frontiers | Research Topics

Emerging trends in cancer research: diagnostic and therapeutic breakthroughs

Edited by
Valentyn Oksenych, Oleksandr Kamyshnyi, Rostyslav Bilyy and Peter Csaba Huszthy

Published in
Frontiers in Molecular Biosciences
Frontiers in Oncology

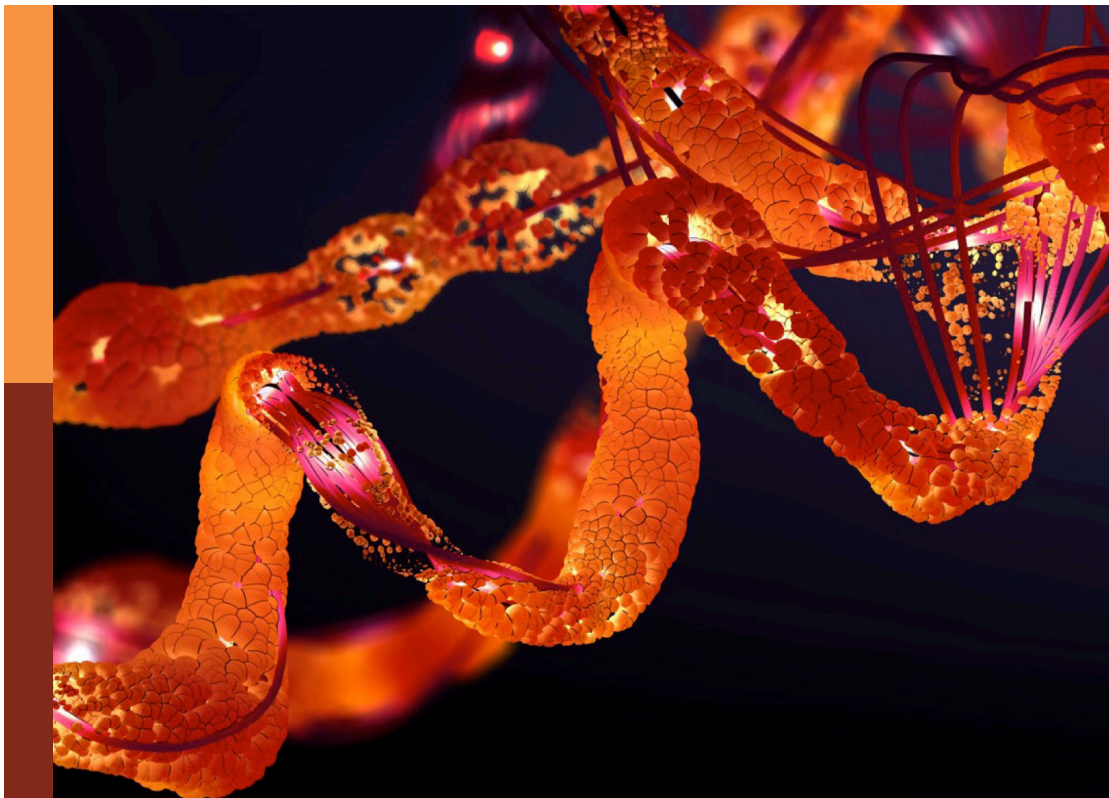

ISSN 1664-8714
ISBN 978-2-8325-7264-1
DOI 10.3389/978-2-8325-7264-1

Generative AI statement
Any alternative text (Alt text) provided alongside figures in the articles in this ebook has been generated by Frontiers with the support of artificial intelligence and reasonable efforts have been made to ensure accuracy, including review by the authors wherever possible. If you identify any issues, please contact us.

About Frontiers

Frontiers is more than just an open access publisher of scholarly articles: it is a pioneering approach to the world of academia, radically improving the way scholarly research is managed. The grand vision of Frontiers is a world where all people have an equal opportunity to seek, share and generate knowledge. Frontiers provides immediate and permanent online open access to all its publications, but this alone is not enough to realize our grand goals.

Frontiers journal series

The Frontiers journal series is a multi-tier and interdisciplinary set of open-access, online journals, promising a paradigm shift from the current review, selection and dissemination processes in academic publishing. All Frontiers journals are driven by researchers for researchers; therefore, they constitute a service to the scholarly community. At the same time, the *Frontiers journal series* operates on a revolutionary invention, the tiered publishing system, initially addressing specific communities of scholars, and gradually climbing up to broader public understanding, thus serving the interests of the lay society, too.

Dedication to quality

Each Frontiers article is a landmark of the highest quality, thanks to genuinely collaborative interactions between authors and review editors, who include some of the world's best academicians. Research must be certified by peers before entering a stream of knowledge that may eventually reach the public - and shape society; therefore, Frontiers only applies the most rigorous and unbiased reviews. Frontiers revolutionizes research publishing by freely delivering the most outstanding research, evaluated with no bias from both the academic and social point of view. By applying the most advanced information technologies, Frontiers is catapulting scholarly publishing into a new generation.

What are Frontiers Research Topics?

Frontiers Research Topics are very popular trademarks of the *Frontiers journals series*: they are collections of at least ten articles, all centered on a particular subject. With their unique mix of varied contributions from Original Research to Review Articles, Frontiers Research Topics unify the most influential researchers, the latest key findings and historical advances in a hot research area.

Find out more on how to host your own Frontiers Research Topic or contribute to one as an author by contacting the Frontiers editorial office: frontiersin.org/about/contact

Emerging trends in cancer research: diagnostic and therapeutic breakthroughs

Topic editors

Valentyn Oksenych — University of Bergen, Norway

Oleksandr Kamyshnyi — Ternopil State Medical University, Ukraine

Rostyslav Bilyy — Danylo Halytsky Lviv National Medical University, Ukraine

Peter Csaba Huszthy — Akershus University Hospital, Norway

Citation

Oksenych, V., Kamyshnyi, O., Bilyy, R., Huszthy, P. C., eds. (2025). *Emerging trends in cancer research: diagnostic and therapeutic breakthroughs*.

Lausanne: Frontiers Media SA. doi: 10.3389/978-2-8325-7264-1

Table of contents

frontiers | Frontiers in Molecular Biosciences

TYPE Editorial
PUBLISHED 02 December 2025
DOI 10.3389/fmolb.2025.1750771

OPEN ACCESS

EDITED AND REVIEWED BY
Matteo Becatti,
University of Firenze, Italy

*CORRESPONDENCE
Valentyn Oksenych,
lab.oksenych@gmail.com
Oleksandr Kamyshnyi,
kamyshnyi_om@tdmu.edu.ua
Rostyslav Bilyy,
r.bilyy@gmail.com

†These authors share senior authorship

RECEIVED 20 November 2025
REVISED 21 November 2025
ACCEPTED 21 November 2025
PUBLISHED 02 December 2025

CITATION
Oksenych V, Kamyshnyi O and Bilyy R (2025) Editorial: Emerging trends in cancer research: diagnostic and therapeutic breakthroughs. *Front. Mol. Biosci.* 12:1750771. doi: 10.3389/fmolb.2025.1750771

Editorial: Emerging trends in cancer research: diagnostic and therapeutic breakthroughs

Valentyn Oksenych[1,2*†], Oleksandr Kamyshnyi[3*†] and Rostyslav Bilyy[4,5,6*†]

[1]Faculty of Medicine, University of Bergen, Bergen, Norway, [2]Oslo Bioconsulting, Oslo, Norway, [3]Department of Microbiology, Virology, and Immunology, I. Horbachevsky Ternopil National Medical University, Ternopil, Ukraine, [4]Institute of Cellular Biology and Pathology "Nicolae Simionescu", Bucharest, Romania, [5]Department of Histology, Cytology and Embryology, Danylo Halytsky Lviv National Medical University, Lviv, Ukraine, [6]Lectinotest R&D, Bucharest, Romania

KEYWORDS

cancer, biomarkers, molecular diagnostics, targeted therapies, immunotherapy, personalized medicine

Editorial on the Research Topic
Emerging trends in cancer research: diagnostic and therapeutic breakthroughs

The Research Topic "*Emerging Trends in Cancer Research: Diagnostic and Therapeutic Breakthroughs*" synthesizes recent advances in oncology, highlighting strategies for early detection, improved prognostic tools, analysis of the complex tumor microenvironment (TME), and development of precision therapies. Despite extensive efforts, cancer remains a major global health challenge, encompassing diverse pathologies with different cellular origins. Hepatocellular carcinoma (HCC), for example, ranks as the third leading cause of cancer-related mortality worldwide, causing over 800,000 deaths annually (Alemayehu et al. and Sung et al., 2021), while cutaneous melanoma (CM) is a highly aggressive skin malignancy, with incidence rates rising dramatically in recent decades (Dudin et al. and Siegel et al., 2022). Addressing these persistent challenges requires breakthroughs in molecular science and integrated clinical strategies. The papers compiled here reflect this imperative, emphasizing minimally invasive molecular diagnostics, immunotherapy targeting the tumor microenvironment (Wan et al., 2025), and advanced genomic approaches to guide personalized treatment. Collectively, they aim to overcome key limitations in late-stage diagnosis and therapy resistance, advancing more effective and precise interventions for cancer management (Alemayehu et al.).

Significant efforts are focused on improving diagnostic and prognostic precision through molecular profiling and liquid biopsy technologies. The value of circulating biomarkers is well illustrated, exemplified by a systematic review and meta-analysis demonstrating that circulating microRNAs hold promise as non-invasive diagnostic biomarkers for hepatocellular carcinoma (Alemayehu et al.). For colorectal cancer (CRC), where early-stage symptoms are often lacking (Bray et al., 2024), novel markers like cystatin S (CST4) are emerging. CST4 demonstrates stability post-chemotherapy and significantly enhances diagnostic sensitivity for malignant

colorectal lesions when combined with conventional tumor markers (CEA, CA125, CA724), representing a 28.4% increase in sensitivity over CST4 alone (Han et al.).

The increasing need for detailed genetic information drives the application of advanced sequencing methods, including Next-Generation Sequencing (NGS) and Third-Generation Sequencing (TGS), to unravel circulating tumor DNA (ctDNA) mutations in liquid biopsies (Da Silva et al.). The requirement for molecular precision is underscored by cases illustrating diagnostic pitfalls, where malignancies like pulmonary Ewing sarcoma (ES) can be misdiagnosed as more common entities such as Small Cell Lung Cancer (SCLC) based solely on histopathology, necessitating early molecular testing for accurate diagnosis and management selection (Waary et al.). Moreover, prognostic models are being refined using routinely available markers, such as assessing uric acid (UR) and the Neutrophil/Lymphocyte Ratio (NLR) in CRC. Elevated UR and NLR levels were found to be independent risk factors for bone metastasis, reflecting the role of systemic inflammation in disease progression (Chen et al.).

Omelianenko et al. investigated the tumor immune microenvironment (TIME) in thyroid adenoma (TA) and carcinoma (TC) to explore its potential diagnostic value in cytopathology. In a pilot study of 72 cases (36 TA, 36 TC) with histological confirmation and preoperative Bethesda III–V cytology, the authors quantified $CD8^+$, $CD68^+$, and $CD163^+$ immune cells and assessed STAT6 and SMAD4 expression. TC exhibited a highly immunogenic profile with abundant $CD8^+$ lymphocytes and macrophages, whereas TA showed low immune infiltration. Immune cell counts in cytology specimens correlated strongly with histological findings. These results suggest that immune cell density in thyroid cytology may serve as an additional criterion for differentiating benign and malignant lesions.

Case report of Yang et al. focuses on a metastatic squamous cell carcinoma of unknown primary (SCCUP) in a 70-year-old female presenting with elevated CA 19–9 and a diaphragmatic mass. Despite extensive evaluation, including PET-CT and a 90-gene expression assay, the primary tumor remained unidentified. The patient underwent surgical resection followed by systemic therapy, achieving 14 months of disease-free survival. This case highlights diagnostic limitations, the potential of multimodal therapy, molecular–clinical discordance, and the need for international collaboration and comprehensive genomic profiling in CUP management.

In therapeutic breakthroughs, a key focus is the multifaceted interplay within the tumor microenvironment (TME) (Anderson and Simon, 2020; Ragunathan et al., 2020). A prominent area involves targeting Tumor-Associated Macrophages (TAMs), which exhibit plasticity, polarizing into M1 (anti-tumor) or M2 (pro-tumor/metastasis promoting) phenotypes (Bai et al.). Therapeutic strategies aim to reprogram M2-TAMs toward the anti-tumor M1 phenotype, utilizing agents like CSF1R inhibitors or blockers targeting the CD47/SIRPα axis, or through common drugs like Metformin, which disrupts M2 polarization by activating the AMP-activated protein kinase (AMPK) pathway (Bai et al.). This emphasis on immunomodulation was heavily featured at the 8th Cancer Immunotherapy and Immunomonitoring (CITIM) conference, which highlighted the critical roles of chronic inflammation, Myeloid-Derived Suppressor Cells (MDSCs), and the emerging understanding of the neuro-metabolic-immune regulation of cancer (Rostyslav Bilyy).

Cutting-edge strategies include novel chemical agents designed to induce immunogenic cell death and prolonged immune stimulation (Arkhypov et al., 2025) and delivery systems critical for overcoming treatment obstacles, particularly in challenging diseases like Triple-Negative Breast Cancer (TNBC) (Tiwari et al.). Extracellular vesicles (EVs) are identified both as essential players in promoting TNBC progression and drug resistance (e.g., through carrying EGFR or lncRNA XIST) and as promising drug carriers for targeted therapies due to their low toxicity and ability to traverse biological barriers, Tiwari et al.

Finally, innovation in clinical safety includes the development of a novel sealant combining an absorbable gelatin sponge (mechanical occlusion) with Agkistrodon acutus-derived hemocoagulase (local coagulation, Chen et al.). This dual mechanical and pharmacological barrier significantly reduced the rate of intervention-requiring pneumothorax in pulmonary biopsies (from a literature rate of 22.1% to 2.38%) and introduced a precision-stratified safety protocol based on D-dimer levels to manage hemorrhage risk, Chen et al.

Collectively, these findings underscore a concerted movement toward integrative cancer management, where precise molecular information and sophisticated TME modulation techniques are combined to deliver more effective, personalized, and safer patient care, Alemayehu et al.

Author contributions

VO: Writing – original draft, Writing – review and editing. OK: Writing – original draft, Writing – review and editing. RB: Writing – original draft, Writing – review and editing.

Funding

The authors declare that financial support was received for the research and/or publication of this article. This work was supported by the European Union–NextGenerationEU and the Romanian Government through the National Recovery and Resilience Plan, Component 9 - Investment 8, HeartCure project, Financing Contract no. 760063/23.05.2023, CF93/15.11.2022; Project SAIL under Partnership Fostering a European Research Area for Health (ERA4Health) (GA N° 101095426 of the EU Horizon Europe Research and Innovation Programme); RB received funding through the MSCA4Ukraine project ID: 101101923, fellowship grant 1194477, which is funded by the European Union. VO was a recipient of the following grants: the Research Council of Norway Young Talent Investigator grant (#249774); the Liaison Committee for Education, Research, and Innovation in Central Norway (#13477; #38811); the Norwegian Cancer Society (#182355); the Research Council of Norway FRIMEDBIO grants (#270491 and #291217); The Outstanding Academic Fellow Program 2.0

at NTNU; and Karolinska Institutet Stiftelser och Fonder (#2020-02155).

Conflict of interest

Author VO was employed by Oslo Bioconsulting. Author RB was employed by Lectinotest R&D.

The remaining author declares that the research was conducted in the absence of any commercial or financial relationships that could be construed as a potential conflict of interest.

The author(s) declared that they were an editorial board member of Frontiers, at the time of submission. This had no impact on the peer review process and the final decision.

Generative AI statement

The authors declare that Generative AI was used in the creation of this manuscript. During the preparation of this work, the authors used ChatGPT-4.1 and Microsoft Copilot to enhance text readability. After using these tools/services, the authors reviewed and edited the content as needed and take full responsibility for the content of the published article.

Any alternative text (alt text) provided alongside figures in this article has been generated by Frontiers with the support of artificial intelligence and reasonable efforts have been made to ensure accuracy, including review by the authors wherever possible. If you identify any issues, please contact us.

Publisher's note

References

Anderson, N. M., and Simon, M. C. (2020). The tumor microenvironment. *Curr. Biol.* 30 (16), R921–R925. doi:10.1016/j.cub.2020.06.081

Arkhypov, A., Klemt, I., Bila, G., Attia, D., Chernii, S., Bilyy, R., et al. (2025). Targeting Lysosomal thiols for immunogenic cancer cell death. *Angew. Chem. Int. Ed. Engl.* 64 (5), e202417509. doi:10.1002/anie.202417509

Bray, F., Laversanne, M., Sung, H., Ferlay, J., Siegel, R. L., Soerjomataram, I., et al. (2024). Global cancer statistics 2022: GLOBOCAN estimates of incidence and mortality worldwide for 36 cancers in 185 countries. *CA Cancer J. Clin.* 74 (3), 229–263. doi:10.3322/caac.21834

Ragunathan, K., Upfold, N. L. E., and Oksenych, V. (2020). Interaction between fibroblasts and immune cells following DNA damage induced by ionizing radiation. *Int. J. Mol. Sci.* 21 (22). doi:10.3390/ijms21228635

Siegel, R. L., Miller, K. D., Fuchs, H. E., and Jemal, A. (2022). Cancer statistics, 2022. *CA Cancer J. Clin.* 72 (1), 7–33. doi:10.3322/caac.21708

Sung, H., Ferlay, J., Siegel, R. L., Laversanne, M., Soerjomataram, I., Jemal, A., et al. (2021). Global cancer statistics 2020: GLOBOCAN estimates of Incidence and Mortality Worldwide for 36 Cancers in 185 Countries. *CA Cancer J. Clin.* 71 (3), 209–249. doi:10.3322/caac.21660

Wan, H., Ren, W., Yang, M., Nie, M., Wasik, A. M., Du, L., et al. (2025). Tumor evolution and immune microenvironment dynamics in primary and relapsed mantle cell lymphoma. *Cell Rep. Med.* 6 (9), 102318. doi:10.1016/j.xcrm.2025.102318

frontiers | Frontiers in Molecular Biosciences

TYPE Review
PUBLISHED 14 May 2024
DOI 10.3389/fmolb.2024.1353547

OPEN ACCESS

EDITED BY
Ashok Kumar,
All India Institute of Medical Sciences, Bhopal, India

REVIEWED BY
Shikha Tiwari,
All India Institute of Medical Sciences, Bhopal, India
Zhi-Wei Guo,
Southern Medical University, China

*CORRESPONDENCE
Ermiyas Alemayehu,
ermiyas0009@gmail.com

†These authors have contributed equally to this work and share first authorship

RECEIVED 10 December 2023
ACCEPTED 30 April 2024
PUBLISHED 14 May 2024

CITATION
Alemayehu E, Fasil A, Ebrahim H, Mulatie Z, Bambo GM, Gedefie A, Teshome M, Worede A and Belete MA (2024), Circulating microRNAs as promising diagnostic biomarkers for hepatocellular carcinoma: a systematic review and meta-analysis.
Front. Mol. Biosci. 11:1353547.
doi: 10.3389/fmolb.2024.1353547

Circulating microRNAs as promising diagnostic biomarkers for hepatocellular carcinoma: a systematic review and meta-analysis

Ermiyas Alemayehu[1*†], Alebachew Fasil[2], Hussen Ebrahim[1], Zewudu Mulatie[1], Getachew Mesfin Bambo[3], Alemu Gedefie[1], Mulugeta Teshome[4], Abebaw Worede[2] and Melaku Ashagrie Belete[1†]

[1]Department of Medical Laboratory Sciences, College of Medicine and Health Sciences, Wollo University, Dessie, Ethiopia, [2]Department of Clinical Chemistry, School of Biomedical and Laboratory Sciences, College of Medicine and Health Sciences, University of Gondar, Gondar, Ethiopia, [3]Department of Medical Laboratory Science, College of Health Sciences, Mizan-Tepi University, Mizan Aman, Ethiopia, [4]Department of Medical Laboratory Science, Dessie Health Science College, Dessie, Ethiopia

Introduction: Hepatocellular carcinoma (HCC), the most common type of liver cancer, is a major global health problem, ranking as the third leading cause of cancer-related death worldwide. Early identification and diagnosis of HCC requires the discovery of reliable biomarkers. Therefore, the study aimed to assess the diagnostic accuracy of miRNAs for HCC. The protocol was registered on PROSPERO website with the registration number CRD42023417494.

Method: A literature search was conducted in PubMed, Scopus, Embase, Wiley Online Library, and Science Direct databases to identify pertinent articles published between 2018 and 30 July 2023. Stata 17.0 software was employed to determine the pooled sensitivity, specificity, positive likelihood ratio (PLR), negative likelihood ratio (NLR), diagnostic ratio (DOR), and area under the curve (AUC) for evaluating the accuracy of miRNAs in diagnosing HCC. The assessment of heterogeneity among studies involved the use of the Cochran-Q test and I^2 statistic tests. Due to the observed significant heterogeneity, the random-effect model was chosen. Subgroup analysis and meta-regression analysis were also undertaken to explore potential sources contributing to heterogeneity. Deeks' funnel plot was used to assess publication bias. In addition, Fagan's nomogram and likelihood ratio scattergram were utilized to assess the clinical validity of miRNAs for HCC.

Result: Twenty-four articles were included, involving 1,668 individuals diagnosed with HCC and 1,236 healthy individuals. The findings revealed pooled sensitivity of 0.84 (95% CI: 0.80–0.88), specificity of 0.81 (95% CI: 0.77–0.84), PLR of 4.36 (95% CI: 3.59–5.30), NLR of 0.19 (95% CI: 0.15–0.25), DOR of 22.47 (95% CI: 14.47–32.64), and an AUC of 0.89 (95% CI: 0.86–0.91) for the diagnosis of HCC using miRNAs. Furthermore, results from the subgroup analysis demonstrated that superior diagnostic performance was observed when utilizing plasma miRNAs, a large sample size (≥100), and miRNA panels.

Conclusion: Hence, circulating miRNAs demonstrate substantial diagnostic utility for HCC and can serve as effective non-invasive biomarkers for the condition. Additionally, miRNA panels, miRNAs derived from plasma, and miRNAs evaluated in larger sample sizes (≥100) demonstrate enhanced diagnostic efficacy for HCC diagnosis. Nevertheless, a large pool of prospective studies and multi-center research will be required to confirm our findings in the near future.

KEYWORDS

miRNAs, non-coding RNAs, diagnostic biomarkers, hepatocellular carcinoma, HCC, liver cancer, meta-analysis

Introduction

Hepatocellular carcinoma (HCC) stands as a formidable global health challenge, representing the most common primary malignancy of the liver accounting for approximately 90% of cases (Singal et al., 2023). It is ranked as the seventh most frequently occurring cancer, and the third leading cause of cancer-related mortality worldwide with over 800,000 deaths annually (Arnold et al., 2020; Sung et al., 2021). The World Health Organization (WHO) forecasts that the annual death rate from HCC will spike to more than 1 million individuals by the year 2030 (World Health Organization, 2020).

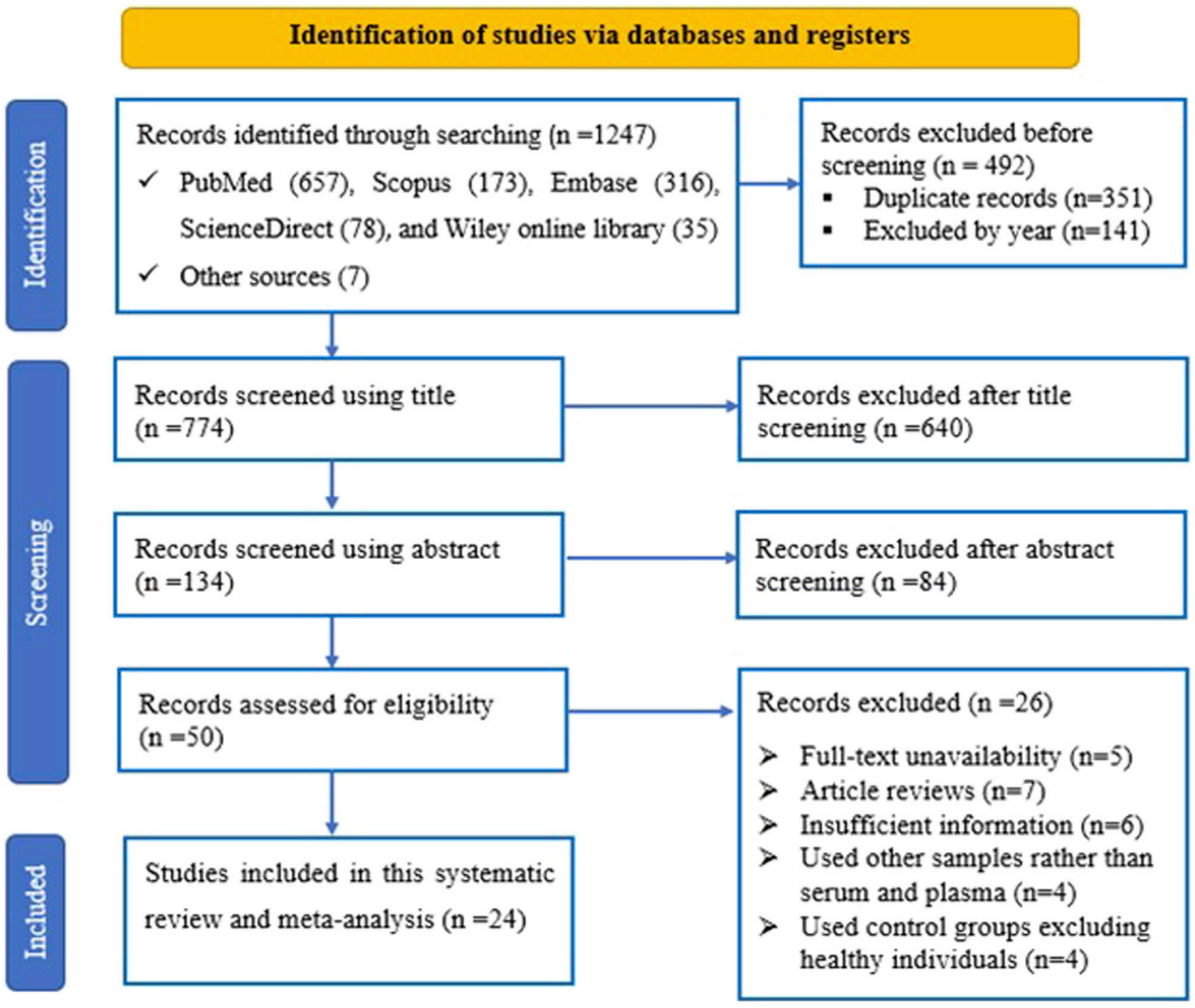

FIGURE 1
The PRISMA flow diagram illustrates the flow of study selection, detailing the number of studies identified, included, and excluded at each stage of the selection process according to predefined criteria.

TABLE 1 Intervening characteristics of the included studies.

Authors	Year	County	miRNAs	Expression	Specimen	Method	References	Participants				Cut-off	Sen (%)	Spe (%)	AUC
								Case	No	Control	No				
Xu et al. (Xu et al., 2018a)	2018	China	miR-125b	Down	Serum	qRT-PCR	U6	HBV-HCC	100	HC	100	2.45	83	96	0.94
Lv et al. (Lv et al., 2018)	2018	China	miR-21	Up	Serum	qRT-PCR	U6	HCC	75	HC	80	NA	69.1	78.3	0.771
Lv et al. (Lv et al., 2018)	2018	China	miR-214	Down	Serum	qRT-PCR	U6	HCC	75	HC	80	NA	79.3	69.6	0.733
Lv et al. (Lv et al., 2018)	2018	China	miR-15b	Up	Serum	qRT-PCR	U6	HCC	75	HC	80	NA	89.7	63.1	0.809
Lv et al. (Lv et al., 2018)	2018	China	miR-21, 214, 15b	NA	Serum	qRT-PCR	U6	HCC	75	HC	80	NA	80.3	87.0	0.887
Han et al. (Han et al., 2019)	2019	China	miR-148a	Down	Plasma	qRT-PCR	U6 snRNA	HCC	155	HC	95	8.12	97.9	92.9	0.980
Zhang et al. (Zhang et al., 2019)	2019	China	miR-130b	Up	Serum	qRT-PCR	U6	HCC	46	HC	55	2.525	82.20	73.72	0.725
Zhang et al. (Zhang et al., 2019)	2019	China	miR-21	Up	Serum	qRT-PCR	U6	HCC	46	HC	55	2.312	81.29	75.74	0.795
Zhang et al. (Zhang et al., 2019)	2019	China	miR-21, 130b	Up	Serum	qRT-PCR	U6	HCC	46	HC	55	NA	92.16	77.51	0.832
Ning et al. (Ning et al., 2019)	2019	China	miR-155	Up	Serum	qRT-PCR	U6	HCC	30	HC	30	NA	93.3	70.0	0.840
Ning et al. (Ning et al., 2019)	2019	China	miR-96	Up	Serum	qRT-PCR	U6	HCC	30	HC	30	NA	70.0	86.7	0.824
Ning et al. (Ning et al., 2019)	2019	China	miR-99a	Down	Serum	qRT-PCR	U6	HCC	30	HC	30	NA	73.3	83.3	0.799
Ning et al. (Ning et al., 2019)	2019	China	miR-155, 96, 99a	NA	Serum	qRT-PCR	U6	HCC	30	HC	30	NA	76.7	96.7	0.931
Chen et al. (Chen and Wang, 2019)	2019	China	miR-195	Down	Serum	qRT-PCR	miR-16	HCC	120	HC	118	1.685	76.7	77.0	0.862
Zeng et al. (Zeng et al., 2020)	2020	China	miR-22	Down	Serum	qRT-PCR	U6	HCC	108	HC	67	1.352	89.3	68.9	0.866
Cao et al. (Cao and Wang, 2020)	2020	China	miR-768-3p	Down	Serum	qRT-PCR	cel-miR-39-3p	HBV-HCC	110	HC	60	0.809	87.27	80	0.908
Wu et al. (Wu et al., 2020)	2020	China	miR-199a	Down	Serum	qRT-PCR	cel-miR-54-5p	HCC	48	HC	50	1.02	91.7	62.0	0.808
Zhao et al. (Zhao et al., 2021)	2021	China	miR-324-3p	Up	Serum	qRT-PCR	cel-miR-39-3p	HBV-HCC	96	HC	76	1.608	77.08	93.42	0.926
Chen et al. (Chen et al., 2021)	2021	China	miR-497	Down	Serum	qRT-PCR	cel-miR-39	HCC	50	HC	50	NA	74.0	66.0	0.726
Chen et al. (Chen et al., 2021)	2021	China	miR-1246	Up	Serum	qRT-PCR	cel-miR-39	HCC	50	HC	50	NA	82.0	80.0	0.865
Chen et al. (Chen et al., 2021)	2021	China	miR-497, 1,246	NA	Serum	qRT-PCR	cel-miR-39	HCC	50	HC	50	NA	94.0	70.0	0.911
Wu et al. (Wu et al., 2022)	2022	China	miR-126	Down	Plasma	qRT-PCR	hsamiR-16-5p	HCC	38	HC	20	2.082	81.6	65	0.751

(Continued on following page)

10.3389/fmolb.2024.1353547

TABLE 1 (*Continued*) Intervening characteristics of the included studies.

Authors	Year	County	miRNAs	Expression	Specimen	Method	References	Participants				Cut-off	Sen (%)	Spe (%)	AUC
								Case	No	Control	No				
Wu et al. (Wu et al., 2022)	2022	China	miR-222	Up	Plasma	qRT-PCR	hsamiR-16-5p	HCC	38	HC	20	2.207	55.3	90	0.686
Wu et al. (Wu et al., 2022)	2022	China	miR-206	Up	Plasma	qRT-PCR	hsamiR-16-5p	HCC	38	HC	20	1.315	51.9	90	0.713
Wu et al. (Wu et al., 2022)	2022	China	miR-126, 206	NA	Plasma	qRT-PCR	hsamiR-16-5p	HCC	38	HC	20	NA	81.6	85	0.887
Fang et al. (Fang et al., 2022)	2022	China	miR-16	Up	Serum	qRT-PCR	hsamiR-21-5p	HCC	100	HC	100	NA	91	58	0.798
Shaheen et al. (Shaheen et al., 2018)	2018	Egypt	miR-150	Down	Serum	qRT-PCR	cel-mir-39	HCV-HCC	40	HC	40	0.674	60	70	0.638
Elmougy et al. (Elmougy et al., 2019)	2019	Egypt	miR-223	Down	Serum	qRT-PCR	SNORD68	HCV-HCC	40	HC	40	1.59	77.5	80.0	0.857
Elmougy et al. (Elmougy et al., 2019)	2019	Egypt	miR-19a	Up	Serum	qRT-PCR	SNORD68	HCV-HCC	40	HC	40	0.65	70	77.5	0.726
Mahdy et al. (El Mahdy et al., 2019)	2019	Egypt	miR-215	Down	Plasma	qRT-PCR	RNU6	HCC	60	HC	60	2.30	80	96.7	0.93
Aly et al. (Aly et al., 2020)	2020	Egypt	miR-143	Down	Serum	qRT-PCR	SNORD68	HCV-HCC	40	HC	40	0.43	62.5	72.5	0.702
Aly et al. (Aly et al., 2020)	2020	Egypt	miR-145	Down	Serum	qRT-PCR	SNORD68	HCV-HCC	40	HC	40	0.462	65	67.5	0.677
Elhendawy et al. (Elhendawy et al., 2020)	2020	Egypt	miR-142-5p	Up	Plasma	NGS	NA	HCC	20	HC	10	1.401	75.0	100.0	0.929
Elhendawy et al. (Elhendawy et al., 2020)	2020	Egypt	miR-191-5p	Down	Plasma	NGS	NA	HCC	20	HC	10	4.426	92.9	80.0	0.929
Elhendawy et al. (Elhendawy et al., 2020)	2020	Egypt	miR-22-3p	Down	Plasma	NGS	NA	HCC	20	HC	10	2.165	76.9	100.0	0.831
Elhendawy et al. (Elhendawy et al., 2020)	2020	Egypt	miR-126-5p	Down	Plasma	NGS	NA	HCC	20	HC	10	2.315	83.0	100.0	0.967
Wahb et al. (Wahb et al., 2021)	2021	Egypt	miR-9-3p	Down	Serum	qRT-PCR	U6 snRNA	HCV-HCC	35	HC	32	1.01	91.43	87.50	N/A
Elfert et al. (Elfert et al., 2022)	2022	Egypt	miR-122	Up	Serum	qRT-PCR	SNORD68	HCV-HCC	90	HC	60	6.55	100	84.1	0.95
Elfert et al. (Elfert et al., 2022)	2022	Egypt	miR-483	Up	Serum	qRT-PCR	SNORD68	HCV-HCC	90	HC	60	2.43	100	82.3	0.986
Elfert et al. (Elfert et al., 2022)	2022	Egypt	miR-335	Down	Serum	qRT-PCR	SNORD68	HCV-HCC	90	HC	60	0.49	100	79.8	0.908

(Continued on following page)

10.3389/fmolb.2024.1353547

TABLE 1 (*Continued*) Intervening characteristics of the included studies.

Authors	Year	County	miRNAs	Expression	Specimen	Method	References	Participants				Cut-off	Sen (%)	Spe (%)	AUC
								Case	No	Control	No				
Youssef et al. (Youssef et al., 2022)	2022	Egypt	miR-326	Up	Plasma	qRT-PCR	RNU6B	HCC	70	HC	20	1.165	97.1	52.0	0.784
Youssef et al. (Youssef et al., 2022)	2022	Egypt	miR-511	Down	Plasma	qRT-PCR	RNU6B	HCC	70	HC	20	2.063	71.4	60.0	0.654
Youssef et al. (Youssef et al., 2022)	2022	Egypt	miR-424	Down	Plasma	qRT-PCR	RNU6B	HCC	70	HC	20	2.462	82.9	48.0	0.559
Yousuf et al. (Yousuf et al., 2022)	2022	India	miR-221	Down	Serum	qRT-PCR	U6	HCC	33	HC	33	1.626	77.14	80.77	0.786
Yousuf et al. (Yousuf et al., 2022)	2022	India	miR-222	Down	Serum	qRT-PCR	U6	HCC	33	HC	33	0.609	86.96	68.75	0.758
Loosen et al. (Loosen et al., 2021)	2021	Germany	miR-107	Up	Serum	qPCR	NA	HCC	45	HC	18	2.63	55.6	100	0.679
Moshiri et al. (Moshiri et al., 2018)	2018	Italy	miR-101-3p	Up	Plasma	ddPCR	NA	HCC	29	HC	25	NA	71.4	58.8	0.71
Moshiri et al. (Moshiri et al., 2018)	2018	Italy	miR-1246	Up	Plasma	ddPCR	NA	HCC	29	HC	25	NA	57.1	78.6	0.83
Moshiri et al. (Moshiri et al., 2018)	2018	Italy	miR-106b-3p	Up	Plasma	ddPCR	NA	HCC	29	HC	25	NA	87.0	83.3	0.95
Moshiri et al. (Moshiri et al., 2018)	2018	Italy	miR-101-3p, 1246,106b-3p	NA	Plasma	ddPCR	NA	HCC	29	HC	25	NA	100.0	100.0	1.00

Note: HC: healthy control; HCC: hepatocellular carcinoma; HCV-HCC: hepatitis C virus related hepatocellular carcinoma; HBV-HCC: hepatitis B virus related hepatocellular carcinoma; NA: not available; NGS: next-generation sequence; qRT-PCR: quantitative real-time polymerase chain reaction; qPCR: quantitative polymerase chain reaction; ddPCR: droplet digital polymerase chain reaction.

10.3389/fmolb.2024.1353547

FIGURE 2
The risk of bias assessment of included studies using the QUADAS-2 tool evaluates the quality of diagnostic accuracy studies across four domains: patient selection, index test, reference standard, and flow and timing.

Despite therapeutic strategies are nowadays advanced, the prognosis for HCC remains suboptimal mainly due to late-stage diagnosis and limited therapeutic options (Guan et al., 2021). This is evidenced by poor overall prognosis worldwide, with global age-standardized incidence and mortality at 9.5 and 8.7 per 100,000 person-years, respectively (Rumgay et al., 2022). Moreover, mainly attributable to the absence of obvious clinical symptoms in patients with early HCC, early diagnosis of HCC is still very difficult and insufficient.

Currently, HCC screening primarily relies on cross-sectional imaging such as magnetic resonance imaging (MRI), computed tomography (CT) scanning, ultrasonography (US), contrast-enhanced ultrasound (CEUS), and some tumor markers, particularly α-fetoprotein (AFP) (Frenette et al., 2019). However, such screening techniques still have major shortcomings in detecting early onset HCC (Sherman, 2014). For instance, low (more than 40%) AFP positivity rate frequently observed for early liver cancer, and as a result of which the American Association for the Study of Liver Diseases (AASLD) and the European Association for the Study of the Liver (EASL) (European Association for the Study of the LiverEuropean Organisation For and Research And Treatment Of Cancer, 2012) have excluded AFP as a diagnostic marker for HCC (Bae, 2012; Parra et al., 2023). Furthermore, pathological tests are invasive and can lead to complications (Martins-Filho and Alves, 2019). Therefore, there is an urgent need for robust, less invasive, and reliable biomarkers that can facilitate early diagnosis, prognosis, and therapeutic monitoring in HCC patients.

Recently, there has been a growing interest in the role of microRNAs (miRNAs) as diagnostic biomarkers for numerous cancers, including HCC. MicroRNAs are a class of small (approximately 19–24 nucleotides), non-coding RNAs that play critical roles in the post-transcriptional regulation of gene expression (Armand-Labit and Pradines, 2017). Their dysregulation has been implicated in the initiation and progression or pathogenesis of different diseases, making them promising targets for biomarker discovery (Valihrach et al., 2020; Kim and Croce, 2023). The stability of circulating miRNAs in body fluids such as blood, plasma serum and urine, and their non-invasive potential make them preferable diagnostic biomarkers unlike tissue-based biomarkers (Wang et al., 2012). This is particularly vital in HCC, where tissue sampling may become invasive and risky, and pose challenges. The ability of circulating miRNAs to indicate the molecular changes in the cancer microenvironment embraces their remarkable utilization in clinical settings (Gramantieri et al., 2021).

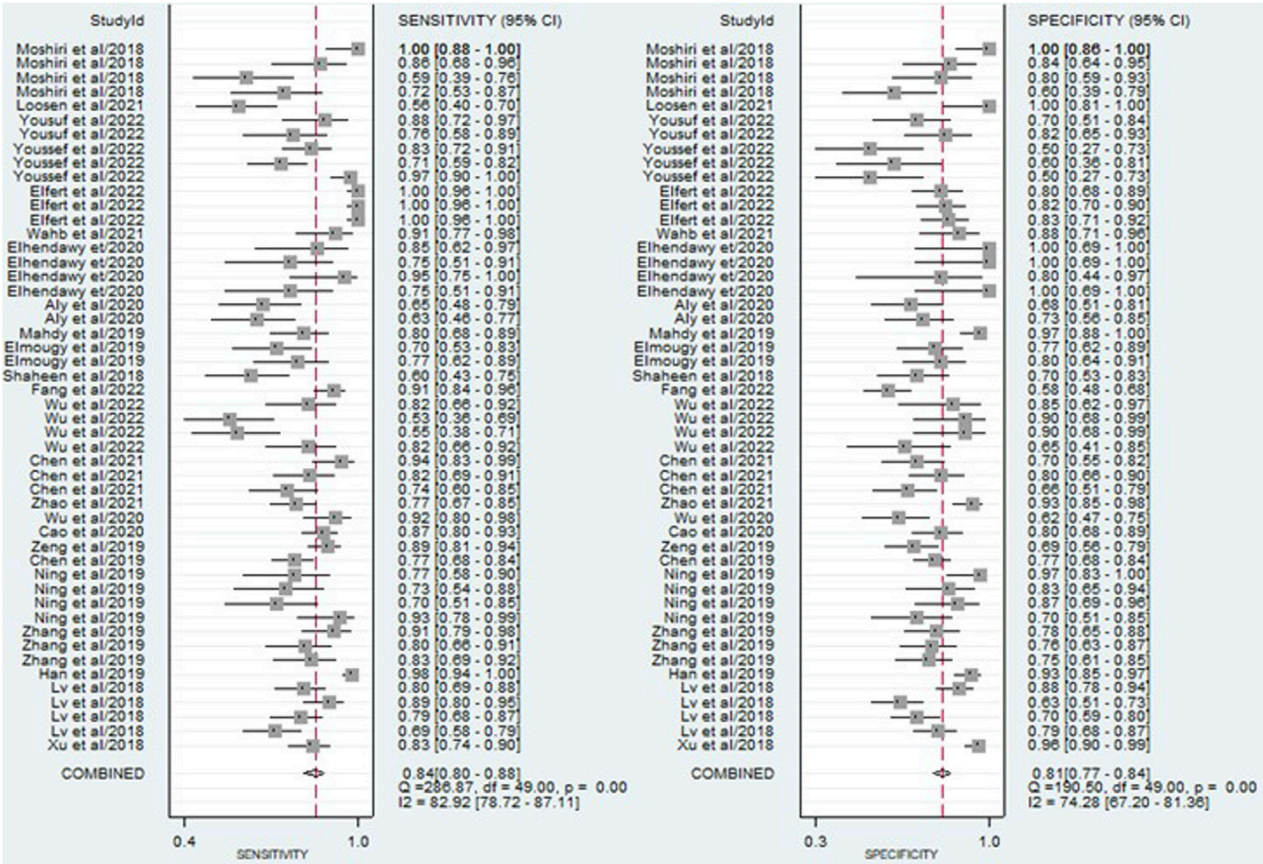

FIGURE 3
A forest plot illustrating the pooled sensitivity and specificity estimates of miRNAs for diagnosing HCC across multiple studies, providing an overview of the diagnostic performance of miRNAs.

Several studies have emphasized the altered expression patterns and dysregulation of specific circulating miRNAs in the development, progression and metastasis of HCC, signifying their utility as promising diagnostic biomarkers (Jin et al., 2019; Fang et al., 2022; Lv and Sun, 2023), but comprehensive and up-to-date evidence-based data is still lacking. In this systematic review and meta-analysis, we aimed to comprehensively evaluate the current state of evidence regarding the diagnostic potential of circulating miRNAs as reliable, non-invasive and clinically applicable biomarkers for the detection of HCC intending to provide an input in addressing the unmet needs in early detection of HCC.

The findings hold significant relevance and applicability in the clinical setting, particularly for improving the early detection of HCC, which is crucial for enhancing patient outcomes, given the disease is often diagnosed at advanced stages when treatment options are limited. Furthermore, the non-invasive nature of circulating miRNA testing makes it particularly appealing for widespread clinical use. Additionally, the clinical utility of circulating miRNAs in HCC diagnosis is underscored by their potential integration into routine screening or diagnostic protocols. By incorporating these biomarkers into existing diagnostic algorithms, the accuracy and effectiveness of HCC detection could be enhanced, ultimately leading to improved patient management and outcomes.

Methods and materials

Registration

This research follows the guidelines outlined in the Preferred Reporting Items for Systematic Reviews and Meta-analysis (PRISMA) statement (Page et al., 2021). The study protocol was registered in the Prospective Register of Systematic Reviews (PROSPERO) under the registration identifier CRD42023417494.

Search strategy and data sources

Two independent researchers (EA and MAB) carried out a comprehensive literature search to collect studies that assessed the diagnostic value of circulating miRNAs for HCC. Various electronic bibliographic databases, including PubMed, Scopus, Embase, Wiley Online Library, and Science Direct, were utilized for this purpose. Additionally, a direct search on Google was performed to identify any relevant studies that might have been omitted during the electronic database searches by checking the bibliographies of the identified studies. The final search was conducted on 30 July 2023. The search strategy incorporated Medical Subject Heading (MeSH) terms and keywords, such as

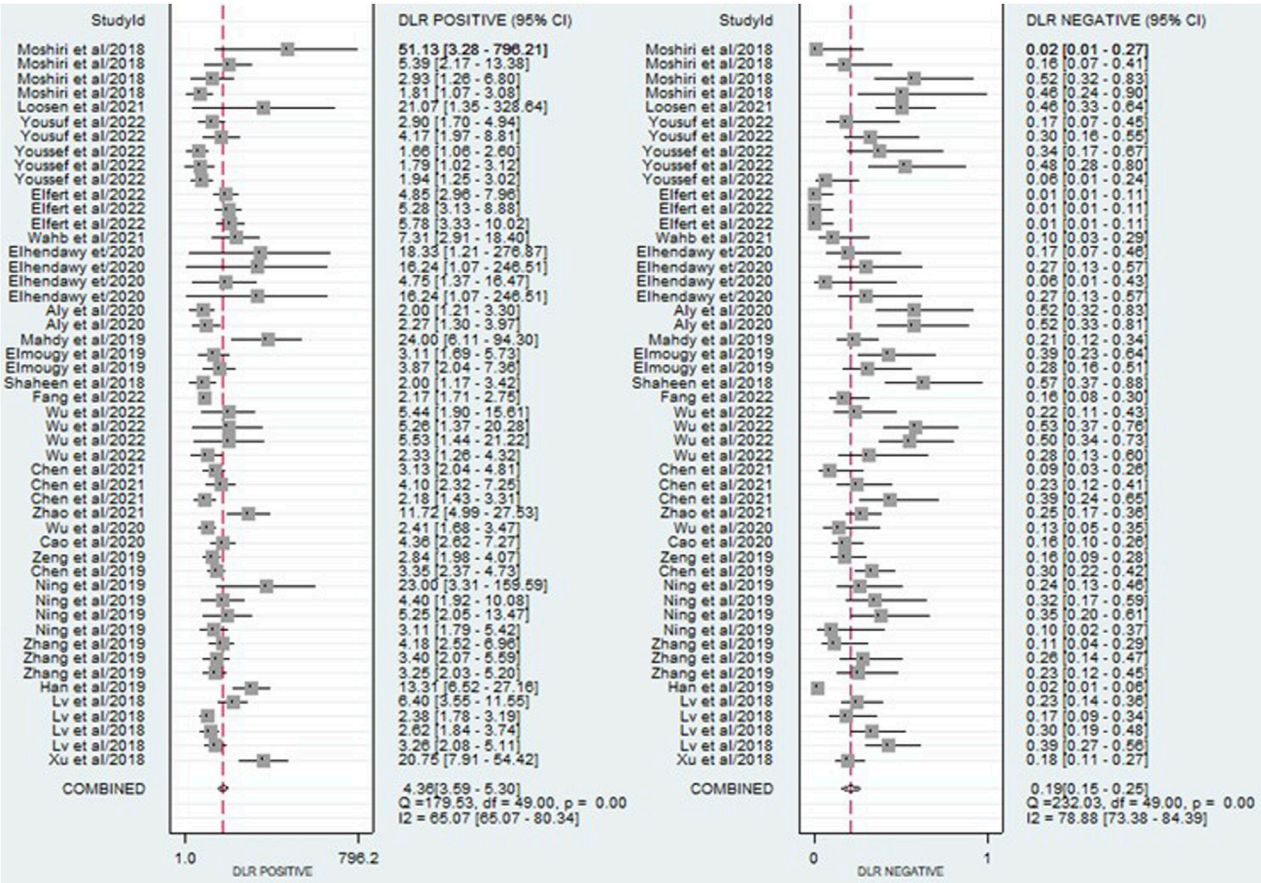

FIGURE 4
A forest plot showing the pooled PLR and NLR estimates of miRNAs for diagnosing HCC, providing insights into the diagnostic utility of miRNAs.

"Serum" OR "plasma" OR "circulating" AND "miRNAs" OR "microRNAs" OR "miRNA" OR "microRNA" OR "miR" AND "diagnosis" AND "hepatocellular carcinoma" OR "HCC". The detailed search strategy is available in the Supplementary Table S1.

Inclusion and exclusion criteria

This review considered specific types of studies, namely, observational studies (including case-control, cross-sectional, and cohort studies) published in peer-reviewed journals since 2018, which explored the utility of circulating miRNAs as a diagnostic tool for distinguishing HCC patients from healthy individuals and examined miRNAs in plasma or serum. In addition, the studies had to provide essential data such as sensitivity, specificity, and sample sizes, enabling the calculation of key diagnostic metrics like true positives (TP), false positives (FP), false negatives (FN), and true negatives (TN). On the other hand, the review excluded review articles, case reports, narrative reviews, conference abstracts, editorials, commentaries, letters to the editor, author replies, studies that did not involve human subjects, and studies lacking the necessary data to calculate TP, FP, TN, and FN. These inclusion and exclusion criteria were employed to guide the selection of studies for the review.

Study selection and data extraction

The studies gathered from the databases mentioned earlier, as well as from direct google search, were imported into EndNote 20 software to identify and eliminate duplicate entries. Subsequently, a thorough screening process was carried out for each selected paper, involving the evaluation of the title, abstract, and full text by two independent reviewers (EA and AF), in accordance with the predetermined eligibility criteria. In cases where discrepancies or disagreements arose between the two reviewers, a discussion took place, and a third reviewer (AG) was involved as needed to make the final determinations regarding which articles would be included in the review.

The selected papers underwent a thorough assessment, during which essential information was collected and organized into an extraction table using Microsoft Office Excel software. This process involved identifying key details, such as the first author, publication year, country of the study, extracted miRNAs, miRNA expression, type of specimen used, internal reference control, sample sizes for both HCC patients and healthy individuals, diagnostic methods, and cut-off values. Additionally, diagnostic parameters including sensitivity, specificity, and the area under the curve (AUC) were extracted by two independent investigators (AW and HE). To ensure accuracy and consistency, the findings were meticulously

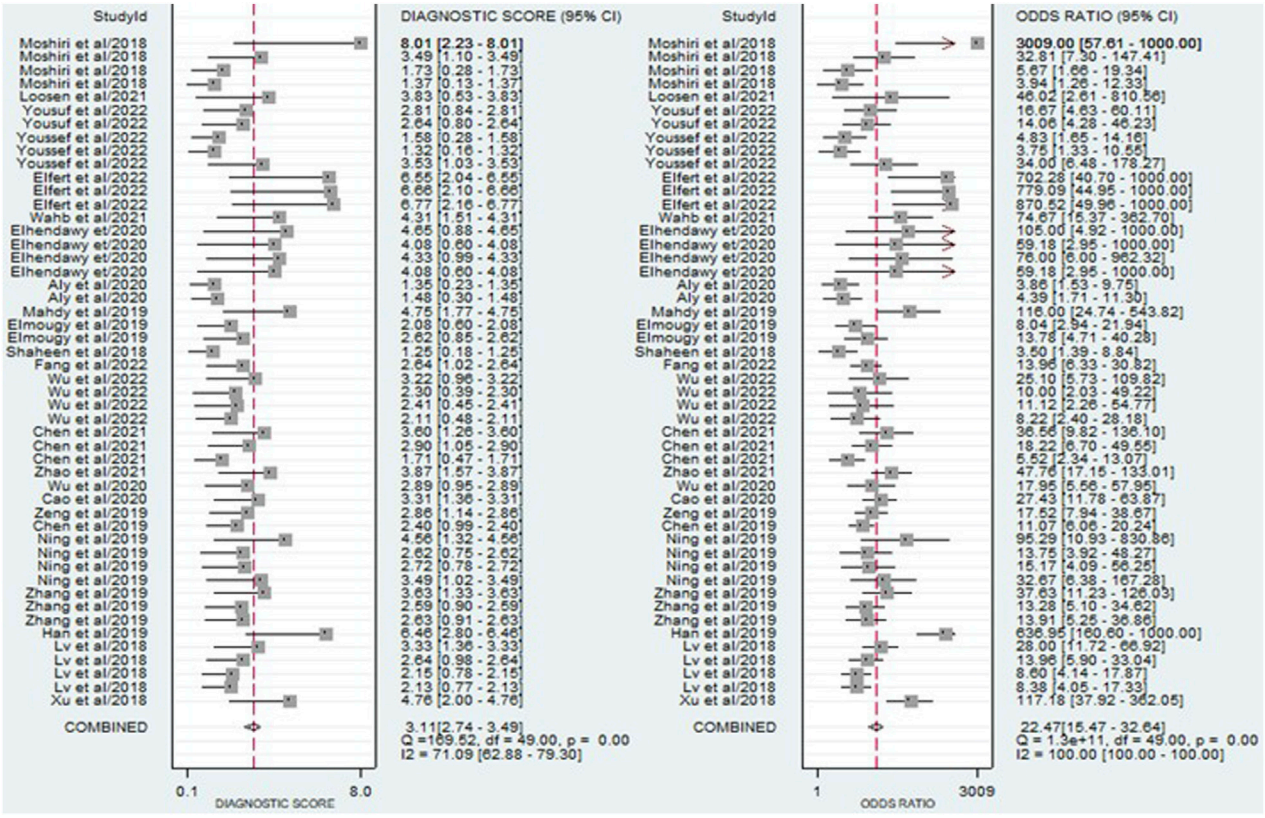

FIGURE 5
A forest plot illustrating the pooled DOR estimates of miRNAs for diagnosing HCC, offering a comprehensive evaluation of the overall diagnostic performance of miRNAs.

cross-checked by the two reviewers, and any discrepancies between the data extractors were resolved through discussion and consensus with the involvement of a third reviewer (GMB), thus verifying the integrity of the collected data.

Quality assessment

The quality of the included studies was assessed using the modified Quality Assessment of Diagnostic Accuracy Studies-2 (QUADAS-2) tool (Freeman et al., 2017), which was carried out with the assistance of Review Manager 5.4 software. Two independent investigators (ZM and EA) conducted this assessment. The QUADAS-2 tool comprises four domains, namely, patient selection, index test, reference standard, and flow and timing. It entailed evaluating the clinical applicability of selected patients, the performance of the index test, and the standard of the reference. The risk of bias was categorized as high, low, or unclear based on this evaluation.

Data analysis

The data analysis was performed using Stata version 17.0 software. To assess the heterogeneity among the studies, Cochrane Q test and I^2 statistics were employed. Considerable heterogeneity was identified when the I^2 test statistics values exceeded 50% and the *p*-value was less than 0.05 (Higgins et al., 2003). The available data were transformed into diagnostic parameters, including TP, FP, FN, and TN. These parameters were used to calculate the pooled sensitivity, specificity, positive likelihood ratio (PLR), negative likelihood ratio (NLR), diagnostic odds ratio (DOR), and area under the curve (AUC) using a random-effects model (Jackson et al., 2010). The AUC and DOR from the summary receiver characteristic curve (SROC) were used to evaluate the overall diagnostic accuracy of circulating miRNAs in diagnosing HCC. The existence of a threshold effect was established through an analysis of the Spearman correlation coefficient and visual inspection of the SROC curve. A *p*-value of less than 0.05 derived from the Spearman correlation coefficient, coupled with the presence of the characteristic "shoulder-arm" shape in the SROC curve, indicated the presence of a threshold effect. Subgroup analyses and meta-regression analyses were conducted to investigate the primary sources of heterogeneity. Deeks' funnel plot asymmetry was employed to assess the presence of publication bias, where a *p*-value greater than 0.10 indicated the absence of publication bias. Moreover, sensitivity analysis was performed to assess the robustness and reliability of the results. Additionally, the Fagan plot and likelihood ratio scattergram were used to evaluate the clinical utility of miRNAs in distinguishing HCC patients from healthy individuals.

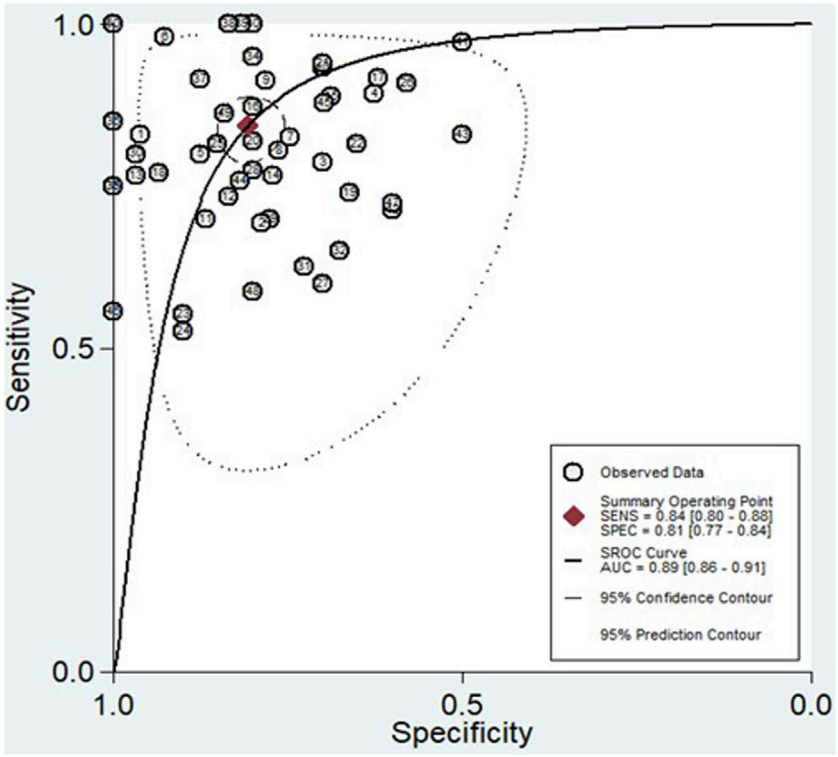

FIGURE 6
The SROC curve, accompanied by the 95% confidence contour and 95% prediction contour, provides a graphical representation of the overall diagnostic accuracy of miRNAs in distinguishing HCC.

Results

Study selection process

A total of 1,266 records were retrieved from various online databases such as PubMed, Scopus, Embase, ScienceDirect, and Wiley library. Initially, 351 duplicated studies were removed, followed by excluding 141 articles based on their publication year. Subsequently, 724 studies including irrelevant ones like reviews, conference proceedings, and commentaries were excluded after reviewing their titles and abstracts. Then, 50 full-text articles were thoroughly assessed against specific criteria, resulting in the exclusion of 26 studies for various reasons. Ultimately, after this rigorous process, 50 studies from 24 articles were deemed suitable and met the criteria for inclusion in the meta-analysis. The visual representation outlining our screening process can be found in Figure 1.

Characteristics, and quality assessment of included studies

Table 1 presents the fundamental characteristics of the literature encompassed in this analysis. The table includes data from 24 papers, which collectively involved 1,668 individuals diagnosed with HCC and 1,236 healthy individuals. These papers were published between 2018 and 2023, with thirteen originating from China (Xu L. et al., 2018; Lv et al., 2018; Chen and Wang, 2019; Han et al., 2019; Ning et al., 2019; Zhang et al., 2019; Cao and Wang, 2020; Wu et al., 2020; Zeng et al., 2020; Chen et al., 2021; Zhao et al., 2021; Fang et al., 2022; Wu et al., 2022), eight from Egypt (Shaheen et al., 2018; El Mahdy et al., 2019; Elmougy et al., 2019; Aly et al., 2020; Elhendawy et al., 2020; Wahb et al., 2021; Elfert et al., 2022; Youssef et al., 2022), one from India (Yousuf et al., 2022), one from Germany (Loosen et al., 2021), and one from Italy (Moshiri et al., 2018). In terms of sample types, eighteen studies utilized serum samples, while six studies used plasma samples for miRNA extraction. Methods for determining miRNA expression varied among the studies: one utilized next-generation sequencing, one used quantitative PCR, one employed droplet digital PCR, while the remaining twenty-two studies utilized quantitative real-time PCR. Regarding miRNA profiling, 44 studies reported on single miRNAs, while 6 studies focused on miRNAs panels. Among the findings, twenty studies reported an upregulation in miRNA expression, whereas twenty-four studies reported a downregulation.

The assessment of the 24 studies' quality was conducted using the QUADAS-2 tool. Given the significance of patient selection in experimental integrity, the data utilized in this meta-analysis predominantly originated from validated groups. Overall, the included studies exhibited satisfactory and qualifying methodological standards. Figure 2 provides a detailed breakdown of the quality assessment criteria.

Overall diagnostic accuracy of circulating miRNAs in diagnosing HCC

The presence of a threshold effect of heterogeneity was evaluated using both the Spearman correlation coefficient and the SROC

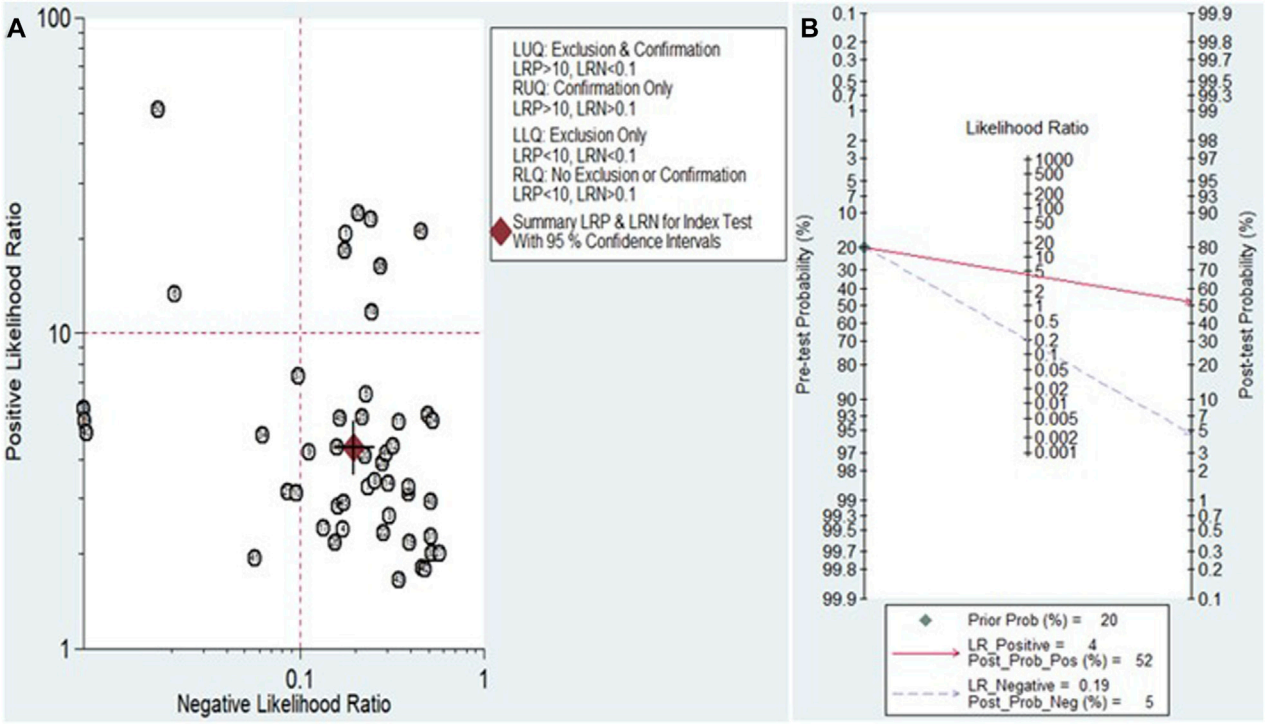

FIGURE 7
Assessment of the clinical applicability of miRNAs for the diagnosis of HCC. **(A)** Likelihood ratio scattergram visually represents the relationship between pre-test and post-test probabilities of HCC diagnosis based on miRNA test results. **(B)** Fagan's nomogram, a graphical tool for estimating the post-test probability of HCC given a specific pre-test probability and miRNA test result.

curve. The findings from the Spearman correlation coefficient (with a rho value of 0.15 and a *p*-value of 0.28) and the absence of the characteristic "shoulder-arm" shape in the SROC curve indicated that there is no evidence of a threshold effect of heterogeneity. In addition, the I^2 values for sensitivity, specificity, PLR, NLR, and DOR were 82.2%, 74.28%, 65.07%, 78.88%, and 100%, respectively. With I^2 results exceeding 50% and *p*-values for all parameters below 0.001, it strongly suggests the presence of substantial non-threshold effect heterogeneity in this study. Therefore, a random-effects model was employed for the meta-analysis.

The findings revealed that circulating miRNAs demonstrated strong diagnostic potential for detecting HCC. The combined sensitivity and specificity were 0.84 (95% CI: 0.80–0.88) and 0.81 (95% CI: 0.77–0.84), respectively (Figure 3). Additionally, the pooled PLR and NLR were 4.36 (95% CI: 3.59–5.30) and 0.19 (95% CI: 0.15–0.25), respectively (Figure 4). Furthermore, the DOR was 22.47 (95% CI: 14.47–32.64) (Figure 5). In assessing diagnostic accuracy, the SROC curve was generated, resulting in an AUC of 0.89 (95% CI: 0.86–0.91) (Figure 6). These results indicate that circulating miRNAs exhibit high diagnostic accuracy in identifying HCC, as an AUC greater than 0.7 is indicative of a strong predictive capability.

Clinical applicability of miRNAs for HCC diagnosis

The Fagan nomogram and likelihood ratio scattergram were used to evaluate the clinical value of miRNAs in HCC diagnosis. The Fagan's nomogram showed encouraging outcomes, revealing post-test probabilities of 0.52 and 0.5 for PLR and NLR respectively, under a pre-test probability set at 20% (Figure 7B). Furthermore, a scattergram depicting the likelihood ratios (PLR and NLR) was generated to assess the clinical utility of miRNAs in HCC diagnosis. The findings indicated that the studies conducted by Han et al. (miR-148a) (Han et al., 2019) and Moshiri et al. (miR-101-3p, miR-1246, and miR-106b-3p) (Moshiri et al., 2018) laid over on a left upper quadrant (PLR >10 and an NLR <0.1) (Figure 7A).

Subgroup analysis, meta-regression and sensitivity analysis

Because significant heterogeneity (I^2 > 50% and p < 0.05) was observed across all diagnostic performance parameters (including sensitivity, specificity, PLR, NLR, DOR, and AUC), meta-regression and subgroup analyses were performed. These analyses aimed to investigate the sources of heterogeneity among the studies by exploring various study characteristics. These characteristics encompass ethnicity, biological specimen, regulation mode, miRNA profiling, method of identification, internal reference, sample size, cut-off value establishment, and the classification of HCC patients.

In the subgroup analysis, plasma-derived miRNAs demonstrated superior diagnostic performance for HCC compared to serum-derived miRNAs. Plasma-derived miRNAs showed higher sensitivity (0.84, 95% CI: 0.75–0.90), specificity

10.3389/fmolb.2024.1353547

TABLE 2 Subgroup analysis of the diagnostic accuracy of miRNAs in HCC.

Subgroup	No of studies	Sen (95% CI)	Spe (95% CI)	PLR (95% CI)	NLR (95% CI)	DOR (95% CI)	AUC (95% CI)
Ethnicity							
Asian	28	0.83 (0.79, 0.87)	0.80 (0.75, 0.84)	4.1 (3.3, 5.2)	0.21 (0.17, 0.27)	20 (14, 28)	0.88 (0.85, 0.91)
Non-Asian	22	0.87 (0.78, 0.93)	0.82 (0.75, 0.88)	5.0 (3.3, 7.4)	0.15 (0.08, 0.28)	33 (15, 87)	0.91 (0.88, 0.93)
Specimen							
Serum	33	0.85 (0.80, 0.89)	0.79 (0.75, 0.82)	4.0 (3.3, 4.8)	0.19 (0.14, 0.26)	20 (14, 30)	0.87 (0.84, 0.90)
Plasma	17	0.84 (0.75, 0.90)	0.86 (0.76, 0.92)	6.0 (3.3, 11.0)	0.19 (0.12, 0.31)	32 (13, 79)	0.92 (0.89, 0.94)
Regulation mode							
Up	20	0.83 (0.74, 0.90)	0.80 (0.74, 0.85)	4.2 (3.2, 5.4)	0.21 (0.13, 0.32)	20 (12, 34)	0.88 (0.85, 0.91)
Down	24	0.84 (0.78, 0.88)	0.79 (0.73, 0.84)	4.0 (3.0, 5.4)	0.21 (0.15, 0.28)	20 (11, 34)	0.88 (0.84, 0.90)
miRNAs profile							
Single	44	0.84 (0.79, 0.88)	0.80 (0.75, 0.83)	4.1 (3.4, 5.0)	0.21 (0.16, 0.27)	20 (13, 29)	0.88 (0.85, 0.91)
Combination	6	0.88 (0.79, 0.94)	0.88 (0.76, 0.94)	7.1 (3.5, 14.6)	0.13 (0.07, 0.24)	53 (19, 144)	0.94 (0.92, 0.96)
References							
U6	15	0.82 (0.78, 0.86)	0.80 (0.74, 0.85)	4.1 (3.2, 5.4)	0.22 (0.18, 0.27)	19 (13, 27)	0.88 (0.85, 0.90)
Others	35	0.86 (0.79, 0.90)	0.81 (0.76, 0.85)	7.5 (3.5, 5.9)	0.18 (0.12, 0.26)	25 (15, 44)	0.89 (0.86, 0.92)
Methods							
qRT-PCR	41	0.85 (0.80, 0.89)	0.79 (0.75, 0.82)	4.0 (3.3, 4.8)	0.19 (0.14, 0.25)	21 (14, 31)	0.88 (0.85, 0.91)
Others	9	0.81 (0.68, 0.90)	0.95 (0.76, 0.99)	14.4 (2.9, 80.8)	0.20 (0.11, 0.36)	77 (11, 538)	0.93 (0.91, 0.95)
Sample size							
<100	30	0.79 (0.74, 0.84)	0.81 (0.75, 0.85)	4.1 (3.1, 5.3)	0.26 (0.20, 0.33)	16 (10, 24)	0.87 (0.83, 0.89)
≥100	20	0.90 (0.83, 0.94)	0.81 (0.75, 0.85)	4.7 (3.5, 6.2)	0.13 (0.08, 0.21)	37 (19, 71)	0.91 (0.88, 0.93)
Cut-off value							
Reported	32	0.85 (0.79, 0.90)	0.82 (0.77, 0.86)	4.7 (3.6, 6.2)	0.18 (0.12, 0.26)	26 (15, 44)	0.90 (0.87, 0.92)
Not reported	18	0.90 (0.83, 0.94)	0.81 (0.75, 0.85)	4.7 (3.5, 6.2)	0.13 (0.08, 0.21)	37 (19, 71)	0.91 (0.88, 0.93)
Participants							
Undefined HCC	38	0.83 (0.78, 0.86)	0.80 (0.75, 0.84)	4.2 (3.3, 5.3)	0.22 (0.17, 0.27)	19 (14, 28)	0.88 (0.85, 0.91)
HCV related HCC	9	0.93 (0.71, 0.99)	0.78 (0.73, 0.82)	4.2 (3.1, 5.6)	0.09 (0.02, 0.46)	48 (7, 317)	0.81 (0.78, 0.85)
HBV related HCC	3	-	-	-	-	-	-

(0.86, 95% CI: 0.76–0.92), PLR (6.0, 95% CI: 3.3–11.0), NLR (0.19, 95% CI: 0.12–0.31), DOR (32, 95% CI: 13–79), and AUC (0.92, 95% CI: 0.89–0.94) compared to serum-derived miRNAs (sensitivity: 0.85, 95% CI: 0.80–0.89; specificity: 0.79, 95% CI: 0.75–0.82; PLR: 4.0, 95% CI: 3.3–4.8; NLR: 0.19, 95% CI: 0.14–0.26; DOR: 20, 95% CI: 14–30; AUC: 0.87, 95% CI: 0.84–0.90). Furthermore, within the subgroups categorized by miRNA profiling, miRNA clusters exhibited higher accuracy in HCC detection compared to individual single miRNAs. MiRNA clusters displayed a sensitivity of 0.88 (95% CI: 0.79–0.94), specificity of 0.88 (95% CI: 0.76–0.94), PLR of 7.1 (95% CI: 3.5–14.6), NLR of 0.13 (95% CI: 0.07–0.24), DOR of 53 (95% CI: 19–144), and an AUC of 0.94 (95% CI: 0.92–0.96).

Regarding sample size, miRNAs demonstrated the highest overall diagnostic accuracy when the sample size was ≥100, with a sensitivity of 0.90 (95% CI: 0.83–0.94), specificity of 0.81 (95% CI: 0.75–0.85), PLR of 4.7 (95% CI: 3.5–6.2), NLR of 0.13 (95% CI: 0.08–0.21), DOR of 37 (95% CI: 19–71), and an AUC of 0.91 (95% CI: 0.88–0.93) compared to cases with a sample size <100. Additionally, miRNAs proved to be highly effective in diagnosing undefined HCC in comparison to HCV-related HCC. For undefined HCC, the diagnostic values were as follows: sensitivity of 0.83 (95% CI: 0.78–0.86), specificity of 0.80 (95% CI: 0.75–0.84), PLR of 4.2 (95% CI: 3.3–5.3), NLR of 0.22 (95% CI: 0.17–0.27), DOR of 19 (95% CI: 14–28), and an AUC of 0.88 (95% CI: 0.85–0.91) (Table 2).

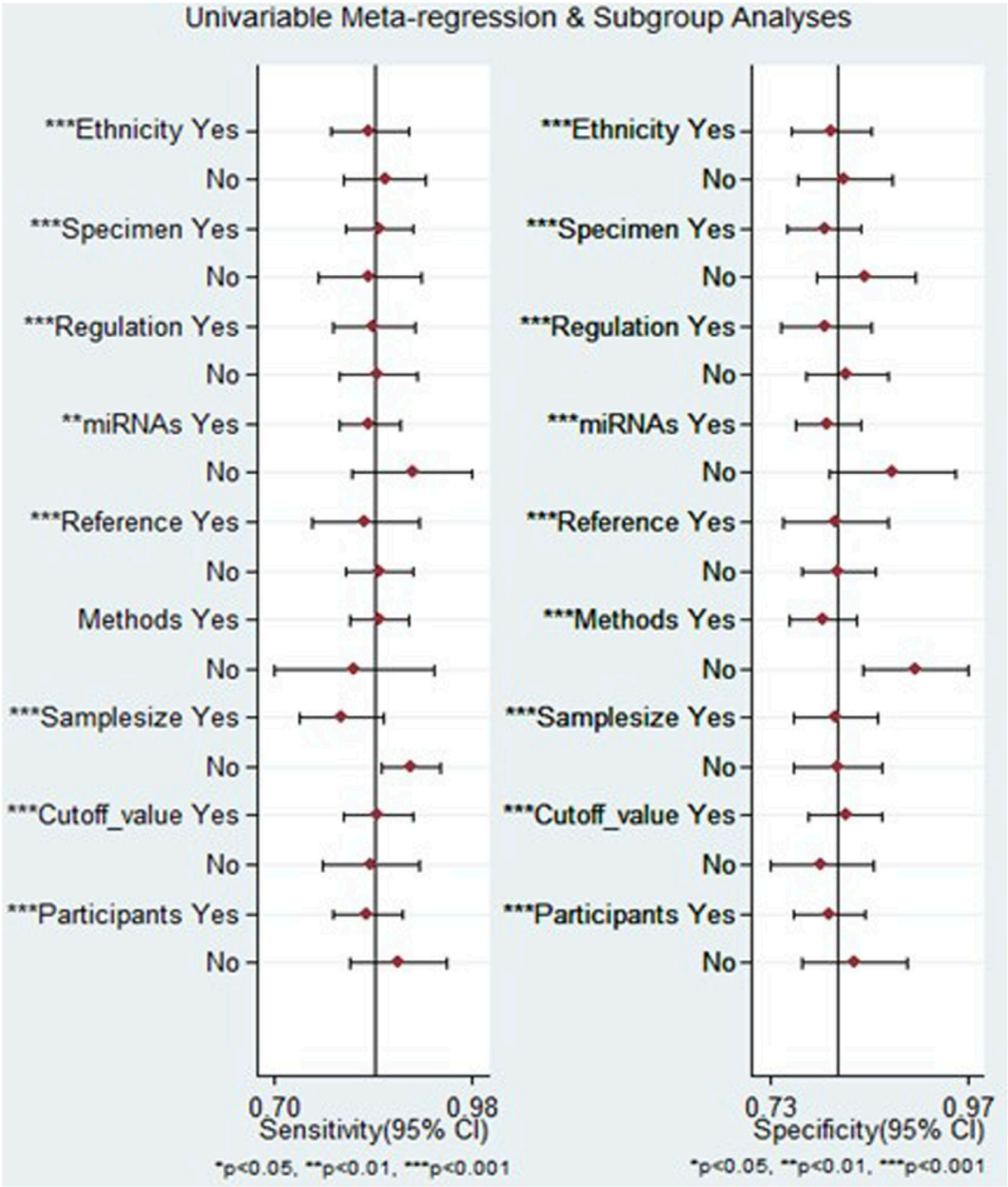

FIGURE 8
The results of meta-regression analysis examining the relationship between sensitivity and specificity of miRNA-based diagnostics for HCC, exploring potential sources of heterogeneity across included studies.

The outcomes of the meta-regression analysis revealed that for both sensitivity and specificity, sources of heterogeneity included ethnicity, biological specimen, regulation mode, miRNA profiling, internal reference, sample size, cut-off value determination, and the classification of HCC patients ($p < 0.05$). In contrast, the method of identification was identified as a source of heterogeneity specifically for specificity ($p < 0.05$) (Figure 8).

The sensitivity analysis can be observed in Figure 9A. Examination of goodness-of-fit and bivariate normality indicated the strength and reliability of the bivariate mixed-effects model for conducting meta-analysis (Figure 9A (a and b)). Moreover, the identification of outliers pointed to potential sources of heterogeneity in the form of two studies conducted by Xu et al. (miR-125b) and Elfert et al. (miR-122, miR-483, and miR-335)

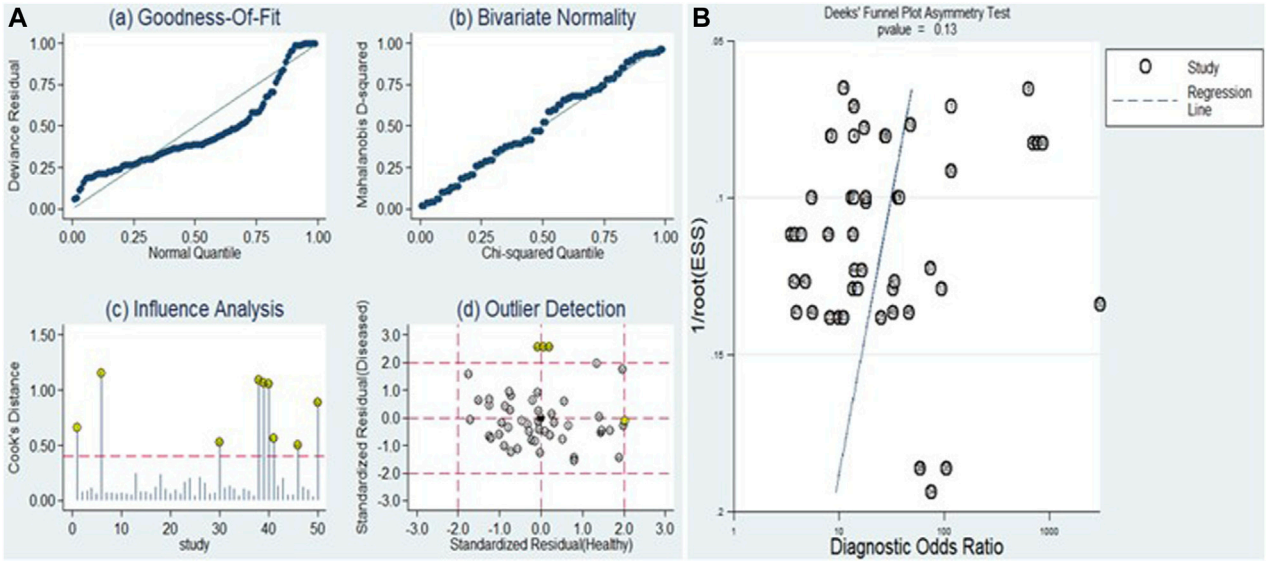

FIGURE 9
Sensitivity analysis and assessment of publication bias. **(A)** Sensitivity analysis evaluates the robustness of pooled estimates by examining the impact of various factors or assumptions on the overall findings. **(B)** Deek's funnel plot is used to detect publication bias by examining the relationship between study size and effect size estimates.

(Figure 9A (d)). Upon removing these outliers, we observed no substantial alterations in the overall sensitivity (0.82, 95% CI: 0.78–0.85), specificity (0.80, 95% CI: 0.76–0.84), PLR (4.1, 95% CI: 3.3–4.9), NLR (0.23, 95% CI: 0.19–0.28), DOR (18, 95% CI: 13–24), and AUC (0.88, 95% CI: 0.84–0.90). This suggests that the sensitivity of the studies included was consistently low, and the results became more resilient and trustworthy.

Publication bias

The Deeks' funnel plot asymmetry test was executed (Figure 9B) to evaluate the presence of publication bias. The resulting *p*-value of 0.13 indicates that there was no evidence of publication bias within the included studies.

Discussion

Hepatocellular carcinoma is a widespread cancer within the digestive system and stands as a primary contributor to global cancer-related fatalities. Challenges persist in detecting the disease at its early stages, coupled with the substantial risk of tumor recurrence and metastasis following surgery. Consequently, HCC continues to pose a significant threat to both human health and survival (Villanueva, 2019). The disease begins gradually and progresses slowly, resulting in atypical early clinical signs. A considerable number of individuals with HCC receive inadequate diagnoses until the disease reaches its mid-to-late stages, leading to the loss of the optimal treatment period (Yang and Heimbach, 2020). Current diagnostic methods for HCC, such as imaging techniques and serum biomarkers, often have limitations in terms of accuracy and invasiveness (Bialecki and Di Bisceglie, 2005). Therefore, there is an urgent need for the identification of non-invasive biomarkers for the detection of HCC.

MiRNAs exhibit resilience in circulation through the formation of inclusion bodies and exosomes, allowing for their extraction and examination from biological fluids like serum and stool samples (Valihrach et al., 2020). Disruption in their expression is a common occurrence in cancer (Shaker et al., 2022). This dysregulation leads to a distinct expression profile that is advantageous for early cancer detection. Specifically, miRNAs linked to tumor growth are often overexpressed, while suppressors are frequently under-expressed (Shaker et al., 2021). In recent years, the role of miRNAs in HCC has garnered increasing attention, attributed to their involvement in key signaling pathways implicated in hepatocarcinogenesis (Ruiz-Manriquez et al., 2022). These miRNAs play crucial roles in modulating various cellular processes integral to HCC pathogenesis, including cell proliferation, apoptosis, migration, invasion, angiogenesis, and drug resistance (Xu X. et al., 2018). Circulating miRNAs, protected from RNases, display notable stability (Cui et al., 2019). This stability persists even in challenging conditions such as boiling, extended storage, numerous freeze–thaw cycles, and exposure to extremely low or high pH (Drees and Pegtel, 2020). These characteristics suggest that miRNAs are widely distributed and hold promise for effective early detection of HCC (Shen et al., 2013). Consequently, this systematic review and meta-analysis aimed to assess the diagnostic accuracy of circulating miRNAs in detecting HCC.

In the present study, a total of 24 articles, involving 1,668 HCC patients and 1,236 healthy controls were included. The results indicate that the pooled sensitivity, specificity, PLR, NLR, DOR, and AUC of miRNAs in the diagnosis of HCC were 0.84 (95% CI: 0.80–0.88), 0.81 (95% CI: 0.77–0.84), 4.36 (95% CI: 3.59–5.30), 0.19

(95% CI: 0.15–0.25), 22.47 (95% CI: 14.47–32.64), and 0.89 (95% CI: 0.86–0.91), respectively. The PLR value of 4.3 suggests that the likelihood of a positive miRNA determination in patients with HCC is approximately 4.3 times higher compared to healthy controls. On the other hand, the NLR of 0.19 indicates that cases with negative test results have about a 19% chance of developing HCC. The DOR serves as an index indicating the discriminatory performance of a test (Glas et al., 2003), and a DOR value exceeding 1 signifies a superior diagnostic test. With a DOR of 22.47, the miRNA exhibits a substantial ability to effectively differentiate between HCC patients and healthy controls. Additionally, the AUC value is a valuable indicator for evaluating a system. An ideal test demonstrating perfect discrimination achieves an AUC of 1.0 (Nahm, 2022). As the AUC value approaches 1.0, the overall effectiveness of the test increases. In this study, miRNA emerges as a best tool for screening HCC patients compared to healthy controls, boasting an AUC value of 0.89, which is in close proximity to 1.0. This suggests that miRNAs possess a relatively high capability to distinguish between HCC patients and healthy controls.

In a meta-analysis conducted by Jiang et al., the effectiveness of miRNAs as diagnostic markers for HCC was explored. The reported diagnostic values of miRNAs are as follows: sensitivity of 0.84 (95% CI, 0.79–0.88), specificity of 0.87 (95% CI, 0.83–0.90), a DOR of 36 (95% CI: 20–64), and an AUC of 0.92 (95% CI, 0.90–0.94). These findings highlight the potential diagnostic value of miRNAs for individuals with HCC (Jiang et al., 2019). Discrepancies in certain pooled diagnostic values between our results and those of Jiang et al. could be attributed to variations in diagnostic criteria, demographic differences, adjustments in sample size, and differences in study design. Additionally, discrepancies may arise from variations in miRNA expression patterns, biological diversity, and temporal changes in the characteristics of HCC, all contributing to differences in the reported pooled diagnostic accuracy.

Due to the presence of heterogeneity among the included studies, subgroup analysis and meta-regression analysis were conducted to investigate potential confounding factors. Subgroup analysis indicated that plasma-derived miRNAs exhibited better diagnostic performance (AUC: 0.92) for HCC compared to serum-derived miRNAs (AUC: 0.87). Our findings align with those reported in a meta-analysis conducted by Wu et al. (Wu et al., 2023). Differences in miRNA concentration between serum and plasma can be attributed to various factors, including platelet contamination along with red and white blood cells (Wang et al., 2012), hemolysis (Kirschner et al., 2011), and the presence of qPCR inhibitors (Kaudewitz et al., 2013). Additionally, beyond sample contamination by miRNA from red blood cell rupture, the miRNA profile in serum and plasma may be influenced by platelet content or activation. Activated platelets are known to release miRNAs incorporated into microparticles or the effector protein Argonaute 2 (Ago2) (Laffont et al., 2013). In serum, platelet-derived miRNAs may be released during the coagulation process, and in the case of plasma, there might be residual contamination even after careful serial centrifugation to deplete platelet content (Binderup et al., 2018).

Furthermore, miRNA panels (AUC: 0.94) demonstrated superior accuracy in detecting HCC compared to single miRNAs (AUC: 0.88). This heightened accuracy could be attributed to the involvement of multiple gene mutations and epigenetic genetic abnormalities in the development of HCC (Stavast and Erkeland, 2019). Consequently, miRNA panels may emerge as more suitable diagnostic biomarkers for HCC, reflecting a future trend in development. Interestingly, our results revealed a significant difference in diagnostic ability between groups with a sample size of ≥100 (AUC: 0.91) and <100 (AUC: 0.87). Thus, validating these findings will necessitate large sample sizes and extensive studies.

The paramount value of biomarkers lies in their contribution to clinical decision-making. Likelihood ratios (Rubinstein et al., 2018) serve as valuable tools for clinicians, offering insights into the likelihood that a patient with a positive or negative test actually has HCC or not. In this study, we summarized PLR and NLR to assess the clinical applicability of miRNAs for diagnosing HCC. A PLR >10 and NLR <0.1 indicate high diagnostic accuracy. Our findings highlight that specific miRNA panels, including miR-101-3p, miR-1246, and miR-106b-3p from Moshiri et al.'s (Moshiri et al., 2018) study, and miRNA-148a from Han et al.'s (Han et al., 2019) study, exhibit high diagnostic accuracy and clinical applicability. These miRNAs exert profound effects on HCC pathogenesis, offering intricate correlations and multifaceted functions. MiRNA-148a emerges as a potent tumor suppressor within HCC, orchestrating anti-tumor activities such as inhibiting cell proliferation, inducing apoptosis, and impeding tumor growth (Babu and Muckenthaler, 2019). Its ability to counteract HCC metastasis through the inhibition of the epithelial-mesenchymal transition process and the suppression of the Wnt/β-catenin signaling pathway underscores its pivotal role in mitigating disease progression (Zhang et al., 2014). Similarly, miR-101-3p functions as a tumor suppressor, exerting inhibitory effects on HCC proliferation, metastasis, and stemness properties through the regulation of oncogenic pathways (Su et al., 2009). In contrast, miR-1246 and miR-106b-3p demonstrate oncogenic potential in HCC, promoting tumor progression by enhancing cell proliferation, migration, invasion, and metastasis (Yau et al., 2013; Chuma et al., 2019). Additionally, Fagan's nomogram reveals promising outcomes, with post-test probabilities of 0.52 and 0.5 for PLR and NLR, respectively, when the pre-test probability was set at 20%. This result suggests that when samples test positive for the presence of miRNAs, patients have a 52% probability of developing HCC. In contrast, the post-test probability of disease is reduced to 5% when the samples test negative for miRNAs. Consequently, miRNAs exhibit a certain diagnostic potential in distinguishing patients with HCC from healthy controls, making them a suitable screening method for HCC.

This meta-analysis has several strengths. It highlights those circulating miRNAs exhibit high diagnostic value in distinguishing healthy controls from patients with HCC, contributing valuable insights for the development of biomarkers in HCC diagnosis. Moreover, the inclusion of studies with high methodological quality minimizes the risk of bias, and the analysis encompasses a more comprehensive list of miRNAs. The incorporation of subgroup analysis and meta-regression analysis addresses the observed heterogeneity in the studies. However, certain limitations exist. Firstly, due to constraints in sample sizes and data within the included studies, the diagnostic efficacy of miRNA in different clinical stages and metastasis of HCC has not been thoroughly analyzed. Second, variations in cutoff values of miRNAs among the studies could contribute to heterogeneity.

Third, the lack of consensus on a unified internal reference may result in inconsistent results in miRNA relative quantitative analysis. Fifth, the representation of only some countries may limit the global applicability of miRNAs' diagnostic performance for HCC. Sixth, the relatively small sample size in each study may affect statistical power. Seventh, the absence of a large number of similar miRNAs for pooling results prevents the identification of specific single miRNA or miRNA panels as the optimal diagnostic biomarkers for HCC. Therefore, while these findings offer valuable insights, caution is warranted in interpretation. The results should be further validated through well-designed studies with larger sample sizes in the future to enhance their reliability and generalizability.

In conclusion, our findings highlight the robust diagnostic potential of circulating miRNAs in detecting HCC. With a combined sensitivity of 0.84 and specificity of 0.81, along with a pooled PLR of 4.36 and a NLR of 0.19, the DOR stood at 22.47. Evaluation of diagnostic accuracy via the SROC curve yielded an AUC of 0.89. These compelling results affirm that circulating miRNAs demonstrate high diagnostic accuracy in identifying HCC, as an AUC exceeding 0.7 signifies a robust predictive capability. Moreover, miRNA panels, plasma-derived miRNAs, and miRNAs analyzed in studies with a large sample size (≥100) demonstrate heightened diagnostic potency in HCC diagnosis. However, to validate and strengthen our findings, a comprehensive collection of prospective studies and multi-center research is essential in the near future.

Author contributions

EA: Conceptualization, Data curation, Formal Analysis, Investigation, Methodology, Software, Supervision, Validation, Writing–original draft, Writing–review and editing. AF: Data curation, Formal Analysis, Investigation, Methodology, Software, Validation, Writing–review and editing. HE: Data curation, Formal Analysis, Investigation, Methodology, Software, Validation, Writing–review and editing. ZM: Data curation, Formal Analysis, Investigation, Methodology, Software, Validation, Writing–review and editing. GB: Data curation, Formal Analysis, Investigation, Methodology, Software, Validation, Writing–review and editing. AG: Data curation, Formal Analysis, Investigation, Methodology, Software, Validation, Writing–review and editing. MT: Data curation, Formal Analysis, Investigation, Methodology, Software, Validation, Writing–review and editing. AW: Data curation, Formal Analysis, Investigation, Methodology, Software, Validation, Writing–review and editing. MB: Conceptualization, Data curation, Formal Analysis, Investigation, Methodology, Software, Supervision, Validation, Writing–original draft, Writing–review and editing.

Funding

The author(s) declare that no financial support was received for the research, authorship, and/or publication of this article.

Conflict of interest

The authors declare that the research was conducted in the absence of any commercial or financial relationships that could be construed as a potential conflict of interest.

Publisher's note

Supplementary material

The Supplementary Material for this article can be found online at: https://www.frontiersin.org/articles/10.3389/fmolb.2024.1353547/full#supplementary-material

References

Aly, D. M., Gohar, N. A.-H., Abd El-Hady, A. A., Khairy, M., and Abdullatif, M. M. (2020). Serum microRNA let-7a-1/let-7d/let-7f and miRNA 143/145 gene expression profiles as potential biomarkers in HCV induced hepatocellular carcinoma. *Asian Pac. J. cancer Prev. APJCP* 21 (2), 555–562. doi:10.31557/APJCP.2020.21.2.555

Armand-Labit, V., and Pradines, A. (2017). Circulating cell-free microRNAs as clinical cancer biomarkers. *Biomol. concepts* 8 (2), 61–81. doi:10.1515/bmc-2017-0002

Arnold, M., Abnet, C. C., Neale, R. E., Vignat, J., Giovannucci, E. L., McGlynn, K. A., et al. (2020). Global burden of 5 major types of gastrointestinal cancer. *Gastroenterology* 159 (1), 335–349. doi:10.1053/j.gastro.2020.02.068

Babu, K. R., and Muckenthaler, M. U. (2019). miR-148a regulates expression of the transferrin receptor 1 in hepatocellular carcinoma. *Sci. Rep.* 9 (1), 1518. doi:10.1038/s41598-018-35947-7

Bae, S. H. (2012). Changes of guidelines diagnosing hepatocellular carcinoma during the last ten-year period. *Clin. Mol. hepatology* 18 (3), 258–267. doi:10.3350/cmh.2012.18.3.258

Bialecki, E. S., and Di Bisceglie, A. M. (2005). Diagnosis of hepatocellular carcinoma. *Hpb* 7 (1), 26–34. doi:10.1080/13651820410024049

Binderup, H. G., Madsen, J. S., Heegaard, N. H. H., Houlind, K., Andersen, R. F., and Brasen, C. L. (2018). Quantification of microRNA levels in plasma–impact of preanalytical and analytical conditions. *PloS one* 13 (7), e0201069. doi:10.1371/journal.pone.0201069

Cao, C., and Wang, C. (2020). Clinical significance of serum miR-768-3p in HBV-related hepatocellular carcinoma and its potential mechanism. *Clin. Exp. Med.* 20 (4), 569–576. doi:10.1007/s10238-020-00646-z

Chen, S., Fu, Z., Wen, S., Yang, X., Yu, C., Zhou, W., et al. (2021). Expression and diagnostic value of miR-497 and miR-1246 in hepatocellular carcinoma. *Front. Genet.* 12, 666306. doi:10.3389/fgene.2021.666306

Chen, X., and Wang, A. (2019). Clinical significance of miR-195 in hepatocellular carcinoma and its biological function in tumor progression. *OncoTargets Ther.* 12, 527–534. doi:10.2147/OTT.S190108

Chuma, M., Toyoda, H., Matsuzaki, J., Saito, Y., Kumada, T., Tada, T., et al. (2019). Circulating microRNA-1246 as a possible biomarker for early tumor recurrence of hepatocellular carcinoma. *Hepatology Res.* 49 (7), 810–822. doi:10.1111/hepr.13338

Cui, M., Wang, H., Yao, X., Zhang, D., Xie, Y., Cui, R., et al. (2019). Circulating microRNAs in cancer: potential and challenge. *Front. Genet.* 10, 626. doi:10.3389/fgene.2019.00626

Drees, E. E., and Pegtel, D. M. (2020). Circulating miRNAs as biomarkers in aggressive B cell lymphomas. *Trends cancer* 6 (11), 910–923. doi:10.1016/j.trecan.2020.06.003

Elfert, A. Y., Salem, A., Abdelhamid, A. M., Salama, A., Sourour, D. A., Shaker, O., et al. (2022). Implication of miR-122, miR-483, and miR-335 expression levels as potential signatures in HCV-related hepatocellular carcinoma (HCC) in Egyptian patients. *Front. Mol. Biosci.* 9, 864839. doi:10.3389/fmolb.2022.864839

Elhendawy, M., Abdul-Baki, E. A., Abd-Elsalam, S., Hagras, M. M., Zidan, A.-A., Abdel-Naby, A. Y., et al. (2020). MicroRNA signature in hepatocellular carcinoma patients: identification of potential markers. *Mol. Biol. Rep.* 47, 4945–4953. doi:10.1007/s11033-020-05521-4

El Mahdy, H. A., Abdelhamid, I. A., Amen, A. I., Abdelsameea, E., and Hassouna, M. M. (2019). MicroRNA-215 as a diagnostic marker in Egyptian patients with hepatocellular carcinoma. *Asian Pac. J. cancer Prev.* 20 (9), 2723–2731. doi:10.31557/APJCP.2019.20.9.2723

Elmougy, F. A. F., Mohamed, R. A., Hassan, M. M., Elsheikh, S. M., Marzban, R. N., Fatma-elzahraa, M. A., et al. (2019). Study of serum microRNA19a and microRNA223 as potential biomarkers for early diagnosis of hepatitis C virus-related hepatocellular carcinoma. *Gene Rep.* 15, 100398. doi:10.1016/j.genrep.2019.100398

European Association for the Study of the LiverEuropean Organisation For Research And Treatment Of Cancer (2012). EASL–EORTC clinical practice guidelines: management of hepatocellular carcinoma. *J. hepatology* 56 (4), 908–943. doi:10.1016/j.jhep.2011.12.001

Fang, Y., Yan, D., Wang, L., Zhang, J., and He, Q. (2022). Circulating microRNAs (miR-16, miR-22, miR-122) expression and early diagnosis of hepatocellular carcinoma. *J. Clin. Laboratory Analysis* 36 (7), e24541. doi:10.1002/jcla.24541

Freeman, K., Mistry, H., Tsertsvadze, A., Royle, P., McCarthy, N., Taylor-Phillips, S., et al. (2017). "Quality Assessment of Diagnostic Accuracy Studies-2 quality appraisal tool and guidance notes," in *Multiplex tests to identify gastrointestinal bacteria, viruses and parasites in people with suspected infectious gastroenteritis: a systematic review and economic analysis* (Southampton (UK): NIHR Journals Library).

Frenette, C. T., Isaacson, A. J., Bargellini, I., Saab, S., and Singal, A. G. (2019). A practical guideline for hepatocellular carcinoma screening in patients at risk. *Mayo Clin. Proc. Innovations, Qual. Outcomes* 3 (3), 302–310. doi:10.1016/j.mayocpiqo.2019.04.005

Glas, A. S., Lijmer, J. G., Prins, M. H., Bonsel, G. J., and Bossuyt, P. M. (2003). The diagnostic odds ratio: a single indicator of test performance. *J. Clin. Epidemiol.* 56 (11), 1129–1135. doi:10.1016/s0895-4356(03)00177-x

Gramantieri, L., Giovannini, C., Piscaglia, F., and Fornari, F. (2021). MicroRNAs as modulators of tumor metabolism, microenvironment, and immune response in hepatocellular carcinoma. *J. Hepatocell. Carcinoma* 8, 369–385. doi:10.2147/JHC.S268292

Guan, M.-C., Wang, M.-D., Liu, S.-Y., Ouyang, W., Liang, L., Pawlik, T. M., et al. (2021). Early diagnosis and therapeutic strategies for hepatocellular carcinoma: from bench to bedside. *World J. Gastrointest. Oncol.* 13 (4), 197–215. doi:10.4251/wjgo.v13.i4.197

Han, J., Li, J., Qian, Y., Liu, W., Liang, J., Huang, Z., et al. (2019). Identification of plasma miR-148a as a noninvasive biomarker for hepatocellular carcinoma. *Clin. Res. Hepatology Gastroenterology* 43 (5), 585–593. doi:10.1016/j.clinre.2018.12.008

Higgins, J. P., Thompson, S. G., Deeks, J. J., and Altman, D. G. (2003). Measuring inconsistency in meta-analyses. *Bmj* 327 (7414), 557–560. doi:10.1136/bmj.327.7414.557

Jackson, D., White, I. R., and Thompson, S. G. (2010). Extending DerSimonian and Laird's methodology to perform multivariate random effects meta-analyses. *Statistics Med.* 29 (12), 1282–1297. doi:10.1002/sim.3602

Jiang, Y., He, J., Li, Y., Guo, Y., and Tao, H. (2019). The diagnostic value of MicroRNAs as a biomarker for hepatocellular carcinoma: a meta-analysis. *BioMed Res. Int.* 2019, 5179048. doi:10.1155/2019/5179048

Jin, Y., Wong, Y. S., Goh, B. K., Chan, C. Y., Cheow, P. C., Chow, P. K., et al. (2019). Circulating microRNAs as potential diagnostic and prognostic biomarkers in hepatocellular carcinoma. *Sci. Rep.* 9 (1), 10464. doi:10.1038/s41598-019-46872-8

Kaudewitz, D., Lee, R., Willeit, P., McGregor, R., Markus, H. S., Kiechl, S., et al. (2013). Impact of intravenous heparin on quantification of circulating microRNAs in patients with coronary artery disease. *Thrombosis haemostasis* 110 (09), 609–615. doi:10.1160/TH13-05-0368

Kim, T., and Croce, C. M. (2023). MicroRNA: trends in clinical trials of cancer diagnosis and therapy strategies. *Exp. Mol. Med.* 55 (7), 1314–1321. doi:10.1038/s12276-023-01050-9

Kirschner, M. B., Kao, S. C., Edelman, J. J., Armstrong, N. J., Vallely, M. P., van Zandwijk, N., et al. (2011). Haemolysis during sample preparation alters microRNA content of plasma. *PloS one* 6 (9), e24145. doi:10.1371/journal.pone.0024145

Laffont, B., Corduan, A., Plé, H., Duchez, A.-C., Cloutier, N., Boilard, E., et al. (2013). Activated platelets can deliver mRNA regulatory Ago2● microRNA complexes to endothelial cells via microparticles. *Blood, J. Am. Soc. Hematol.* 122 (2), 253–261. doi:10.1182/blood-2013-03-492801

Loosen, S. H., Castoldi, M., Jördens, M. S., Roy, S., Vucur, M., Kandler, J., et al. (2021). Serum levels of circulating microRNA-107 are elevated in patients with early-stage HCC. *Plos one* 16 (3), e0247917. doi:10.1371/journal.pone.0247917

Lv, Y., and Sun, X. (2023) Role of miRNA in pathogenesis, diagnosis, and prognosis in hepatocellular carcinoma. *Chem Biol Drug Des.* 103 (1), e14352. doi:10.1111/cbdd.14352

Lv, Z., Tao, Y., Cai, X., Zhou, X., and Li, Y. (2018). Cluster of specified microRNAs in tissues and serum as biomarkers for early diagnosis of hepatocellular carcinoma. *Int. J. Clin. Exp. Pathology* 11 (2), 990–997.

Martins-Filho, S. N., and Alves, V. A. F. (2019). The strengths and weaknesses of gross and histopathological evaluation in hepatocellular carcinoma: a brief review. *Surg. Exp. Pathology* 2, 23–12. doi:10.1186/s42047-019-0047-6

Moshiri, F., Salvi, A., Gramantieri, L., Sangiovanni, A., Guerriero, P., De Petro, G., et al. (2018). Circulating miR-106b-3p, miR-101-3p and miR-1246 as diagnostic biomarkers of hepatocellular carcinoma. *Oncotarget* 9 (20), 15350–15364. doi:10.18632/oncotarget.24601

Nahm, F. S. (2022). Receiver operating characteristic curve: overview and practical use for clinicians. *Korean J. Anesthesiol.* 75 (1), 25–36. doi:10.4097/kja.21209

Ning, S., Liu, H., Gao, B., Wei, W., Yang, A., Li, J., et al. (2019). miR-155, miR-96 and miR-99a as potential diagnostic and prognostic tools for the clinical management of hepatocellular carcinoma. *Oncol. Lett.* 18 (3), 3381–3387. doi:10.3892/ol.2019.10606

Page, M. J., McKenzie, J. E., Bossuyt, P. M., Boutron, I., Hoffmann, T. C., Mulrow, C. D., et al. (2021). The PRISMA 2020 statement: an updated guideline for reporting systematic reviews. *Int. J. Surg.* 88, 105906. doi:10.1016/j.ijsu.2021.105906

Parra, N. S., Ross, H. M., Khan, A., Wu, M., Goldberg, R., Shah, L., et al. (2023). Advancements in the diagnosis of hepatocellular carcinoma. *Int. J. Transl. Med.* 3 (1), 51–65. doi:10.3390/ijtm3010005

Rubinstein, M. L., Kraft, C. S., and Parrott, J. S. (2018). Determining qualitative effect size ratings using a likelihood ratio scatter matrix in diagnostic test accuracy systematic reviews. *Diagnosis* 5 (4), 205–214. doi:10.1515/dx-2018-0061

Ruiz-Manriquez, L. M., Carrasco-Morales, O., Sanchez, Z. E. A., Osorio-Perez, S. M., Estrada-Meza, C., Pathak, S., et al. (2022). MicroRNA-mediated regulation of key signaling pathways in hepatocellular carcinoma: a mechanistic insight. *Front. Genet.* 13, 910733. doi:10.3389/fgene.2022.910733

Rumgay, H., Arnold, M., Ferlay, J., Lesi, O., Cabasag, C. J., Vignat, J., et al. (2022). Global burden of primary liver cancer in 2020 and predictions to 2040. *J. Hepatology* 77 (6), 1598–1606. doi:10.1016/j.jhep.2022.08.021

Shaheen, N. M. H., Zayed, N., Riad, N. M., Tamim, H. H., Shahin, R. M. H., Labib, D. A., et al. (2018). Role of circulating miR-182 and miR-150 as biomarkers for cirrhosis and hepatocellular carcinoma post HCV infection in Egyptian patients. *Virus Res.* 255, 77–84. doi:10.1016/j.virusres.2018.07.004

Shaker, O., Ayeldeen, G., and Abdelhamid, A. (2021). The impact of single nucleotide polymorphism in the long non-coding MEG3 gene on microRNA-182 and microRNA-29 expression levels in the development of breast cancer in Egyptian women. *Front. Genet.* 12, 683809. doi:10.3389/fgene.2021.683809

Shaker, O. G., Ayeldeen, G., and Abdelhamid, A. M. (2022). Circulating microRNA-944 and its target gene EPHA7 as a potential biomarker for colorectal cancer. *Archives Physiology Biochem.* 128 (5), 1181–1187. doi:10.1080/13813455.2020.1762658

Shen, J., Wang, A., Wang, Q., Gurvich, I., Siegel, A. B., Remotti, H., et al. (2013). Exploration of genome-wide circulating microRNA in hepatocellular carcinoma: MiR-483-5p as a potential biomarker. *Cancer Epidemiol. biomarkers Prev.* 22 (12), 2364–2373. doi:10.1158/1055-9965.EPI-13-0237

Sherman, M. (2014). Limitations of screening for hepatocellular carcinoma. *Hepatic Oncol.* 1 (2), 161–163. doi:10.2217/hep.13.22

Singal, A. G., Kanwal, F., and Llovet, J. M. (2023). Global trends in hepatocellular carcinoma epidemiology: implications for screening, prevention and therapy. *Nat. Rev. Clin. Oncol.* 20, 864–884. doi:10.1038/s41571-023-00825-3

Stavast, C. J., and Erkeland, S. J. (2019). The non-canonical aspects of microRNAs: many roads to gene regulation. *Cells* 8 (11), 1465. doi:10.3390/cells8111465

Su, H., Yang, J.-R., Xu, T., Huang, J., Xu, L., Yuan, Y., et al. (2009). MicroRNA-101, down-regulated in hepatocellular carcinoma, promotes apoptosis and suppresses tumorigenicity. *Cancer Res.* 69 (3), 1135–1142. doi:10.1158/0008-5472.CAN-08-2886

Sung, H., Ferlay, J., Siegel, R. L., Laversanne, M., Soerjomataram, I., Jemal, A., et al. (2021). Global cancer statistics 2020: GLOBOCAN estimates of incidence and mortality worldwide for 36 cancers in 185 countries. *CA a cancer J. Clin.* 71 (3), 209–249. doi:10.3322/caac.21660

Valihrach, L., Androvic, P., and Kubista, M. (2020). Circulating miRNA analysis for cancer diagnostics and therapy. *Mol. Aspects Med.* 72, 100825. doi:10.1016/j.mam.2019.10.002

Villanueva, A. (2019). Hepatocellular carcinoma. *N. Engl. J. Med.* 380, 1450–1462. doi:10.1056/NEJMra1713263

Wahb, AMSE, El Kassas, M., Khamis, A. K., Elhelbawy, M., Elhelbawy, N., and Habieb, M. S. E. (2021). Circulating microRNA 9-3p and serum endocan as potential biomarkers for hepatitis C virus-related hepatocellular carcinoma. *World J. Hepatology* 13 (11), 1753–1765. doi:10.4254/wjh.v13.i11.1753

Wang, K., Yuan, Y., Cho, J.-H., McClarty, S., Baxter, D., and Galas, D. J. (2012) *Comparing the MicroRNA spectrum between serum and plasma*.

World Health Organization (2020) *Projections of mortality and causes of death, 2016 to 2060*.

Wu, J., Wu, Y., Luo, Y., Li, X., Lin, N., Yang, X., et al. (2020). Circulating miRNA-199a and miRNA-122 levels as potential diagnostic and prognostic biomarkers for hepatocellular carcinoma. *Ann. Clin. Laboratory Sci.* 50 (2), 219–227.

Wu, N., Sun, H., Sun, Q., Zhang, F., Ma, L., Hu, Y., et al. (2023). Circulating microRNAs as diagnostic biomarkers for melanoma: a systematic review and meta-analysis. *BMC cancer* 23 (1), 414–14. doi:10.1186/s12885-023-10891-6

Wu, X., Wan, R., Ren, L., Yang, Y., Ding, Y., and Wang, W. (2022). Circulating MicroRNA panel as a diagnostic marker for hepatocellular carcinoma. *Turkish J. Gastroenterology* 33 (10), 844–851. doi:10.5152/tjg.2022.21183

Xu, L., Wei, B., Hui, H., and Liu, Y. (2018a). Association of serum microRNA-125b and HBV-related hepatocellular carcinoma in Chinese Han patients. *Int. J. Clin. Exp. Med.* 11 (4), 3699–3703.

Xu, X., Tao, Y., Shan, L., Chen, R., Jiang, H., Qian, Z., et al. (2018b). The role of MicroRNAs in hepatocellular carcinoma. *J. Cancer* 9 (19), 3557–3569. doi:10.7150/jca.26350

Yang, J. D., and Heimbach, J. K. (2020). New advances in the diagnosis and management of hepatocellular carcinoma. *Bmj* 371, m3544. doi:10.1136/bmj.m3544

Yau, W. L., Lam, C. S. C., Ng, L., Chow, A. K. M., Chan, S. T. C., Chan, J. Y. K., et al. (2013). Over-expression of miR-106b promotes cell migration and metastasis in hepatocellular carcinoma by activating epithelial-mesenchymal transition process. *PloS one* 8 (3), e57882. doi:10.1371/journal.pone.0057882

Youssef, S. S., Elfiky, A., Nabeel, M. M., Shousha, H. I., Elbaz, T., Omran, D., et al. (2022). Assessment of circulating levels of microRNA-326, microRNA-424, and microRNA-511 as biomarkers for hepatocellular carcinoma in Egyptians. *World J. Hepatology* 14 (8), 1562–1575. doi:10.4254/wjh.v14.i8.1562

Yousuf, T., Dar, S. B., Bangri, S. A., Choh, N. A., Rasool, Z., Shah, A., et al. (2022). Diagnostic implication of a circulating serum-based three-microRNA signature in hepatocellular carcinoma. *Front. Genet.* 13, 929787. doi:10.3389/fgene.2022.929787

Zeng, Z., Dong, J., Li, Y., Dong, Z., Liu, Z., Huang, J., et al. (2020). The expression level and diagnostic value of microRNA-22 in HCC patients. *Artif. cells, nanomedicine, Biotechnol.* 48 (1), 683–686. doi:10.1080/21691401.2019.1703723

Zhang, J., Zeng, C., Xu, L., Gong, J., Fang, J., and Zhuang, S. (2014). MicroRNA-148a suppresses the epithelial–mesenchymal transition and metastasis of hepatoma cells by targeting Met/Snail signaling. *Oncogene* 33 (31), 4069–4076. doi:10.1038/onc.2013.369

Zhang, N., Hu, Z., Qiang, Y., and Zhu, X. (2019). Circulating miR-130b-and miR-21-based diagnostic markers and therapeutic targets for hepatocellular carcinoma. *Mol. Genet. genomic Med.* 7 (12), e1012. doi:10.1002/mgg3.1012

Zhao, L., Yang, Q., and Liu, J. (2021). Clinical value evaluation of microRNA-324-3p and other available biomarkers in patients with HBV infection-related hepatocellular carcinoma. *Open Forum Infect. Dis.* 8 (6), ofab108. doi:10.1093/ofid/ofab108

frontiers | Frontiers in Molecular Biosciences

TYPE Review
PUBLISHED 06 August 2024
DOI 10.3389/fmolb.2024.1423470

OPEN ACCESS

EDITED BY
Carmela De Marco,
Magna Græcia University of Catanzaro, Italy

REVIEWED BY
Claudia Veneziano,
Magna Græcia University, Italy
Yunfan Fan,
Bristol Myers Squibb, United States

*CORRESPONDENCE
Tamires Ferreira da Silva,
ferreiradasilvatamires81@gmail.com
Danielle Queiroz Calcagno,
danicalcagno@gmail.com

RECEIVED 25 April 2024
ACCEPTED 11 July 2024
PUBLISHED 06 August 2024

CITATION
Silva TFd, Azevedo JCd Jr, Teixeira EB, Casseb SMM, Moreira FC, Assumpção PPd, Santos SEBd and Calcagno DQ (2024), From haystack to high precision: advanced sequencing methods to unraveling circulating tumor DNA mutations.
Front. Mol. Biosci. 11:1423470.
doi: 10.3389/fmolb.2024.1423470

From haystack to high precision: advanced sequencing methods to unraveling circulating tumor DNA mutations

Tamires Ferreira da Silva[1,2]*, Juscelino Carvalho de Azevedo Jr[1,2], Eliel Barbosa Teixeira[2], Samir Mansour Moraes Casseb[2], Fabiano Cordeiro Moreira[2], Paulo Pimentel de Assumpção[2], Sidney Emanuel Batista dos Santos[2] and Danielle Queiroz Calcagno[1,2]*

[1]Programa de Residência Multiprofissional em Saúde (Oncologia), Hospital Universitário João de Barros Barreto, Universidade Federal do Pará, Belém, Brazil, [2]Núcleo de Pesquisas em Oncologia, Universidade Federal do Pará, Belém, Brazil

Identifying mutations in cancer-associated genes to guide patient treatments is essential for precision medicine. Circulating tumor DNA (ctDNA) offers valuable insights for early cancer detection, treatment assessment, and surveillance. However, a key issue in ctDNA analysis from the bloodstream is the choice of a technique with adequate sensitivity to identify low frequent molecular changes. Next-generation sequencing (NGS) technology, evolving from parallel to long-read capabilities, enhances ctDNA mutation analysis. In the present review, we describe different NGS approaches for identifying ctDNA mutation, discussing challenges to standardized methodologies, cost, specificity, clinical context, and bioinformatics expertise for optimal NGS application.

KEYWORDS

precision medicine, ctDNA mutation, non-targeted next-generation sequencing, targeted next-generation sequencing, bioinformatics

Background

Cancer is a multifaceted and constantly evolving disease, which has a progression of genetically distinct clones that guide its course (Lomakin et al., 2022). In the era of precision medicine, the identification of mutations within cancer-associated genes assumes paramount significance, as it serves as a compass guiding the therapeutic journey for patients (Malone et al., 2020).

As a groundbreaking stride, liquid biopsies have risen as a complementary approach to traditional tissue biopsies, offering molecular insights into tumors that can revolutionize early cancer detection, patient stratification, treatment efficacy assessment, and post-treatment vigilance. Unlike tissue biopsies, this minimally invasive approach stands out for its increased uniformity, mitigating sampling bias across diverse tumor regions (Martins et al., 2021). Central to this methodology are mainly circulating tumor DNA (ctDNA) and circulating tumor cells (CTCs) (Jiang et al., 2021).

In particular, ctDNA corresponds to DNA fragments at about 160–200 base pairs (bp) that contain tumor-specific mutations which potentially represent the real-time status of the

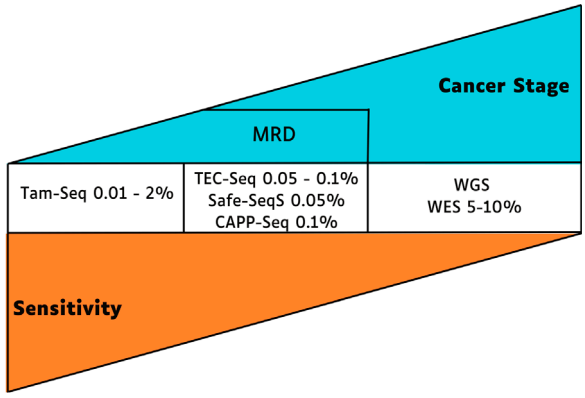

FIGURE 1
Sensitivity and applicability of techniques for identifying ctDNA mutations, the early stage of cancer requires more sensitive next-generation sequencing techniques to detect mutations in ctDNA. MRD, minimal residual disease; TEC-Seq, Targeted error correction sequencing; Safe-SeqS, Safe-Sequencing System; CAPP-Seq, Cancer Personalized Profiling by Deep Sequencing; WGS, Whole-Genome Sequencing; WES, Whole Exome Sequencing.

tumor genome (Chen and Zhao, 2019; Noguchi et al., 2020; Yu et al., 2022). Consequently, the assessment of ctDNA at specific time points—such as the clinical management and the detection of minimal residual disease (MRD)—has emerged as a pivotal factor in prognostication for a multitude of cancer types, encompassing breast cancer, colorectal cancer and leukemia (Parikh et al., 2021; Fürstenau et al., 2022; Turner et al., 2023).

The ctDNA concentrations represent about 0.01% of cell-free DNA (cfDNA); these low percentages lead to challenges in acquiring enough quality material for detection, especially at the early stages of tumor development (Huerta et al., 2021). According to individual tumor features, a specific analysis methodology is required, and the technique's sensitivity for identifying ctDNA mutations is inversely proportional to the tumor stage (Elazezy and Joosse, 2018; Oliveira et al., 2020; Sanz-Garcia et al., 2022) (Figure 1).

In 2016, the U.S. Food and Drug Administration (FDA) and the European Medicines Agency approved the first ctDNA-based test to prescribe *EGFR* inhibitors in patients with non-small cell lung cancer (NSCLC) - Cobas *EGFR* mutation test v2 (Kwapisz, 2017; U.S Food and Drug Administration, 2022; U.S Food and Drug Administration, 2023). This ctDNA *EGFR* mutation testing leads to cost reductions and enables more effective treatment, resulting in a positive economic impact. Table 1 shows other current ctDNA tests approved for application in the clinical management of different cancer types.

Advances in next-generation sequencing (NGS) technology and a large demand for ctDNA mutation analysis to support clinical studies have facilitated the emergence of sequencing assays covering cancer-related genes (Yu et al., 2022). Because it is rare, detection of mutations in ctDNA can be challenging, even with the increased feasibility of its analysis through NGS, which can present error rates of 0.1%–1% depending on the platform used (Glenn, 2011).

Currently, sequencing technologies have two distinct approaches with different methods and applications. The non-targeted sequencing often provides an overview of the entire genome and captures coding and non-coding regions. Also, it enables new genetic discovery without previous knowledge (Bagger et al., 2024). Conversely, targeted sequencing focuses on specific genes or regions of interest previously known, which participate in biological processes and diseases (Figure 2) (Singh, 2022).

Recently, long-read sequencers, known as third-generation sequencing (TGS), have emerged to surpass NGS technologies. This approach allows the reading of single DNA molecules in real time without the need for prior PCR amplification steps, offering high precision and speed. Furthermore, TGS is capable of detecting epigenetic modifications, and its rapid results make it attractive for disease diagnosis, particularly in precision oncology (Ling et al., 2023; Scarano et al., 2024).

In the present study, we described NGS and TGS approaches and discussed standardized methodologies and challenges for the identification of ctDNA mutation. Additionally, we explore cost-effectiveness, specificity, clinical utility, and bioinformatic implications for optimal NGS application in ctDNA analysis from cancer patients.

Next-generation sequencing

The NGS technology has revolutionized the field of genomics by enabling rapid and affordable large-scale DNA and RNA sequencing. This methodology is based on analyzing several millions of short DNA fragments in parallel, followed by either sequence alignment to a reference genome or *de novo* sequence assembly (Lin et al., 2021). Therefore, this technology can be useful for real-time monitoring of tumor progression through detection with high accuracy of genetic status from primary and metastatic tumors (Hess et al., 2020).

Usually, library preparation is a critical step that precedes sequencing and varies according to study type and available financial resources. This process consists of ensuring genetic material is appropriate to be sequenced by high-throughput sequencing platforms and may include separation of large fragments, recovery of small fragments through probes, repair of DNA ends, connector connection, and addition of a special connector from the sequencing kit (Liang et al., 2020; Bohers et al., 2021). A technological advance within library preparation is the use of molecular barcoding by inserting random sequences prior to PCR amplification to obtain counts of original DNA molecules without unbiased results and with increased sensitivity (Bohers et al., 2021; Szadkowska et al., 2022).

In ctDNA, the identification of mutations is challenging due to its representation of a small fraction of cfDNA and the need for high levels of plasma DNA for analysis (Dang and Park, 2022). However, the various NGS tools offer potential applicability, specificity, sensitivity and low input, making them invaluable in ctDNA research (Elazezy and Joosse, 2018). This includes non-targeted (Diefenbach et al., 2019; Ganesamoorthy et al., 2022) and targeted approaches (Phallen et al., 2017; Elazezy and Joosse, 2018; Gale et al., 2018; Peng et al., 2019; Zhao et al., 2020; Kato et al., 2021; Hallermayr et al., 2022) (Table 2).

10.3389/fmolb.2024.1423470

TABLE 1 FDA approved tests for identifying mutations used in liquid biopsy.

Year	Name test	Technology	Company	Biomarker	Molecular alteration	Cancer
2016	cobas® EGFR Mutation Test v2	real-time PCR	Roche Molecular Systems, Inc	*EGFR*	42 *EGFR* mutations in exons 18, 19, 20, and 21	NSCLC
2019	Therascreen PIK3CA RGQ PCR Kit	real-time PCR	QIAGEN GmbH	*PIK3CA*	11 mutations in exons 7, 9, and 20	Breast Cancer
2020	FoundationOne® Liquid CDx	NGS	Foundation Medicine, Inc	*PIK3CA*	*PIK3CA* mutations C420R, E542K, E545A, E545D [1635G>T only], E545G, E545K, Q546E, Q546R; and H1047L, H1047R, and H1047Y	Breast Cancer
				BRCA1, BRCA2, ATM.	*BRCA1, BRCA2, ATM* alterations	Prostate Cancer
				BRCA1, BRCA2	*BRCA1, BRCA2* alterations	Ovarian Cancer
				MET, EGFR, ALK.	*ALK, EGFR, MET*	NSCLC
2022	Agilent Resolution ctDx FIRST assay	NGS	Resolution Bioscience, Inc	*KRAS*	*KRAS* G12C	NSCLC
				EGFR	Single nucleotide variants (SNVs) and deletions	
2023	Guardant 360 CDx	NGS	Guardant Health	*ERS1*	*ESR1* missense mutations between codons 310–547	Breast Cancer
2023	FoundationOne® Liquid CDx	NGS	Foundation Medicine, Inc	*BRAF*	*BRAF V600E* alteration	Colorectal Cancer

Adapted table of U.S Food and Drug Administrations https://www.fda.gov/medical-devices/in-vitro-diagnostics/list-cleared-or-approved-companion-diagnostic-devices-in-vitro-and-imaging-tools and https://www.accessdata.fda.gov/cdrh_docs/pdf19/P190032S010A.pdf

PCR, polymerase chain reaction; NGS, Next-Generation Sequencing; Non-Small Cell Lung Cancer.

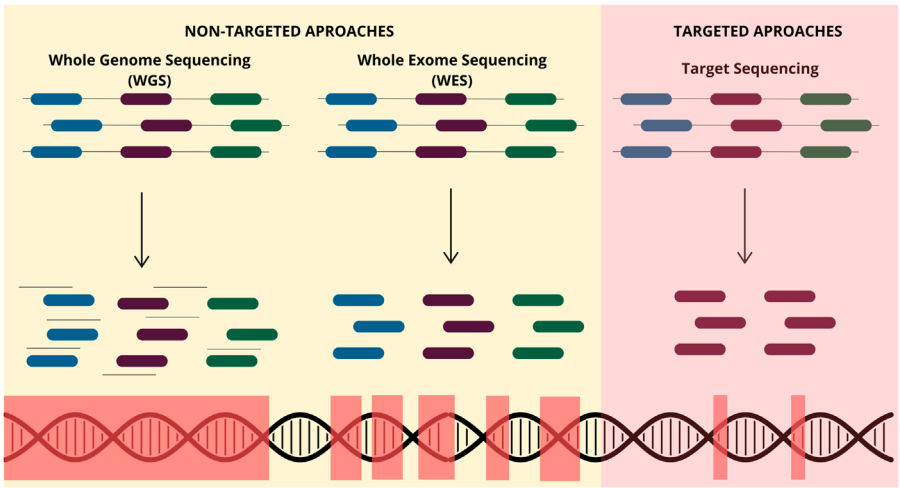

FIGURE 2
Different NGS-based approaches available for ctDNA analysis. The non-targeted approach includes whole-genome sequencing (WGS), which captures the entire genome from a biological sample, including coding and noncoding regions. Additionally, whole-exome sequencing (WES) captures only coding regions. Contrastly, targeted techniques capture only the molecular alterations of genes of interest that are previously known.

TABLE 2 Sequencing NGS- and TGS-bated methods used for ctDNA analysis.

Technology		Methods	Sensitivity (%)	Specificity (%)	Input (ng)	Applications	Alteration	Reference
NGS	Non targeted	WGS	5–10	99.85	1–30	Cancer localization and origin, early detection (early and late stage), for research us	Structural and non-coding variations: genome-wide copy number aberrations, methylation profiles and fragmentation patterns	(Ganesamoorthy et al., 2022)
		WES	5	96	5	Cancer detection, monitoring of resistant clones in metastasis, for research use	Exploring unknown mutations	Diefenbach et al. (2019)
	Targeted	Safe-SeqS/UMI-based	0.01–0.05	98.9	3	Cancer detection and monitoring, classification, targetable alterations, for research use	Known point mutation and number copy variation	(Elazezy and Joosse, 2018)
		Tam-Seq	2	99.9997	0.9–20	Cancer detection and monitoring, classification, targetable alterations, for research use	Known point mutation	(Gale et al., 2018)
		CancerSEEK	69–98	99	0.11–119	Early cancer detection	Mutations nonsense, insertions or deletions, synonymous mutations and intronic mutations	Cohen et al. (2018)
		eTam-Seq	0.2	99.9997	6.6–53	Cancer detection and monitoring, classification, targetable alterations, for research use	Low frequency mutations, short (indels)	(Gale et al., 2018)
		CAPP-SEQ	0.02	99.99	32	Molecular Profiling, Treatment Monitoring, ctDNA MRD	Known point mutation, number copy variation and rearrangements	(Kato et al., 2021)
		Ig-HTS	10–6	98.3	500	Minimal residual disease in hematologic malignancy and cancer monitoring	Not mentioned	Rezazadeh et al. (2024)

(Continued on the following page)

TABLE 2 (*Continued*) Sequencing NGS- and TGS-bated methods used for ctDNA analysis.

Technology		Methods	Sensitivity (%)	Specificity (%)	Input (ng)	Applications	Alteration	Reference
NGS	Targeted	TEC-Seq	0.05–0.01	99.99	2.9–49.5	Molecular Profiling, Treatment Monitoring, ctDNA MRD	Point mutations, small insertions, and deletions	Phallen et al. (2017)
		Single primer extension (SPE)	0.05–1	94	1–50	Cancer detection and monitoring, classification, targetable alterations, for research use	Point mutations	(Zhao et al., 2020)
		SPE-duplex UMI	0.1–0.2	95	40	Cancer detection and monitoring, classification, targetable alterations, for research use	Single-nucleotide variant and Indel mutations	(Peng et al., 2019)
		Duplex Sequencing	0.001–0.1	96.91	64	Cancer detection and monitoring, classification, targetable alterations, for research use	Known and unknown mutations, indels, CNV, chromosomal rearrangements (capture)	(Hallermayr et al., 2022)
TGS	Single Molecular Real-time		Not mentioned	Not mentioned	Not mentioned	Reading of repetitive elements and allele phasing in long fragments	Not mentioned	Choy et al. (2022)
	Nanopore	CyclomicsSeq	Not mentioned	Not mentioned	1500	Real-time monitoring of tumors	Nonsense mutation, missense and deletion	(Marcozzi et al., 2021)

WGS, Whole-genome sequencing; WES., Whole-exome sequencing; Safe-SeqS, Safe-Sequencing System; UMI, unique molecular identifier; Tam-Seq, Tagged-amplicon deep sequencing; eTam-seq, enhanced Tam-Seq; CAPP-Seq, Cancer Personalized Profiling by Deep Sequencing; TEC-Seq, Targeted error correction sequencing; Ig-HTS, Immunoglobulin high-throughput sequencing; SPE, single primer extension.

Non-targeted NGS technologies

In the realm of non-targeted sequencing, the focus broadens to include the entire genome or exome using methods such as whole-genome sequencing (WGS) and whole-exome sequencing (WES), allowing for the simultaneous identification of multiple mutations (Elazezy and Joosse, 2018; Chen and Zhao, 2019; Esteva-Socias et al., 2020). In ctDNA analysis, these methodologies can be applied to discover new molecular alterations, recognize new drug targets, and screen for drug resistance clones (Bohers et al., 2021).

In particular, WGS technologies are better suited to identifying structural and non-coding variations in ctDNA, composing a potential promise for the diagnosis of rare diseases (Bos et al., 2020; Marshall et al., 2020; Sun et al., 2021; Ibañez et al., 2022). The goal of the technique is to detect mutations, chromosomal alterations, genetic rearrangements, and somatic copy number alterations (Daya and Mahfouz, 2018).

According to Zviran et al. (2020) the WGS approach allowed dynamic tracking of tumor burden and detection of single nucleotide variations in postoperative residual disease in colorectal cancer with sensitivity ±SE = 90% ± 0.069%, specificity ±SE = 98% ± 0.006% (AUC ±SE = 0.97 ± 0.025). In addition, showed an association with shorter recurrence-free survival for 36.8% (7/19) of post-operative ctDNA-positive patients $P = 0.03$.

Recently, a study used ultra-low-pass whole-genome sequencing (ULP-WGS), an emergent tool for ctDNA analysis in hepatocellular carcinoma (HC) patients. This technique is cheaper compared to WGS and has a total ctDNA input of 2.5 ng but a very low coverage (<0.05), which can leave gaps in the sequencing. The results showed that 30.1% (22/73) of HC patients had detectable ctDNA levels. Furthermore, a pattern of chromosomal changes was found, such

as the loss of 5q (36.3%) and 16q (40.9%) with an association with positive ctDNA as a predictor of worse prognosis and a biomarker of tumor aggressiveness (Sogbe et al., 2024).

In contrast, WES is a limited method only for coding regions (Sabatier et al., 2022). It is generally used to detect genetic variants that are associated with diseases and detect mutations (Glotov et al., 2023). In a comparative study, WES was applied to paired ctDNA and tumor biopsy in 15 patients for breast cancer, sarcoma, gastrointestinal cancer and melanoma. It was observed that the ctDNA fraction <16.4% is insufficient for detecting tumor-specific variants with a median number of 3 variants, in contrast, a value >30% of ctDNA fraction detected 95 non-synonymous variants. Furthermore, the results showed that ctDNA captures tumor heterogeneity by sharing 22 variants between melanoma (primary tumor) and liver (metastatic) and 12 additional variants that are unique to a tumor site, as well as being able to identify more frequently mutated genes concordant between WES ctDNA and tissue for breast cancer such as *ESR1, KRAS, PIK3CA, PIK3R1, FAT1* and *MED12*, for gastrointestinal cancer *APC, CASP8, GRIN2A, MYH9, TP53, ASXL1, CDH11* and *KRAS*; and melanoma *PSIP1, RSPO2* and *SF3B1* (Leenanitikul et al., 2023).

Nevertheless, it is adequate to detect mutation in patients with advanced tumors and increased ctDNA fractions (Bohers et al., 2021). A study by Diefenbach et al., 2019 showed that ctDNA WES can be used to profile mutations and capture clinically relevant alterations in metastatic melanoma, such as *BRAF* and *NRAS* melanoma driver gene mutations in 6/10 patients when applying a mutant allele frequency (MAF) cutoff of at least 10%.

Notably, WES presents a cost-effective approach compared to WGS by exclusively scrutinizing exons. However, both WGS and WES demand substantial DNA input to ensure the acquisition of high-quality data for the sequencing process and high-throughput. Therefore, these techniques are expensive, which makes their clinical application challenging. Additionally, these methods exhibit limited sensitivity, rendering them less suitable for early-stage cancer detection (Ganesamoorthy et al., 2022).

Targeted NGS-based methods

The targeted strategies allow the detection of single or few tumor-specific mutations in ctDNA through pre-selected panels previously described, such as *BRAF, KRAS, TP53, PIK3CA, APC* and *EGFR* (Elazezy and Joosse, 2018; Mallampati et al., 2019; Liu et al., 2020; Kato et al., 2021; Jiménez-Rodríguez et al., 2022). These techniques could be useful in clinical management for monitoring MRD, early detection of relapse or screening for resistant mutations (Bohers et al., 2021; Lin et al., 2021; Sanz-Garcia et al., 2022).

Generally, customized panels are constructed based on mutations captured during tissue sequencing and applied to detect tumor-specific mutations in plasma (Sanz-Garcia et al., 2022). In addition, laboratories have no standardization in the clinical implementation of NGS panel design. It is widespread to use pre-designed panels from suppliers or to create your panels. However, developing a targeted panel from scratch is challenging, as investments in operational infrastructure and bioinformatics are required (Shi et al., 2022).

Amplicon

Target NGS technologies require enrichment by amplicon or hybrid-capture (Figure 3) (Lin et al., 2021; Sanz-Garcia et al., 2022). Amplicon sequencing, a targeted NGS method able to analyze genetic variation in specific genomic regions, consists of a multiplex PCR-based method that uses oligonucleotides to target and capture regions of interest. PCR is used to create DNA sequences known as amplicons, which can be multiplexed by adding a barcode or index to the samples for identification. Before, the samples must be transferred into libraries by adding adapters and enriching targets using PCR amplification. The adapters allow the formation of indexed amplicons and their adherence to the flow cell for sequencing (Hung et al., 2018). Currently, some amplicon-based methods are described in the literature.

Safe-sequencing system (Safe-SeqS)

Safe-SeqS is an amplicon method that uses DNA molecular barcodes to increase sequencing sensitivity before PCR and uses the unique identifier (UID), which allows fragments with the same UID to be considered mutants if more than 95% have the same mutation. Barcode error correction increases sensitivity to 0.05% and identifies rare mutations (Tuaeva et al., 2019; Bohers et al., 2021). Tie et al. (2021) designed Safe-SeqS to evaluate a previously detected mutation with a higher allele frequency in 54 patients with resectable colorectal liver metastases (CRLM) and evaluated the prognostic impact of postoperative ctDNA in patients with CRLM. As a result, ctDNA was most detectable in patients at baseline (T0) 85% (46/54) with a median MAF for positive ctDNA of 1.86% (IQR, 0.44%–8.2%) and in patients after surgery (TP) 24% (12/49) 0.09% (IQR, 0.02%–1.3%).

Nowadays, Safe-seqS is recognized as Unique Molecular Identifier (UMI)-based sequencing and highlights in new nomenclature the use of unique molecular identifiers (UMIs) to track and correct errors during the process, with greater accuracy in the detection of rare mutations and in the quantification of nucleic acids (Salk et al., 2018). UMI-based sequencing technology was used to investigate somatic mutations in ctDNA of patients with lung squamous cell carcinoma (LUSC), which were detected in 80.8% (20/26) of patients and mutations with maximum allele fraction (maxAF) > 5% compared to maxAF ≤5% (P = 0.020) reflected shorter overall survival. The most frequently mutated gene was *TP53* with 73.0% (19/26), and the classic lung cancer driver mutations, *PIK3CA* (n = 3), *EGFR* amplification (n = 2), *EGFR* exon 19 deletion (n = 1), *KRAS* Q61R (n = 1), and *MET* amplification (n = 1) were detected (Liu et al., 2020).

Tagged-amplicon deep sequencing (Tam-seq)

Tam-seq uses an enrichment matrix with primers and barcodes in the construction of an amplicon library, which goes through steps of targeted pre-amplification and selective amplification with single-plex reactions, as well as PCR is performed for the addition of adapters and barcodes for sample identification (Zhao et al.,

10.3389/fmolb.2024.1423470

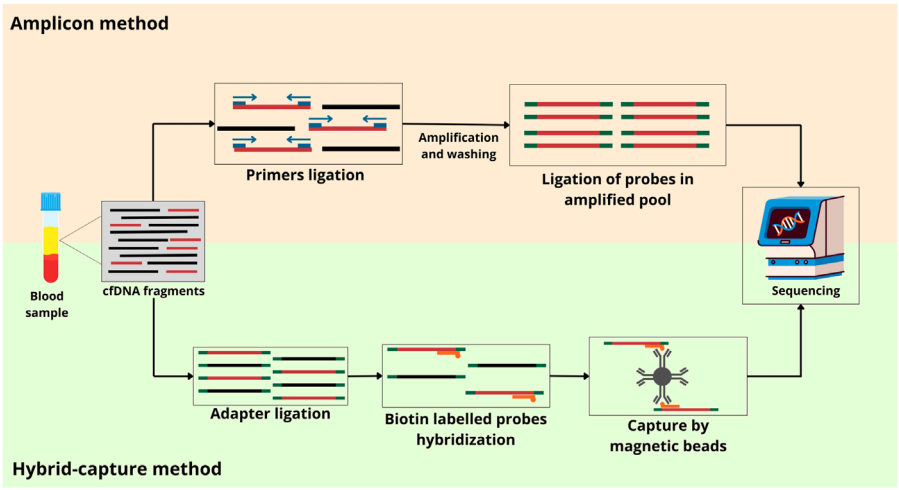

FIGURE 3
Two NGS-based targeted approaches for ctDNA analysis. The amplicon approach is based on the PCR method, which amplifies specific regions of the genome. The hybrid-capture approach uses probes to capture and enrich specific genomic regions of interest before sequencing. cfDNA, cell-free DNA.

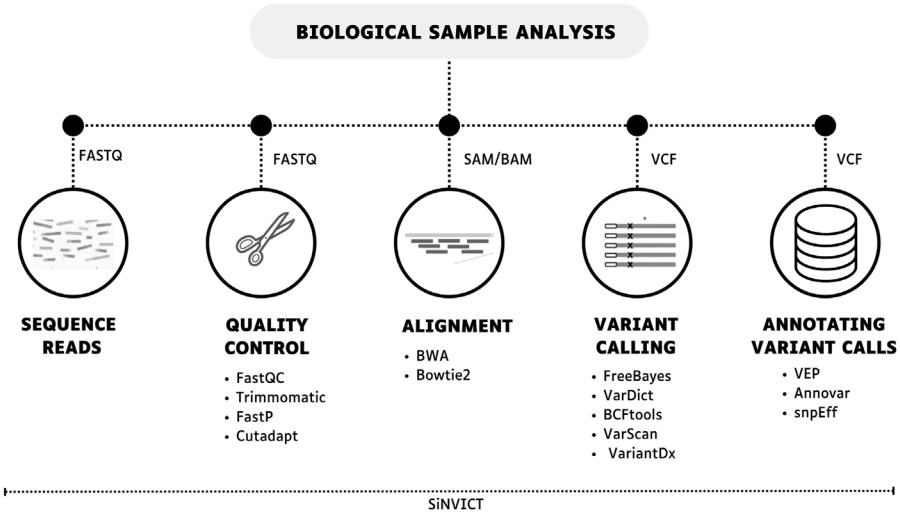

FIGURE 4
Bioinformatics workflow for data-seq for ctDNA evaluation. This process generally includes obtaining sequence reads, performing quality control, genomic alignment, variant calling, and annotating variant calls. Multiple tools are available for each step, or a single tool can be used to complete all the steps (SiNVICT).

2020). This technique showed high sensitivity 0.01%–2.0% and specificity >97% to detect mutations in circulating DNA, as a ctDNA analysis method that allows for an ultra-low detection limit and broad patient coverage, as well as showing digital PCR-like sensitivity for hotspot alleles and can simultaneously interrogate thousands of additional genomic positions without your sensitivity or specificity are affected (Noguchi et al., 2020). The technique requires knowledge of recurrent cancer mutations available in databases and uses a selector (biotinylated oligonucleotide probes) to target large segments of the studied regions (Bohers et al., 2021).

In 2018, Gale et al. described enhanced Tam-Seq (eTam-Seq), which consists of an expanded assay to target hotspots and entire coding regions of 35 genes for common cancer types, based on a primer design that allows amplification of highly fragmented DNA and in library preparation does not use microfluidics. This technique aims to identify single nucleotide variants (SNVs) and short insertions/deletions (indels) and identify copy number variants (CNVs). The validation test results of this tool indicated high specificity 99.9997% (95% (CI): 99.9989%–99.9999% by base specificity) and sensitivity 100% (90% (CI): 99.01%–100%) in low

input samples at 2%–2.5% AF, 99.17% (90% CI: 97.40%–99.85%) in medium input samples at 1%–1.3% AF and 95.45% (90% CI: 93.09%–97.18%) in high input samples at 0.25%–0.33% AF (Gale et al., 2018).

On the other hand, the hybrid-capture, also known as hybridization-based sequencing, is based on using long, biotinylated probes or baits complementary to the region of interest. This method involved the fragmentation of physical or enzymatic DNA followed by enzymatic repair of the ends of the molecules and ligation of platform-specific adapters. These adapters usually contain index bases that comprise a sequence that is unique to the sample or the barcode of the sample (Bohers et al., 2021). Unlike amplicon sequencing, this method does not require PCR primer design. Thus, it is less likely to miss mutations and is said to be better at performing in terms of sequence complexity. The capacity of this method for mutation detection makes it best suited to cancer research. Moreover, its sequence complexity and scalability make it good for WES (Wu et al., 2022).

Hybrid capture

When choosing panels in the hybridization method, cfDNA fragmentation must be taken into account, as it may result in heterogeneous coverage between target exons (Lin et al., 2021; Shen et al., 2021). This enrichment step prevents loss of the variant of interest if they are on the edges of the fragments because the probe binding to the target region is sufficient to capture the variant. However, the fragments may not amplify because they do not have a binding sequence with the primers during NGS library preparation (Mallampati et al., 2019). Several hybrid capture-based technologies have been described.

Cancer personalized profiling by deep sequencing (CAPP-Seq)

CAPP-Seq developed the ability to simultaneously detect several types of changes: SNVs, rearrangements, insertions/deletions, and copy number changes (Elazezy and Joosse, 2018). Additionally, CAPP-Seq has been enhanced with Integrated Digital Error Suppression (iDES), combining CAPP-Seq with duplex barcode sequencing technology and a computational algorithm that removes stereotyped errors associated with the CAPP-Seq hybridization step (Peng et al., 2019). According to Kato et al. (2021), CAPP-SEq applied to ctDNA mutation analysis allowed the identification of mechanisms of resistance to osimertinib in *EGFR* T790M-positive NSCLC patients. In addition, the assay also detected *EGFR*-activating mutation in 70% (14/20) of patients, and these results were associated with a larger tumor volume through the sum analysis of the largest diameters of the target lesions ($P = 0.04$). In addition, for patients with *EGFR* activating mutation, mutations were observed in the genes *PIK3CA* (3/14) 21%, *KRAS* (2/14) (14%) and or *BRAF* (3/14) 21% and copy number gain alterations for *EGFR* (9/14) 64%, *ERBB2* (4/14) 29% or *MET* (4/14) 29%. Additionally, the identified alterations were more common in patients with innate resistance 8 (57%) compared to patients with acquired resistance 6 (43%) (Kato et al., 2021).

Others technologies

Some approaches described use different combinations of technologies to optimize results. Some methods do not apply to the amplicon enrichment or hybrid capture standards.

Immunoglobulin high-throughput sequencing (Ig-HTS)

Ig-HTS is an ultra-deep genomic DNA sequencing method developed for minimal residual disease in hematologic malignancy that uses multiplex PCR arrays to identify a tumor-specific clonotype from rearranged gene regions of IgH, IgK, and IgL receptors. This technology enables cancer monitoring through quantifying ctDNA with a sensitivity of 10%–6% (Bohers et al., 2021). In 2022, Rezazedeh et al. demonstrated that Ig-HTS as a Food and Drug Administration-proven tool clonoSEQ (Adaptive Biotechnologies) allows the minimization of surveillance imaging in patients with B-cell lymphomas from ctDNA analysis, in which the result of the MRD assay was predictive of relapse before imaging in 92% of patients (11/12) (Rezazadeh et al., 2024).

Targeted error correction sequencing (TEC-Seq)

TEC-Seq is a method that combines targeted sequencing and error correction approaches, which has a sensitivity of 94.7% and is capable of detecting mutations in early-stage solid cancers, as well as being a method capable of identifying true mutations and false-positive variants (Phallen et al., 2017; Bohers et al., 2021). Serrano et al. employed TEC-Seq for serial monitoring of ctDNA from patients with gastrointestinal stromal tumors to evaluate the combination of sunitinib and regorafenib as a new add-on drug treatment regimen. In this study, somatic mutations, point mutations, small insertions, and deletions were analyzed. This approach resulted in primary mutations in 89% (8/9) and secondary mutations in 78% (7/9) of patients (Serrano et al., 2019).

Single primer extension (SPE)

SPE is a method developed by QIAGEN that redefines amplicon enrichment and sequencing (QIAseq SPE technology for Illumina: Redefining amplicon sequencing - QIAGEN, 2018). The method is based on the extension of a single gene-specific primer by DNA polymerase to amplify each genomic region with uniform coverage, allowing the detection of single nucleotide polymorphisms (SNPs) and specific mutations with high accuracy. Initially, the primer is hybridized to the DNA template strand in the target region, where there are subsequent adapter ligation repair steps. Then, the primer is extended from the 3′ end, and each genomic region is targeted by only one region-specific primer plus a universal adapter primer that binds to sequences introduced through adapters. These adapters are linked to primers and a molecular barcoding technology used to uniquely tag each molecule in the sample library, Unique Molecular Index (UMI), with a sensitivity of 0.5%–1%

(Bentley et al., 2008; Peng et al., 2019; Zhao et al., 2020). In SPE, the use of UMI reduces amplification errors and increases the sensitivity of variant detection, which provides error correction and higher accuracy during sequencing. Additionally, SPE can be enhanced through duplex UMI adapters (duplex SP-UMI), multiplex PCR-based enrichment and sequencing, which increases sensitivity to 0.1%–0.2% (Peng et al., 2019).

Recently, this technology was used by Jiménez-Rodríguez et al. (2022) for the analysis of ctDNA from BC patients and a sequencing panel composed of exonic regions of 33 genes in 75 plasma samples was developed. As a result of the study, 21.31% (13/61) of tumor mutations were found in both plasma and corresponding tumors, and the most frequently mutated genes were *TP53* (53.84%) and *PIK3CA* (23.07%). In addition, it presented a sensitivity of 0.03% and a specificity of 86.36%.

Duplex sequencing

Duplex sequencing is a method that aims to achieve accuracy and reduce sequencing errors based on double-strand consensus analysis. This technique begins with the fragmentation of DNA into smaller pieces and the addition of specific adapters. The fragmented DNA is encapsulated in emulsion drops where PCR amplification occurs, generating single-strand readings. The single strands are paired to form duplex readings. The analysis of the two strands is compared to eliminate random errors that can be identified by the lack of correspondence between the single-strand readings (Mallampati et al., 2019; Bohers et al., 2021; Shields et al., 2022). This approach was demonstrated by Mallampati et al. (2019) to monitor disease progression in patients with stage IV colorectal cancer. In this research, a CRC23 panel with 78.81 kb was created involving 85% of mutated targets and exon regions for the *TP53, APC, KRAS, NRAS, BRAF, PIK3CA* and *ERBB2* genes and hotspot coding exons of 16 other genes. Furthermore, a detection limit of 0.3% of variant frequency was observed, as well as diagnostic accuracy of 96.15% (95% CI, 94.28%–97.55%), sensitivity of 87.23% (95% CI, 74.26%–95.17%) and specificity of 96.91% (95% CI, 95.11%–98.19%).

Although the targeted strategy makes cancer monitoring extremely sensitive, these approaches require prior genetic knowledge of the tumor. This may not be useful in characterizing new molecular alterations that occur during tumor treatment (Elazezy and Joosse, 2018; Sanz-Garcia et al., 2022).

Third generation of sequencing

Additionally to NGS, the advent of the third generation of sequencing (TGS) has provided new features and capabilities for real-time reading, long-fragment reading, portability, and ease of use which are fundamental to understanding cancer genetics, and currently PacBio Sequencing (Menlo Park, CA, United States) and Oxford Nanopore Technologies (ONT, Oxford, United Kingdom) are the two TGS technology platforms (Amarasinghe et al., 2020; Scarano et al., 2024).

Single Molecular Real-Time (SMRT) (Pacific Biosciences, California) is a method based on reading made on SMRT chips which is composed of metal film containing zero-mode waveguides (ZMW) which are special nanophotonic visualization chambers. Inside chambers in the flow cell are ZMW that capture signals from phospholinked dNTP labeled with fluorophores which are incorporated by DNA polymerase and released fluorescence pulse that is identified by laser at a specific wavelength in real time (Treffer and Deckert, 2010). This SMRT technology enables the reading of repetitive elements and allele phasing in long fragments (Ardui et al., 2018). In the analysis of ctDNA, SMRT sequencing was used to evaluate long DNA properties and methylation patterns, since analyses usually focus on short fragments. The assay results showed the detection of fragments up to 13.6 kb in length in samples from 13 patients with hepatocellular carcinoma. Additionally, it was observed that non-tumor cfDNA was generally longer than tumor cfDNA, in which plasma DNA molecules longer than 600 bp were 55.1% carrying mutant alleles and 64.8% wild-type, and molecules longer than 1 kb were 43.4% carrying mutant alleles and 56.4% wild-type. Furthermore, complete reads were performed in 85.79% (IQR: 83.11%–88.69%) of the fragments. Another important point to be analyzed was the detection of long cfDNA fragments containing a mutant allele, which can generate changes in cfDNA analyses for the inclusion of long molecules (Choy et al., 2022).

Furthermore, nanopore sequencing (Oxford Nanopore Technologies) is a technology that consists of real-time readings of changes in electrical current during the passage of the DNA molecule through a biosensor, which is composed of an electrically resistant membrane. The nanopores are arranged in the flow cell in micro-scaffolds and can be categorized as solid and biological. Each nanopore is an electrode connected to the channel inside the sensor chip where the electrical current is measured. When the electrical current is interrupted by the passage of a molecule, the so-called "squiggle" occurs and this information becomes corresponding to a specific nucleotide. This method has capacity for long-read sequencing, empowering the direct analysis of DNA or RNA fragments sans the prerequisite of prior amplification (Wang et al., 2021; Scarano et al., 2024). This TGS technology was employed to analyze genomic and fragmentomic data from liquid biopsies in 8 urine samples from bladder cancer patients and 22 plasma samples from lung cancer patients. ONT sequencing performed on the MinION showed structural properties of cfDNA and the ability to recover somatic copy number aberrations (SCNAs) in 24 h with a median of 800,183 reads and ~0.1X coverage. Although cfDNA is described in the literature as short and fragmented molecules (167 bp), the results obtained from this research showed increased recovery of long cfDNA (>300 bp) in plasma from lung cancer patients, and compared to short-read sequencing (5.3%), ONT sequencing had 54.1% of fragments larger than 300 bp (van der Pol et al., 2023).

CyclomicsSeq is a technology based on the circularization and concatemerization of DNA molecules and an optimized DNA sequence in combination with Oxford Nanopore sequencing created for real-time monitoring of tumors based on the analysis of ctDNA levels. The protocol of this technology uses amplicons and is divided into four steps, which involve the circularization of the insert and backbone (DNA adapter), rolling circle amplification (RCA), long-read sequencing and data processing. The detection of ctDNA through this technology allows the identification of mutations based on somatic variants. Real-time monitoring can

be done by identifying mutations in the *TP53* gene, in which a *TP53* mutation was observed in a trial with patients with head and neck squamous cell cancer negative for the human papillomavirus (HPV) at a frequency of 0.02%. During the trial, the single nucleotide error false positive rate (snFP rate) was also analyzed, which had a median <6, 10^{-4} in all *TP53* exons to evaluate the use of CyclomicsSeq for mutation detection in liquid biopsy (Marcozzi et al., 2021).

Although TGS can generate long reads and detect complex structural variants, its use in ctDNA analysis still has challenges. ctDNA fragments are rare in cfDNA, and reads of long fragments can induce the appearance of false base substitution mutations and indels (Ardui et al., 2018; Marcozzi et al., 2021; Scarano et al., 2024). These errors can make it difficult to accurately detect relevant mutations that could interfere with the clinical management of cancer patients.

Sequencing data analysis

Data sequencing analysis is a critical process for ctDNA evaluation and consists of three main steps: quality analysis, alignment, and variant calling (Figure 4) (Wadapurkar and Vyas, 2018). Firstly, quality control of the reads is crucial for the bioinformatics analysis since high throughput NGS generates a massive volume of data and improves confidence in the data. In general, programs like FastQC provide a comprehensive per-base analysis, ensuring that the sequence is accurate and not compromised by issues generated during the sequencing run (Andrews, 2010; Trivedi et al., 2014; Mahamdallie et al., 2018). Moreover, reads can be contaminated by other sequences, such as primers or adapters in library preparation. Thus, several tools may be used to remove low-quality bases and sequences from adapters, such as Cutadapt, FastP, and Trimmomatic (Bolger et al., 2014; Chen et al., 2018; Martins et al., 2021).

Based on the provenance of the data and the size of the fragments, several aligners can be useful for ctDNA, including BWA and Bowtie2 (Li and Durbin, 2009; Langmead and Salzberg, 2012). In target sequencing, the alignment process consists of comparing the generated sequences to verify the degree of similarity using a reference genome or a customized file containing only the regions of interest of the study as a parameter. Moreover, it is worth noting that the version of the genome used during the analysis should be the same in order to avoid later disagreements (Reinert et al., 2015; Dilliott et al., 2018; Kang et al., 2020).

The last step seeks the identification of variants that differ from the reference used, typically FreeBayes, VarScan, BCFtools, VarDict and VariantDx are among the tools used to find SNPS, indels during the calling process in ctDNA analysis (Liu et al., 2013; Kang et al., 2020). Finally, the variants found go through the annotation process, which is querying existing databases. The VarDict is an ultra-sensitive variant caller pipeline that has already been used for the identification of ctDNA variants in cancer samples (Lai et al., 2016; Leal et al., 2020).

A sufficient number of reads is extremely important for correct mapping, identifying genetic alterations, and ruling out putative execution errors, especially data from devices that show errors in base changes. Targeted sequencing provides just that, contributing to the identification of variants at low abundance, which is characteristic of ctDNA. Therefore, high coverages (>30,000×) are expected in this type of experiment.

In addition, variant detection in ctDNA samples can be challenging due to the low frequency of total cfDNA and PCR artifacts in library preparation. Thus, Kockan et al. (2017) introduced SiNVICT, which consists of a tool for the detection of SNVs and short indels in ctDNA at very low variant allele percentages with high accuracy and sensitivity. This approach includes pre-processing, SNV/indel calling, and post-processing steps. SiNVICT also allows for analyzing samples collected at different time points and evaluating the temporal clonal evolution of tumors, which could be useful for the detection of resistance mutations and therapy selection (Kockan et al., 2017).

Conclusion and future perspectives

Currently, ctDNA analysis represents a crucial approach to guide cancer diagnosis, management and monitoring, but the clinical implementation of ctDNA is still limited (Oliveira et al., 2020). NGS has shown great potential for advancing clinical practices through the development of a diverse panel for identifying ctDNA mutations in different cancer types, but finding the optimal approach remains a challenge (Table 3). Studies based on non-targeted NGS have the highest cost but are necessary for the construction of mutational panels, especially in cases of tumors lacking biomarkers (Hess et al., 2020; Christodoulou et al., 2023). With these studies, it is expected that new techniques will be developed to detect ctDNA mutations even at low frequencies in the bloodstream.

One of the tests approved by the FDA based on NGS panels most used in clinical oncology practice is still Foundation One® Liquid Cdx, used with both tissue biopsies and ctDNA in NSCLC, breast, prostate, ovarian, and colorectal cancer (Newman et al., 2016; Shahnoor et al., 2023). This test allows comprehensive genomic profiling that guides more effective therapy and predicts patient prognosis (Woodhouse et al., 2020).

Another technology that is quite promising for application in clinical practice is CancerSEEK is an amplicon-based method that uses multiplex PCR in the enrichment step and was developed in 2018 as a blood test for early cancer detection through quantifying the levels of circulating proteins and cfDNA (Cohen et al., 2018; Duffy et al., 2021; Dao et al., 2023).

CancerSEEK is capable of detecting 8 types of non-metastatic cancer (ovarian, liver, stomach, pancreas, esophagus, colorectal, lung or breast) through the construction of a panel for 16 genes (*NRAS, CTNNB1, PIK3CA, FBXW7, APC, EGFR, BRAF, CDKN2A, PTEN, FGFR2, HRAS, KRAS, AKT1, TP53, PPP2R1A, GNAS*) composed of 61 amplifiers containing on average 33 base pairs each amplicon. This assay has shown results, after application in 1,005 patients, of sensitivities of 69%–98% for 5 types of cancer (ovarian, liver, stomach, pancreas and esophagus) and specificity >99% in 0.86% (7/812) of healthy controls. In addition, it was observed that the maximum ctDNA detection capacity of the assay

10.3389/fmolb.2024.1423470

TABLE 3 Sequencing technologies are available for ctDNA analysis, as well as its principles, advantages, and disadvantages.

Sequencing technology	Classification	Method	Principle	Advantages	Disadvantages
NGS	Non-targeted	WGS	Determining the complete DNA sequence from a genome captures exons (coding) and introns (non-coding) regions, providing a comprehensive view of the genetic information	Provides a genome-wide view, capturing all genetic variations without requiring prior knowledge of regions of interest	Presents high cost and generates large amounts of data, requiring substantial computational resources for analysis
		WES	Performs only sequencing of the coding regions of the genome	It is cost-effective and efficient in identifying clinically relevant mutations	Does not provide information on non-coding regions and it also requires comprehensive bioinformatics tools for analysis
	Targeted	Amplicon	Analyze genetic sequences by amplifying specific regions of the genome before sequencing	Exhibits high sensitivity, is customizable according to the needs of the study, has high performance, and has a shorter response time	Only provides information about the selected regions; the design of primers for regions with high genetic variability can be complex, and errors arising from the amplification steps can lead to false-positive results
		Hybrid-capture	Uses biotinylated oligonucleotide probes to hybridize and enrich the regions of interest before sequencing	It has high coverage and specificity, can be targeted to various genomic regions, and has no amplification bias	The workflow is more complex, expensive, and time-consuming due to the steps in the protocol. Errors in hybridization can lead to inadequate capture and false results
TGS		SMRT	Based on SMRT (Single Molecule, Real-Time) chips, fluorophore-labeled nucleotides are added to DNA polymerase, and when incorporated into the DNA strand, fluorescent light is recorded at a specific wavelength	Long DNA sequence reads allow identification of structural rearrangements and mutations that may be difficult to detect with short-read methods	Limitation on coverage and processing time
	Nanopore	CyclomicsSeq	Performs amplification and repeated cyclic reading of circular DNA molecules to achieve accurate detection of low-frequency variants	Presents high precision and sensitivity for detecting low-frequency mutations, and random errors are reduced due to the cyclic reading of the fragments	It has a high cost and technical complexity for its execution, in addition to having a lower yield compared to NGS and requiring sophisticated bioinformatics tools to analyze the results

NGS, Next-Generation Sequencing; TGS, third generation sequencing; WGS, Whole-Genome Sequencing; WES, Whole-Exome Sequencing; SMRT, Single Molecular Real-time.

could vary according to the type of tumor (60% for liver cancer and 100% for ovarian cancer) and DNA concentrations in plasma ranged from 0.11 to 119 ng/mL. The test identified rare mutations: nonsense, insertions or deletions, canonical splice site mutations, synonymous mutations, except at exon ends and intronic mutations, except at splice sites. Regarding the reading model, CancerSEEK uses reference sequences and custom scripts in Python, SQL and C# (In Silico Solutions, Falls Church, VA) (Cohen et al., 2018).

Although the CancerSEEK test has been recognized as a Breakthrough Device by the U.S. Food and Drug Administration for the detection of genetic mutations and proteins associated with pancreatic and ovarian cancers, it still needs to be validated in large-scale screening studies for commercialization (Duffy et al., 2021).

Therefore, it is expected that more target NGS-based technologies will be developed to increase the sensitivity of ctDNA detection. Additionally, as NGS-based experimental designs become more affordable and popular, there is an escalating demand for software capable of collating, manipulating, and visually presenting quality control (QC) logs and reports, especially when dealing with a substantial number of samples. Also, multiple factors, including cost, yield, specificity, cancer type, disease stage, clinical application, and bioinformatics analysis need to be considered.

Author contributions

TS: Writing–review and editing, Writing–original draft. JA: Writing–original draft, Supervision, Writing–review and editing. ET: Writing–review and editing. SC: Writing–review and editing. FM: Writing–review and editing. PP: Writing–review and editing. SS: Writing–review and editing. DC: Writing–review and editing, Writing–original draft.

Funding

The author(s) declare that financial support was received for the research, authorship, and/or publication of this article. This study was supported by Universidade Federal do Pará and Brazilian funding agencies: Coordenação de Aperfeiçoamento de Pessoal de Nível Superior (CAPES; to ET, TS, and JA), Conselho Nacional de Desenvolvimento Científico e Tecnológico (CNPq; to DC, 315643/2023-4) for financial support.

Conflict of interest

The authors declare that the research was conducted in the absence of any commercial or financial relationships that could be construed as a potential conflict of interest.

Publisher's note

References

Amarasinghe, S. L., Su, S., Dong, X., Zappia, L., Ritchie, M. E., and Gouil, Q. (2020). Opportunities and challenges in long-read sequencing data analysis. *Genome Biol.* 21, 30. doi:10.1186/s13059-020-1935-5

Andrews, S. (2010). Babraham bioinformatics - FastQC A quality control tool for high throughput sequence data. Available at: http://www.bioinformatics.babraham.ac.uk/projects/fastqc/ (Accessed June 14, 2024).

Ardui, S., Ameur, A., Vermeesch, J. R., and Hestand, M. S. (2018). Single molecule real-time (SMRT) sequencing comes of age: applications and utilities for medical diagnostics. *Nucleic Acids Res.* 46, 2159–2168. doi:10.1093/nar/gky066

Bagger, F. O., Borgwardt, L., Jespersen, A. S., Hansen, A. R., Bertelsen, B., Kodama, M., et al. (2024). Whole genome sequencing in clinical practice. *BMC Med. Genomics* 17, 39. doi:10.1186/s12920-024-01795-w

Bentley, D. R., Balasubramanian, S., Swerdlow, H. P., Smith, G. P., Milton, J., Brown, C. G., et al. (2008). Accurate whole human genome sequencing using reversible terminator chemistry. *Nature* 456, 53–59. doi:10.1038/nature07517

Bohers, E., Viailly, P.-J., and Jardin, F. (2021). cfDNA sequencing: technological approaches and bioinformatic issues. *Pharmaceuticals* 14, 596. doi:10.3390/ph14060596

Bolger, A. M., Lohse, M., and Usadel, B. (2014). Trimmomatic: a flexible trimmer for Illumina sequence data. *Bioinformatics* 30, 2114–2120. doi:10.1093/bioinformatics/btu170

Bos, M. K., Angus, L., Nasserinejad, K., Jager, A., Jansen, M. P. H. M., Martens, J. W. M., et al. (2020). Whole exome sequencing of cell-free DNA – a systematic review and Bayesian individual patient data meta-analysis. *Cancer Treat. Rev.* 83, 101951. doi:10.1016/j.ctrv.2019.101951

Chen, M., and Zhao, H. (2019). Next-generation sequencing in liquid biopsy: cancer screening and early detection. *Hum. Genomics* 13, 34. doi:10.1186/s40246-019-0220-8

Chen, S., Zhou, Y., Chen, Y., and Gu, J. (2018). fastp: an ultra-fast all-in-one FASTQ preprocessor. *Bioinformatics* 34, i884–i890. doi:10.1093/bioinformatics/bty560

Choy, L. Y. L., Peng, W., Jiang, P., Cheng, S. H., Yu, S. C. Y., Shang, H., et al. (2022). Single-molecule sequencing enables long cell-free DNA detection and direct methylation analysis for cancer patients. *Clin. Chem.* 68, 1151–1163. doi:10.1093/clinchem/hvac086

Christodoulou, E., Yellapantula, V., O'Halloran, K., Xu, L., Berry, J. L., Cotter, J. A., et al. (2023). Combined low-pass whole genome and targeted sequencing in liquid biopsies for pediatric solid tumors. *Npj Precis. Oncol.* 7, 21–11. doi:10.1038/s41698-023-00357-0

Cohen, J. D., Li, L., Wang, Y., Thoburn, C., Afsari, B., Danilova, L., et al. (2018). Detection and localization of surgically resectable cancers with a multi-analyte blood test. *Science* 359, 926–930. doi:10.1126/science.aar3247

Dang, D. K., and Park, B. H. (2022). Circulating tumor DNA: current challenges for clinical utility. *J. Clin. Investig.* 132, e154941. doi:10.1172/JCI154941

Dao, J., Conway, P. J., Subramani, B., Meyyappan, D., Russell, S., and Mahadevan, D. (2023). Using cfDNA and ctDNA as oncologic markers: a path to clinical validation. *Int. J. Mol. Sci.* 24, 13219. doi:10.3390/ijms241713219

Daya, S. A., and Mahfouz, R. (2018). Circulating tumor DNA, liquid biopsy, and next generation sequencing: a comprehensive technical and clinical applications review - ScienceDirect. Available at: https://www.sciencedirect.com/science/article/pii/S2214540018301439?via%3Dihub (Accessed June 2, 2024).

Diefenbach, R. J., Lee, J. H., Strbenac, D., Yang, J. Y. H., Menzies, A. M., Carlino, M. S., et al. (2019). Analysis of the whole-exome sequencing of tumor and circulating tumor DNA in metastatic melanoma. *Cancers* 11, 1905. doi:10.3390/cancers11121905

Dilliott, A. A., Farhan, S. M. K., Ghani, M., Sato, C., Liang, E., Zhang, M., et al. (2018). Targeted next-generation sequencing and bioinformatics pipeline to evaluate genetic determinants of constitutional disease. *J. Vis. Exp.*, 57266. doi:10.3791/57266

Duffy, M. J., Diamandis, E. P., and Crown, J. (2021). Circulating tumor DNA (ctDNA) as a pan-cancer screening test: is it finally on the horizon? *Clin. Chem. Lab. Med. CCLM* 59, 1353–1361. doi:10.1515/cclm-2021-0171

Elazezy, M., and Joosse, S. A. (2018). Techniques of using circulating tumor DNA as a liquid biopsy component in cancer management. *Comput. Struct. Biotechnol. J.* 16, 370–378. doi:10.1016/j.csbj.2018.10.002

Esteva-Socias, M., Enver-Sumaya, M., Gómez-Bellvert, C., Guillot, M., Azkárate, A., Marsé, R., et al. (2020). Detection of the EGFR G719S mutation in non-small cell lung cancer using droplet digital PCR. *Front. Med.* 7, 594900. doi:10.3389/fmed.2020.594900

Fürstenau, M., Weiss, J., Giza, A., Franzen, F., Robrecht, S., Fink, A.-M., et al. (2022). Circulating tumor DNA–based MRD assessment in patients with CLL treated with obinutuzumab, acalabrutinib, and venetoclax. *Clin. Cancer Res.* 28, 4203–4211. doi:10.1158/1078-0432.CCR-22-0433

Gale, D., Lawson, A. R. J., Howarth, K., Madi, M., Durham, B., Smalley, S., et al. (2018). Development of a highly sensitive liquid biopsy platform to detect clinically-relevant cancer mutations at low allele fractions in cell-free DNA. *PLOS ONE* 13, e0194630. doi:10.1371/journal.pone.0194630

Ganesamoorthy, D., Robertson, A. J., Chen, W., Hall, M. B., Cao, M. D., Ferguson, K., et al. (2022). Whole genome deep sequencing analysis of cell-free DNA in samples with low tumour content. *BMC Cancer* 22, 85. doi:10.1186/s12885-021-09160-1

Glenn, T. C. (2011). Field guide to next-generation DNA sequencers. *Mol. Ecol. Resour.* 11, 759–769. doi:10.1111/j.1755-0998.2011.03024.x

Glotov, O. S., Chernov, A. N., and Glotov, A. S. (2023). Human exome sequencing and prospects for predictive medicine: analysis of international data and own experience. *J. Pers. Med.* 13, 1236. doi:10.3390/jpm13081236

Hallermayr, A., Neuhann, T. M., Steinke-Lange, V., Scharf, F., Laner, A., Ewald, R., et al. (2022). Highly sensitive liquid biopsy Duplex sequencing complements tissue biopsy to enhance detection of clinically relevant genetic variants. *Front. Oncol.* 12, 1014592. doi:10.3389/fonc.2022.1014592

Hess, J. F., Kohl, T. A., Kotrová, M., Rönsch, K., Paprotka, T., Mohr, V., et al. (2020). Library preparation for next generation sequencing: a review of automation strategies. *Biotechnol. Adv.* 41, 107537. doi:10.1016/j.biotechadv.2020.107537

Huerta, M., Roselló, S., Sabater, L., Ferrer, A., Tarazona, N., Roda, D., et al. (2021). Circulating tumor DNA detection by digital-droplet PCR in pancreatic ductal adenocarcinoma: a systematic review. *Cancers* 13, 994. doi:10.3390/cancers13050994

Hung, S. S., Meissner, B., Chavez, E. A., Ben-Neriah, S., Ennishi, D., Jones, M. R., et al. (2018). Assessment of capture and amplicon-based approaches for the development of a targeted next-generation sequencing pipeline to personalize lymphoma management. *J. Mol. Diagn* 20, 203–214. doi:10.1016/j.jmoldx.2017.11.010

Ibañez, K., Polke, J., Hagelstrom, R. T., Dolzhenko, E., Pasko, D., Thomas, E. R. A., et al. (2022). Whole genome sequencing for the diagnosis of neurological repeat expansion disorders in the UK: a retrospective diagnostic accuracy and prospective clinical validation study. *Lancet Neurol.* 21, 234–245. doi:10.1016/S1474-4422(21)00462-2

Jiang, M., Jin, S., Han, J., Li, T., Shi, J., Zhong, Q., et al. (2021). Detection and clinical significance of circulating tumor cells in colorectal cancer. *Biomark. Res.* 9, 85. doi:10.1186/s40364-021-00326-4

Jiménez-Rodríguez, B., Alba-Bernal, A., López-López, E., Quirós-Ortega, M. E., Carbajosa, G., Garrido-Aranda, A., et al. (2022). Development of a novel NGS methodology for ultrasensitive circulating tumor DNA detection as a tool for early-stage breast cancer diagnosis. *Int. J. Mol. Sci.* 24, 146. doi:10.3390/ijms24010146

Kang, J.-K., Heo, S., Kim, H.-P., Song, S.-H., Yun, H., Han, S.-W., et al. (2020). Liquid biopsy-based tumor profiling for metastatic colorectal cancer patients with ultra-deep targeted sequencing. *PLOS ONE* 15, e0232754. e0232754–e0232754. doi:10.1371/journal.pone.0232754

Kato, R., Hayashi, H., Sakai, K., Suzuki, S., Haratani, K., Takahama, T., et al. (2021). CAPP-seq analysis of circulating tumor DNA from patients with EGFR T790M–positive lung cancer after osimertinib. *Int. J. Clin. Oncol.* 26, 1628–1639. doi:10.1007/s10147-021-01947-3

Kockan, C., Hach, F., Sarrafi, I., Bell, R. H., McConeghy, B., Beja, K., et al. (2017). SiNVICT: ultra-sensitive detection of single nucleotide variants and indels in circulating tumour DNA. *Bioinformatics* 33, 26–34. doi:10.1093/bioinformatics/btw536

Kwapisz, D. (2017). The first liquid biopsy test approved. Is it a new era of mutation testing for non-small cell lung cancer? *Ann. Transl. Med.* 5, 46. doi:10.21037/atm.2017.01.32

Lai, Z., Markovets, A., Ahdesmaki, M., Chapman, B., Hofmann, O., McEwen, R., et al. (2016). VarDict: a novel and versatile variant caller for next-generation sequencing in cancer research. *Nucleic Acids Res.* 44, e108. doi:10.1093/nar/gkw227

Langmead, B., and Salzberg, S. L. (2012). Fast gapped-read alignment with Bowtie 2. *Nat. Methods* 9, 357–359. doi:10.1038/nmeth.1923

Leal, A., van Grieken, N. C. T., Palsgrove, D. N., Phallen, J., Medina, J. E., Hruban, C., et al. (2020). White blood cell and cell-free DNA analyses for detection of residual disease in gastric cancer. *Nat. Commun.* 11, 525. doi:10.1038/s41467-020-14310-3

Leenanitikul, J., Chanchaem, P., Mankhong, S., Denariyakoon, S., Fongchaiya, V., Arayataweegool, A., et al. (2023). Concordance between whole exome sequencing of circulating tumor DNA and tumor tissue. *PLOS ONE* 18, e0292879. doi:10.1371/journal.pone.0292879

Li, H., and Durbin, R. (2009). Fast and accurate short read alignment with Burrows–Wheeler transform. *Bioinformatics* 25, 1754–1760. doi:10.1093/bioinformatics/btp324

Liang, J., Zhao, W., Lu, C., Liu, D., Li, P., Ye, X., et al. (2020). Next-generation sequencing analysis of ctDNA for the detection of glioma and metastatic brain tumors in adults. *Front. Neurol.* 11, 544. doi:10.3389/fneur.2020.00544

Lin, C., Liu, X., Zheng, B., Ke, R., and Tzeng, C.-M. (2021). Liquid biopsy, ctDNA diagnosis through NGS. *Life* 11, 890. doi:10.3390/life11090890

Ling, X., Wang, C., Li, L., Pan, L., Huang, C., Zhang, C., et al. (2023). Third-generation sequencing for genetic disease. *Clin. Chim. Acta Int. J. Clin. Chem.* 551, 117624. doi:10.1016/j.cca.2023.117624

Liu, X., Han, S., Wang, Z., Gelernter, J., and Yang, B.-Z. (2013). Variant callers for next-generation sequencing data: a comparison study. *PLoS ONE* 8, e75619. doi:10.1371/journal.pone.0075619

Liu, Y., Feng, Y., Hou, T., Lizaso, A., Xu, F., Xing, P., et al. (2020). Investigation on the potential of circulating tumor DNA methylation patterns as prognostic biomarkers for lung squamous cell carcinoma. *Lung Cancer Res.* 9, 2356–2366. doi:10.21037/tlcr-20-1070

Lomakin, A., Svedlund, J., Strell, C., Gataric, M., Shmatko, A., Rukhovich, G., et al. (2022). Spatial genomics maps the structure, nature and evolution of cancer clones. *Nature* 611, 594–602. doi:10.1038/s41586-022-05425-2

Mahamdallie, S., Ruark, E., Yost, S., Münz, M., Renwick, A., Poyastro-Pearson, E., et al. (2018). The Quality Sequencing Minimum (QSM): providing comprehensive, consistent, transparent next generation sequencing data quality assurance. *Wellcome Open Res.* 3, 37. doi:10.12688/wellcomeopenres.14307.1

Mallampati, S., Zalles, S., Duose, D. Y., Hu, P. C., Medeiros, L. J., Wistuba, I. I., et al. (2019). Development and application of duplex sequencing strategy for cell-free DNA–based longitudinal monitoring of stage IV colorectal cancer. *J. Mol. Diagn* 21, 994–1009. doi:10.1016/j.jmoldx.2019.06.008

Malone, E. R., Oliva, M., Sabatini, P. J. B., Stockley, T. L., and Siu, L. L. (2020). Molecular profiling for precision cancer therapies. *Genome Med.* 12, 8. doi:10.1186/s13073-019-0703-1

Marcozzi, A., Jager, M., Elferink, M., Straver, R., van Ginkel, J. H., Peltenburg, B., et al. (2021). Accurate detection of circulating tumor DNA using nanopore consensus sequencing. *NPJ Genomic Med.* 6, 106. doi:10.1038/s41525-021-00272-y

Marshall, C. R., Chowdhury, S., Taft, R. J., Lebo, M. S., Buchan, J. G., Harrison, S. M., et al. (2020). Best practices for the analytical validation of clinical whole-genome sequencing intended for the diagnosis of germline disease. *Npj Genomic Med.* 5, 47. doi:10.1038/s41525-020-00154-9

Martins, I., Ribeiro, I. P., Jorge, J., Gonçalves, A. C., Sarmento-Ribeiro, A. B., Melo, J. B., et al. (2021). Liquid biopsies: applications for cancer diagnosis and monitoring. *Genes.* 12, 349. doi:10.3390/genes12030349

Noguchi, T., Sakai, K., Iwahashi, N., Matsuda, K., Matsukawa, H., Yahata, T., et al. (2020). Changes in the gene mutation profiles of circulating tumor DNA detected using CAPP-Seq in neoadjuvant chemotherapy-treated advanced ovarian cancer. *Oncol. Lett.* 19, 2713–2720. doi:10.3892/ol.2020.11356

Oliveira, K. C. S., Ramos, I. B., Silva, J. M. C., Barra, W. F., Riggins, G. J., Palande, V., et al. (2020). Current perspectives on circulating tumor DNA, precision medicine, and personalized clinical management of cancer. *Mol. Cancer Res.* 18, 517–528. doi:10.1158/1541-7786.MCR-19-0768

Parikh, A. R., Van Seventer, E. E., Siravegna, G., Hartwig, A. V., Jaimovich, A., He, Y., et al. (2021). Minimal residual disease detection using a plasma-only circulating tumor DNA assay in patients with colorectal cancer. *Clin. Cancer Res.* 27, 5586–5594. doi:10.1158/1078-0432.CCR-21-0410

Peng, Q., Xu, C., Kim, D., Lewis, M., DiCarlo, J., and Wang, Y. (2019). Targeted single primer enrichment sequencing with single end duplex-UMI. *Sci. Rep.* 9, 4810. doi:10.1038/s41598-019-41215-z

Phallen, J., Sausen, M., Adleff, V., Leal, A., Hruban, C., White, J., et al. (2017). Direct detection of early-stage cancers using circulating tumor DNA. *Sci. Transl. Med.* 9, eaan2415. doi:10.1126/scitranslmed.aan2415

QIAseq SPE technology for Illumina (2018). Redefining amplicon sequencing - QIAGEN. Available at: https://www.qiagen.com/us/resources/resourcedetail?id=b3363886-aaed-4e0d-8d4b-3291b28593c5&lang=en (Accessed July 5, 2024).

Reinert, K., Langmead, B., Weese, D., and Evers, D. J. (2015). Alignment of next-generation sequencing reads. *Annu. Rev. Genomics Hum. Genet.* 16, 133–151. doi:10.1146/annurev-genom-090413-025358

Rezazadeh, A., Pruett, J., Detzner, A., Edwin, N., Hamadani, M., Shah, N. N., et al. (2024). Immunoglobulin high throughput sequencing (Ig-HTS) minimal residual disease (MRD) analysis is an effective surveillance tool in patients with mantle cell lymphoma. *Clin. Lymphoma Myeloma Leuk.* 24, 254–259. doi:10.1016/j.clml.2023.12.006

Sabatier, R., Garnier, S., Guille, A., Carbuccia, N., Pakradouni, J., Adelaide, J., et al. (2022). Whole-genome/exome analysis of circulating tumor DNA and comparison to tumor genomics from patients with heavily pre-treated ovarian cancer: subset analysis of the PERMED-01 trial. *Front. Oncol.* 12, 946257. doi:10.3389/fonc.2022.946257

Salk, J. J., Schmitt, M. W., and Loeb, L. A. (2018). Enhancing the accuracy of next-generation sequencing for detecting rare and subclonal mutations. *Nat. Rev. Genet.* 19, 269–285. doi:10.1038/nrg.2017.117

Sanz-Garcia, E., Zhao, E., Bratman, S. V., and Siu, L. L. (2022). Monitoring and adapting cancer treatment using circulating tumor DNA kinetics: current research, opportunities, and challenges. *Sci. Adv.* 8, eabi8618. doi:10.1126/sciadv.abi8618

Scarano, C., Veneruso, I., De Simone, R. R., Di Bonito, G., Secondino, A., and D'Argenio, V. (2024). The third-generation sequencing challenge: novel insights for the omic sciences. *Biomolecules* 14, 568. doi:10.3390/biom14050568

Serrano, C., Leal, A., Kuang, Y., Morgan, J. A., Barysauskas, C. M., Phallen, J., et al. (2019). Phase I study of rapid alternation of sunitinib and regorafenib for the treatment

of tyrosine kinase inhibitor refractory gastrointestinal stromal tumors. *Clin. Cancer Res.* 25, 7287–7293. doi:10.1158/1078-0432.CCR-19-2150

Shen, W., Shan, B., Liang, S., Zhang, J., Yu, Y., Zhang, Y., et al. (2021). Hybrid capture-based genomic profiling of circulating tumor DNA from patients with advanced ovarian cancer. *Pathol. Oncol. Res.* 27, 581534. doi:10.3389/pore.2021.581534

Shi, Z., Lopez, J., Kalliney, W., Sutton, B., Simpson, J., Maggert, K., et al. (2022). Development and evaluation of ActSeq: a targeted next-generation sequencing panel for clinical oncology use. *PLoS ONE* 17, e0266914. doi:10.1371/journal.pone.0266914

Shields, M. D., Chen, K., Dutcher, G., Patel, I., and Pellini, B. (2022). Making the rounds: exploring the role of circulating tumor DNA (ctDNA) in non-small cell lung cancer. *Int. J. Mol. Sci.* 23, 9006. doi:10.3390/ijms23169006

Singh, R. R. (2022). Target enrichment approaches for next-generation sequencing applications in oncology. *Diagnostics* 12, 1539. doi:10.3390/diagnostics12071539

Sogbe, M., Bilbao, I., Marchese, F. P., Zazpe, J., De Vito, A., Pozuelo, M., et al. (2024). Prognostic value of ultra-low-pass whole-genome sequencing of circulating tumor DNA in hepatocellular carcinoma under systemic treatment. *Clin. Mol. Hepatol.* 30, 177–190. doi:10.3350/cmh.2023.0426

Sun, Y., Liu, F., Fan, C., Wang, Y., Song, L., Fang, Z., et al. (2021). Characterizing sensitivity and coverage of clinical WGS as a diagnostic test for genetic disorders. *BMC Med. Genomics* 14, 102. doi:10.1186/s12920-021-00948-5

Szadkowska, P., Roura, A.-J., Wojtas, B., Wojnicki, K., Licholai, S., Waller, T., et al. (2022). Improvements in quality control and library preparation for targeted sequencing allowed detection of potentially pathogenic alterations in circulating cell-free DNA derived from plasma of brain tumor patients. *Cancers* 14, 3902. doi:10.3390/cancers14163902

Tie, J., Wang, Y., Cohen, J., Li, L., Hong, W., Christie, M., et al. (2021). Circulating tumor DNA dynamics and recurrence risk in patients undergoing curative intent resection of colorectal cancer liver metastases: a prospective cohort study. *PLOS Med.* 18, e1003620. e1003620–e1003620. doi:10.1371/journal.pmed.1003620

Treffer, R., and Deckert, V. (2010). Recent advances in single-molecule sequencing. *Curr. Opin. Biotechnol.* 21, 4–11. doi:10.1016/j.copbio.2010.02.009

Trivedi, U. H., Cã©zard, T., Bridgett, S., Montazam, A., Nichols, J., Blaxter, M., et al. (2014). Quality control of next-generation sequencing data without a reference. *Front. Genet.* 5, 111. doi:10.3389/fgene.2014.00111

Tuaeva, F., Porozov, N., Trukhan, K., Nosyrev, A. E., Kovatsi, L., Spandidos, D. A., et al. (2019). Translational application of circulating DNA in oncology: review of the last decades achievements. *Cells* 8, 1251. doi:10.3390/cells8101251

Turner, N. C., Swift, C., Jenkins, B., Kilburn, L., Coakley, M., Beaney, M., et al. (2023). Results of the c-TRAK TN trial: a clinical trial utilising ctDNA mutation tracking to detect molecular residual disease and trigger intervention in patients with moderate- and high-risk early-stage triple-negative breast cancer. *Ann. Oncol.* 34, 200–211. doi:10.1016/j.annonc.2022.11.005

U.S Food And Drug Administration (2022). List of cleared or approved companion diagnostic devices (*in vitro* and imaging tools). Available at: https://www.fda.gov/medical-devices/in-vitro-diagnostics/list-cleared-or-approved-companion-diagnostic-devices-in-vitro-and-imaging-tools.

U.S Food And Drug Administration (2023). List of cleared or approved companion diagnostic devices (*in vitro* and imaging tools). Available at: https://www.fda.gov/medical-devices/recently-approved-devices/foundationone-liquid-cdx-f1-liquid-cdx-p190032s010 (Accessed January 10, 2024).

van der Pol, Y., Tantyo, N. A., Evander, N., Hentschel, A. E., Wever, B. M., Ramaker, J., et al. (2023). Real-time analysis of the cancer genome and fragmentome from plasma and urine cell-free DNA using nanopore sequencing. *EMBO Mol. Med.* 15, e17282. doi:10.15252/emmm.202217282

Wadapurkar, R. M., and Vyas, R. (2018). Computational analysis of next generation sequencing data and its applications in clinical oncology. *Inf. Med. Unlocked* 11, 75–82. doi:10.1016/j.imu.2018.05.003

Wang, Y., Zhao, Y., Bollas, A., Wang, Y., and Au, K. F. (2021). Nanopore sequencing technology, bioinformatics and applications. *Nat. Biotechnol.* 39, 1348–1365. doi:10.1038/s41587-021-01108-x

Wu, X.-B., Hou, S.-L., Zhang, Q.-H., Jia, N., Hou, M., and Shui, W. (2022). Circulating tumor DNA characteristics based on next generation sequencing and its correlation with clinical parameters in patients with lymphoma. *Front. Oncol.* 12, 901547. doi:10.3389/fonc.2022.901547

Yu, L., Lopez, G., Rassa, J., Wang, Y., Basavanhally, T., Browne, A., et al. (2022). Direct comparison of circulating tumor DNA sequencing assays with targeted large gene panels. *PLOS ONE* 17, e0266889. doi:10.1371/journal.pone.0266889

Zhao, C., Pan, Y., Wang, Y., Li, Y., Han, W., Lu, L., et al. (2020). A novel cell-free single-molecule unique primer extension resequencing (cf-SUPER) technology for bladder cancer non-invasive detection in urine. *Transl. Androl. Urol.* 9, 1222–1231. doi:10.21037/tau-19-774

Zviran, A., Schulman, R. C., Shah, M., Hill, S. T. K., Deochand, S., Khamnei, C. C., et al. (2020). Genome-wide cell-free DNA mutational integration enables ultra-sensitive cancer monitoring. *Nat. Med.* 26, 1114–1124. doi:10.1038/s41591-020-0915-3

frontiers | Frontiers in Molecular Biosciences

TYPE Review
PUBLISHED 09 December 2024
DOI 10.3389/fmolb.2024.1463061

OPEN ACCESS

EDITED BY
Pia Giovannelli,
University of Campania Luigi Vanvitelli, Italy

REVIEWED BY
Mithlesh Kumar Temre,
National Institute on Aging (NIH),
United States
Asha Thomas,
Case Western Reserve University,
United States

*CORRESPONDENCE
Xing Gao,
zoecat2@126.com

†These authors have contributed equally to this work

RECEIVED 11 July 2024
ACCEPTED 21 October 2024
PUBLISHED 09 December 2024

CITATION
Bai B, Xie S, Wang Y, Wu F, Chen Y, Bian J and Gao X (2024) Development of anti-cancer drugs for tumor-associated macrophages: a comprehensive review and mechanistic insights.
Front. Mol. Biosci. 11:1463061.
doi: 10.3389/fmolb.2024.1463061

Development of anti-cancer drugs for tumor-associated macrophages: a comprehensive review and mechanistic insights

Bingjun Bai[1†], Shangzhi Xie[2†], Ya Wang[3], Fei Wu[4], Yao Chen[5], Jia Bian[6] and Xing Gao[7*]

[1]Department of Colorectal Surgery, Sir Run Run Shaw Hospital, School of Medicine, Zhejiang University, Hangzhou, China, [2]Institute of Genomic Medicine, Wenzhou Medical University, Wenzhou, China, [3]Department of Hospital Infection-Control, Zhejiang Cancer Hospital, Hangzhou, China, [4]Institute of Systemic Medicine, Zhejiang University School of Medicine, Hangzhou, China, [5]Department of Medical Oncology, Sir Run Run Shaw Hospital, School of Medicine, Zhejiang University, Hangzhou, China, [6]Department of Gynecology and Obstetrics, The Affiliated People's Hospital of Ningbo University, Ningbo, Zhejiang, China, [7]Department of Oncology, The Second Affiliated Hospital of Soochow University, Suzhou, Jiangsu, China

This review provides an in-depth summary of the development of anti-cancer drugs for tumor-associated macrophages (TAMs), with a particular focus on the development and tissue specialization of macrophages, and factors influencing the polarization of M1 and M2 macrophages, and mechanistic insights underlying the targeting therapeutic approaches. TAMs, pivotal in the tumor microenvironment, exhibit notable plasticity and diverse functional roles. Influenced by the complex milieu, TAMs polarize into M1-type, which suppresses tumors, and M2-type, which promotes metastasis. Notably, targeting M2-TAMs is a promising strategy for tumor therapy. By emphasizing the importance of macrophages as a therapeutic target of anti-cancer drugs, this review aims to provide valuable insights and research directions for clinicians and researchers.

KEYWORDS

tumor-associated macrophages (TAMs), tumor microenvironment (TME), TAMs-targeted therapies, macrophage polarization, M1 and M2 macrophages

1 Introduction

1.1 Macrophages: development and tissue specialization

Macrophages, initially detailed by Ilya Metchnikoff (Stefater et al., 2011), possess the capacity to engulf and eliminate cellular components from both living and dead organisms and host cells (Ji et al., 2024). Macrophages can be categorized into two main subtypes: tissue-resident macrophages and monocyte-derived inflammatory macrophages. Tissue-resident macrophages primarily execute anti-tumor functions through cytotoxicity and antibody-dependent cell-mediated cytotoxicity (ADCC). In contrast, monocyte-derived inflammatory macrophages tend to promote tumor metastasis and suppress T cell-mediated immune responses (Sun et al., 2023). The predominant population, tissue-resident macrophages, originates embryonically and is distributed across various tissues where microcellular invasion or foreign body accumulation occurs frequently, such as the liver, lymph nodes, and spleen. Recent research has highlighted the indispensable

role of tissue-resident macrophages in responding to lung injury post-trauma or stroke through specific inflammatory pathways (Aegerter et al., 2022). Notably, investigations have revealed that depleting tissue-resident macrophages, instead of impeding the recruitment of monocyte-derived macrophages, effectively mitigates lung injury after trauma or stroke events (Hoyer et al., 2019). Over time, the belief that tumor-associated macrophages (TAMs) were primarily recruited from peripheral sites has shifted due to novel insights from gene pedigree tracing, xenogeneic reproduction, and bone marrow chimera studies, indicating both embryonic and pathological origins as key sources (1) (Rodell et al., 2019; Fu et al., 2020). In a steady state, most tissue-resident macrophages are derived from the yolk sac and fetal liver. However, during pathological conditions, monocytes turned out to be a prominent source (van de Laar et al., 2016). These findings about mature macrophage proliferation prompt us to re-evaluate the interplay between macrophage proliferation and differentiation. Each organ harbors a unique macrophage subpopulation that, following birth, is renewed by circulating monocytes, establishing a distinct regeneration pattern.

1.2 Tumor microenvironment and tumor-associated macrophages

The tumor microenvironment (TME), consisting of various cellular and non-cellular components, is the complex ecosystem that surrounds and interacts with cancer cells within a tumor. As one of the most concerned cellular components, immune cells include innate immune system cells (including macrophages, neutrophils, myelogenic suppressor cells, dendritic cells and natural killer cells) and adaptive immune system cells (T and B lymphocytes) (Ji et al., 2024; Anderson and Simon, 2020; Ruf et al., 2023). The TME is highly dynamic and can influence cancer cell behavior, drug resistance, and treatment outcomes (Escamilla et al., 2015). Understanding and targeting the TME has become an important focus in cancer research and therapy development, leading to new approaches such as immunotherapy and strategies to modify the tumor microenvironment to enhance treatment efficacy (Ruf et al., 2023).

Tumor metastasis, a leading cause of cancer-related deaths, is propelled not only by intrinsic alterations in tumor cells but also by the intricate interactions between cancer cells and their evolving microenvironment (Neophytou et al., 2021). TAMs are crucial in these interactions, orchestrating the production of cytokines, chemokines, and growth factors by T cells, while also promoting the release of inhibitory immune checkpoint proteins that foster an immunosuppressive microenvironment (Sun et al., 2023). Although evidence indicates that various types of macrophages can coexist in tumors, recruited macrophages may account for the majority of TAMs (Bied et al., 2023). By influencing cancer cell metastasis and offering targets for immunotherapy, TAMs play a central role in tumor progression. Simultaneously, they offer several targets for blocking immunotherapy at some checkpoints to combat tumor progression. As their relationship with malignant tumors becomes clearer, TAMs are garnering recognition as potential biomarkers for cancer diagnosis and prognostic assessment. Moreover, they have emerged as promising therapeutic targets in cancer treatment, spurring active research in this field (Dallavalasa et al., 2021). However, quantifying the respective contributions of these macrophage subtypes at different stages of tumor progression remains challenging. Therefore, further investigations aimed at characterizing TAMs across different human cancers are warranted (Dallavalasa et al., 2021).

1.3 Factors influencing the polarization of macrophages

Macrophage polarization is a complex biological process intricately governed by a multitude of factors, with cytokines and signaling pathways playing pivotal roles. Pathways such as PI3K/Akt, MAPK, and NF- κB are central to this regulatory network (Hu et al., 2002; Jia et al., 2023; Tosic and Frank, 2021). Macrophages express various markers from different subtypes depending on their microenvironment and activation state so that their classifications are not rigid. CD68 is a pan-macrophage marker widely used to identify macrophages in human tissues but lacks specificity. CD80 and CD86 are co-stimulatory molecules expressed on activated macrophages, which are often associated with pro-inflammatory (M1) macrophages (Van Dyken and Locksley, 2013). In contrast, CD206 is another marker associated with anti-inflammatory (M2) macrophages. Besides, CD163, a number of the scavenger receptor family, offers greater specificity and is exclusive to the monocyte/macrophage lineage (Tardito et al., 2019). CD115, also named the receptor for colony-stimulating factor 1 (CSF1R), is important for macrophage development. CD204 is expressed on tissue macrophages. What's more, advanced techniques like flow cytometry, immunohistochemistry, and single-cell RNA sequencing are used to analyze these markers and characterize macrophage populations in complex tissues or cell mixtures.

Researchers often use combinations of several markers to more accurately characterize macrophage populations in specific circumstances. The M1/M2 classification is a simplification of macrophage activation states. These two distinct types of macrophages have different functions and characteristics, and they play crucial roles in various physiological and pathological processes. M1 macrophages, also known as "Killer" macrophages, differentiate from monocytes in response to type 1 T helper cell (Th1) cytokines like INF-γ, granulocyte-macrophage colony-stimulating factor and lipopolysaccharide (Pasca et al., 2020). M1 macrophages are involved in the pro-inflammatory response, host defense against pathogens, and anti-tumor activities. They produce high levels of pro-inflammatory cytokines, such as interleukin (IL)-1, IL-6, IL-12, IL-23, and tumor necrosis factor (TNF) (Klichinsky et al., 2020). Besides, M1 macrophages produce high levels of nitric oxide through expressing inducible Nitric Oxide Synthase (iNOS). In contrast, M2 macrophages, termed "Repair" macrophages, are activated by anti-inflammatory cytokines, such as IL-4, IL-13, IL-10, macrophage colony-stimulating factor (M-CSF), prostaglandin F (PGF), and vitamin D3. The main functions of M2 macrophages are tissue repair, wound healing, and immunoregulation. They mainly produce anti-inflammatory cytokines such as IL-10, TGF-β, VEGF-A, and matrix metalloproteinase 2 (MMP2). A higher expression level of arginase-1 enables M2 macrophages to have the function of

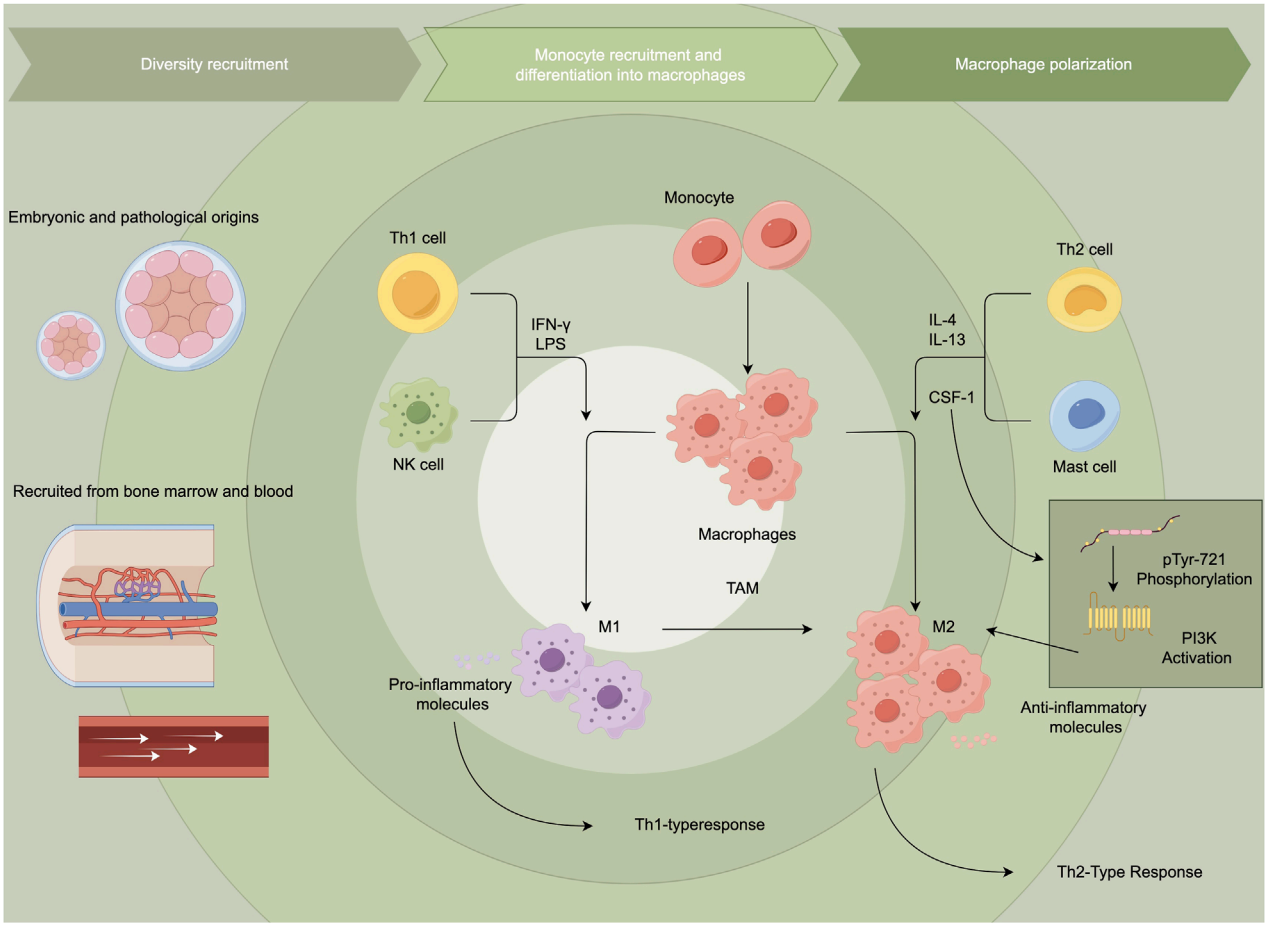

FIGURE 1
Tumor-associated macrophages and macrophage polarization. This figure illustrates the recruitment and differentiation of monocytes into macrophages, highlighting their polarization into pro-inflammatory M1 or anti-inflammatory M2 phenotypes. M1 macrophages promote Th1 responses, while M2 macrophages, often associated with tumor-associated macrophages, support Th2 responses and tumor progression.

tissue repair and fibrosis. M2 macrophages promote angiogenesis by producing growth factors, like VEGF. At the level of transcriptional modification, most changes in histone methylation and acetylation modifiers are concentrated in M1 macrophages (Zhang et al., 2024), for example, histone acetylation mediated by acetyl-CoA enhances the expression of pro-inflammatory genes in LPS-activated macrophages (Sun et al., 2022), while almost all modifiers related to histone crotonylation are activated in M2 macrophages. In the tumor microenvironment, TAMs are commonly categorized as M2-like macrophages, distinguished by elevated levels of anti-inflammatory cytokines, scavenger receptors, angiogenic factors, and proteases. The signaling axis of CSF-1 and its receptor CSF-1R remarkably influence the survival and activation of TAMs. Tumor cells secrete CSF-1, which not only promotes the recruitment of macrophages but also polarizes them towards an M2-like TAM phenotype (Pedersen et al., 2014). When CSF-1R is activated, phosphorylation at the Y721 site (pTyr-721) provides a critical binding and activation site for PI3K (Figure 1) (Guo et al., 2006; Caescu et al., 2015).

Across various cancer types, including non-small cell lung cancer (NSCLC), ovarian, gastric, melanoma, and breast cancers, CD68 expression is associated with a poorer prognosis and reduced survival rates (Zhang et al., 2017). Specifically in NSCLC, CD68-positive macrophages inversely correlate with patient survival and are associated with increased tumor IL-8 expression. This relationship suggests a potential contribution to heightened tumor angiogenesis (Zhang et al., 2017). Elevated levels of CD68-positive infiltrating TAMs in gastric cancer (GC) are associated with increased metastasis and poor prognostic outcomes. Moreover, these TAMs also exhibit features of epithelial-mesenchymal transition (EMT), characterized by the loss of E-cadherin expression and positivity for vimentin (Yang et al., 2019). Similarly, in melanoma, an abundance of CD68+ macrophages correlates with a poorer prognosis and increased melanoma-specific mortality (Tariq et al., 2017). Zhang et al. suggest that the reduction of CD206+ TAMs in gastric cancer is associated with prolonged disease-free survival (DFS), highlighting their significance as prognostic indicators (Zhang et al., 2021). Recent studies also reveal a notable positive correlation between the infiltration of CD206-expressing TAMs in ovarian and renal cancers and lower patient survival rates (Sun et al., 2020). Stabilin-1, a multifunctional scavenger receptor found in alternatively activated macrophages, is critical for removing unwanted autologous material from the body (Manta et al., 2022).

Extensive infiltration of Stabilin-1-expressing TAMs has been observed in metastatic lesions of human primary breast tumors. Notably, these TAMs show tumor growth-promoting properties in a mouse model of mammary adenocarcinoma (Riabov et al., 2016).

2 Therapeutic target of cancer

TAMs are instrumental in enhancing tumor cell resistance to chemotherapy and radiotherapy by delivering survival factors and activating anti-apoptotic mechanisms. Consequently, anticancer therapeutic targeting TAMs have a solid theoretical basis and are expected to be a promising strategy for enhancing therapeutic efficacy. Approaches to target TAMs include: 1) inhibiting monocyte recruitment from systemic circulation to tumor sites; 2) reprogramming TAMs towards an anti-tumor phenotype; 3) disrupting TAM activation pathways to reduce their pro-tumor activities; and 4) integrating TAM targeting with conventional treatments like chemotherapy or radiotherapy (Anfray et al., 2019).

2.1 Inhibition of monocyte induction from systemic circulation to the tumor tissue

Tumor cells promote the migration of myeloid-derived suppressor cells (MDSCs) and macrophages into the tumor microenvironment by secreting chemokines such as CCL2, CCL5, and CXCL12. Disrupting these recruitment pathways can effectively slow tumor growth and progression (Groth et al., 2019). Carlumab, a monoclonal antibody targeting CCL2, has shown efficacy in reducing prostate-specific antigen levels and inhibiting tumor progression in a phase II clinical trial (Martori et al., 2022). Similarly, Bindarit inhibits key inflammatory chemokines including MCP-1 (CCL2), MCP-3 (CCL7), and MCP-2 (CCL8), significantly affecting the NF-κB signaling pathway associated with monocyte recruitment without impacting other pathways, demonstrating its specificity and potential in reducing monocyte recruitment into tumors (Wolfsberger et al., 2021).

Inhibiting monocyte induction from systemic circulation to tumor tissue is a pivotal strategy in cancer treatment. Targeting the chemokine signaling pathways that facilitate monocyte recruitment offers a promising approach to alter the tumor microenvironment and potentially boost the efficacy of cancer therapies. Table 1 below highlights several drugs currently explored for their role in inhibiting monocyte induction and influencing TAM behavior across various cancer types: BLZ945 and PLX3397, targeting CSF-1R, are crucial in modulating the tumor microenvironment by reducing monocyte recruitment and enhancing T cell infiltration. These interventions, evidenced in trials NCT02829723 and NCT02371369, not only impede tumor progression but also strengthen the overall immune response within the tumor milieu. Cabiralizumab, another CSF-1R inhibitor, disrupts monocyte recruitment pathways, significantly impacting the development and progression of solid tumors as indicated in clinical trial NCT03502330. CCX872 targets CCR2, playing a significant role in monocyte recruitment to tumor sites. By blocking this pathway, CCX872 aims to reduce the number of macrophages in the tumor microenvironment, potentially limiting tumor growth and metastasis, particularly in pancreatic cancer, as studied in NCT02345408.

2.2 Reprogramming of TAMs

Reprogramming TAMs to adopt an anti-tumor phenotype represents a promising avenue in cancer immunotherapy. This approach aims to shift their behavior from pro-tumor (M2-like) to anti-tumor (M1-like) activities, thereby harnessing the immune system's natural defenses against cancer. Various therapeutic strategies have been developed to achieve this goal, including the use of CSF1R inhibitors, immune checkpoint inhibitors, and other reprogramming agents. This intervention works by encouraging TAMs to enhance immune cell recruitment, augment phagocytic activity, and produce cytotoxic molecules that directly attack tumor cells. By remodeling the tumor microenvironment towards an immune-supportive state, these approaches not only suppress tumor growth but also synergistically enhance the efficacy of existing cancer treatments, potentially leading to improved clinical outcomes for patients (Genard et al., 2017; Khan et al., 2023).

Thymosin-α, a small bioactive polypeptide secreted by thymus tissue, has garnered significant attention in cancer immunotherapy due to its unique capacity to reprogram TAMs into functional dendritic cells. This transformation profoundly impacts T cell differentiation and activation, ultimately amplifying the anti-tumor immune response (Sun et al., 2023). This reprogramming is leveraged in treatments for metastatic melanoma and advanced non-small cell lung cancer (NSCLC). Clinical studies have demonstrated that Thymosin-α-based therapies can significantly prolong patient survival, offering a promising adjunct to conventional cancer treatments. Moreover, its capacity to modulate the tumor microenvironment and enhance immune surveillance has sparked interest in combining Thymosin-α with other immunotherapeutic approaches, potentially opening new avenues for more effective and personalized cancer management strategies (Singh et al., 2017). Overall, the reprogramming of TAMs represents a promising area in cancer therapy, focusing on converting the immunosuppressive tumor environment into an immunostimulatory one.

2.3 Targeting the activation of TAMs

Legumain, a lysosomal cysteine protease, is highly expressed in many solid tumors, TAMs and endothelial cells of tumor neovascularization. Angiogenesis, tumor invasion, proliferation, and metastasis are pivotal events in malignant tumor progression, intricately linked to various biological processes within the tumor microenvironment. Recent studies have unveiled that a DNA vaccine targeting legumain can effectively stimulate $CD8^+$ T cells to attack TAMs, leading to a significant reduction in TAM density within tumor tissues. Furthermore, this vaccine markedly decreases the release of multiple angiogenic factors from TAMs, including transforming growth factor-β (TGF-β), tumor necrosis factor-α (TNF-α), matrix metalloproteinase-9 (MMP-9), and vascular endothelial growth factor (VEGF). This approach holds the potential to inhibit tumor angiogenesis and metastasis, presenting a novel

TABLE 1 Proposed tumor-associated macrophages targeting therapy.

Drug/Compound	Target	Tumor type	Phase	Clinical trials
BLZ945	CSF-1R	Advanced solid tumors	I/II	NCT02829723
PLX3397	CSF-1R	Tenosynovial giant cell tumor	III	NCT02371369
Cabiralizumab	CSF-1R	Advanced solid tumors	I	NCT03502330
Biophosphonates	TAMs	Various solid tumors	II	Multiple trials
Ibrutinib	BTK	Various cancers	II/III	Multiple trials
CCX872	CCR2	Pancreatic cancer	I/II	NCT02345408
Trabectedin	TAMs	Soft tissue sarcoma	III	Various trials exploring

strategy for cancer treatment. Therefore, Legumain based DNA vaccine can effectively inhibit the growth and metastasis of tumor cells in mouse models of breast cancer, non-small cell lung cancer and colon cancer (Ngambenjawong et al., 2017). Furthermore, CD200S, a variant of CD200, plays a significant role in the reprogramming of TAMs by inducing their trans-differentiation into dendritic cells. This alteration enhances immune responses against tumor cells, effectively targeting the activation pathways of TAMs to curb tumor growth, as shown in a mouse glioma model (Liu et al., 2020).

Recent research highlights the novel application of lovastatin in cancer therapy, particularly its capacity to reduce the population of TAMs. Through gene chip analysis, lovastatin has been observed to downregulate the expression of placental growth factor (PlGF), which is closely associated with enhanced TAM activity. Thus, beyond its conventional role in managing cholesterol, lovastatin presents a new avenue for modulating anti-tumor immunity, offering a fresh strategy for cancer treatment (Yang et al., 2020). Moreover, the role of protein deacetylases in regulating TAM activity has been emphasized in studies involving TMP195, a small molecule inhibitor of class IIa histone deacetylase. Research using the MMTV-PyMT transgenic breast cancer model demonstrated that TMP195 not only stabilizes tumor volume but also significantly reduces the incidence of lung metastases by about threefold. This suggests that by altering TAM functions, TMP195 induces profound changes in the tumor microenvironment, effectively inhibiting tumor growth and the spread of metastasis. These outcomes support the potential of targeted immunotherapy in cancer treatment (Lopez-Yrigoyen et al., 2021).

Nuclear Factor-kappa B (NF-κB) plays a critical role in regulating inflammatory responses, which are heavily implicated in various tumor processes such as promoting Epithelial-Mesenchymal Transition (EMT), enhancing tumor cell migration, and generating Tumor-Initiating Stem Cells (TSCs) (Zhu et al., 2021). These activities collectively contribute to the malignant progression and metastatic potential of tumors. Importantly, TAMs, influenced by NF-κB signals, are known to promote and mediate angiogenesis through the production of interleukins like IL-10, VEGF, and IL-8, making NF-κB a viable target for treating cancers such as urinary bladder cancer (UBC) (Iacona and Lutz, 2019). BAY11-7082, an inhibitor of the NF-κB pathway, effectively reduces the invasiveness of bladder cancer cells and prevents the M2 polarization of TAMs, highlighting its role in macrophage polarization and its potential in modulating tumor microenvironments (Zhang et al., 2019).

2.4 Targeting TAMs in combination with standard therapies

Signal regulatory protein α (SIRP α) is a membrane protein primarily expressed on macrophages and other myeloid immune cells. It can be activated by various mitogens and phosphorylated, transmitting inhibitory signals through binding to SHP-1 and SHP-2 via its immunoreceptor tyrosine-based inhibition motif (ITIM) domain. Additionally, SIRP α can inhibit the activation of downstream pathways and convey negative signals by interacting with CD47 ligands. The blockers of exosomes SIRP α and CD47 can enhance the phagocytic function of cancer cells, suggesting that targeting SIRP α with antibodies presents a promising immunotherapy approach for treating tumors exhibiting high expression of SIRP α, such as renal cell carcinoma and melanoma (Yanagita et al., 2017). Anti-CD47 antibodies are currently demonstrating significant therapeutic potential as agents targeting the CD47/SIRP α signaling axis. Several CD47 antagonists are undergoing extensive investigation in clinical trials, including Hu5F9-G4, humanized anti-human CD47 monoclonal antibody CC-90002, and TTI-621. These drugs operate through various mechanisms to obstruct the interaction between CD47 and SIRP α, thereby stimulating the phagocytosis of tumor cells by macrophages. Consequently, they enhance the immune system's ability to combat tumors, offering novel strategies for treating multiple types of cancer (Weiskopf, 2017; Folkes et al., 2018). Humanized anti-human CD47 monoclonal antibody CC-90002 is currently under investigation for use in both solid tumors and hematological malignancies. TTI-621 is composed of the Ig-V-like domain of human SIRP α connected to the Fc region of human IgG1, which can enhance the phagocytosis of tumor cells and effectively control tumor growth. The potential of targeting CD47 lies in its combination with immunotherapy agents like PD-1 antibodies, aiming to maximize its therapeutic efficacy (Ansell et al., 2021; Feng et al., 2019).

Metformin, a biguanide widely used in diabetes management, has gained attention for its potential applications in the field

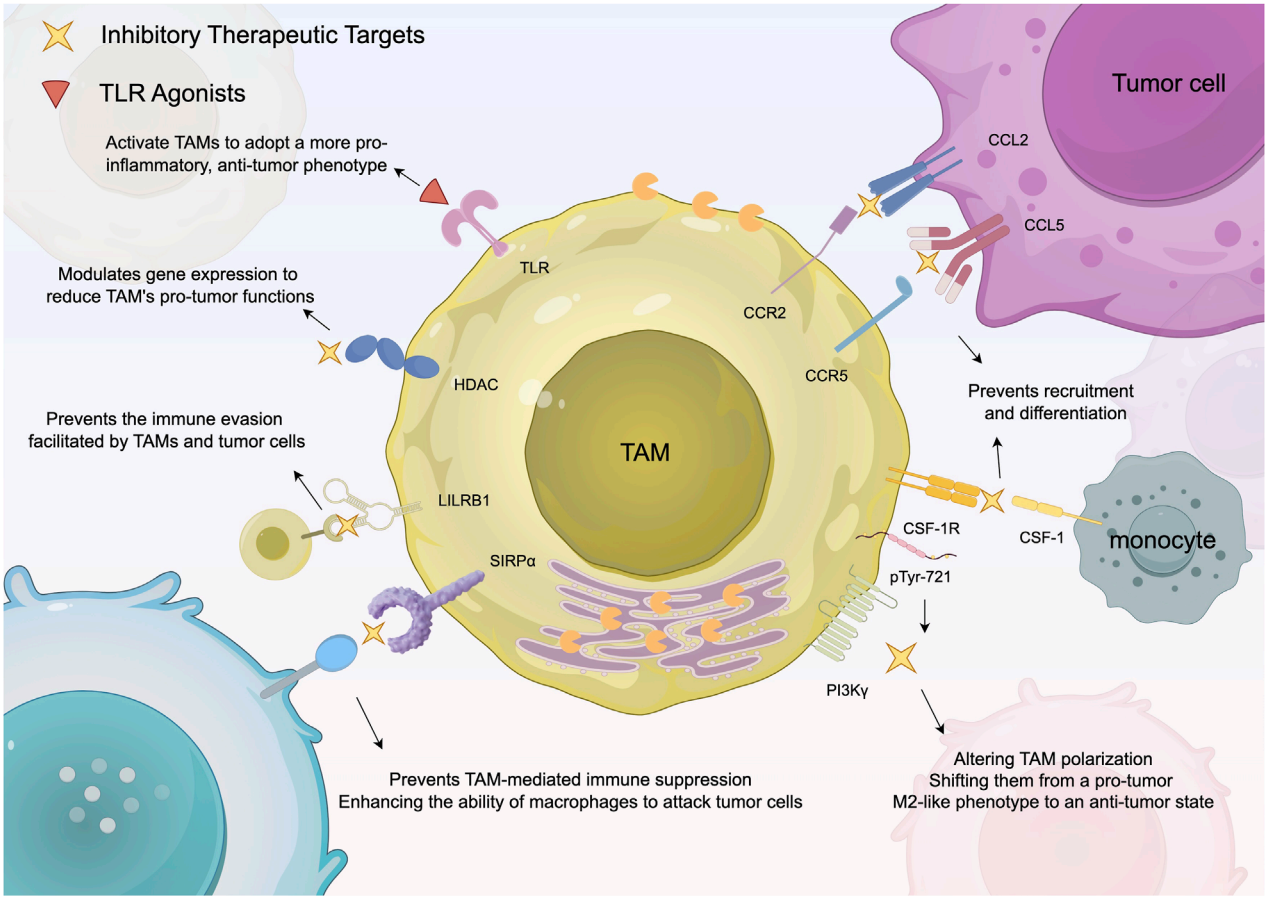

FIGURE 2
Summarizes the existing strategies for targeting TAMs to boost anti-tumor immune responses. This diagram outlines therapeutic strategies targeting TAMs in cancer treatment. It focuses on specific pathways, such as CSF-1R inhibition and CAR-M therapy, that either suppress the tumor-supporting function of M2 macrophages or reprogram them to enhance the immune response against tumors.

of antitumor therapy. This effect is primarily attributed to the activation of the AMP-activated protein kinase (AMPK) signaling pathway, which disrupts the M2 polarization of macrophages. These findings suggest that metformin may exert an anti-tumor metastatic effect, providing a new scientific rationale for its use in anti-tumor therapy. Moreover, these discoveries may further expand the therapeutic potential of metformin in tumor populations (Neophytou et al., 2021).

Resveratrol, a non-flavonoid polyphenolic compound, has garnered significant attention due to its diverse biological activities, including its role as an antioxidant, anti-inflammatory, and anti-cancer agent. It has been observed to inhibit the activation of M2-type macrophages, impacting the tumor microenvironment significantly. One of its mechanisms involves the reduction of STAT3 activation and the decrease in F4/80-positive cells, which contributes to its anti-tumor effects, particularly in inhibiting lung cancer growth. However, the complexities of resveratrol's mechanisms require further investigation to fully understand and harness its potential in cancer therapy (Ge and Ding, 2020).

A novel and promising therapeutic approach for targeting TAMs within the tumor microenvironment involves the use of Chimeric Antigen Receptor T (CAR-T) cells. While traditional CAR-T therapies have been effective in hematological malignancies, the application of this technology to solid tumors has faced significant challenges. However, recent advancements have focused on engineering CAR-T cells to specifically target TAMs, which play a key role in promoting tumor growth and suppressing anti-tumor immunity. By utilizing CAR-T cells directed against macrophage markers such as F4/80, researchers have demonstrated significant reductions in TAM populations within tumors, leading to delayed tumor progression and enhanced immune responses. Importantly, these CAR-T cells not only deplete TAMs but also trigger the release of cytokines, such as IFN-γ, which reprogram the tumor microenvironment to favor immune cell infiltration and activation. This innovative strategy holds promise for improving outcomes in solid tumors by targeting the immunosuppressive components of the tumor microenvironment, potentially paving the way for more effective immunotherapies in the future (Sánchez-Paulete et al., 2022).

Recent advances have introduced CAR-T cell therapies targeting specific TAM markers, such as F4/80, as a novel treatment strategy. This approach not only depletes TAM populations but also reprograms them toward a pro-inflammatory (M1-like) state, enhancing anti-tumor immune responses (Xiang et al., 2021).

Current trends in cancer treatment research increasingly emphasize the development of integrative therapeutic approaches that combine chemotherapy with immunotherapy. For instance, the combination of immune checkpoint inhibitors targeting PD-1, PD-L1, and CTLA-4 with traditional chemotherapies has shown significant survival benefits in treating metastatic tumors, marking substantial progress in oncological therapeutics (Larionova et al., 2019).

Paclitaxel, a naturally derived anticancer drug, has gained wide application in treating various cancers, including breast, ovarian, and lung cancer. By combining paclitaxel with a CSF1R signaling antagonist, studies have shown an effective reduction in macrophage recruitment to tumor sites, thereby enhancing the drug's effectiveness and reducing tumor progression and metastasis in preclinical models (Mantovani et al., 2022). Moreover, this combination has been demonstrated to improve the efficacy of paclitaxel on breast tumors and extend survival in a mouse model with mammary tumors, highlighting the potential of TAM-targeted combination therapies in clinical settings (Brown et al., 2017).

Recent advancements have shown that targeting tumor-associated macrophages can significantly enhance the effectiveness of gemcitabine, particularly in treating pancreatic cancer and NSCLC (Rohila et al., 2023). By inhibiting CSF1R or targeting the CCR2 receptor, both key to macrophage recruitment in tumors, the therapeutic effectiveness of gemcitabine is improved. This approach decreases the number of tumor-promoting macrophages and bolsters anti-tumor T cell responses, thereby reducing tumor growth and metastasis. Such strategies underscore the potential of integrating TAM-targeting therapies with traditional chemotherapy to better manage cancer progression (Poh and Ernst, 2021).

Oncolytic viruses are tumor-killing viruses with the ability to replicate. They invade tumor cells through cell surface molecules. One effective strategy of oncolytic virus therapy involves engineering oncolytic viruses to target specific receptors that are overexpressed in tumor cells. This allows the viruses to invade tumor cells and carry out subsequent functions, enhancing the specificity and efficacy of the therapy (Kubli et al., 2021). A recent study explored the therapeutic use of oncolytic viruses that encode IL-12, a pro-inflammatory cytokine that has previously been shown to be important for the anti-tumor ability of myeloid cells (Nguyen et al., 2020). The findings related to this are illustrated in Figure 2. After the virus particles are transported to glioblastoma, TAMs undergo a transformation to the M2 phenotype, thus killing cancer cells (Malfitano et al., 2020). The transition of TAMs to an M2 phenotype renders gliomas more susceptible to immune checkpoint inhibitors, such as anti-PD-1 and anti-CTLA-4 antibodies. Additionally, when these immune checkpoint inhibitors are administered in combination with viral therapy, they can substantially improve patient survival rates. This integrated approach presents a promising avenue for treating resistant tumors like glioma by activating and bolstering the patient's immune response (Malfitano et al., 2020).

3 Conclusion and perspectives

TAMs play a pivotal yet multifaceted role in the tumor microenvironment, exhibiting both pro- and anti-tumor growth depending on their M1 or M2 polarization states (Ji et al., 2024). This complex behavior has made TAMs as significant targets for anticancer therapies aimed at reducing tumor growth, immune evasion, and metastasis. However, broad-spectrum macrophage targeting presents considerable challenges, including potential systemic toxicity that might affect healthy tissues, limited efficacy in completely controlling tumor progression, and the risk of treatment resistance. These issues necessitate the ongoing development of novel strategies to maintain therapeutic efficacy. The field is evolving with a focus on more refined targeting techniques, such as identifying TAM-specific markers or pathways for more precise intervention. Combining TAM-targeted therapies with other anticancer treatments shows promise in enhancing overall treatment effectiveness and mitigating drug resistance. An emerging strategy involves reprogramming TAMs from a tumor-promoting M2 phenotype to a tumor-inhibiting M1 phenotype, potentially reshaping the tumor microenvironment and bolstering immune responses against cancer.

As research into macrophage functions and the tumor microenvironment advances, more precise and personalized therapeutic strategies are emerging. These advancements may involve the development of highly specific treatments tailored to individual patient profiles, which aim to minimize side effects and improve outcomes. Current progress in the field is expected to address the complexities of TAM-targeted therapies more comprehensively, paving the way for more effective and individualized cancer treatments that leverage the unique dynamics of the tumor microenvironment.

In contrast to other reviews, we emphasize the integration of cutting-edge treatments, such as CAR-T cell therapies, specifically designed to target TAMs, along with the latest advancements in reprogramming macrophages from a tumor-promoting (M2-like) to a tumor-suppressing (M1-like) phenotype. Additionally, our review introduces novel mechanistic insights into the pathways regulating macrophage polarization, utilizing recent advances in single-cell RNA sequencing to provide a more granular understanding of TAM heterogeneity. The combination of these innovations, alongside a thorough examination of ongoing clinical trials and future directions for personalized therapies, ensures that this review not only summarizes current knowledge but also offers forward-looking perspectives that are underexplored in the existing literature.

Author contributions

BB: Writing–original draft, Writing–review and editing. SX: Writing–original draft. YW: Data curation, Formal Analysis, Methodology, Project administration, Writing–review and editing. FW: Resources, Software, Writing–original draft. YC: Supervision, Validation, Writing–review and editing. JB: Validation, Visualization, Writing–review and editing. XG: Conceptualization, Funding acquisition, Supervision, Writing–original draft, Writing–review and editing.

Funding

The author(s) declare that financial support was received for the research, authorship, and/or publication of this article. This

work was supported by Zhejiang Provincial Medical and Health Technology Plan Project (ID: 2023KY302).

Conflict of interest

The authors declare that the research was conducted in the absence of any commercial or financial relationships that could be construed as a potential conflict of interest.

Publisher's note

References

Aegerter, H., Lambrecht, B. N., and Jakubzick, C. V. (2022). Biology of lung macrophages in health and disease. *Immunity* 55 (9), 1564–1580. doi:10.1016/j.immuni.2022.08.010

Anderson, N. M., and Simon, M. C. (2020). The tumor microenvironment. *Curr. Biol.* 30 (16), R921–R925. doi:10.1016/j.cub.2020.06.081

Anfray, C., Ummarino, A., Andón, F. T., and Allavena, P. (2019). Current strategies to target tumor-associated-macrophages to improve anti-tumor immune responses. *Cells* 9 (1), 46. doi:10.3390/cells9010046

Ansell, S. M., Maris, M. B., Lesokhin, A. M., Chen, R. W., Flinn, I. W., Sawas, A., et al. (2021). Phase I study of the CD47 blocker TTI-621 in patients with relapsed or refractory hematologic malignancies. *Clin. Cancer Res.* 27 (8), 2190–2199. doi:10.1158/1078-0432.CCR-20-3706

Bied, M., Ho, W. W., Ginhoux, F., and Blériot, C. (2023). Roles of macrophages in tumor development: a spatiotemporal perspective. *Cell. and Mol. Immunol.* 20 (9), 983–992. doi:10.1038/s41423-023-01061-6

Brown, J. M., Recht, L., and Strober, S. (2017). The promise of targeting macrophages in cancer therapy. *Clin. Cancer Res.* 23 (13), 3241–3250. doi:10.1158/1078-0432.CCR-16-3122

Caescu, C. I., Guo, X., Tesfa, L., Bhagat, T. D., Verma, A., Zheng, D., et al. (2015). Colony stimulating factor-1 receptor signaling networks inhibit mouse macrophage inflammatory responses by induction of microRNA-21. *Blood* 125 (8), e1–e13. doi:10.1182/blood-2014-10-608000

Dallavalasa, S., Beeraka, N. M., Basavaraju, C. G., Tulimilli, S. V., Sadhu, S. P., Rajesh, K., et al. (2021). The role of tumor associated macrophages (TAMs) in cancer progression, chemoresistance, angiogenesis and metastasis-current status. *Curr. Med. Chem.* 28 (39), 8203–8236. doi:10.2174/0929867328666210720143721

Escamilla, J., Schokrpur, S., Liu, C., Priceman, S. J., Moughon, D., Jiang, Z., et al. (2015). CSF1 receptor targeting in prostate cancer reverses macrophage-mediated resistance to androgen blockade therapy. *Cancer Res.* 75 (6), 950–962. doi:10.1158/0008-5472.CAN-14-0992

Feng, M., Jiang, W., Kim, B. Y. S., Zhang, C. C., Fu, Y. X., and Weissman, I. L. (2019). Phagocytosis checkpoints as new targets for cancer immunotherapy. *Nat. Rev. Cancer* 19 (10), 568–586. doi:10.1038/s41568-019-0183-z

Folkes, A. S., Feng, M., Zain, J. M., Abdulla, F., Rosen, S. T., and Querfeld, C. (2018). Targeting CD47 as a cancer therapeutic strategy: the cutaneous T-cell lymphoma experience. *Curr. Opin. Oncol.* 30 (5), 332–337. doi:10.1097/CCO.0000000000000468

Fu, L.-Q., Du, W. L., Cai, M. H., Yao, J. Y., Zhao, Y. Y., and Mou, X. Z. (2020). The roles of tumor-associated macrophages in tumor angiogenesis and metastasis. *Cell. Immunol.* 353, 104119. doi:10.1016/j.cellimm.2020.104119

Ge, Z., and Ding, S. (2020). The crosstalk between tumor-associated macrophages (TAMs) and tumor cells and the corresponding targeted therapy. *Front. Oncol.* 10, 590941. doi:10.3389/fonc.2020.590941

Genard, G., Lucas, S., and Michiels, C. (2017). Reprogramming of tumor-associated macrophages with anticancer therapies: radiotherapy versus chemo-and immunotherapies. *Front. Immunol.* 8, 828. doi:10.3389/fimmu.2017.00828

Groth, C., Hu, X., Weber, R., Fleming, V., Altevogt, P., Utikal, J., et al. (2019). Immunosuppression mediated by myeloid-derived suppressor cells (MDSCs) during tumour progression. *Br. J. cancer* 120 (1), 16–25. doi:10.1038/s41416-018-0333-1

Guo, J., Marcotte, P. A., McCall, J. O., Dai, Y., Pease, L. J., Michaelides, M. R., et al. (2006). Inhibition of phosphorylation of the colony-stimulating factor-1 receptor (c-Fms) tyrosine kinase in transfected cells by ABT-869 and other tyrosine kinase inhibitors. *Mol. Cancer Ther.* 5 (4), 1007–1013. doi:10.1158/1535-7163.MCT-05-0359

Hoyer, F. F., Naxerova, K., Schloss, M. J., Hulsmans, M., Nair, A. V., Dutta, P., et al. (2019). Tissue-specific macrophage responses to remote injury impact the outcome of subsequent local immune challenge. *Immunity* 51 (5), 899–914. doi:10.1016/j.immuni.2019.10.010

Hu, X., Herrero, C., Li, W. P., Antoniv, T. T., Falck-Pedersen, E., Koch, A. E., et al. (2002). Sensitization of IFN-gamma Jak-STAT signaling during macrophage activation. *Nat. Immunol.* 3 (9), 859–866. doi:10.1038/ni828

Iacona, J. R., and Lutz, C. S. (2019). miR-146a-5p: expression, regulation, and functions in cancer. *Wiley Interdiscip. Rev. RNA* 10 (4), e1533. doi:10.1002/wrna.1533

Ji, S., Shi, Y., and Yin, B. (2024). Macrophage barrier in the tumor microenvironment and potential clinical applications. *Cell Commun. Signal* 22 (1), 74. doi:10.1186/s12964-023-01424-6

Jia, L., Wang, Y., Ma, X., Wang, H., and Fu, R. (2023). A study on the role of Wip1 in renal fibrosis by modulating macrophage phenotype. *Arch. Med. Res.* 54 (4), 332–338. doi:10.1016/j.arcmed.2023.04.003

Khan, S. U., Khan, M. U., Azhar Ud Din, M., Khan, I. M., Khan, M. I., Bungau, S., et al. (2023). Reprogramming tumor-associated macrophages as a unique approach to target tumor immunotherapy. *Front. Immunol.* 14, 1166487. doi:10.3389/fimmu.2023.1166487

Klichinsky, M., Ruella, M., Shestova, O., Lu, X. M., Best, A., Zeeman, M., et al. (2020). Human chimeric antigen receptor macrophages for cancer immunotherapy. *Nat. Biotechnol.* 38 (8), 947–953. doi:10.1038/s41587-020-0462-y

Kubli, S. P., Berger, T., Araujo, D. V., Siu, L. L., and Mak, T. W. (2021). Beyond immune checkpoint blockade: emerging immunological strategies. *Nat. Rev. Drug Discov.* 20 (12), 899–919. doi:10.1038/s41573-021-00155-y

Larionova, I., Cherdyntseva, N., Liu, T., Patysheva, M., Rakina, M., and Kzhyshkowska, J. (2019). Interaction of tumor-associated macrophages and cancer chemotherapy. *Oncoimmunology* 8 (7), e1596004. doi:10.1080/2162402X.2019.1596004

Liu, J.-Q., Hu, A., Zhu, J., Yu, J., Talebian, F., and Bai, X. F. (2020). CD200-CD200R pathway in the regulation of tumor immune microenvironment and immunotherapy. *Adv. Exp. Med. Biol.* 1223, 155–165. doi:10.1007/978-3-030-35582-1_8

Lopez-Yrigoyen, M., Cassetta, L., and Pollard, J. W. (2021). Macrophage targeting in cancer. *Ann. N. Y. Acad. Sci.* 1499 (1), 18–41. doi:10.1111/nyas.14377

Malfitano, A. M., Pisanti, S., Napolitano, F., Di Somma, S., Martinelli, R., and Portella, G. (2020). Tumor-associated macrophage status in cancer treatment. *Cancers* 12 (7), 1987. doi:10.3390/cancers12071987

Manta, C.-P., Leibing, T., Friedrich, M., Nolte, H., Adrian, M., Schledzewski, K., et al. (2022). Targeting of scavenger receptors stabilin-1 and stabilin-2 ameliorates atherosclerosis by a plasma proteome switch mediating monocyte/macrophage suppression. *Circulation* 146 (23), 1783–1799. doi:10.1161/CIRCULATIONAHA.121.058615

Mantovani, A., Allavena, P., Marchesi, F., and Garlanda, C. (2022). Macrophages as tools and targets in cancer therapy. *Nat. Rev. Drug Discov.* 21 (11), 799–820. doi:10.1038/s41573-022-00520-5

Martori, C., Sanchez-Moral, L., Paul, T., Pardo, J. C., Font, A., Ruiz de Porras, V., et al. (2022). Macrophages as a therapeutic target in metastatic prostate cancer: a way to overcome immunotherapy resistance? *Cancers* 14 (2), 440. doi:10.3390/cancers14020440

Neophytou, C. M., Panagi, M., Stylianopoulos, T., and Papageorgis, P. (2021). The role of tumor microenvironment in cancer metastasis: molecular mechanisms and therapeutic opportunities. *Cancers* 13 (9), 2053. doi:10.3390/cancers13092053

Ngambenjawong, C., Gustafson, H. H., and Pun, S. H. (2017). Progress in tumor-associated macrophage (TAM)-targeted therapeutics. *Adv. Drug Deliv. Rev.* 114, 206–221. doi:10.1016/j.addr.2017.04.010

Nguyen, K. G., Vrabel, M. R., Mantooth, S. M., Hopkins, J. J., Wagner, E. S., Gabaldon, T. A., et al. (2020). Localized interleukin-12 for cancer immunotherapy. *Front. Immunol.* 11, 575597. doi:10.3389/fimmu.2020.575597

Pasca, S., Jurj, A., Petrushev, B., Tomuleasa, C., and Matei, D. (2020). MicroRNA-155 implication in M1 polarization and the impact in inflammatory diseases. *Front. Immunol.* 11, 625. doi:10.3389/fimmu.2020.00625

Pedersen, M. B., Danielsen, A. V., Hamilton-Dutoit, S. J., Bendix, K., Nørgaard, P., Møller, M. B., et al. (2014). High intratumoral macrophage content is an adverse prognostic feature in anaplastic large cell lymphoma. *Histopathology* 65 (4), 490–500. doi:10.1111/his.12407

Poh, A. R., and Ernst, M. (2021). Tumor-associated macrophages in pancreatic ductal adenocarcinoma: therapeutic opportunities and clinical challenges. *Cancers* 13 (12), 2860. doi:10.3390/cancers13122860

Riabov, V., Yin, S., Song, B., Avdic, A., Schledzewski, K., Ovsiy, I., et al. (2016). Stabilin-1 is expressed in human breast cancer and supports tumor growth in mammary adenocarcinoma mouse model. *Oncotarget* 7 (21), 31097–31110. doi:10.18632/oncotarget.8857

Rodell, C. B., Koch, P. D., and Weissleder, R. (2019). Screening for new macrophage therapeutics. *Theranostics* 9 (25), 7714–7729. doi:10.7150/thno.34421

Rohila, D., Park, I. H., Pham, T. V., Weitz, J., Hurtado de Mendoza, T., Madheswaran, S., et al. (2023). Syk inhibition reprograms tumor-associated macrophages and overcomes gemcitabine-induced immunosuppression in pancreatic ductal adenocarcinoma. *Cancer Res.* 83 (16), 2675–2689. doi:10.1158/0008-5472.CAN-22-3645

Ruf, B., Greten, T. F., and Korangy, F. (2023). Innate lymphoid cells and innate-like T cells in cancer—at the crossroads of innate and adaptive immunity. *Nat. Rev. Cancer* 23 (6), 351–371. doi:10.1038/s41568-023-00562-w

Sánchez-Paulete, A. R., Mateus-Tique, J., Mollaoglu, G., Nielsen, S. R., Marks, A., Lakshmi, A., et al. (2022). Targeting macrophages with CAR T cells delays solid tumor progression and enhances antitumor immunity. *Cancer Immunol. Res.* 10 (11), 1354–1369. doi:10.1158/2326-6066.CIR-21-1075

Singh, Y., Pawar, V. K., Meher, J. G., Raval, K., Kumar, A., Shrivastava, R., et al. (2017). Targeting tumor associated macrophages (TAMs) via nanocarriers. *J. Control. Release* 254, 92–106. doi:10.1016/j.jconrel.2017.03.395

Stefater, J. A., Ren, S., Lang, R. A., and Duffield, J. S. (2011). Metchnikoff's policemen: macrophages in development, homeostasis and regeneration. *Trends Mol. Med.* 17 (12), 743–752. doi:10.1016/j.molmed.2011.07.009

Sun, D., Luo, T., Dong, P., Zhang, N., Chen, J., Zhang, S., et al. (2020). CD86+/CD206+ tumor-associated macrophages predict prognosis of patients with intrahepatic cholangiocarcinoma. *PeerJ* 8, e8458. doi:10.7717/peerj.8458

Sun, L., Zhang, H., and Gao, P. (2022). Metabolic reprogramming and epigenetic modifications on the path to cancer. *Protein Cell* 13 (12), 877–919. doi:10.1007/s13238-021-00846-7

Sun, Y., Cronin, M. F., Mendonça, M. C. P., Guo, J., and O'Driscoll, C. M. (2023). Sialic acid-targeted cyclodextrin-based nanoparticles deliver CSF-1R siRNA and reprogram tumour-associated macrophages for immunotherapy of prostate cancer. *Eur. J. Pharm. Sci.* 185, 106427. doi:10.1016/j.ejps.2023.106427

Tardito, S., Martinelli, G., Soldano, S., Paolino, S., Pacini, G., Patane, M., et al. (2019). Macrophage M1/M2 polarization and rheumatoid arthritis: a systematic review. *Autoimmun. Rev.* 18 (11), 102397. doi:10.1016/j.autrev.2019.102397

Tariq, M., Zhang, J. Q., Liang, G. K., He, Q. J., Ding, L., and Yang, B. (2017). Gefitinib inhibits M2-like polarization of tumor-associated macrophages in Lewis lung cancer by targeting the STAT6 signaling pathway. *Acta Pharmacol. Sin.* 38 (11), 1501–1511. doi:10.1038/aps.2017.124

Tosic, I., and Frank, D. A. (2021). STAT3 as a mediator of oncogenic cellular metabolism: pathogenic and therapeutic implications. *Neoplasia* 23 (12), 1167–1178. doi:10.1016/j.neo.2021.10.003

van de Laar, L., Saelens, W., De Prijck, S., Martens, L., Scott, C. L., Van Isterdael, G., et al. (2016). Yolk sac macrophages, fetal liver, and adult monocytes can colonize an empty niche and develop into functional tissue-resident macrophages. *Immunity* 44 (4), 755–768. doi:10.1016/j.immuni.2016.02.017

Van Dyken, S. J., and Locksley, R. M. (2013). Interleukin-4- and interleukin-13-mediated alternatively activated macrophages: roles in homeostasis and disease. *Annu. Rev. Immunol.* 31, 317–343. doi:10.1146/annurev-immunol-032712-095906

Weiskopf, K. (2017). Cancer immunotherapy targeting the CD47/SIRPα axis. *Eur. J. cancer* 76, 100–109. doi:10.1016/j.ejca.2017.02.013

Wolfsberger, J., Sakil, H. A. M., Zhou, L., van Bree, N., Baldisseri, E., de Souza Ferreira, S., et al. (2021). TAp73 represses NF-κB–mediated recruitment of tumor-associated macrophages in breast cancer. *Proc. Natl. Acad. Sci.* 118 (10), e2017089118. doi:10.1073/pnas.2017089118

Xiang, X., Wang, J., Lu, D., and Xu, X. (2021). Targeting tumor-associated macrophages to synergize tumor immunotherapy. *Signal Transduct. Target Ther.* 6 (1), 75. doi:10.1038/s41392-021-00484-9

Yanagita, T., Murata, Y., Tanaka, D., Motegi, S. I., Arai, E., Daniwijaya, E. W., et al. (2017). Anti-SIRPα antibodies as a potential new tool for cancer immunotherapy. *JCI Insight* 2, e89140. doi:10.1172/jci.insight.89140

Yang, C., Wei, C., Wang, S., Shi, D., Zhang, C., Lin, X., et al. (2019). Elevated CD163+/CD68+ ratio at tumor invasive front is closely associated with aggressive phenotype and poor prognosis in colorectal cancer. *Int. J. Biol. Sci.* 15 (5), 984–998. doi:10.7150/ijbs.29836

Yang, Q., Guo, N., Zhou, Y., Chen, J., Wei, Q., and Han, M. (2020). The role of tumor-associated macrophages (TAMs) in tumor progression and relevant advance in targeted therapy. *Acta Pharm. Sin. B* 10 (11), 2156–2170. doi:10.1016/j.apsb.2020.04.004

Zhang, J., Chang, L., Zhang, X., Zhou, Z., and Gao, Y. (2021). Meta-analysis of the prognostic and clinical value of tumor-associated macrophages in hepatocellular carcinoma. *J. Investigative Surg.* 34 (3), 297–306. doi:10.1080/08941939.2019.1631411

Zhang, Q., Mao, Z., and Sun, J. (2019). NF-κB inhibitor, BAY11-7082, suppresses M2 tumor-associated macrophage induced EMT potential via miR-30a/NF-κB/Snail signaling in bladder cancer cells. *Gene* 710, 91–97. doi:10.1016/j.gene.2019.04.039

Zhang, S., Zhu, L. C., Jiang, Y. P., Zhang, J., Xu, R. J., Xu, Y. S., et al. (2017). Efficacy of afatinib, an irreversible ErbB family blocker, in the treatment of intracerebral metastases of non-small cell lung cancer in mice. *Acta Pharmacol. Sin.* 38 (2), 233–240. doi:10.1038/aps.2016.107

Zhang, Y., Jiang, H., Dong, M., Min, J., He, X., Tan, Y., et al. (2024). Macrophage MCT4 inhibition activates reparative genes and protects from atherosclerosis by histone H3 lysine 18 lactylation. *Cell Rep.* 43 (5), 114884. doi:10.1016/j.celrep.2024.114884

Zhu, S., Yi, M., Wu, Y., Dong, B., and Wu, K. (2021). Roles of tumor-associated macrophages in tumor progression: implications on therapeutic strategies. *Exp. Hematol. and Oncol.* 10, 60–17. doi:10.1186/s40164-021-00252-z

frontiers | Frontiers in Molecular Biosciences

TYPE Original Research
PUBLISHED 28 January 2025
DOI 10.3389/fmolb.2025.1542821

OPEN ACCESS

EDITED BY
Peter Csaba Huszthy,
Akershus University Hospital, Norway

REVIEWED BY
Mithlesh Kumar Temre,
National Institute on Aging (NIH), United States
Yuling Shen,
Shanghai Jiao Tong University School of Medicine, China

*CORRESPONDENCE
Tetyana Falalyeyeva,
tfalalyeyeva@gmail.com

RECEIVED 10 December 2024
ACCEPTED 09 January 2025
PUBLISHED 28 January 2025

CITATION
Omelianenko I, Kobyliak N, Falalyeyeva T, Seleznov O, Botsun P, Ostapchenko L, Korotkyi O, Domylivska L, Tsyryuk O, Mykhalchyshyn G, Shapochka T and Sulaieva O (2025) Immune cells in thyroid adenoma and carcinoma: uncovering a hidden value of assessing tumor-host interplay and its potential application in thyroid cytopathology.
Front. Mol. Biosci. 12:1542821.
doi: 10.3389/fmolb.2025.1542821

Immune cells in thyroid adenoma and carcinoma: uncovering a hidden value of assessing tumor-host interplay and its potential application in thyroid cytopathology

Iryna Omelianenko[1,2], Nazarii Kobyliak[1,3], Tetyana Falalyeyeva[1,2]*, Oleksii Seleznov[1], Pavlina Botsun[1], Lyudmila Ostapchenko[2], Oleksandr Korotkyi[2], Liudmyla Domylivska[2], Olena Tsyryuk[2], Galyna Mykhalchyshyn[3], Tetiana Shapochka[1] and Oksana Sulaieva[1,4]

[1]Medical Laboratory CSD, Pathology Department, Kyiv, Ukraine, [2]Educational-Scientific Center "Institute of Biology and Medicine" Taras Shevchenko National University of Kyiv, Kyiv, Ukraine, [3]Endocrinology Department, Bogomolets National Medical University, Kyiv, Ukraine, [4]Pathology Department, Kyiv Medical University, Kyiv, Ukraine

Introduction: Although the role of tumor immune microenvironment (TIME) in thyroid cancer is well established, little data exists about the differences in immune cell presence in thyroid adenomas and carcinomas. We assume that immune cell density could be an additional diagnostic criterion for differentiating benign and malignant tumors in thyroid aspirates.

Aim: The current study compared the immune contexture of thyroid adenoma (TA) and thyroid carcinoma (TC) in histological and cytological specimens of III-V categories.

Materials and methods: This pilot study included 72 cases (36 of TA and 36 of TC) with verified histological diagnosis and pre-operative cytology corresponding to categories III, IV and V according to the Bethesda system for reporting thyroid cytology. The number of CD8+, CD68+ and CD163+ cells was assessed in histological samples of TA and TC with further comparison to cytological specimens. Besides, the expression of STAT6 and SMAD4 as potential regulators of TIME was evaluated in the study.

Results: TC demonstrated an immune-rich profile representing abundant tumor-associated CD8+ lymphocytes, CD68 and CD163+ macrophages. In contrast, TA represented mostly a low immune cell infiltration. The higher immunogenicity of TC was accompanied by the more profound expression of STAT6 and SMAD4 in tumor cells. The number of immune cells in cytological specimens correlated with CD8+ ($r = 0.693$; $p < 0.001$) and CD163+ cells ($r = 0.559$; $p < 0.001$) in histological samples, reflecting the differences in

the tumor immune microenvironment between benign and malignant thyroid neoplasms.

Conclusion: TC demonstrated high immunogenicity compared to TA, which correlated to the number of immune cells in cytological specimens. The number of immune cells in thyroid cytology samples could be an additional criterion in cytological diagnostics for III-V Bethesda categories. Further investigations are needed to validate the findings of the study.

KEYWORDS

thyroid cancer, immune cells, immune microenvironment, thyroid adenoma, papilary thyroid carcinoma

Introduction

Thyroid cancer (TC) is one of the most common endocrine malignancies (Siegel et al., 2021). The incidence of TC morbidity has been increasing for the last decades leading to a sharp increase in thyroid surgery, the need for lifelong hormone replacement therapy and disturbances of endocrine regulation and metabolism (Rahib et al., 2014; Lim et al., 2017). Among the various types of TC papillary thyroid cancer prevails, while follicular, medullary and anaplastic carcinoma represents a smaller proportion of thyroid malignancies. Genetic and epigenetic research advances have identified the differences in mutagenesis and signaling pathway alterations in different thyroid cancers. It was shown that various histological types of TC are rooted in distinct molecular alterations and possess different evolution (Xing, 2013). These findings were incorporated into diagnostic algorithms relying on molecular testing applications in the case of "grey zone" categories of cytological diagnostics of thyroid fine needle aspiration biopsy (FNA) (Ali et al., 2023a). Although molecular testing provides a valuable impact on distinguishing benign and malignant tumors of the thyroid, its availability and affordability are limited especially in low- and middle-income countries. Seeking alternative approaches for discerning benign and malignant thyroid neoplasia shifted researchers' attention toward the tumor immune microenvironment (TIME).

TIME is considered to be one of the crucial factors influencing the development and progression of malignant tumors. It comprises different types of immune cells, signaling molecules, and growth factors (Yang et al., 2021). TIME discovery has illuminated the bidirectional and multivariable interplay between tumor cells and the host immune system, defining the formation of conditions for malignancy and progression of tumor growth (Ferrari et al., 2019). The link between thyroid carcinoma and inflammation has been reported in many studies (Zheng et al., 2024; Wang et al., 2022; Li et al., 2024), uncovering both mechanisms of immune-mediated tumor destruction and tumor cell-dictated immune evasion (Menicali et al., 2021). However, little is known about the differences in immune cells' presence in TA. These data could be essential for developing a new approach for differentiating benign and malignant thyroid tumors at the pre-operative stage that is based on assessing cytological features of FNA biopsy of thyroid nodules (Goldstein et al., 2002). Although FNA is approved as the best diagnostic approach for primary cytological assessment of thyroid nodules using the Bethesda system, it is still challenging to discriminate between benign and malignant thyroid tumors (Sulaieva et al., 2019). About 10%–20% of lesions, diagnosed by FNA as categories III (atypia of undetermined significance; AUS), IV (follicular neoplasm; FN) or V (suspicious for malignancy (SFM) still represent some uncertainty and require molecular testing for further patients management (Ali et al., 2023b). Although molecular evolution and profile of thyroid neoplasms are well discovered and various types of molecular testing were validated and approved for clinical practice, the high costs of molecular testing reduce its wide application, especially in low-resource settings (Fagin and Nikiforov, 2023). Beyond various ancillary tests focused on tumor cell biomarkers, signaling and genomics, assessment of TIME could be beneficial, as it reflects host-tumor interplay and its nature.

A complex interplay between various immune cells infiltrating thyroid carcinomas defines the balance between protumor and antitumor effects, impacting tumor cells' behavior and prognosis (Li et al., 2024). Previous studies uncovered a prognostic role of CD8+ T-cells in papillary thyroid carcinoma (PTC) prognosis (Galdiero et al., 2016). Naturally, the functioning of CD8+ lymphocytes responsible for cell-mediated immunity was associated with antitumor defense and efficiency in killing tumor cells (Giles et al., 2023). Other studies addressed the involvement of CD4+ cells and B lymphocytes in PTC development and progression (Menicali et al., 2021; French et al., 2010). Tumor-associated macrophages (TAMs), including both M1 (CD68+) and M2-type (CD163+), were shown to be the most numerous immune cells infiltrating thyroid carcinoma (Liu et al., 2022). The impact of CD163+ tumor-associated macrophages representing the M2-anti-inflammatory type includes the production of a wide spectrum of growth factors, promoting cancer growth (Song et al., 2023). Their amount was linked to various clinicopathological features and positively correlated with larger tumor size, invasiveness and decreased survival in PTC (Gong et al., 2021; Jung et al., 2015). However, the precise mechanisms defining the scale and polarization of immune cells response within different thyroid tumors still need clarification.

Numerous studies addressed factors affecting the immune contexture of TC. In addition to various cytokines and chemokines, regulatory molecules involved in their signaling cascades have been placed at the center of studies. For instance, the recent study defined the prognostic role of the transcription factor of signal transducer and activator of transcription (STAT) family–STAT6, in thyroid cancer (Wang et al., 2020). In addition to the cell cycle, cell adhesion and apoptosis control STAT6 can impact immune infiltration of B

cells, CD4+ T cells, neutrophils, macrophages, and dendritic cells. STAT6 also affects macrophage polarization due to IL-4 and IL-13 effects mediated through STAT6 signaling. Besides activated macrophages secrete transforming growth factor β (TGF-β) which also can affect immune cells response and TIME through SMAD4 signaling pathways (Wang et al., 2020). Although the role of STAT6 and SMAD4 is in the focus of active discovery there are still little data about the role of these molecules in TA and TC (Wang et al., 2020).

Although the immune microenvironment of thyroid malignancies is quite well established, it is still little known about the difference between the immune contexture of thyroid adenoma and carcinoma. This pilot case-control study aimed to compare the TIME of thyroid adenomas and carcinomas with respect to the potential mechanisms impacting tumor immune contexture and the correlation between histological and cytological representation.

Materials and methods

Ethics statement

This case-control study was approved by the Ethics Commission of the Medical Laboratory CSD (Protocol No. 1D from 02.10.2023). It was performed following the principles of the Declaration of Helsinki. The Ethics Commission of the Medical Laboratory CSD waived informed consent.

Patients' characteristics

72 cases of III-V categories of the Bethesda system and histologically confirmed diagnoses of TC (group 1, 36 cases, 12 cases of each Bethesda category) and TA (group 2, 36 cases, 12 cases of each Bethesda category) were selected for the study (Figure 1). All enrolled patients met the following criteria: 1) thyroid cytology corresponded to Bethesda categories III, IV or V; 2) histologically confirmed diagnosis of thyroid neoplasia, 3) age between 21 and 60 years, and 4) patients had no autoimmune thyroid diseases (Grave`s disease or Hashimoto`s thyroiditis); 5) absence of other malignancies at the time of examination. As far as PTC was the most common type of thyroid malignancy, only individuals with PTC were included in this study. Exclusion criteria were as follows: 1) age under 21 or over 60; 2) Bethesda category I, II, or VI at cytology; 3) patients having any co-existing immune-mediated thyroid pathology (Hashimoto thyroiditis, Graves' disease, etc.); 4) other histological types of TC (follicular thyroid carcinoma or medullary thyroid carcinoma); 5) individuals having synchronous or metachronous malignancies.

The age of patients with TA was 37 (IQR 29–53) and the age of TC comprised 42.5 (IQR 27–54). Other clinical and demographic data are represented in Table 1.

Histology and immunohistochemistry

The number of immune cells infiltrating thyroid tumors was assessed in histological specimens. Special attention was paid to T-lymphocytes ($CD8^+$), B-lymphocytes ($CD19^+$) and macrophages ($CD163+$ and $CD68^+$). The expression of the signaling molecules STAT6 and SMAD4, which play a crucial role in regulating the immune response and the tumor microenvironment, was also analyzed. Evaluating the expression of these markers allows for a better understanding of the mechanisms of tumor interaction with the immune system and the role of immunosuppression in the progression of the tumor process.

Immunohistochemistry was applied to visualize different immune cells and evaluate STAT6 and SMAD4 expression (Table 2). Briefly, paraffin tissue sections with a thickness of 4 μm were prepared and placed on SuperFrost Plus slides (Menzel, Germany). Deparaffinization and restoration of antigenicity were performed in TRS High pH buffer (DAKO, Denmark) at a temperature of 98°C for 40 min in a DAKO PT Module apparatus. The following primary antibodies were used for staining: CD8 (clone C8/144B, DAKO), CD4 (clone 4B12, DAKO), CD19 (clone LE-CD19, DAKO), CD68 (clone KP1, DAKO), CD163 (clone MRQ-26, Cell Marque), STAT6 (clone EP325, Cell Marque), and SMAD4 (clone JM56, Novocastra). Appropriate detection systems were used with incubation of primary antibodies for 30 min and subsequent treatment with DAB solution.

Immune cells in histological slides were counted in 10 fields of view at ×40 magnification using light microscopy (Leica Microsystems, DM3000). The number of immunopositive cells was evaluated per square millimeter. In addition, the density of immune cell infiltration was assessed in a dichotomic way as high or low. The threshold for such discrimination was based on the Median (9 per 1 mm^2 for CD8 lymphocytes and 17 per 1 mm^2 for $CD68^+$ and $CD163^+$ macrophages).

Two independent cytologists assessed cytological specimens of the enrolled cases to verify the category according to the Bethesda system and estimate the number of immune cells (lymphocytes and macrophages). The number of immune cells in cytological slides was evaluated semi-quantitatively (0 – lack of immune cells, 1 – few immune cells, 2 – moderate number of immune cells and 3 – high number of immune cells).

In addition, the expression levels of STAT6 and SMAD4, being important factors involved in tumor signaling cascades, were evaluated (Table 2). Expression levels of these proteins were evaluated in both stromal and tumor cells. The expression of STAT6 and SMAD4 in tumor cells was evaluated semi-quantitatively using an intensity scale from 0 to 3 (0 - negative, 1 - weak, 2 - moderate, 3 -strong) and the percentage of positive cells (0% - negative, 1%–25% - 1+, 26%–50% - 2+, >50% - 3+) (Sulaieva et al., 2020a). The total score was calculated by multiplying the degree of staining by the percentage of positive cells, which allows us to estimate the relative degree of expression of these factors in the tumor tissue. A blind histologic analysis was performed by two independent pathologists.

Statistical analysis

Statistical analysis was performed using MedCalc software (MedCalc Software, Mariakerke, Belgium) and GraphPad Prism, version 10.4.0 (GraphPad Software, Inc., La Jolla, CA, United States) for creating diagrams. The data distribution was analyzed using the Shapiro-Wilk test for normality. All continuous variables were presented as the Median with interquartile range (IQR), and categorical variables were presented as %.

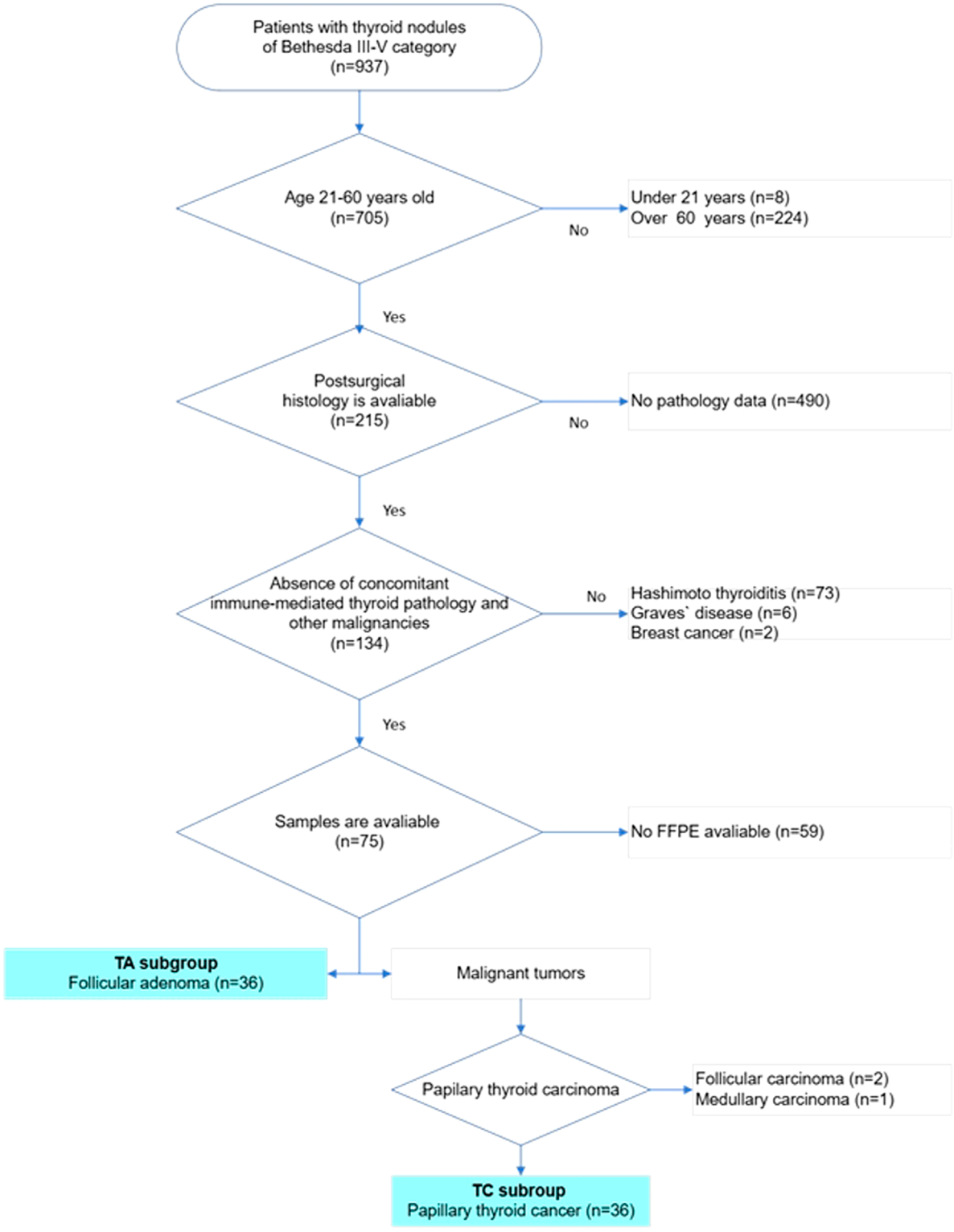

FIGURE 1
Flowchart of patients' selection in the study. The multistep selection algorithm was applied in the study. After selecting cases in which thyroid cytology corresponded to categories III, IV or V according to the Bethesda system for reporting thyroid cytology, patients were checked for age. Only patients of age 21–60 were included in the study. Next, all cases were checked for follow-up surgery and a histopathology report was available. Cases with complete pathology reports were reviewed and all cases with reported autoimmune thyroid diseases were excluded. After that cases with available FFPE blocks were revised for diagnosis, 36 cases with follicular adenoma and 36 cases with papillary thyroid carcinoma were included in the final study sample.

10.3389/fmolb.2025.1542821

TABLE 1 Clinic pathological characteristics of patients.

Patients characteristics	TA group	TC group
Number of patients	**36**	**36**
Sex		
Females	34	35
Males	2	1
Age	37 (IQR 29–53)	42.5 (IQR 27–54)
Laterality of lesions		
Unilateral	36	35
Bilateral	0	1

the bold indicates significant changes.

For comparing quantitative data between TA and TC Mann-Whitney test was applied. Categorical variables were analyzed by utilizing a χ^2 test. Spearman's correlation analysis was used to assess associations between different immune cells and biomarker expression. p-value ≤0.05 was considered statistically significant.

Results

Immune cells in TA and TC

The immune microenvironment of TC was enriched with immune cells with the prevalence of tumor-associated lymphocytes and macrophages. CD8+ lymphocyte number was significantly higher in TC compared to TA ($p < 0.001$, Figure 2). Surprisingly, only scarce CD4+ and CD19+ cells (from 0 to 3 cells per 1 mm^2) were found in samples of TC and TA (Figure 3).

Likewise, CD8+ cells, the number of tumor-associated macrophages was significantly higher in carcinomas ($p < 0.001$). CD68+ and CD163+ cells were abundant in TC forming a network within the tumors (Figure 2; Table 3). Notably, the density of infiltration by M1 and M2 macrophages displayed a high heterogeneity in patients of both groups. Although the Medians of CD68+ and CD163+ cells in the TC group were almost similar, the balance of M1 and M2 macrophages varied significantly inside the group, so the CD68/CD163 ratio was low in patients with papillary thyroid carcinoma, comprising 0.563 (0.082–3.0). In contrast, in TA the proportion of CD68+ to CD163+ cells was significantly higher ($p = 0.036$) reaching 1.04 (0.467–3.0).

When applying dichotomic assessment of immune cell numbers as low or high in thyroid tumors, we found that most TA demonstrated a low number of CD8+, CD68+ and CD163 cells. Alternatively, about 80% of TC demonstrated high immunogenicity, being "hot" in terms of T-cell infiltration, and more than half of them possessed a high number of macrophages (Figures 4A–F). These facts reflect a higher immunogenicity of thyroid carcinoma as compared to benign tumors.

For uncovering the potential mechanisms affecting tumor immune contexture, at the next step, we assessed the expression of signaling biomarkers involved in carcinogenesis and immune modulation.

STAT6 and SMAD4 expression in TA and TC: relation to diagnosis and immune cell number

Differences in immune cell count between benign and malignant thyroid tumors were also associated with distinction in STAT6 and SMAD4 expression (Figure 5). A significantly higher expression of STAT6 s SMAD4 was found in TC, compared to TA. In adenomas, about half of tumor cells showed mild cytoplasmic expression of STAT6, whereas in TC STAT6 demonstrated moderate expression in a higher proportion of tumor cells ($p = 0.008$) (Table 3). STAT6 score in TC moderately correlated with the number of CD163+ macrophages ($r = 0.394$; $p < 0.001$) and $CD68^+$ cells ($r = 0.317$; $p < 0.001$).

Nuclear expression of SMAD4 was detected in less than half of tumor cells in TA but showed diffuse moderate expression in carcinoma cells (Figure 5). Interestingly, SMAD4 expression correlated with STAT6 ($r = 0.495$, $p < 0.001$) and was also linked to the number of CD163+ cells ($r = 0.41$; $p < 0.001$) in TC.

Correlations between cytological and histological features of thyroid tumors immune contexture

Similar to histological samples, cytological specimens demonstrated significant differences in lymphocyte and macrophage numbers between cases diagnosed as TA and TC. The proportion of cases with high and moderate numbers of lymphocytes and macrophages was significantly higher in TC compared to TA ($p < 0.001$). While most TA cases demonstrated a lack or low number of macrophages, cases verified as TC were more commonly rich in macrophages (Figure 4G) and/or lymphocytes (Figure 4I).

The number of macrophages in cytological specimens correlated with the amount of CD163+ cells in histological samples ($r = 0.559$; $p < 0.001$). Similarly, lymphocyte density in cytological slides correlated to the amount of C8+ cells ($r = 0.693$; $p < 0.001$) although we did not find a correlation between the number of immune cells in FNA specimens and the expression of STAT6 and SMAD4 in histological samples.

To illustrate the relationship of thyroid tumors' immune contexture in cytological and histological specimens, herein we provide several examples.

Example 1: A woman, 50 years old, single thyroid nodule 2 cm in diameter, Bethesda category 3 with architectural or nuclear atypia at cytology. Cytological specimens demonstrated a low number of lymphocytes and only a few macrophages. After repetitive FNA, the results of cytology were the same. According to the patient`s preferences, a lobectomy was performed. Follicular adenoma was diagnosed after a histopathological study. Assessment of tumor immunogenicity by immunohistochemistry revealed the following

TABLE 2 Characteristics of biomarkers used for immunohistochemistry.

Marker	Clone	Manufacturer	Interpretation
CD8	C8/144B	DAKO	A T-cell marker that detects cytotoxic/suppressor cells in lymphocytes; also found on NK-cells
CD68	KP1	DAKO	Lysosomal membrane glycoproteins expressed on monocyte-macrophage cells
CD163	MRQ-26	Cell Marque	Acute phase regulatory transmembrane protein that induces signaling and is found only in cells of monocytic origin
STAT6	EP325	Cell Marque	A transcription factor involved in signaling pathways associated with immune responses, including macrophage polarization and Th2 cell differentiation; STAT6 is activated by cytokines such as IL-4 and IL-13
SMAD 4	JM56	Novocastra	A protein that plays an important role in the signaling pathway activated by TGF-β (transforming growth factor beta). It is a central mediator of signaling in this pathway and is involved in the regulation of cell growth, differentiation and apoptosis, and immune response and inflammation

number of immune cells: CD8+ cells - 11 per 1 mm^2, CD68+ – 6 per 1 mm^2, CD163+ macrophages – 3 per 1 mm^2. The ratio of CD68/CD163 macrophages comprised 2. STAT6 score was 2, and SMAD4 score reached 2.

Example 2: A woman, 54 years old, unilateral thyroid nodule 2 cm in size, Bethesda class 3 with architectural and nuclear atypia. There was a moderate number of macrophages and a mild number of lymphocytes in cytological specimens. After surgery, the histological diagnosis was Papillary thyroid carcinoma. Assessment of tumor immunogenicity by immunohistochemistry revealed the following number of immune cells: CD8+ cells - 15 per 1 mm^2, CD68+ – 7 per 1 mm^2, CD163+ macrophages – 35 per 1 mm^2. The ratio of CD68/CD163 macrophages comprised 0,2. STAT6 score was 6, and SMAD4 score reached 4.

Thus, the number of immune cells in cytological specimens correlated with $CD8^+$ and $CD163^+$ cells in histological samples (Figure 4H) and can reflect the differences in the immune tumor microenvironment between benign and malignant thyroid tumors that could be applied as additional criteria in cytological diagnostics for III-V Bethesda categories.

Discussion

The results of our research showed a significantly higher level of infiltration of TC by tumor-infiltrating CD8+ lymphocytes and tumor-associated macrophages compared to adenomas, which confirms the role of the immune microenvironment in the development and progression of papillary thyroid carcinoma (PTC). In particular, we found that the majority of immune cells in carcinomas are CD8+ cells, the number of which was more than three times greater in TC than in TA. This reflects a higher immunogenicity of carcinomas compared to benign tumors. CD8+ cytotoxic T-lymphocytes are well-known effector cells of cell-mediated immunity, are responsible for the elimination of tumor cells (Huang et al., 2019). Research by Modi et al., found that patients with PTC who had dense $CD8^+$ T-cell infiltration showed slower tumor progression, smaller tumor sizes, and lower recurrence rates (Modi et al., 2003). This emphasizes the importance of the immune response mediated by cytotoxic T-cells in suppressing the tumor process and improving the prognosis for patients. This is consistent with previous studies indicating an important role of $CD8^+$ T-cells in the antitumor response and regulating the immune microenvironment in various cancers, including thyroid cancer (Giles et al., 2023), although some studies highlighted the possible role of CD8+ in prognosticating TC recurrence (Cunha et al., 2015). It is also important to note that CD8+ cells were the most numerous immune cells in TC, prevailing under B-cells and tumor-associated macrophages that can explain the relatively slow tumor progression, satisfactory prognosis and high survival rate of papillary thyroid cancer, the most common histological type of TC (Sheridan et al., 1995; Ulisse et al., 2021). In this study we found only scarce CD4+ and CD19+ cells, reflecting a weak role of T-helpers and humoral immunity cells in thyroid tumors microenvironment. This surprising finding could be related to the exclusion of patients with coexisting thyroiditis from the study. As it was shown in recent studies, autoreactive CD4+ T cells and CD8+ cytotoxic T cells, as well as plasma cells producing autoantibodies play a central role in Hashimoto thyroiditis, which is often associated with thyroid tumor development (Chistiakov, 2005). However, in the absence of concomitant immune-mediated thyroid pathology, the role of CD4+ and CD19+ cells is much less significant. At the same time, it is worth noting that in this study we did not focus on discovering the role of various CD4+ cell and B-lymphocyte subsets, but rather explored the core differences of immune contexture of benign and malignant tumors of the thyroid and their correlation to cytological features of FNA (Chistiakov, 2005).

Of particular interest is the increased number of CD163+ macrophages in carcinomas compared to adenomas. Tumor-associated macrophages in the tumor microenvironment express a number of markers, such as CD163, indicating an M2-like polarization state of macrophages with tumor-protective functions (Aras and Zaidi, 2017; Sulaieva et al., 2020b). We found that the number of CD163+ cells in carcinomas was three times higher than in adenomas, confirming the role of these cells in the progression of PCOS. This trend of increased presence of M2 macrophages correlates with the data of other studies, which indicate that they will prevail in the tumor microenvironment (Sari et al., 2022). Moreover, the CD68/CD163 ratio was significantly lower in the TC group demonstrating the prevalence of anti-inflammatory M2-macrophages producing a wide range of angiogenic and tumor-promoting growth factors, cytokines and chemokines. In contrast

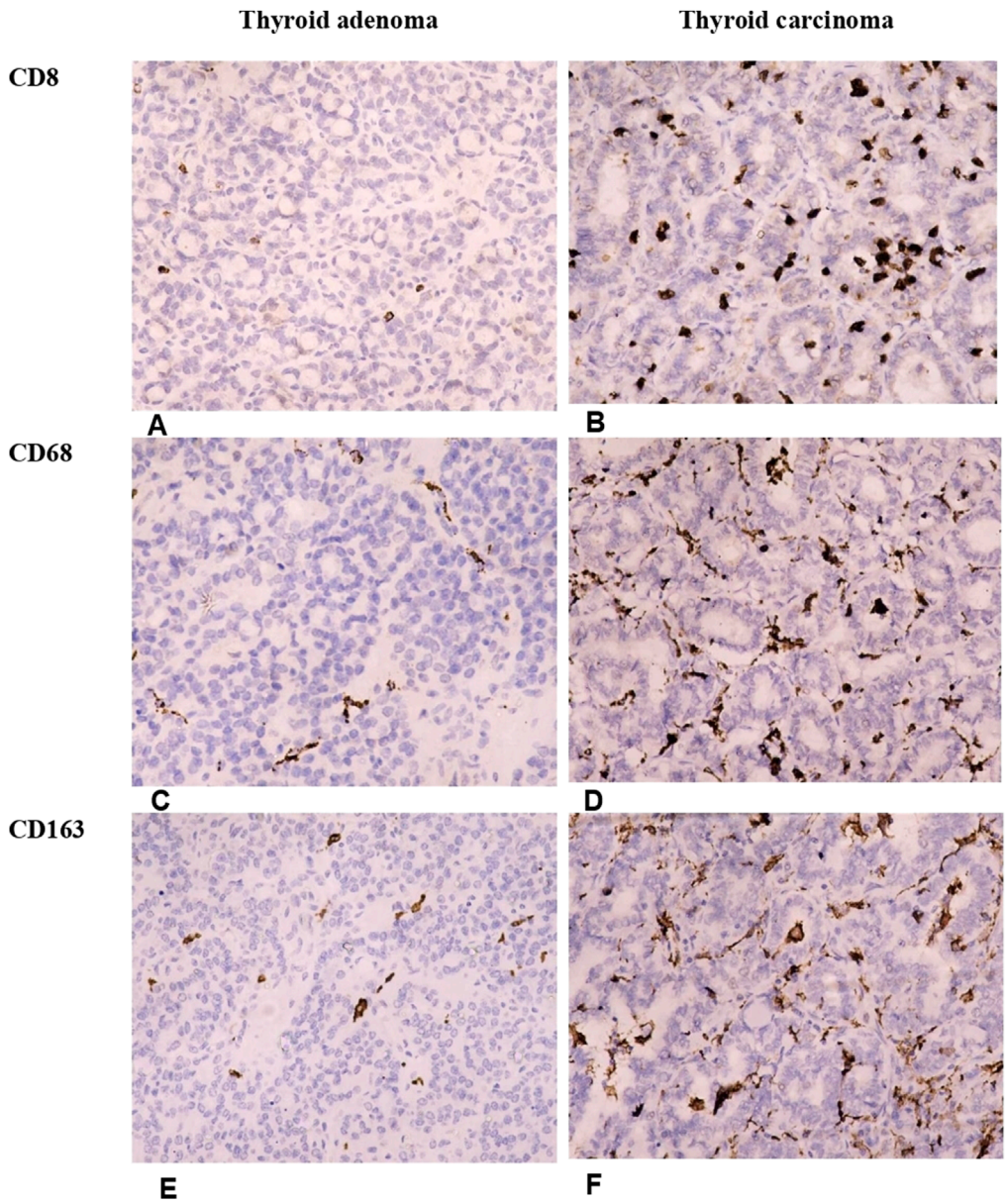

FIGURE 2
Differences in the number of T-cytotoxic lymphocytes and macrophages in thyroid adenomas and papillary carcinomas. Thyroid adenoma demonstrates a low number of tumor-infiltrating lymphocytes and macrophages. In contrast, the immune cells were significantly more numerous in thyroid carcinoma. **(A, B)** Illustrate the number of CD8+ T-cytotoxic lymphocytes in follicular adenoma **(A)** and papillary thyroid carcinoma **(B)**. **(C, D)** Represent infiltration of follicular adenoma **(C)** and papillary thyroid carcinoma **(D)** by CD68+ macrophages. **(E, F)** Show the density of tumor-infiltrating M2-macrophages in follicular adenoma **(E)** and papillary thyroid carcinoma **(F)**. Immunohistochemistry. Magnification 200.

to M1-macrophages, producing proinflammatory cytokines (tumor necrosis factor-alpha - TNF-α, IL-1β, IL-12, and IL-23) reactive oxygen species and NO, medicating inflammatory reaction with activating tumor-killing mechanisms (Chen et al., 2023), M2-macrophages contribute to cell dedifferentiation, tumor growth promotion, angiogenesis and enhanced invasiveness of cancer cells (Liu et al., 2022). These effects are rooted in the extensive secretion of Wnt1 and Wnt3 ligands, inducing activation of β-catenin activation, growth factors (VEGF, IGF, EGF, etc.) and anti-inflammatory cytokines (IL-6, IL-10, IL-18, TGFβ1 etc.) (Lv et al., 2021; Zhang et al., 2021).

The correlation between CD163+ cells and CD8+ (r = 0.395) may indicate the relationship between innate and adaptive immunity reactions during tumor evolution. Significant differences in the number of immune cells of innate and adaptive immunity allow generating the hypothesis that the difference in the immune context of benign and malignant thyroid tumors and carcinomas should be taken into account at the stage of cytological diagnosis of FNA. However, due to the limitations of our study (small sample size and lack of long-term follow-up), there is a need for further thorough research to test this hypothesis and to define clear criteria that will allow differentiation of different

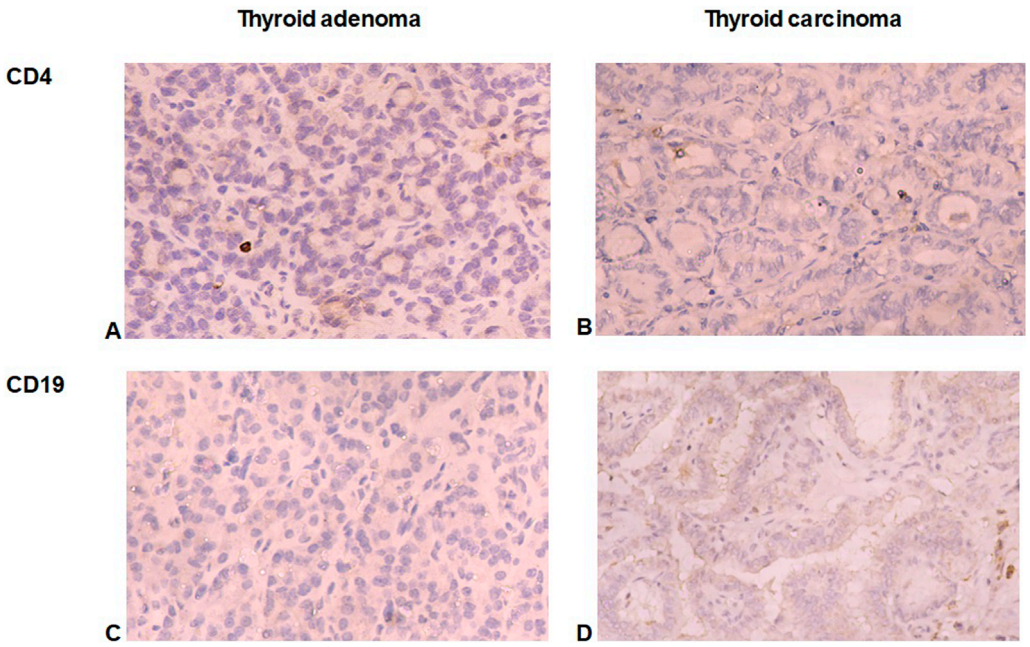

FIGURE 3
CD4+ and CD19+ cells in thyroid tumors. **(A, B)** Demonstrate a little number of CD4+ cells in follicular adenoma **(A)** and papillary thyroid carcinoma **(B)**. **(C, D)** Illuminate scarce CD19+ B-lymphocytes in follicular adenoma **(C)** and papillary thyroid carcinoma **(D)**. Immunohistochemistry. Magnification 200.

TABLE 3 Characteristics of immune contexture of TA and TC.

Immune cells	TC	TA	p
Immune cells count within the tumor			
CD8	6 (1.2–19.5)	37 (13.5–77)	$p < 0.001$
CD68	9 (4–15)	21 (6–46)	$p < 0.001$
CD163	7 (2–12.5)	21 (4.5–45)	$p < 0.001$
CD68/CD163 ratio	0.563 (0.082–3.0)	1.04 (0.467–3.0)	$p = 0.036$
IHC score of transcription factors expression			
STAT6	1 (0–1.5)	3 (1–6)	$p = 0.008$
SMAD4	3.5 (1–6)	6 (1–6)	$p = 0.026$

The data are presented as the Me (Q_I - Q_{III}).

thyroid tumors taking into account immune cells in thyroid cytopathology practice.

Our results demonstrate that STAT6 and SMAD4 molecules are interconnected with the number of certain classes of immune cells, and therefore may play a role in the regulation of the immune microenvironment of thyroid tumors. STAT6 demonstrated a moderate positive correlation with cytotoxic T-lymphocytes (CD8+) and M2-macrophages (CD163+), which reflects the involvement of this transcription factor in the regulation of not only adaptive immune reactions but also the modulation of the macrophage phenotype towards the M2-phenotype, which promotes immunosuppression and tumor growth (Chen et al., 2023). The unique role of STAT6 in the polarization of macrophages to the M2 phenotype, which is associated with tumor progression, should be emphasized. STAT6 impacts the function of immune cells by inducing the transcription of genes involved in cell-mediated and humoral immunity (Hebenstreit et al., 2006). Typically, STAT6 stimulation occurs in response to IL-4 and IL-13 receptor binding and JAK1/JAK3 activation. Enhanced STAT6 expression in immune cells defines the polarization of macrophages toward M2-type (Chen et al., 2023). However, over the last decades, the elevated expression of STAT6 was found in various cancers. Researchers argue that STAT6 might play a prominent role in tumorigenesis and malignant transformation (Todaro et al., 2008; Wang et al., 2010). Beyond immune reaction, STAT6 can orchestrate cancer cell proliferation and apoptosis, cell adhesion and invasiveness, chromatin compaction and DNA damage response (Liu et al., 2017). STAT6 expression in tumor cells can impact the formation and composition of the tumor microenvironment facilitating immune cell recruitment and macrophage polarization (Sulaieva et al., 2020a).

In this study, we also found that TC demonstrated much higher expression of SMAD4 in tumor cells compared to TA. SMAD4 as a key signal transducer of TGFβ impacts a wide range of cellular processes, including proliferation, differentiation and apoptosis (D'Inzeo et al., 2012). Dysregulation of TGFβ signaling was shown to play an important role in tumor progression, affecting such processes as epithelial-mesenchymal transition, cell invasiveness and immune evasion mechanisms. Previous studies showed that reduction of SMAD4 may play a significant role in thyroid carcinogenesis, while overexpression of SMAD4,

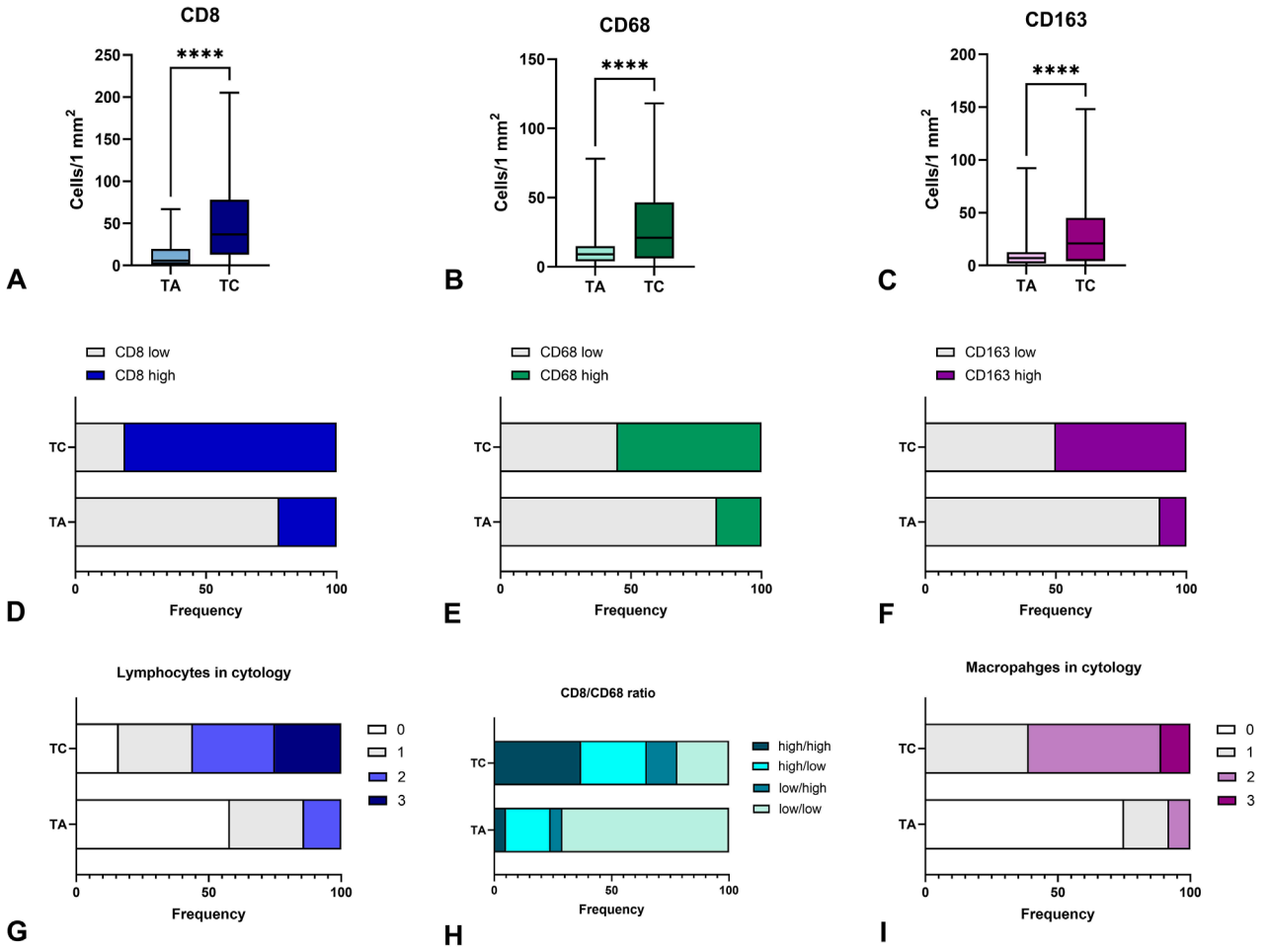

FIGURE 4
Immunogenicity of thyroid carcinomas and adenomas. **(A–C)** – demonstrate the number of CD8+, CD68+, and CD163+ cells per 1 mm^2 in thyroid tumors, respectively. TC demonstrated a higher number of CD8+ T-cells, CD68+ and CD163 macrophages infiltrating the tumor as compared to TA. **(D–F)** – represent the shares of cases with low or high numbers of CD8+, CD68+ and CD163+ cells in thyroid tumors, respectively. More than half of TC cases demonstrated high infiltration by immune cells. **(G)** - demonstrates the proportion of cases with different lymphocyte numbers in FNA cytology of confirmed TA and TC, where 0 corresponds to the lack of lymphocytes, 1, 2 and 3 demonstrate categories of mild, moderate and high numbers of lymphocytes in cytological specimens. More than half of TC cases showed a high or moderate number of lymphocytes in cytological specimens. **(H)** - represents the proportion of cases with different CD8+/CD163+ cell ratio. **(I)** - demonstrates the proportion of cases with different macrophage numbers in FNA cytology of confirmed TA and TC, where 0 corresponds to the lack of lymphocytes, 1, 2 and 3 demonstrate categories of mild, moderate and high numbers of macrophages in cytological specimens. More than half of TC cases showed a high or moderate number of macrophages in cytological specimens. TA – thyroid adenoma, TC – thyroid adenoma.

can facilitate antiproliferative response to TGFβ, reducing the invasive behavior of these cells (D'Inzeo et al., 2010). On the other hand, the recent discovery of the relations between SMAD4 expression and TIME defined the opposite results. Enhanced TGFβ secretion was illuminated in various malignancies, promoting cell invasiveness and tumor progression (Derynck et al., 2021). It was shown that TGF-β acting through SMAD4 and SMAD7 transduction enhances the recruitment of monocytes and activation of macrophages, suppresses the functioning of anti-tumor T-cells and generates immunosuppressive TIME facilitating immune evasion mechanisms and tumor progression (Derynck et al., 2021; Ivanova et al., 2018). These data are supported by the results of our study showing that SMAD4 expression in tumor cells correlated with the number of CD163+ macrophages. This reveals the potential role of the TGF-β-SMA4 signaling pathway in the malignancy-associated modulation of TIME and stimulates further discovery of the diagnostic and prognostic role of STAT6 and SMAD4 in thyroid tumors.

Finally, we found the correlation between cytological and histological reflections of tumor immunogenicity. Previous descriptive studies also highlighted the importance of assessing minor morphological features for navigating decisions in case of uncertain categories defined according to the Bethesda system (Rocha et al., 2023). In our study, we focused exclusively on TIME assuming that differences in benign and malignant tumors immunogenicity could be detected during thyroid FNA cytopathological review. Indeed, the assessment of hidden differences in tumor-host interplay allows rethinking the approach for cytological diagnostics shifting focus from follicular toward immune cells in challenging cases. Herein we showed that while

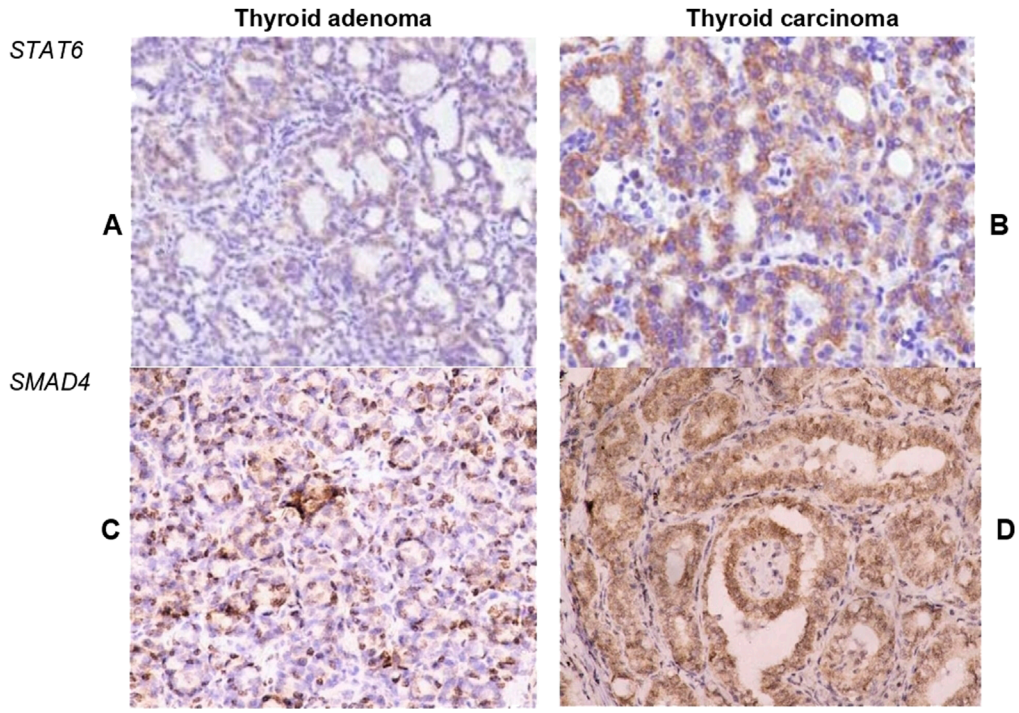

FIGURE 5
Expression of STAT6 and SMAD4 in thyroid tumors. **(A, B)** Demonstrate STAT6 expression in tumor cells within follicular adenoma **(A)** and papillary thyroid carcinoma **(B)**. TC demonstrated significantly higher intensity and extension of STAT6 expression. **(C, D)** Illustrate the expression of SMAD4 in cells of follicular adenoma **(C)** and papillary thyroid carcinoma **(D)**. Most cells of TC demonstrated moderate to high nuclear and cytoplasmic expression of SMAD4. Immunohistochemistry. Magnification 200.

most TA demonstrated a low level of immune cells, TC represented much more prominent immunogenicity, reflected in a number of immune cells in cytological samples. Cytological "grey zone" samples taken during FNA demonstrate significant differences in risk of malignancy and require further follow-up, molecular testing, or diagnostic lobectomy. Molecular testing, including Afirma Genomic Sequencing Classifier (GSC) and ThyroSeq v3, demonstrates high diagnostic performance and provides important prognostic data (Hu et al., 2022). It is informative for stratifying cytologically indeterminate FNA samples and defining high-risk patients with thyroid nodules. On the flip side, molecular testing is expensive, and its applications are not feasible in many countries due to high costs and technological barriers. This dictates the need for developing affordable and cost-effective approaches for managing cases of cytologically indeterminate thyroid nodules, and current data on immunogenetics of thyroid neoplasia could drive the novel approach based on considering immune microenvironment of thyroid lesions.

The findings of this pilot study demonstrate a hidden value of assessing immune cells in the case of follicular cell atypia and uncertainty of cytopathological conclusions.

Limitations

The pilot study was conducted with limited sample size and did not count tumor stage, comorbid pathology and genetic alterations. Besides, this study did not cover the clinical data, cytokine profile and molecular testing results. The observations of this pilot study did not include Hashimoto thyroiditis, Graves' disease and other immune-mediated pathologies of the thyroid gland. Taking into account the design of the study and limited sample size, further large-scale studies (preferably longitudinal investigations) for validating the approach and estimating the predictive values of assessing immune cells in FNA samples are needed.

Conclusion

Thyroid carcinomas demonstrate high immunogenicity compared to adenomas with extensive infiltration by CD8+, CD68+ and CD163+ macrophages, associated with increased expression of SMAD4 and STAT6 in tumor cells. The number of immune cells in cytological specimens correlates with TILs and TAMs count in histological slides and can reflect the differences in the immune tumor microenvironment between benign and malignant thyroid tumors that could be applied as additional criteria in cytological diagnostics for III-V Bethesda categories.

Data availability statement

The raw data supporting the conclusions of this article will be made available by the authors, without undue reservation.

Ethics statement

The studies involving humans were approved by Medical Laboratory CSD (Protocol No. 1D from 02.10.2023). The studies were conducted in accordance with the local legislation and institutional requirements. The human samples used in this study were acquired from a by-product of routine care or industry. Written informed consent for participation was not required from the participants or the participants' legal guardians/next of kin in accordance with the national legislation and institutional requirements.

Author contributions

IO: Conceptualization, Investigation, Supervision, Validation, Writing–original draft. NK: Data curation, Formal Analysis, Methodology, Visualization, Writing–original draft. TF: Conceptualization, Project administration, Supervision, Validation, Writing–original draft. OS: Formal Analysis, Investigation, Methodology, Writing–review and editing. PB: Formal Analysis, Investigation, Methodology, Writing–review and editing. LO: Formal Analysis, Methodology, Writing–review and editing. OK: Formal Analysis, Methodology, Writing–review and editing. LD: Formal Analysis, Methodology, Writing–review and editing. OT: Formal Analysis, Methodology, Writing–review and editing. GM: Formal Analysis, Methodology, Writing–review and editing. TS: Formal Analysis, Investigation, Methodology, Writing–review and editing. OS: Conceptualization, Data curation, Project administration, Supervision, Validation, Writing–original draft.

Funding

The author(s) declare that no financial support was received for the research, authorship, and/or publication of this article.

Conflict of interest

The authors declare that the research was conducted in the absence of any commercial or financial relationships that could be construed as potential conflicts of interest.

The author(s) declared that they were an editorial board member of Frontiers, at the time of submission. This had no impact on the peer review process and the final decision.

Generative AI statement

The authors declare that no Generative AI was used in the creation of this manuscript.

Publisher's note

References

Ali, S. Z., Baloch, Z. W., Cochand-Priollet, B., Schmitt, F. C., Vielh, P., and Vanderlaan, P. A. (2023a). The 2023 Bethesda system for reporting thyroid cytopathology. *Thyroid* 33, 1039–1044. doi:10.1089/THY.2023.0141

Ali, S. Z., VanderLaan, P. A., Baloch, Z., Cochand-Priollet, B., Schmitt, F., and Vielh, P. (2023b). *The Bethesda system for reporting thyroid cytopathology: definitions, criteria, and explanatory notes*. 3rd Edition. Springer, 1–290. doi:10.1007/978-3-031-28046-7/COVER

Aras, S., and Zaidi, M. R. (2017). TAMeless traitors: macrophages in cancer progression and metastasis. *Br. J. Cancer* 117, 1583–1591. doi:10.1038/BJC.2017.356

Chen, S., Saeed, AFUH, Liu, Q., Jiang, Q., Xu, H., Xiao, G. G., et al. (2023). Macrophages in immunoregulation and therapeutics. *Signal Transduct. Target. Ther.* 8, 207. doi:10.1038/S41392-023-01452-1

Chistiakov, D. A. (2005). Immunogenetics of Hashimoto's thyroiditis. *J. Autoimmune Dis.* 2, 1. doi:10.1186/1740-2557-2-1

Cunha, L. L., Marcello, M. A., Nonogaki, S., Morari, E. C., Soares, F. A., Vassallo, J., et al. (2015). CD8+ tumour-infiltrating lymphocytes and COX2 expression may predict relapse in differentiated thyroid cancer. *Clin. Endocrinol.* 83, 246–253. doi:10.1111/CEN.12586

Derynck, R., Turley, S. J., and Akhurst, R. J. (2021). TGFβ biology in cancer progression and immunotherapy. *Nat. Rev. Clin. Oncol.* 18, 9–34. doi:10.1038/S41571-020-0403-1

D'Inzeo, S., Nicolussi, A., Donini, C. F., Zani, M., Mancini, P., Nardi, F., et al. (2012). A novel human Smad4 mutation is involved in papillary thyroid carcinoma progression. *Endocrine-Related Cancer* 19, 39–55. doi:10.1530/ERC-11-0233

D'Inzeo, S., Nicolussi, A., Ricci, A., Mancini, P., Porcellini, A., Nardi, F., et al. (2010). Role of reduced expression of SMAD4 in papillary thyroid carcinoma. *J. Mol. Endocrinol.* 45, 229–244. doi:10.1677/JME-10-0044

Fagin, J. A., and Nikiforov, Y. E. (2023). Progress in thyroid cancer genomics: a 40-year journey. *Thyroid* 33, 1271–1286. doi:10.1089/THY.2023.0045

Ferrari, S. M., Fallahi, P., Galdiero, M. R., Ruffilli, I., Elia, G., Ragusa, F., et al. (2019). Immune and inflammatory cells in thyroid cancer microenvironment. *Int. J. Mol. Sci.* 20, 4413. doi:10.3390/IJMS20184413

French, J. D., Weber, Z. J., Fretwell, D. L., Said, S., Klopper, J. P., and Haugen, B. R. (2010). Tumor-associated lymphocytes and increased FoxP3+ regulatory T cell frequency correlate with more aggressive papillary thyroid cancer. *J. Clin. Endocrinol. Metabolism* 95, 2325–2333. doi:10.1210/JC.2009-2564

Galdiero, M. R., Varricchi, G., and Marone, G. (2016). The immune network in thyroid cancer. *Oncoimmunology* 5, e1168556. doi:10.1080/2162402X.2016.1168556

Giles, J. R., Globig, A. M., Kaech, S. M., and Wherry, E. J. (2023). CD8+ T cells in the cancer-immunity cycle. *Immunity* 56, 2231–2253. doi:10.1016/J.IMMUNI.2023.09.005

Goldstein, R. E., Netterville, J. L., Burkey, B., and Johnson, J. E. (2002). Implications of follicular neoplasms, atypia, and lesions suspicious for malignancy diagnosed by fine-needle aspiration of thyroid nodules. *Ann. Surg.* 235, 656–664. doi:10.1097/00000658-200205000-00007

Gong, J., Jin, B., Shang, L., and Liu, N. (2021). Characterization of the immune cell infiltration landscape of thyroid cancer for improved immunotherapy. *Front. Mol. Biosci.* 8, 714053. doi:10.3389/FMOLB.2021.714053

Hebenstreit, D., Wirnsberger, G., Horejs-Hoeck, J., and Duschl, A. (2006). Signaling mechanisms, interaction partners, and target genes of STAT6. *Cytokine Growth Factor Rev.* 17, 173–188. doi:10.1016/J.CYTOGFR.2006.01.004

Hu, T. X., Nguyen, D. T., Patel, M., Beckett, K., Douek, M., Masamed, R., et al. (2022). The effect modification of ultrasound risk classification on molecular testing in predicting the risk of malignancy in cytologically indeterminate thyroid nodules. *Thyroid* 32, 905–916. doi:10.1089/THY.2021.0659

Huang, Y., Fang, S., Li, D., Zhou, H., Li, B., and Fan, X. (2019). The involvement of T cell pathogenesis in thyroid-associated ophthalmopathy. *Eye Lond. Engl.* 33, 176–182. doi:10.1038/S41433-018-0279-9

Ivanova, K., Manolova, I., Ignatova, M. M., and Gulubova, M. (2018). Immunohistochemical expression of TGF-B1, SMAD4, SMAD7, TGFβRII and

CD68-positive TAM densities in papillary thyroid cancer. *Open Access Macedonian J. Med. Sci.* 6, 435–441. doi:10.3889/OAMJMS.2018.105

Jung, K. Y., Cho, S. W., Kim, Y. A., Kim, D., Oh, B. C., Park, D. J., et al. (2015). Cancers with higher density of tumor-associated macrophages were associated with poor survival rates. *J. Pathology Transl. Med.* 49, 318–324. doi:10.4132/JPTM.2015.06.01

Li, D., Shao, F., Yu, Q., Wu, R., Tuo, Z., Wang, J., et al. (2024). The complex interplay of tumor-infiltrating cells in driving therapeutic resistance pathways. *Cell Commun. Signal. CCS* 22, 405. doi:10.1186/S12964-024-01776-7

Lim, H., Devesa, S. S., Sosa, J. A., Check, D., and Kitahara, C. M. (2017). Trends in thyroid cancer incidence and mortality in the United States, 1974-2013. *JAMA* 317, 1338–1348. doi:10.1001/JAMA.2017.2719

Liu, H., Antony, S., Roy, K., Juhasz, A., Wu, Y., Lu, J., et al. (2017). Interleukin-4 and interleukin-13 increase NADPH oxidase 1-related proliferation of human colon cancer cells. *Oncotarget* 8, 38113–38135. doi:10.18632/ONCOTARGET.17494

Liu, Q., Sun, W., and Zhang, H. (2022). Roles and new insights of macrophages in the tumor microenvironment of thyroid cancer. *Front. Pharmacol.* 13, 875384. doi:10.3389/FPHAR.2022.875384

Lv, J., Feng, Z. P., Chen, F. K., Liu, C., Jia, L., Liu, P. J., et al. (2021). M2-like tumor-associated macrophages-secreted Wnt1 and Wnt3a promotes dedifferentiation and metastasis via activating β-catenin pathway in thyroid cancer. *Mol. Carcinog.* 60, 25–37. doi:10.1002/MC.23268

Menicali, E., Guzzetti, M., Morelli, S., Moretti, S., and Puxeddu, E. (2021). Immune landscape of thyroid cancers: new insights. *Front. Endocrinol.* 11, 637826. doi:10.3389/FENDO.2020.637826

Modi, J., Patel, A., Terrell, R., Tuttle, R. M., and Francis, G. L. (2003). Papillary thyroid carcinomas from young adults and children contain a mixture of lymphocytes. *J. Clin. Endocrinol. Metabolism* 88, 4418–4425. doi:10.1210/JC.2003-030342

Rahib, L., Smith, B. D., Aizenberg, R., Rosenzweig, A. B., Fleshman, J. M., and Matrisian, L. M. (2014). Projecting cancer incidence and deaths to 2030: the unexpected burden of thyroid, liver, and pancreas cancers in the United States. *Cancer Res.* 74, 2913–2921. doi:10.1158/0008-5472.CAN-14-0155

Rocha, J. T. Q., Kanda, R. G., Marques, M. E. A., Tagliarini, J. V., da Silva Mazeto, G. M. F., and Oliveira, C. C. (2023). Bethesda Category III thyroid nodules: descriptive cytological aspects of a series. *Surg. Exp. Pathology* 6 (1), 16–17. doi:10.1186/S42047-023-00141-1

Sari, S., Özdemir, Ç., and Çilekar, M. (2022). The relationship of tumour-associated macrophages (CD68, CD163, CD11c) and cancer stem cell (CD44) markers with prognostic parameters in breast carcinomas. *Pol. J. Pathology* 73, 299–309. doi:10.5114/PJP.2022.125424

Sheridan, R. L., Schomaker, K. T., Lucchina, L. C., Hurley, J., Yin, L. M., Tompkins, R. G., et al. (1995). Burn depth estimation by use of indocyanine green fluorescence: initial human trial. *J. Burn Care Rehabilitation* 16, 602–604. doi:10.1097/00004630-199511000-00007

Siegel, R. L., Miller, K. D., Fuchs, H. E., and Jemal, A. (2021). Cancer statistics, 2021. *CA a Cancer J. Clin.* 71, 7–33. doi:10.3322/CAAC.21654

Song, M., Liu, Q., Sun, W., and Zhang, H. (2023). Crosstalk between thyroid carcinoma and tumor-correlated immune cells in the tumor microenvironment. *Cancers* 15, 2863. doi:10.3390/CANCERS15102863

Sulaieva, O., Chernenko, O., Chereshneva, Y., Tsomartova, D., and Larin, O. (2019). Thyroid stimulating hormone levels and BRAFV600E mutation contribute to pathophysiology of papillary thyroid carcinoma: relation to outcomes? *Pathophysiology* 26, 129–135. doi:10.1016/J.PATHOPHYS.2019.05.001

Sulaieva, O., Chernenko, O., Selesnov, O., Nechay, O., Maievskyi, O., Falalyeyeva, T., et al. (2020a). Mechanisms of the impact of Hashimoto thyroiditis on papillary thyroid carcinoma progression: relationship with the tumor immune microenvironment. *Endocrinol. Metabolism (Seoul, Korea)* 35, 443–455. doi:10.3803/ENM.2020.35.2.443

Sulaieva, O., Selezniov, O., Shapochka, D., Belemets, N., Nechay, O., Chereshneva, Y., et al. (2020b). Hashimoto's thyroiditis attenuates progression of papillary thyroid carcinoma: deciphering immunological links. *Heliyon* 6, e03077. doi:10.1016/J.HELIYON.2019.E03077

Todaro, M., Alea, M. P., Scopelliti, A., Medema, J. P., and Stassi, G. (2008). IL-4-mediated drug resistance in colon cancer stem cells. *Cell Cycle Georget. Tex* 7, 309–313. doi:10.4161/CC.7.3.5389

Ulisse, S., Baldini, E., Lauro, A., Pironi, D., Tripodi, D., Lori, E., et al. (2021). Papillary thyroid cancer prognosis: an evolving field. *Cancers* 13, 5567. doi:10.3390/CANCERS13215567

Wang, C. G., Ye, Y. J., Yuan, J., Liu, F. F., Zhang, H., and Wang, S. (2010). EZH2 and STAT6 expression profiles are correlated with colorectal cancer stage and prognosis. *World J. Gastroenterology* 16, 2421–2427. doi:10.3748/WJG.V16.I19.2421

Wang, L., Yu, S., Yin, Y., and Hao, Y. (2020). STAT6 correlates with response to immune checkpoint blockade therapy and predicts worse survival in thyroid cancer. *Biomarkers Med.* 14, 955–967. doi:10.2217/BMM-2020-0125

Wang, Y., He, Y., Cao, L., Peng, X., Gu, Z., and Yan, J. (2022). Exploring the correlation analysis of immune microenvironment, mutation burden and prognosis of papillary thyroid carcinoma based on Estimate algorithm. *Gland. Surg.* 11, 860–867. doi:10.21037/gs-22-211

Xing, M. (2013). Molecular pathogenesis and mechanisms of thyroid cancer. *Nat. Rev. Cancer* 13, 184–199. doi:10.1038/NRC3431

Yang, Z., Wei, X., Pan, Y., Xu, J., Si, Y., Min, Z., et al. (2021). A new risk factor indicator for papillary thyroid cancer based on immune infiltration. *Cell Death Dis.* 12, 51. doi:10.1038/S41419-020-03294-Z

Zhang, S., Chen, S., Wang, Y., Zhan, Y., Li, J., Nong, X., et al. (2021). Association of a novel prognosis model with tumor mutation burden and tumor-infiltrating immune cells in thyroid carcinoma. *Front. Genet.* 12, 744304. doi:10.3389/FGENE.2021.744304

Zheng, X., Sun, R., and Wei, T. (2024). Immune microenvironment in papillary thyroid carcinoma: roles of immune cells and checkpoints in disease progression and therapeutic implications. *Front. Immunol.* 15, 1438235. doi:10.3389/FIMMU.2024.1438235

frontiers | Frontiers in Molecular Biosciences

TYPE Original Research
PUBLISHED 07 February 2025
DOI 10.3389/fmolb.2025.1543148

OPEN ACCESS

EDITED BY
Rostyslav Bilyy,
Danylo Halytsky Lviv National Medical University, Ukraine

REVIEWED BY
Peng Liu,
Sun Yat-sen University, China
Surjendu Maity,
Duke University, United States

*CORRESPONDENCE
Oksana Sulaieva,
o.sulaieva@csd.com.ua

RECEIVED 10 December 2024
ACCEPTED 20 January 2025
PUBLISHED 07 February 2025

CITATION
Dudin O, Mintser O, Gurianov V, Kobyliak N, Kozakov D, Livshun S and Sulaieva O (2025) Defining the high-risk category of patients with cutaneous melanoma: a practical tool based on prognostic modeling.
Front. Mol. Biosci. 12:1543148.
doi: 10.3389/fmolb.2025.1543148

Defining the high-risk category of patients with cutaneous melanoma: a practical tool based on prognostic modeling

Oleksandr Dudin[1,2], Ozar Mintser[2], Vitalii Gurianov[3], Nazarii Kobyliak[1,3], Denys Kozakov[1], Sofiia Livshun[1] and Oksana Sulaieva[1,4]*

[1]Pathology Department, Medical Laboratory CSD, Kyiv, Ukraine, [2]Department of Fundamental Disciplines and Informatics, Shupyk National Healthcare University of Ukraine, Kyiv, Ukraine, [3]Endocrinology Department, Bogomolets National Medical University, Kyiv, Ukraine, [4]Kyiv Medical University, Pathology Department, Kyiv, Ukraine

Introduction: Although most cutaneous melanoma (CM) in its early stages is treatable, the risk of recurrence remains high and there is a particular ambiguity on patients prognosis. This drives to identification of prognostic biomarkers for predicting CM recurrence to guide appropriate treatment in patients with localized melanoma.

Aim: This study aimed to develop a prognostic model for assessing the risk of recurrence in patients with CM, enabling prompt prognosis-driven further clinical decision-making for high-risk patients.

Materials and methods: This case-control study included 172 patients with CM recurrence (high-risk group) and 30 patients with stable remission (low-risk group) 3 years after primary diagnosis. The impact of sex, age at diagnosis, anatomical site, histological characteristics (the histological type, pathological stage, ulceration; the depth of invasion, mitotic rate, lymphovascular invasion, neurotropism, association with a nevus, tumor-infiltrating lymphocyte density, tumor regression and *BRAF* codon 600 mutation status) on CM recurrence was evaluated.

Results: Five independent variables, including nodal status, a high mitotic rate, Breslow thickness, lymphovascular invasion, perineural invasion and regression features were identified as the most significant. A 5-factor logistic regression model was developed to assess the risk of melanoma recurrence. The sensitivity and specificity of the model were 86.1% and 72.7%, respectively.

Conclusion: The developed model, which relies on routine histological features, allows the identification of individuals at high risk of CM recurrence to tailor their further management.

KEYWORDS

cutaneous melanoma, BRAF mutations, histological subtype, recurrence, prognostic model

Introduction

Cutaneous melanoma (CM) is a highly aggressive skin malignancy whose incidence has increased dramatically in recent decades (Siegel et al., 2022). Although CM represents approximately 4% of all skin malignancies, it is responsible for approximately 75% of skin cancer-related deaths (Gosman et al., 2023; Davis et al., 2019). According to the available data, a majority of melanoma cases diagnosed at stages III and IV are associated with high mortality (Dudin et al., 2023). More than 65%–90% of CMs diagnosed at early stages are treatable, with a high overall survival rate (Orzan et al., 2015). Nonetheless, the risk of recurrence remains high, reaching 50% in stage III melanoma (Garbe et al., 2022; Helvind et al., 2023). Even in localized stage I-II melanoma, 15%–20% of patients relapse locally or in/transit (Orzan et al., 2015), ~50% in regional lymph nodes and ~29% at distant metastatic sites (Salama et al., 2013). The follow-up strategy for CM patients depends on the stage of disease based on the criteria defined by the American Joint Committee on Cancer (AJCC) staging manual (8th edition). The current guidelines, however, present a degree of ambiguity where the question of follow-up in patients with localized CM remains unresolved, with the recommendation to conduct only regular skin examinations during the first 5 years (Swetter et al., 2021). This drives researchers' interest in identifying prognostic biomarkers for predicting CM recurrence and progression to guide appropriate treatment in patients with localized melanoma.

There are various patterns of recurrence, including local, satellite or transit metastases, as well as lymph node and systemic metastases. While advanced melanoma is prone to a high risk of systemic metastasis, early-stage CM tends to recur at the locoregional level (Peirano et al., 2023). The risk of CM recurrence is related to various factors, including stage, sex, age, depth of invasion, mitotic rate, host response to tumor growth, genetic alterations, etc. (Elder et al., 2005). The stage and melanoma thickness have been shown to play crucial roles in predicting tumor behavior and shaping patient management (Rothberg and Rimm, 2014). Sentinel lymph node (SLN) involvement in the development of malignant melanoma is associated with an increased risk of recurrence or progression (Lund, 2022). However, correct SLN identification and accurate assessment of lymph node status require advanced preoperative planning via 3D imaging with SPECT/CT for better intraoperative decision-making. Moreover, the rate of false-negative results in SLN assessment is still high, ranging from 5% to 21% (Peirano et al., 2023).

Similarly, Breslow thickness, ulceration, the rate of proliferation, the anatomical site, and the CM histological subtype have also been reported to be prognostically significant factors for predicting tumor behavior and disease progression. The recent systematic review devoted to identifying prognostic models for melanoma survival, recurrence and metastasis in patients with CM of I and II stages highlighted the feasibility of using clinicopathological features for prognostication. The most common features used for prognostic models included ulceration, Breslow thickness/depth, sociodemographic status and primary site of melanoma lesions (Kunonga et al., 2023). Other studies confirmed the prognostic significance of CM location and ulceration (Rashid et al., 2011). They also illuminated the role of histological type and patients age. Besides tumor-infiltrating lymphocytes (TILs) were shown to have prognostic and predictive value in some types of CM (Lee et al., 2013). While Wan et al. (2022) applied machine-learning algorithms for predicting CM recurrence based on 36 clinical and histopathologic features and demonstrated that Breslow tumor thickness and mitotic rate were the most predictive features (Wan et al., 2022). Nevertheless, the accuracy and affordability of various prognostic models based on clinical and histological parameters is still under debate. Assessment of these parameters might not be sufficient to identify individuals at high risk of recurrence (Salama et al., 2013; Homsi et al., 2005). Various immunohistochemical markers, including Bcl-6, MUC18, metalloproteinase-2, Ki-67, p16, p27, iNOS, etc. (Alonso et al., 2004; Ekmekcioglu et al., 2006), are related to melanoma prognosis, yet only a few of these markers have been confirmed to be linked to the likelihood of recurrence in CM patients (Ding et al., 2022). Several novel biomarkers, including exosomal melanoma inhibitory activity (MIA), serum S100B, epidermal AMBRA1 and loricrin, have been described in the context of disease prognosis. For example, the loss of peritumoral AMBRA1 and loricrin has been considered a prognostic biomarker of a low risk of recurrence in patients with stage I-II melanoma (Ewen et al., 2023). In the context of immunotherapy, the biomarkers LAG3 and TIGIT and tumor-infiltrating immune cell signatures have been described as both prognostic and predictive in CM (Naimy et al., 2023). Similarly, the expression profiles of ferroptosis genes together with clinical data from The Cancer Genome Atlas (TCGA) database were used to construct a model for predicting disease progression. The model stratified patients into low-risk and high-risk groups according to the prognostic value of ferroptosis-related gene expression. The expression profiles of ferroptosis-related genes correlate with disease progression in patients with melanoma. However, immune-activating pathway expression was related to the low-risk group (Kunonga et al., 2023). Although the stratification of patients is effective for evaluating disease progression, the limited data and availability of these biomarkers for routine testing prevent their application in clinical practice (Ding et al., 2022). The novel prognostic model can effectively stratify patients with respect to disease-associated risk; however, the currently available data to support these models to aid in clinical decision-making are still lacking (Wen et al., 2020). Risk factor-driven models and risk-associated biomarkers of CM recurrence are yet to provide commonly available practical tools for stratifying high-risk groups of patients and guiding further decision-making.

This study aims to develop a prognostic model for assessing the risk of recurrence in patients with CM, enabling prompt prognosis-driven further clinical decision-making for high-risk patients.

Materials and methods

Setting and participants

A total of 202 CM patients were included in this case-control study. The patients enrolled in this study had a history of observation for at least 3 years within the period from 2017 to 2022. This study was submitted for and formally exempted from Institutional Review Board approval because of the anonymous nature of the retrieved retrospective data. Informed consent was waived because of the fully anonymous nature of the delivery of the retrospective study data.

Methodology

Clinical, histopathological and molecular testing on BRAF mutation status data were retrieved from the database. In the first step, we selected all cases with histologically confirmed CM with complete clinical, histological and molecular data. Next, we selected only cases obtained by excision with histologically confirmed negative surgical (resection) margins. Finally, only cases with follow-up with histological data available were enrolled in the study cohort. The following inclusion criteria were applied: histologically confirmed diagnosis of CM of stages I-III, negative surgical (resection) margins after excision (to exclude the direct impact of positive margins on melanoma recurrence), known pathological stage and histological tumor features, and known *BRAF* codon 600 mutation status, follow-up histological data within 3 years after diagnosis. The exclusion criteria were as follows: incisional biopsy of skin melanoma instead of excision, positive surgical (resection) margins, lack of histological data according to the CAP protocol, presence of distant metastasis at the time of primary diagnosis, unknown *BRAF* status, and lack of follow-up data with confirmed outcomes. Thus, all patients were characterized with respect to clinical and histopathological tumor features and were tested for *BRAF* codon 600 mutations.

To estimate the sample size, we used the G*Power statistical power analysis tool and calculated sample size for $\alpha = 0.05$, Power = 0.8 and strong influence of the factor (OR ≤ 0.33) (Faul et al., 2007). According to calculations the minimal sample size was equal to 152 patients.

According to the results of follow-up histology and defined outcome patients we divided into groups. The high-risk group included 172 patients with melanoma recurrence within 3 years after primary diagnosis. Recurrence status was recorded in cases of true scar recurrence, local satellite/in-transit recurrence, and nodal or distant metastasis. Thirty patients who achieved stable remission 3 years after primary diagnosis were assigned to the low-risk group.

Methods and variables analyzed

The collected clinicopathological data included the patient's sex, age at diagnosis, and anatomical site of the primary melanoma. Relevant histological characteristics according to CAP protocols for CM were retrieved. The data included the histological type of CM according to the WHO classification (WHO); pathological stage, including tumor size (pT) and lymph node status (pN); ulceration; and tumor regression. The depth of invasion was evaluated according to the maximum tumor (Breslow) thickness (in mm) and anatomic (Clark) level. Breslow thickness (or maximum tumor thickness) was measured with an ocular micrometer at a right angle to the lesion surface from the upper edge of the granular layer of the epidermis (or the base of the ulcer in case of ulceration) to the deepest site of tumor invasion. Foci of neurotropism, lymphovascular invasion or microsatellites were not included in tumor thickness measurements. Anatomic (Clark) levels were identified according to CAP protocol as follows: I - Intraepidermal tumor growth (melanoma *in situ*), II - Tumor present in but does not fill and/or expand papillary dermis, III - Tumor fills and expands papillary dermis, IV - Tumor invades into reticular dermis, V Tumor invades subcutaneous layer.

The roles of factors such as the mitotic rate (per 1 mm^2), lymphovascular invasion, neurotropism (perineural or intraneural invasion), association with a nevus, tumor-infiltrating lymphocyte density, and tumor regression at the time of primary diagnosis were assessed in terms of patient prognosis. Tumor regression was defined by the following features: replacement of tumor cells by lymphohistiocytic infiltration, or attenuation of the epidermis and non-laminated dermal fibrosis with inflammatory cells, melanophagocytosis, and telangiectasia (Aung et al., 2017).

In addition, the potential impact of the *BRAF* codon 600 mutation status on CM recurrence was evaluated. Tumor-infiltrating lymphocytes (TILs) were evaluated in a dichotomous manner according to the pathology report description: the absence of lymphocytes or a low number of tumor-infiltrated lymphocytes were considered TIL-low infiltration, whereas moderate or high-intensity lymphocytic infiltrates were considered TIL-high infiltration.

Molecular testing for detecting BRAF codon 600 mutations was conducted on tissue samples via formalin-fixed paraffin-embedded blocks with verified tumor content. Ten 10 μm-thick sections were obtained from each paraffin block containing a representative tumor area (>20% tumor cells, >200 cells in the sample, <20% necrosis area). DNA was extracted using ZYTOVISION VisionArray FFPE DNA Extraction Kit according to the manufacturer's instructions. The detection of BRAF codon 600 mutations was performed by real-time polymerase chain reaction (RT-PCR) using Easy PGX-ready BRAF system (Diatech Pharmacogenetics, Italy). The assay is designed to detect 5 types of *BRAF* mutations in codon 600: V600E (1799T > A), V600E (1799_1800TG > AA), V600 K (1798_1799GT > AA), V600D (1799_1800TG > AT), and V600 R (1798_1799GT > AG).

Statistical analysis

Statistical analysis was conducted using MedCalc® Statistical Software version 22.016 (MedCalc Software Ltd., Ostend, Belgium; https://www.medcalc.org; 2023) and GraphPad Prism (GraphPad Prism Version 10.0.3 (217) GraphPad Software, San Diego, California, United States; www.graphpad.com). Descriptive statistics for continuous variables (such as age, mitotic rate, and Breslow thickness) were presented as the Mean and SEM for normally distributed data or Median and Interquartile Range for non-normally distributed data. Quantitative data were assessed as frequencies (%). The χ^2 test or Fisher's exact test were applied to compare frequencies. An unpaired *t*-test or non-parametric Mann-Whitney test were used to compare continuous variables between high- and low-risk groups. The developed model was developed to predict the risk of melanoma recurrence within 3 years (binary outcome), so logistic regression was used. Univariate and multivariate logistic regression analysis models were used to assess the impact of various variables on the risk of relapse. The stepwise method was used to identify the set of variables with the highest impact on outcome and define the best-fitting multivariable logistic regression model. To assess the effect of variables on the outcome, odds ratios (OR) with 95% confidence interval (95% CI) were calculated. The diagnostic performance of the logistic regression

models was evaluated using Receiver Operating Characteristic (ROC) curve analysis. The area under the ROC curve (AUROC) and its 95% CI were calculated. The P-value <0.05 was considered statistically significant for all of the tests.

Results

Patients' characteristics

A total of 202 cases with primary CM and 3-year follow-up data are reported in this study. Among the enrolled cases, 103 were males (51%) and 99 (49%) were females, aged 52.6 ± 1.51 (95% CI 49.6–55.6) and 52.0 ± 1.46 (95% CI 49.2–54.9), respectively. The high-risk group included 84 males (48.9%) and 88 females (51.1%). Among patients with remission, there was a higher rate of males (19 of 30, 63.3%) and females represented 36.7% (11 of 30) of the group.

The high-risk group included 172 patients aged 52.2 ± 1.14 years (95% CI 49.9–54.5). The low-risk group comprised 30 patients with stable remission aged 52.9 ± 2.76 years (95% CI 47.3–58.54). There was no significant difference in age and gender distribution between the high- and low-risk groups (Table 1).

In both groups CM at trunk predominated comprising 36.1% in high-risk group and 43.3% in low-risk patients. Similarly, there were no differences in the frequency of various histological types of CM between groups. The most common types were SSM (44.8% and 53.5% of cases in high- and low-risk groups, respectively) and NM comprising correspondingly 27.3% and 30%. At the same time, 7 cases (4.1%) were reported with Spitzoid or desmoplastic CM in the high-risk group. However, we did not find statistically significant differences in the anatomical site of the primary tumor between groups.

Among the observed cases, 19 (9.4%) were characterized as stage I, 133 (65.8%) as stage II and 50 (24.8%) as stage III CM. All patients with affected lymph nodes (stage III) were in the high-risk group, with confirmed recurrence. CM recurrence was characterized by either locoregional or distant metastasis within 3 years of the follow-up period. Within the high-risk group, 13 cases (7.6%) were identified as stage I, 109 cases (63.4%) as stage II, and 50 cases (29%) as stage III CM according to the AJCC tumor staging system. Alternatively, the low-risk group demonstrated 20% of Stage I and 80% of Stage II CM. There were no node-positive cases in this group. This defined a statistically significant difference in staging between patients with recurrence and remission (P < o.oo1).

Finally, we did not find a difference in the BRAF mutation rate between groups, which reached 61.6% in the high-risk group and 60% in patients with remission.

The impact of histological and molecular features on CM recurrence

Regarding the anatomical site of the primary tumor, most cases (n = 75, 37.1%) were located at the trunk, 56 CMs (26.7%) were located in the upper or lower limbs, 17 at the face or scalp areas (8.4%), and the remaining 54 cases had no specified primary CM site (26.7%). There was no significant difference between the groups in the anatomical site of the primary tumor (P = 0.645), the histological subtype of CM (P = 0.518), or the incidence of *BRAF* codon 600 mutation (P > 0.999).

Although there was no difference in ulceration of primary melanoma between high- and low-risk groups (P = 0.241), we observed a significantly greater mitotic rate (P = 0.026) and Breslow thickness (P = 0.01) in the high-risk group than in the low-risk group. At the same time, LVI (P < 0.001), PNI (P < 0.001) and tumor regression features (P < 0.001) were observed at a higher rate in patients with CM recurrence (Figure 1).

There were 124 *BRAF*-mutation-positive cases (61.4% of the observed cohort). The rate of BRAF codon 600 mutations did not differ between the high- and low-risk groups (Table 2). In patients with recurrence, BRAF codon 600 mutation was detected in 61.6% of patients (106 of 172), whereas in the low-risk group, it was identified in 60% of cases (17 of 30, P > 0.999).

Logistic regression analysis for predicting CM recurrence

Single-factorial logistic regression analysis was conducted to identify the features with a moderate degree of relationship with patient outcome (AUROC = 0.6–0.7). These factors included the following: nodal status (stage), mitotic rate, Breslow thickness, LVI, PNI, and regression features.

The risk of recurrence is increased significantly in N-positive tumors (stage III) (P < 0.001; OR = 4.41; 95% CI 1.98–9.87). Similarly, a high mitotic rate, Breslow thickness, LVI, PNI, and regression features affected the probability of CM recurrence (Table 2). To define the minimal set of variables for predicting CM recurrence in a multifactorial logistic regression model, stepwise analysis was employed (stepwise threshold of inclusion $p < 0.05$, threshold of exclusion $p > 0.1$). Five independent variables were identified as the most significant. The independent variables were independent of each other (the Variance Inflation Factor for predictors did not exceed 1.1). Clark level, Breslow thickness correlated with the Stage ($r = 0.47$ and $r = 0.45$, $p < 0.001$, correspondingly), they were excluded from the multiple regression model using Stepwise method. The 5-factors regression model includes only independent significant variables. If we add Breslow's thickness to the model (for example) then the coefficient does not differ to zero (P = 0.531).

The adequacy of the constructed model was confirmed by its characteristics ($\chi^2 = 42.9$, at 5 degrees of freedom; P < 0.001). The AUROC of 0.88 (95% CI 0.81–0.93) reflects the strong link between the risk of progression and tumor characteristics such as stage, mitotic rate, LVI, PNI and tumor regression features (Table 3; Figure 1). When defining the optimal model threshold $Y_{crit} > 0.5221$ the sensitivity and specificity of the model were 86.1% (95% CI 78.4%–91.8%) and 72.7% (95% CI 49.8%–89.3%), respectively. The positive predictive value PPV comprised 94.3% (95% CI 89.3%–97.0%), while the negative predictive value NPV was found to reach 50% (95% CI 37.2%–2.8%). The model can be represented by Formula 1:

$$\ln(Y/(1-Y)) = 21.6 * X1 + 1.02 * X2 + 22.1 * X3 + 21.6 * X4 + 2.49 * X5 + 0.09 \quad (1)$$

10.3389/fmolb.2025.1543148

TABLE 1 Characteristics of patients of the study.

Parameters	Total (n = 202)	High-risk group (recurrence) (n = 172)	Low-risk group (remission) (n = 30)	P-value
Age, years	52.3 + 1.05 (50.3–54.4)	52.2 ± 1.14 (49.9–54.5)	52.9 ± 2.76 (47.3–58.54)	0.819
Sex				
Male	103 (51.0%)	84 (48.9%)	19 (63.3%)	0.618
Female	99 (49.0%)	88 (51.1%)	11 (36.7%)	
The stage at the time of diagnosis				
I	19 (9.4%)	13 (7.6%)	6 (20%)	<0.001
II	133 (65.8%)	109 (63.4%)	24 (80%)	
III	50 (24.8%)	50 (29.0%)	0	
Anatomical site of the primary tumor				
Face & Scalp	17 (8.4%)	16 (9.3%)	1 (3.3%)	0.645
Limbs	56 (26.7%)	47 (27.3%)	9 (30%)	
Trunk	75 (37.1%0	62 (36.1%)	13 (43.3%)	
NOS	54 (26.7%)	47 (27.3%)	7 (23.4%)	
Histological type				
SSM	93 (46%)	77 (44.8%)	16 (53.3%)	0.518
NM	56 (27.7%)	47 (27.3%)	9 (30%)	
Spitzoid + Desmoplastic	7 (3.5%)	7 (4.1%)	0	
NOS	46 (22.8%)	41 (23.8%)	5 (16.7%)	
BRAF codon 600 mutation status				
BRAF-mutated	124 (61.4%)	106 (61.6%)	18 (60%)	>0.999
BRAF-wt	78 (39.6%)	66 (39.4%)	12 (40%)	

Data presented as M±SE (95%CI) or % (n).

where Y is the risk of CM recurrence; X1 = 0 for Stages 1–2 and X1 = 1 for Stage 3; X2 = 0 for mitotic rate <=5 and X2 = 1 for mitotic rate>5; X3 = LVI (0/1); X3 = PNI (0/1); and X5 = regression (0/1).

For practical application of the 5-factor model, the tool for calculating patient risk prediction was implemented in Excel.

Discussion

Although various indicators are considered prognostic at the time of diagnosis, predicting the risk of recurrence in early-stage CM is still challenging. Whereas it is widely accepted that the clinicopathological and demographic features of primary tumors impact prognosis, various authors have applied different sets of histopathological criteria to predict melanoma recurrence (Abbas et al., 2014; Chousakos et al., 2023). Here, we evaluated the relationships between demographic, clinical, and histopathological data and patient outcomes. We analyzed the effects of positive nodal status, histological type, mitotic rate, Breslow thickness, LVI, PNI and tumor regression features on the risk of CM recurrence. Moreover, we found no impact of age, sex, Clark level of invasion, microsatellites, ulceration, association with nevus, or the presence or type of *BRAF* codon 600 mutations on patient prognosis. Ulceration, Breslow thickness and the mitotic rate were found to have the highest statistical power for predicting outcomes in a study by Vita et al. (2023). Besides, multivariable analysis by Buja A. et al. revealed that age, primary tumor site, histological subtype, mitotic count, and tumor stage were independently associated with disease prognosis (Buja et al., 2021). The differences in prognostic criteria could be explained

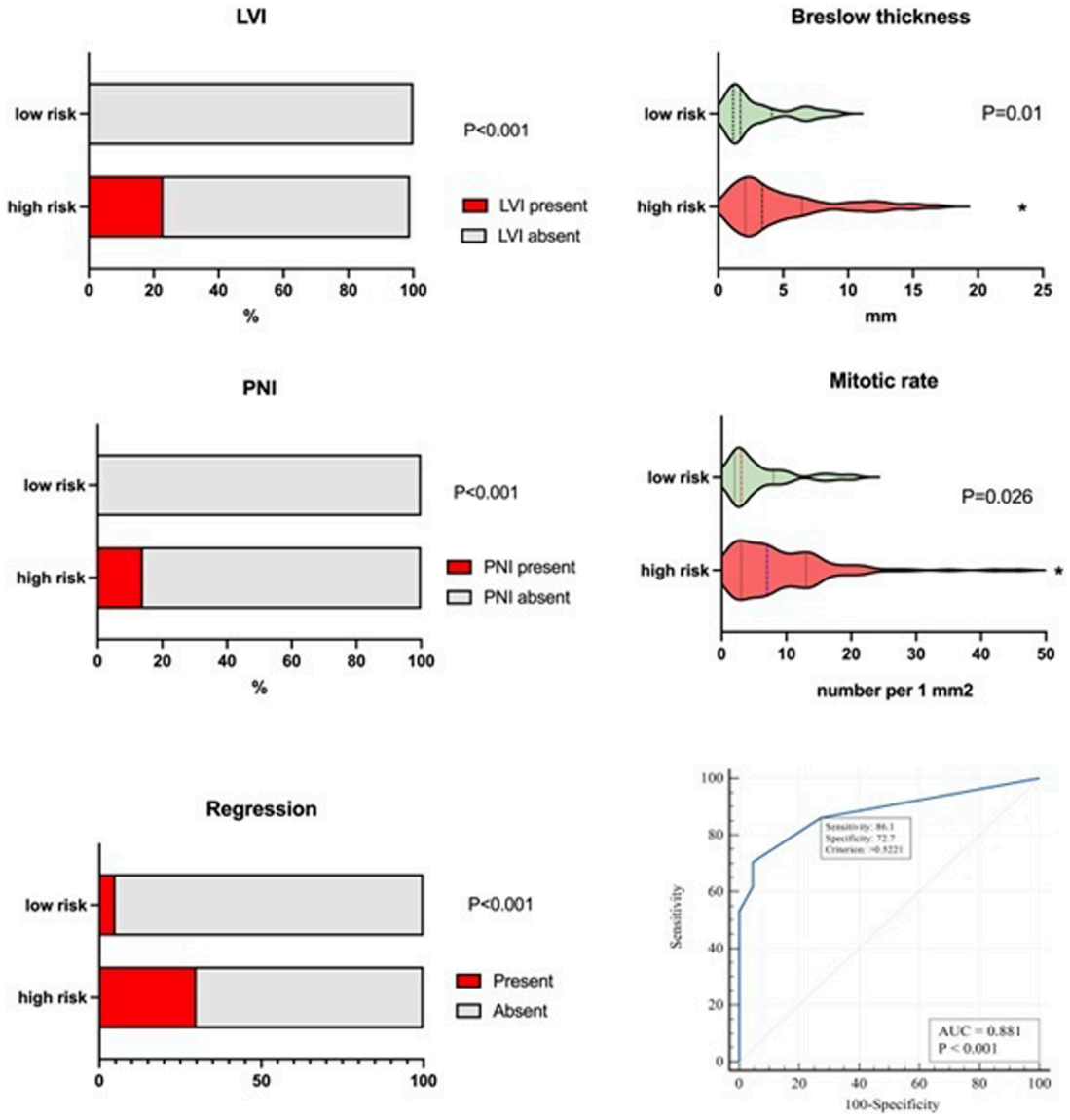

FIGURE 1
Difference in histological features between high- and low-risk groups. The high-risk group demonstrated a significantly higher rate of mitosis, depth of invasion assessed via Breslow thickness, LVI and PNI, and tumor regression features. ROC curve of these 5-factorial logistic regression model for predicting the risk of CM recurrence demonstrates the area under the curve of AUC = 0.88 (95% CI 0.81–0.93) reflecting the strong link between the risk of recurrence and the selected variables The sensitivity and specificity of the model are 86.1% (95% CI 78.4%–91.8%) and 72.7% (95% CI 49.8%–89.3%), respectively.

by the heterogeneity of CM patient populations used in these studies, various inclusion and exclusion criteria, and different endpoints. Importantly, the lists of selected primary factors to be analyzed for predicting patient outcomes presented a high degree of variability between the studies. The common idea, however, is based upon the need to identify subgroups of CM patients at a higher risk for recurrence to optimize management for such patients (Chousakos et al., 2023).

This study elucidated the 5 main tumor features associated with a high risk of CM recurrence, including positive nodal status (stage III), mitotic rate, lymphovascular or perineural invasion, and features of tumor regression. TNM staging was previously shown to be vital in predicting melanoma outcomes (Cozzolino et al., 2023). This enables to prognose the patient outcome based on five widely used features reported by pathologists according to standard protocols. The simplicity and affordability of variables used for assessing the risk of recurrence make the developed model attractive for clinical application at least for the preliminary risk assessment and making decisions concerning every particular patient management based on his or her stage, mitotic rate, tumor invasiveness and regression features.

Comparing the developed model with already existing tools it is important to highlight that many studies apply machine learning-based algorithms which also defined the significance of

10.3389/fmolb.2025.1543148

TABLE 2 Impact of clinical and histopathological features on the risk of recurrence in stage I-III CM (in univariable logistic regression model).

Variables		Model coefficient, b ± m	P	Or (95% CI)	AUROC (95% CI)
Sex	F	Referent			–
	M	−0.59 + 0.41	0.147	–	
Stage		1.49 ± 0.41	<0.001	4.42 (1.98–9.87)	0.69 (0.62–0.75)
Age		−0.003 + 0.013	0.519	–	–
Anatomical site of primary tumor	NOS	Referent			–
	Limbs	−0.25 ± 0.54	0.644	–	
	Face or Scapl	0.87 ± 1.11	0.433	–	
	Trunk	−0.34 ± 0.51	0.500	–	
BRAF wt Vs. mutation		0.07 ± 0.40	0.866	–	–
Mutation type	WT	Referent			–
	V600 K	0.78 ± 1.09	0.473	–	
	V600 E	0.01 ± 0.41	0.990	–	
Positive Nodal status (Stage 3)		1.49 ± 0.41	<0.001	4.41 (1.98–9.87)	0.69 (0.62–0.75)
Histological type	NOS	Referent			0.60 (0.53–0.66)
	NM	−0.73 ± 0.59	0.216	–	
	Spitz	18.1	0.764	–	
	SSM	−0.86 ± 0.54	0.120	–	
Ulceration		0.32 ± 0.45	0.482	–	–
Mitosis more than 5		0.099 ± 0.045	0.028	1.10 (1.01–1.21)	0.66 (0.57–0.73)
Clark level		0.50 ± 0.27	0.063	–	–
Breslow thickness		0.29 ± 0.11	0.007	1.33 (1.08–1.64)	0.71 (0.63–0.79)
TILs high		−0.15 ± 0.21	0.478	–	–
LVI presence		21.1	0.031	22.2 (1.32–373)	0.64 (0.56–0.72)
PNI presence		19.9	0.138	–	0.57 (0.49–0.65)
Regression presence		2.25 ± 1.04	0.031	9.51 (1.23–73.3)	0.63 (0.54–0.71)
Microsatellite presence		1.16 ± 1.06	0.274	–	–
Association with nevus		1.33 ± 1.06	0.207	–	–

Nodal status, BRAF, status, ulceration, LVI, PNI, regression and microsatellite were considered as binary variables. The presence of the feature was considered when assessing the model coefficients.

variables in this study. For instance, using artificial intelligence tools for predicting short-term mortality in CM patients, Aung et al. (2017) showed that both distant and nodal metastasis aggravated the outcome in patients with CM. In addition, patient age, sex, tumor site, histological type and growth phase also contributed significantly to predicting overall survival. In our study focused on predicting CM recurrence, we also demonstrated the role of staging and underscored the prognostic role of other factors. Notably, the mitotic rate and tumor invasiveness features were considered to be tightly linked to melanoma aggressiveness and prognosis in recent

10.3389/fmolb.2025.1543148

TABLE 3 Characteristics of the 5-variables logistic regression model for assessing the risk of CM recurrence.

Variables		Model coefficient, b ± m	P	Or (95% CI)	AUROC (95% CI)
Stage	1–2	Referent			0.88 (0.81–0.93)
	3	21.8	All patients had a recurrence		
Mitotic rate	≤5	Referent			
	>5	1.02 ± 0.58	0.078	4.57 (1.26–16.6)	
LVI	0	Referent			
	1	22.1	All patients had a recurrence		
PNI	0	Referent			
	1	21.6	All patients had a recurrence		
Regression		2.49 ± 1.07	0.020	12.0 (1.48–97.9)	

studies (Thompson et al., 2011). Another study utilizing such tools as MLP, Adaptive Boosting (AB), Bagging (BAG), logistic regression (LR), Gradient Boosting Machine (GBM), and eXtreme Gradient Boosting (XGB) algorithms developed a model for predicting metastasis in patients with nodular melanoma (Serra et al., 2024). The MLP was found as the optimal. It demonstrated the best parameters reaching AUC = 0.932, F1 = 0.855, Accuracy = 0.856, Sensitivity = 0.878. In contrast to our study, this model was focused on nodular melanoma. However, it also highlighted the prognostic significance of the primary site and stage. Another cohort study performed at 4,718 patients with CM developed a model for prognosticating brain metastasis. Based on multivariate logistic regression analysis, authors identified the following significant risk factors of CNS metastasis of melanoma: a higher Breslow index, mitotic rate ≥1 mm^2, ulceration, and microscopic satellites. These data partly correlate with our findings, although it included patients with stage IV, mucosal melanoma and was focused on CNS metastasis and outcome (Serra et al., 2024). Similarly, in Romanian study, the Breslow thickness >2 mm, high Clark level, high mitotic rate and ulceration were defined as the most significant prognostic factors for lymph nodal involvement in CM (Vița et al., 2023). Other studies also illuminated the prognostic significance of LVI associated with recurrent disease (P = 0.003) and metastatic disease (P = 0.008) (Tas and Erturk, 2017). Multivariate analysis also uncovered that lymph node metastasis, Breslow thickness, LVI, and angiotropism are predictors of the overall survival of patients with CM. Moreover, LVI was also shown to correlate with neurotropism, Breslow's thickness and lymph node involvement (Tas and Erturk, 2017). Alternatively in an early-stage melanoma study performed on 1,720 patients, utilizing machine learning algorithms, only Breslow tumor thickness and mitotic rate were identified as the most informative features. Notably, models were evaluated internally by five-fold cross-validation of the MGB cohort, and externally via independent evaluation of training and testing cohorts. A recurrence classification performance of AUC in the internal and external validations comprised 0.845 and 0.812, respectively (Wan et al., 2022). These results are comparable with the performance of the model developed in our study.

Although Breslow thickness is an important histological parameter that can predict the outcome of primary CMs, this factor had a less prominent effect on the risk of recurrence in the observed cohort than the other factors selected for this model. According to the National Comprehensive Cancer Network guidelines, SLN biopsy is recommended for all CMs thicker than 1 mm (Carr et al., 2022). Nevertheless, some patients with thin lesions develop local or distant metastasis. This provoked a discussion on whether sentinel lymphadenectomy should be performed in addition to wide local excision for primary lesions ≤1.00 mm. Several studies have evaluated different approaches for identifying histopathological features and/or genetic markers for predicting SLN positivity and improving patient management (Carr et al., 2022). Although recommendations for SLN biopsy and complete lymph node dissection are still under discussion, the correct assessment of lymph node status is essential for accurate CM staging and prognosis, as it allows stratification of low- and high-risk groups and leads to improvements in regional disease control (Faries et al., 2017). Nevertheless, further prospective studies and clinical validation of the developed models are needed to implement personalized risk-assessment and management.

Interestingly, regression in primary CM was defined in our study as an important prognostic factor. According to recent studies, the prognostic value of regression in CM is quite controversial. While some studies have demonstrated a lack of correlation between regression and patient outcomes (Kaur et al., 2008), other authors have reported that regression predicts a greater risk of lymph node involvement (Oláh et al., 2003) and CM metastasis (Guitart et al., 2002). These controversies may be related to discrepancies in regression definitions and assessments, the different stages of melanoma included in the respective studies, the subjectivity of regression reporting and interpretation, the treatment used, *etc.* (McClain et al., 2012). Histologically, regression is characterized by a decrease in the number of melanoma cells associated with the host response, including inflammatory infiltrates, dermal fibrosis, melanophages, an increased number of ectatic blood and lymphatic vessels,

and the apoptosis of keratinocytes or melanocytes (Aung et al., 2017). It reflects the tumor-host interplay at the site of the primary disease (Aung et al., 2017).

Tumor-host interplay in areas of regression can affect CM outcomes in different ways via changes in the tumor immune microenvironment (TIME), the selection of tumor subclones with different genetic profiles or the use of various cell death mechanisms. First, the melanoma-host interplay can significantly affect various phases of tumor growth and development, depending on the host immune response. This may involve various populations of lymphocytes and macrophages and be associated with alternative polarization of the immune reaction. Importantly, a recent study revealed that regression is highly correlated with TILs (Morrison et al., 2022). Importantly, however, only TILs, but not regression features, were linked with SLN status and survival in CM. Thus, the presence of $CD8^+$ tumor-infiltrating lymphocytes impacts patient outcomes of CM. Alternatively, Yun et al. suggested that the negative impact of regression on CM prognosis can be related to increased dermal lymphatic vessel density, resulting in an enhanced risk of lymphovascular invasion (Yun et al., 2011). Moreover, the elimination of recognizable subpopulations of melanoma cells can benefit the remaining clones of aggressive melanoma cells, assisting their growth and tumor development.

Importantly, the predictive strength of the tumor regression features in our model was lower than that of stage or melanoma invasiveness. It works as a predictor of higher-risk CM only when it is combined with other factors, such as increased mitotic activity or perineural invasion, indicating aggressive melanoma tumor behavior. Importantly, the elimination of melanoma cells in areas of regression can be realized by various immune cells and through different cell death mechanisms. Aside from the classic antitumor immune reaction through $CD8^+$ cytotoxic lymphocytes, alternative activation of the host immune response, with the prevalence of Ms-macrophages, myeloid-derived immunosuppressive cells or activation of immune escape mechanisms, can foster and shape the further development of malignancies (Mashukov et al., 2021; Stakhovskyi et al., 2022). Within their works on deciphering TIME-related expression, Liang Z. and coauthors revealed several promising immune-related biomarkers, demonstrating that high expression levels of the *GZMB*, *C1QA*, and *C1QB* genes correlate with favorable prognosis in patients (Liang et al., 2022). Similarly, Zhang et al. demonstrated the relevance of TIME assessment via genomic and epigenomic scores for defining high-risk and low-risk groups of CM patients to guide personalized melanoma treatment (Zhang et al., 2023). Finally, the tumor regression features in primary CM may be related to the shift between the apoptosis and necroptosis pathways (Yang et al., 2023). A lack of apoptosis signaling can lead to an alternative cell death pathway known as necroptosis, a recently discovered pathway of programmed cell death that bypasses apoptosis and might be involved in pathological oncogenic processes. This process is associated with mitochondrial dysfunction and is promoted by increased generation of reactive oxygen species in melanoma cells, resulting in mutagenesis and cell death (Basit et al., 2017). Recently developed models for prognosis and accurate prediction of the response to immunotherapy demonstrated a close link between necroptosis-related genes and immune cell signatures, identifying novel approaches for identifying high-risk patients and personalizing their treatment.

Heterogeneity of the existing data and models concerning the risk factors and prognostic models allowing to prediction of CM recurrence are related to numerous factors, including differences in populations involved and CM characteristics (stage, histological types, etc.), clinical and pathological data sets, approaches for data handling and outcomes applied. This reflects insufficient evidence to make robust conclusions for clinical decision-making in the management of patients with CM. The developed model could provide clinical usefulness for stratifying patients with a high risk of melanoma recurrence. Despite the relatively low figures of NPV, the model enables predicting the high risk of recurrence with good accuracy. Considering existing clinical data concerning the risk of CM recurrence varying according to different data from 50% to 80% in CM of I-III stages, the developed model allows for prediction recurrence in 94.1% of patients with CM of I-III stage though further external and clinical validation of the model are needed (Leiter et al., 2014; Stucky et al., 2010). In the future, a prognostic model could be used to tailor patient management during counseling and/or integrate predictive models in electronic healthcare systems. Accurate risk assessment could support physicians' and patients' decision-making in clinical settings to plan individualized follow-up and treatment to prevent disease progression and improve patients' outcomes. The developed model could be also adjusted for navigating patients' management after immunotherapy. However future multi-center trials are needed to justify the model's application in populations treated with immunotherapy. The findings of the study also stimulate a comprehensive investigation of tumor regression mechanisms and interpretations for a better understanding of its role in CM behavior and progression.

Conclusion

This study demonstrated the prognostic significance of tumor stage, mitosis rate, and invasion features, as well as tumor regression features, on CM patient outcomes. The application of the 5-factor model, which is based on routinely assessed histological markers, allows the definition of high-risk groups of patients with a high likelihood of CM recurrence. Its application could be useful for guiding guide personalized management strategies. Further prospective studies are needed to validate the model.

Limitations of the study

This study is limited to a retrospective analysis of patient data over a three-year follow-up period. This study did not focus on the therapeutic schemes used for various patients in the cohort. Moreover, the sample included only patients with CM of the I-III stage, and we did not differentiate outcomes between groups. Due to the retrospective type of the study, there is a potential bias in data collection. For instance, the high- and low-risk groups were not equal in terms of CM staging. Logistic regression analysis instead of Cox proportional hazards regression was applied because of the lack of accurate follow-up data concerning the timing

of recurrence onset. The developed prognostic model was based on logistic regression analysis and needs validation in further multicenter studies.

Data availability statement

The raw data supporting the conclusions of this article will be made available by the authors, without undue reservation.

Ethics statement

The requirement of ethical approval was waived by the Medical Laboratory CSD (Kyiv, Ukraine) for the studies on humans because of the anonymous nature of the retrieved retrospective data. The studies were conducted in accordance with the local legislation and institutional requirements. Written informed consent for participation was not required from the participants or the participants' legal guardians/next of kin in accordance with the national legislation and institutional requirements. The human samples used in this study were acquired from a by-product of routine care or industry.

Author contributions

OD: Conceptualization, Data curation, Project administration, Supervision, Writing–original draft. OM: Formal Analysis, Methodology, Writing–review and editing. VG: Data curation, Formal Analysis, Methodology, Visualization, Writing–review and editing. NK: Conceptualization, Validation, Writing–original draft. DK: Formal Analysis, Methodology, Writing–review and editing. SL: Formal Analysis, Methodology, Writing–review and editing. OS: Conceptualization, Data curation, Project administration, Supervision, Validation, Writing–original draft.

Funding

The author(s) declare that no financial support was received for the research, authorship, and/or publication of this article.

Conflict of interest

The authors declare that the research was conducted in the absence of any commercial or financial relationships that could be construed as potential conflicts of interest.

The author(s) declared that they were an editorial board member of Frontiers, at the time of submission. This had no impact on the peer review process and the final decision.

Generative AI statement

The author(s) declare that no Generative AI was used in the creation of this manuscript.

Publisher's note

References

Abbas, O., Miller, D. D., and Bhawan, J. (2014). Cutaneous malignant melanoma: update on diagnostic and prognostic biomarkers. *Am. J. Dermatopathol.* 36, 363–379. doi:10.1097/DAD.0B013E31828A2EC5

Alonso, S. R., Ortiz, P., Pollán, M., Pérez-Gómez, B., Sánchez, L., Acuña, M. J., et al. (2004). Progression in cutaneous malignant melanoma is associated with distinct expression profiles: a tissue microarray-based study. *Am. J. pathology* 164, 193–203. doi:10.1016/S0002-9440(10)63110-0

Aung, P. P., Nagarajan, P., and Prieto, V. G. (2017). Regression in primary cutaneous melanoma: etiopathogenesis and clinical significance. *Laboratory investigation; a J. Tech. methods pathology* 97, 657–668. doi:10.1038/LABINVEST.2017.8

Basit, F., Van Oppen, LMPE, Schöckel, L., Bossenbroek, H. M., Van Emst-De Vries, S. E., Hermeling, J. C. W., et al. (2017). Mitochondrial complex I inhibition triggers a mitophagy-dependent ROS increase leading to necroptosis and ferroptosis in melanoma cells. *Cell death and Dis.* 8, e2716. doi:10.1038/CDDIS.2017.133

Buja, A., Bardin, A., Damiani, G., Zorzi, M., De Toni, C., Fusinato, R., et al. (2021). Prognosis for cutaneous melanoma by clinical and pathological profile: a population-based study. *Front. Oncol.* 11, 737399. doi:10.3389/FONC.2021.737399

Carr, M. J., Monzon, F. A., and Zager, J. S. (2022). Sentinel lymph node biopsy in melanoma: beyond histologic factors. *Clin. and Exp. metastasis* 39, 29–38. doi:10.1007/S10585-021-10089-9

Chousakos, E., Zugna, D., Dika, E., Boada, A., Podlipnik, S., Carrera, C., et al. (2023). Topographical and chronological analysis of thin cutaneous melanoma's progressions: a multicentric study. *Cancers* 15, 3989. doi:10.3390/CANCERS15153989

Cozzolino, C., Buja, A., Rugge, M., Miatton, A., Zorzi, M., Vecchiato, A., et al. (2023). Machine learning to predict overall short-term mortality in cutaneous melanoma. *Discov. Oncol.* 14, 13. doi:10.1007/S12672-023-00622-5

Davis, L. E., Shalin, S. C., and Tackett, A. J. (2019). Current state of melanoma diagnosis and treatment. *Cancer Biol. and Ther.* 20, 1366–1379. doi:10.1080/15384047.2019.1640032

Ding, L., Gosh, A., Lee, D. J., Emri, G., Huss, W. J., Bogner, P. N., et al. (2022). Prognostic biomarkers of cutaneous melanoma. *Photodermatol. Photoimmunol. and Photomed.* 38, 418–434. doi:10.1111/PHPP.12770

Dudin, O., Mintser, O., Kobyliak, N., Kaminskyi, D., Shabalkov, R., Matvieieva, A., et al. (2023). Incidence of BRAF mutations in cutaneous melanoma: histopathological and molecular analysis of a Ukrainian population. *Melanoma Manag.* 10, MMT64. doi:10.2217/MMT-2023-0005

Ekmekcioglu, S., Ellerhorst, J. A., Prieto, V. G., Johnson, M. M., Broemeling, L. D., and Grimm, E. A. (2006). Tumor iNOS predicts poor survival for stage III melanoma patients. *Int. J. cancer* 119, 861–866. doi:10.1002/IJC.21767

Elder, D. E., Gimotty, P. A., and Guerry, D. P. (2005). Cutaneous melanoma: estimating survival and recurrence risk based on histopathologic features. *Dermatol. Ther.* 18, 369–385. doi:10.1111/J.1529-8019.2005.00044.X

Ewen, T., Husain, A., Stefanos, N., Barrett, P., Jones, C., Ness, T., et al. (2023). Validation of epidermal AMBRA1 and loricrin (AMBLor) as a prognostic biomarker for nonulcerated American Joint Committee on Cancer stage I/II cutaneous melanoma. *Br. J. dermatology* 190, 549–558. doi:10.1093/BJD/LJAD459

Faries, M. B., Thompson, J. F., Cochran, A. J., Andtbacka, R. H., Mozzillo, N., Zager, J. S., et al. (2017). Completion dissection or observation for sentinel-node metastasis in melanoma. *N. Engl. J. Med.* 376, 2211–2222. doi:10.1056/NEJMOA1613210

Faul, F., Erdfelder, E., Lang, A. G., and Buchner, A. (2007). G*Power 3: a flexible statistical power analysis program for the social, behavioral, and biomedical sciences. *Behav. Res. methods* 39, 175–191. doi:10.3758/BF03193146

Garbe, C., Amaral, T., Peris, K., Hauschild, A., Arenberger, P., Basset-Seguin, N., et al. (2022). European consensus-based interdisciplinary guideline for melanoma. Part 1: diagnostics: Update 2022. *Eur. J. cancer (Oxford, Engl. 1990)* 170 (170), 236–255. doi:10.1016/J.EJCA.2022.03.008

Gosman, L. M., Țăpoi, D. A., and Costache, M. (2023). Cutaneous melanoma: a review of multifactorial pathogenesis, immunohistochemistry, and emerging biomarkers for early detection and management. *Int. J. Mol. Sci.* 24, 15881. doi:10.3390/IJMS242115881

Guitart, J., Lowe, L., Piepkorn, M., Prieto, V. G., Rabkin, M. S., Ronan, S. G., et al. (2002). Histological characteristics of metastasizing thin melanomas: a case-control study of 43 cases. *Archives dermatology* 138, 603–608. doi:10.1001/ARCHDERM.138.5.603

Helvind, N. M., Brinch-Møller Weitemeyer, M., Chakera, A. H., Hendel, H. W., Ellebæk, E., Svane, I. M., et al. (2023). Stage-specific risk of recurrence and death from melanoma in Denmark, 2008-2021: a national observational cohort study of 25 720 patients with stage ia to IV melanoma. *JAMA dermatol.* 159, 1213–1222. doi:10.1001/JAMADERMATOL.2023.3256

Homsi, J., Kashani-Sabet, M., Messina, J. L., and Daud, A. (2005). Cutaneous melanoma: prognostic factors. *Cancer control J. Moffitt Cancer Cent.* 12, 223–229. doi:10.1177/107327480501200403

Kaur, C., Thomas, R. J., Desai, N., Green, M. A., Lovell, D., Powell, BWEM, et al. (2008). The correlation of regression in primary melanoma with sentinel lymph node status. *J. Clin. pathology* 61, 297–300. doi:10.1136/JCP.2007.049411

Kunonga, T. P., Kenny, R. P. W., Astin, M., Bryant, A., Kontogiannis, V., Coughlan, D., et al. (2023). Predictive accuracy of risk prediction models for recurrence, metastasis and survival for early-stage cutaneous melanoma: a systematic review. *BMJ open* 13, e073306. doi:10.1136/BMJOPEN-2023-073306

Lee, S. J., Lim, H. J., Choi, Y. H., Chang, Y. H., Lee, W. J., Kim, D. W., et al. (2013). The clinical significance of tumor-infiltrating lymphocytes and microscopic satellites in acral melanoma in a Korean population. *Ann. dermatology* 25, 61–66. doi:10.5021/AD.2013.25.1.61

Leiter, U., Eigentler, T., and Garbe, C. (2014). Follow-up in patients with low-risk cutaneous melanoma: is it worth it? *Melanoma Manag.* 1, 115–125. doi:10.2217/MMT.14.22

Liang, Z., Pan, L., Shi, J., and Zhang, L. (2022). C1QA, C1QB, and GZMB are novel prognostic biomarkers of skin cutaneous melanoma relating tumor microenvironment. *Sci. Rep.* 12, 20460. doi:10.1038/S41598-022-24353-9

Lund, A. W. (2022). Standing watch: immune activation and failure in melanoma sentinel lymph nodes. *Clin. cancer Res. official J. Am. Assoc. Cancer Res.* 28, 1996–1998. doi:10.1158/1078-0432.CCR-22-0214

Mashukov, A., Shapochka, D., Seleznov, O., Kobyliak, N., Sulaieva, O., Falalyeyeva, T., et al. (2021). Histological differentiation impacts the tumor immune microenvironment in gastric carcinoma: relation to the immune cycle. *World J. gastroenterology* 27, 5259–5271. doi:10.3748/WJG.V27.I31.5259

McClain, S. E., Shada, A. L., Barry, M., Patterson, J. W., and Slingluff, C. L. (2012). Outcome of sentinel lymph node biopsy and prognostic implications of regression in thin malignant melanoma. *Melanoma Res.* 22, 302–309. doi:10.1097/CMR.0B013E328353E673

Morrison, S., Han, G., Elenwa, F., Vetto, J. T., Fowler, G., Leong, S. P., et al. (2022). Is there a relationship between TILs and regression in melanoma? *Ann. Surg. Oncol.* 29, 2854–2866. doi:10.1245/S10434-021-11251-Z

Naimy, S., Bzorek, M., Eriksen, J. O., Løvendorf, M. B., Litman, T., Dyring-Andersen, B., et al. (2023). LAG3 and TIGIT expression on tumor infiltrating lymphocytes in cutaneous melanoma. *Dermatol. Basel, Switz.* 240, 156–163. doi:10.1159/000533932

Oláh, J., Gyulai, R., Korom, I., Varga, E., and Dobozy, A. (2003). Tumour regression predicts higher risk of sentinel node involvement in thin cutaneous melanomas. *Br. J. dermatology* 149, 662–663. doi:10.1046/J.1365-2133.2003.05502.X

Orzan, O. A., Şandru, A., and Jecan, C. R. (2015). Controversies in the diagnosis and treatment of early cutaneous melanoma. *J. Med. Life* 8, 132–141.

Peirano, D., Donoso, F., Vargas, S., Hidalgo, L., Agüero, R., Uribe, P., et al. (2023). Patterns of recurrence of cutaneous melanoma: a literature review. *Dermatology Pract. and Concept.* 13, e2023304. doi:10.5826/DPC.1304A304

Rashid, O. M., Schaum, J. C., Wolfe, L. G., Brinster, N. K., and Neifeld, J. P. (2011). Prognostic variables and surgical management of foot melanoma: review of a 25-year institutional experience. *ISRN Dermatol.* 2011, 384729. doi:10.5402/2011/384729

Rothberg, B. E. G., and Rimm, D. L. (2014). Construction and analysis of multiparameter prognostic models for melanoma outcome. *Methods Mol. Biol. Clift. NJ* 1102, 227–258. doi:10.1007/978-1-62703-727-3_13

Salama, A. K. S., de Rosa, N., Scheri, R. P., Pruitt, S. K., Herndon, J. E., Marcello, J., et al. (2013). Hazard-rate analysis and patterns of recurrence in early stage melanoma: moving towards a rationally designed surveillance strategy. *PloS one* 8, e57665. doi:10.1371/JOURNAL.PONE.0057665

Serra, E., Abarzua-Araya, Á., Arance, A., Martin-Huertas, R., Aya, F., Olondo, M. L., et al. (2024). Predictive and prognostic factors in melanoma central nervous system metastases-A cohort study. *Cancers* 16, 2272. doi:10.3390/CANCERS16122272

Siegel, R. L., Miller, K. D., Fuchs, H. E., and Jemal, A. (2022). Cancer statistics, 2022. *CA a cancer J. Clin.* 72, 7–33. doi:10.3322/CAAC.21708

Stakhovskyi, O., Kobyliak, N., Voylenko, O., Stakhovskyi, E., Ponomarchuk, R., and Sulaieva, O. (2022). Immune microenvironment of muscular-invasive urothelial carcinoma: the link to tumor immune cycle and prognosis. *Cells* 11, 1802. doi:10.3390/CELLS11111802

Stucky, C. C. H., Gray, R. J., Dueck, A. C., Wasif, N., Laman, S. D., Sekulic, A., et al. (2010). Risk factors associated with local and in-transit recurrence of cutaneous melanoma. *Am. J. Surg.* 200, 770–774. doi:10.1016/J.AMJSURG.2010.07.025

Swetter, S. M., Thompson, J. A., Albertini, M. R., Barker, C. A., Baumgartner, J., Boland, G., et al. (2021). NCCN Guidelines® insights: melanoma: cutaneous, version 2.2021. *J. Natl. Compr. Cancer Netw. JNCCN* 19, 364–376. doi:10.6004/JNCCN.2021.0018

Tas, F., and Erturk, K. (2017). Histological lymphovascular invasion is associated with nodal involvement, recurrence, and survival in patients with cutaneous malignant melanoma. *Int. J. dermatology* 56, 166–170. doi:10.1111/IJD.13405

Thompson, J. F., Soong, S. J., Balch, C. M., Gershenwald, J. E., Ding, S., Coit, D. G., et al. (2011). Prognostic significance of mitotic rate in localized primary cutaneous melanoma: an analysis of patients in the multi-institutional American Joint Committee on Cancer melanoma staging database. *J. Clin. Oncol. official J. Am. Soc. Clin. Oncol.* 29, 2199–2205. doi:10.1200/JCO.2010.31.5812

Vița, O., Jurescu, A., Văduva, A., Cornea, R., Cornianu, M., Tăban, S., et al. (2023). Invasive cutaneous melanoma: evaluating the prognostic significance of some parameters associated with lymph node metastases. *Med. Kaunas. Lith.* 59, 1241. doi:10.3390/MEDICINA59071241

Wan, G., Nguyen, N., Liu, F., DeSimone, M. S., Leung, B. W., Rajeh, A., et al. (2022). Prediction of early-stage melanoma recurrence using clinical and histopathologic features. *NPJ Precis. Oncol.* 6, 79. doi:10.1038/S41698-022-00321-4

Wen, X., Li, D., Zhao, J., Li, J., Yang, T., Ding, Y., et al. (2020). Time-varying pattern of recurrence risk for localized melanoma in China. *World J. Surg. Oncol.* 18, 6. doi:10.1186/S12957-019-1775-5

Yang, B., Xie, P., Huai, H., and Li, J. (2023). Comprehensive analysis of necroptotic patterns and associated immune landscapes in individualized treatment of skin cutaneous melanoma. *Sci. Rep.* 13, 21094. doi:10.1038/S41598-023-48374-0

Yun, S. J., Gimotty, P. A., Hwang, W. T., Dawson, P., Van Belle, P., Elder, D. E., et al. (2011). High lymphatic vessel density and lymphatic invasion underlie the adverse prognostic effect of radial growth phase regression in melanoma. *Am. J. Surg. pathology* 35, 235–242. doi:10.1097/PAS.0B013E3182036CCD

Zhang, M., Yang, L., Wang, Y., Zuo, Y., Chen, D., and Guo, X. (2023). Comprehensive prediction of immune microenvironment and hot and cold tumor differentiation in cutaneous melanoma based on necroptosis-related lncRNA. *Sci. Rep.* 13, 7299. doi:10.1038/S41598-023-34238-0

frontiers | Frontiers in Molecular Biosciences

TYPE Review
PUBLISHED 14 April 2025
DOI 10.3389/fmolb.2025.1561464

OPEN ACCESS

EDITED BY
Valentyn Oksenych,
University of Bergen, Norway

REVIEWED BY
Dwijendra K. Gupta,
Allahabad University, India
Mithlesh Kumar Temre,
National Institute on Aging (NIH),
United States
Meden Fruel Isaac-Lam,
Purdue University Northwest, United States
Parth Hemantkumar Desai,
North Carolina Agricultural and Technical State University, United States
Jessica Pullan,
Southern Utah University, United States
Ashutosh Gupta,
Manipal University, India

*CORRESPONDENCE
Sanjay Kumar,
sanjay.kumar7@sharda.ac.in

RECEIVED 15 January 2025
ACCEPTED 25 February 2025
PUBLISHED 14 April 2025

CITATION
Tiwari PK, Chaudhary AA, Gupta S, Chouhan M, Singh HN, Rustagi S, Khan S-U and Kumar S (2025) Extracellular vesicles in triple-negative breast cancer: current updates, challenges and future prospects. *Front. Mol. Biosci.* 12:1561464. doi: 10.3389/fmolb.2025.1561464

Extracellular vesicles in triple-negative breast cancer: current updates, challenges and future prospects

Prashant Kumar Tiwari[1], Anis Ahmad Chaudhary[2], Saurabh Gupta[3], Mandeep Chouhan[1], Himanshu Narayan Singh[4], Sarvesh Rustagi[5], Salah-Ud-Din Khan[6] and Sanjay Kumar[1]*

[1]Biological and Bio-Computational Lab, Department of Life Sciences, School of Basic Sciences and Research, Sharda University, Greater Noida, Uttar Pradesh, India, [2]Department of Biology, College of Science, Imam Mohammad Ibn Saud Islamic University (IMSIU), Riyadh, Saudi Arabia, [3]Department of Biotechnology, GLA University, Mathura, Uttar Pradesh, India, [4]Department of Systems Biology, Columbia University Irving Medical Center, New York, NY, United States, [5]Department of Food Technology, School of Applied and Life science, Uttaranchal University, Dehradun, Uttarakhand, India, [6]Department of Biochemistry, College of Medicine, Imam Mohammad Ibn Saud Islamic University (IMSIU), Riyadh, Saudi Arabia

Breast cancer (BC) remains a complex and widespread problem, affecting millions of women worldwide, Among the various subtypes of BC, triple-negative breast cancer (TNBC) is particularly challenging, representing approximately 20% of all BC cases, and the survival rate of TNBC patients is generally worse than other subtypes of BC. TNBC is a heterogeneous disease characterized by lack of expression of three receptors: estrogen (ER), progesterone (PR), and human epidermal growth factor receptor 2 (HER2), resulting conventional hormonal therapies are ineffective for its management. Despite various therapeutic approaches have been explored, but no definitive solution has been found yet for TNBC. Current treatments options are chemotherapy, immunotherapy, radiotherapy and surgery, although, these therapies have some limitations, such as the development of resistance to anti-cancer drugs, and off-target toxicity, which remain primary obstacles and significant challenges for TNBC. Several findings have shown that EVs exhibit significant therapeutic promise in many diseases, and a similar important role has been observed in various types of tumor. Studies suggest that EVs may offer a potential solution for the management of TNBC. This review highlights the multifaceted roles of EVs in TNBC, emphasizing their involvement in disease progression, diagnosis and therapeutic approach, as well as their potential as biomarkers and drug delivery.

KEYWORDS

extracellular vesicles, biomarkers, therapeutic challenges, non-coding RNAs, drug delivery

1 Introduction

Cancer remains a major concern worldwide, after skin cancer, BC is the most common among women. According to NIH statistical data, about 3 lakh cases were expected with

7.1% mortality rate. BC increasing steadily over the past two decades (Aravindan et al., 2024), and one of the most prevalent diseases affecting women worldwide (Arnold et al., 2022). Several studies and their results from different perspectives unanimously classify BC as a highly heterogeneous disease molecular and histological both level (Viale, 2012). Over time, several molecular markers have been discovered to classify BC based on factors like genomic instability, genetic changes, and gene activity. Advanced technologies have made it much easier for us to understand why BC is so diverse by identifying biomarkers like ER, PR, and HER2. These markers have helped classify BC into five subtypes, including luminal A, luminal B, HER2-enriched, triple-negative (or basal-like), and normal-like breast cancer. This classification helps to predict disease progression and choose effective treatments (Zubair et al., 2021). According to cancer statistics and several studies, the proportion of TNBC is higher in Asian countries. Primarily, Indian data shows that 100,000 people are diagnosed with breast cancer every year. It is estimated that by 2025, global cancer cases will reach approximately 30 million, while deaths will increase to 17 million. Like the United States, breast cancer is the second leading cause of cancer-related deaths in India after lung cancer. The diagnosis of breast cancer presents a significant challenge in effectively managing the disease. According to WHO, survival rates vary across regions, ranging from about 90% in high-income countries, 60% in India and 40% in South Africa (Gupta et al., 2024).

Of all these subtypes of BC, TNBC has received significant attention. TNBC is an aggressive subtype that represent around 11%–20% of all BC cases (Loizides and Constantinidou, 2023). It is characterized by the lack of estrogen receptor (ER), progesterone receptor (PR), as well as lack of overexpression or amplification of human epidermal growth factor receptor 2 (HER2) (Tiwari et al., 2023). Consequently, TNBC is frequently unresponsive to hormone-based therapies, which specifically target ER and PR, as well as strategy designed to address HER2 receptors. The lack of these receptor targets hinders the effectiveness of conventional hormone-based and HER2-targeted therapies in managing TNBC cases (Saleh et al., 2021). TNBC primarily affects young, premenopausal women to a more significant number and has been observed more frequently in African-American women. This is often associated with inherited gene mutations involving the BRCA1 and BRCA2 genes (Howard and Olopade, 2021). The highly aggressive nature of TNBC poses a significant challenge in its diagnosis and prognosis. TNBC have more propensity to metastasize to different body parts in compression of other subtypes of BC (Azim et al., 2020).

Prognostic biomarkers may play in significant role in the initial diagnosis of TNBC. Lipids, circulating tumors DNA (ctDNA), glycogen, tumors-infiltrating lymphocytes (TILs), immune checkpoint molecules (PD-L1), circulating tumors cells (CTCs), and microRNAs (miRNAs) are considered as next-generation predictive biomarkers and promise significant potential for enhance the prognosis of TNBC. Glycogen and lipid show pathology-associated metabolic changes and give important insights into malignancy growth and treatment response. ctDNA serves as a non-invasive methodology to assess tumors genetics and monitor pathological conditions (Alismail, 2024; Banerjee et al., 2024). Patients with early-stage TNBC who have not received adjuvant or neoadjuvant chemotherapy have been shown to have significantly better survival when they have significant quantities of TILs in their BC tissues. These studies results confirm, abundance of TILs in BC may serve as a crucial prognostic factor for early-stage TNBC patients (Leon-Ferre et al., 2024). PD-L1, a protein that involved in immune evasion, mostly exhibit in aggressive type neoplasm. In BC, its expression is related with high histologic grade and negative hormone receptor status. Approximately 20% of TNBC tumors express PD-L1 (Mittendorf et al., 2014).

Currently, the primary therapeutic approach for TNBC involve a combination of surgery, radiation, chemotherapy, and neoadjuvant therapy (Baranova et al., 2022). Though there are some approved chemotherapeutics such as platinum agent (carboplatin and cisplatin), doxorubicin, paclitaxel, capecitabine, gemcitabine, and eribulin, but their efficacy are limited (Twelves et al., 2016). Moreover, most of these drugs cannot cross the blood-brain barrier, posing a challenge in treating brain tumors resulting from TNBC metastasis. Approximately one-third of TNBC patients develop brain metastases, which currently have no available cure, leading to short survival times (Kadamkulam Syriac et al., 2023; Kannan and Cheng, 2023). Some TNBC patients with BRCA1/2 mutations can receive intervention with poly (ADP-ribose) polymerase inhibitors like olaparib and talazoparib, however these options are limited (Hobbs et al., 2021). Therefore, there is a pressing need for developing new and effective therapies with high specificity for BC and minimal damage to healthy tissues.

EVs are tiny particles surrounded by lipid bilayers that are released into the circulation by various types cells, including tumor cells, and these diverse membranous vesicles secreted into the extracellular space (Dixson et al., 2023), which engage in numerous functions, including intercellular communication, immune regulation, disease progression and development, and tissue repair. Additionally, EVs carries cargo such as, proteins, lipids, metabolites DNA and various type RNA, which play a crucial role in biological processes (Yue et al., 2023). Initially, until the late 1990s, EVs did not receive significant attention in the field of research, because in the early stages it was believed that these vesicles were waste material of cells (Yuan et al., 2023). Primarily based on their biogenesis and size, EVs have been classified into three different types (Liu and Wang, 2023), (i) Exosomes range in size from 30 to 150 nm. Their biogenesis occurs within multivesicular bodies (MVBs) via the endocytic pathway, following ESCRT-dependent complexes, and they are released into the extracellular space via exocytosis (Yin et al., 2023). The presence of various biomarkers including tetraspanins (CD9, CD63, CD81), endosomal proteins (TSG101, Rab-GTPase), and heat shock chaperones (HSP70, HSP90) characterize exosomes (Banerjee and Rajeswari, 2023). (ii) Microvesicles are formed through outward of the plasma membrane under stimuli and calcium-dependent pathways. These vesicles range in size from 50 to 1,000 nm and are released through outward budding and fission of the membrane. These include various biomarkers including flotillin-2, CD40 ligand, and annexin (Rani et al., 2023), and (iii) apoptotic bodies which is greater than 1,000 nm in size, formed during the apoptosis process, compared to other EVs it has phosphatidylserine, cytochrome c and DNA histones as major markers (Wen et al., 2023) (Detailed classification and characteristics of EVs mentioned in Table 1).

Tumor cell-derived EVs promote tumor development and metastasis through diverse mechanisms by influencing the tumor microenvironment (TME), modulating cellular interactions, and

TABLE 1 Extracellular vesicle classification, based on category, size, formation, pathways and marker.

1.	Category	Size	Formation	Biogenesis pathway	Markers	References
2.	Exosomes	30–120 nm	Multivesicular bodies fusion (MVBs) with the plasma membrane	ESCRT-dependent	Tetraspanins (CD9, CD63, CD81), Endosome system proteins (TSG101, Rab-GTPase), and Heat shock chaperones (HSP70, HSP90)	Xu et al. (2022); Banerjee and Rajeswari (2023)
3.	Microvesicle	40–1,000 nm	Outward blebbing of the plasma membrane	Stimuli-dependent, Ca2+-dependent, cell-dependent	Flotllin-2, CD40 ligand, Selectin, Annexin 1	Ståhl et al. (2019)
4.	Apoptotic bodies	>1,000 nm	Plasma membrane budding of Apoptotic cells	Apoptosis-related	Phosphatidylserine, Annexin V, DNA histones	Ståhl et al. (2019), Hu et al. (2020b)

signaling pathways (Tian et al., 2023). TME play crucial role in the TNBC progression, by utilizing different biological mechanisms such as immune suppression, proliferation, angiogenesis, and apoptosis inhibition. Dynamic interactivity between surrounding stromal, endothelial, immune cells, and neoplasm cells builds niche, that facilitated tumor development, metastasis, and epithelial-to-TNBC stem cell transition (Deepak et al., 2020). TME composed diverse types of cells and biological molecule, including ECM components, immune cells, tumor-associated fibroblasts (CAFs), blood vessels and cancer stem cells (CSCs), ECM generate signals for numerus key processes like cell proliferation, replicative immortality, invasion, and apoptosis evasion. CAFs are prime contributors to drug resistance and disease progression by producing growth factors and chemokines, additionally play crucial role in immune cell infiltration (Otranto et al., 2012).

EVs can be collected from various bodily fluids such as blood or urine, providing a non-invasive method to obtain real-time information about the status and types of malignant cells (Kalra et al., 2016). They got special attention in the clinical field due to verity of function like precisely targeted drug delivery (vaccines and therapeutic agents), interaction with specific cell and tissue. This observation has led to the exploration of EVs as potential cargo carriers for delivering (Wang et al., 2020). Notably EVs secreted from body enable them to work well with the same because they are natural and are less likely to cause an adverse reaction or be seen as foreign particles by the immune system of body (Song et al., 2022). EVs surface is made of the cellular proteins and can escape from our immune system. Additionally they can also pass through the protective blood-brain barrier and prevent drugs from breaking down (Kooijmans et al., 2016).

2 Biogenesis of extracellular vesicle

Endosomes are membrane-bound compartments within cells that play an essential role in sorting and trafficking various cellular materials, including proteins and lipids. The early endosome is the first step in the endocytic pathway, where the material is internalized from the cell surface via endocytosis (Simonetti et al., 2023). Endosomes mature into late endosomes or multivesicular bodies (MVBs), and specific cargo inside the endosomal membrane forms tiny buds that separate from the membrane. These buds synthesize tiny intraluminal vesicles (ILVs) within the endosome's inner space, and these ILVs are later released through exocytosis. So based on this process exosomes biogenesis can be categorized into two main pathways, i.e., ESCRT (endosomal sorting complex required for transport)-dependent pathway and the ESCRT-independent pathway (Han et al., 2022).

2.1 Biogenesis of exosomes through ESCRT-dependent pathway

The ESCRT machinery is a multi-protein complex comprised of approximately 30 distinct proteins, which can be classified into four different complexes: ESCRT-0, ESCRT-I, ESCRT-II, and ESCRT-III. These protein complexes play crucial roles in the biogenesis of exosomes (Camacho et al., 2023). The investigation of ESCRT complexes has yielded significant insights into the intricate cellular mechanisms underlying the formation and release of exosomes, enhancing our understanding of intercellular communication and cellular trafficking processes (Ho et al., 2022). The biogenesis of ILVs begins by placing cargo on the outer surface of MVBs, and this action is facilitated by the ESCRT-0 complex. ESCRT-0 functions like a team management, capable of capturing the biomolecule utilized two crucial components: hepatocyte growth factor-regulated tyrosine kinase substrate (HRS) and signal transducing adaptor molecule (STAM). Both help the team to identify and attach to the cargo, preparing it for the subsequent stages in forming ILVs (Jin et al., 2022). The ESCRT-0 complex have ten binding sites that facilitate the capture of polyubiquitylated cargo (Dixson et al., 2023). Upon attachment of marked polyubiquitylated cargo to ESCRT-0, the HRS-STAM complex presents an opportunity for the ESCRT-I complex to participate in the process (Mirzaei et al., 2022). ESCRT-I, aided by the molecule TSG-101 (Tumor susceptibility gene 101), which binds to ubiquitin, facilitates the transport of the cargo (Mishra et al., 2023). Subsequently, ESCRT-I recruits the subsequent complex, ESCRT-II,

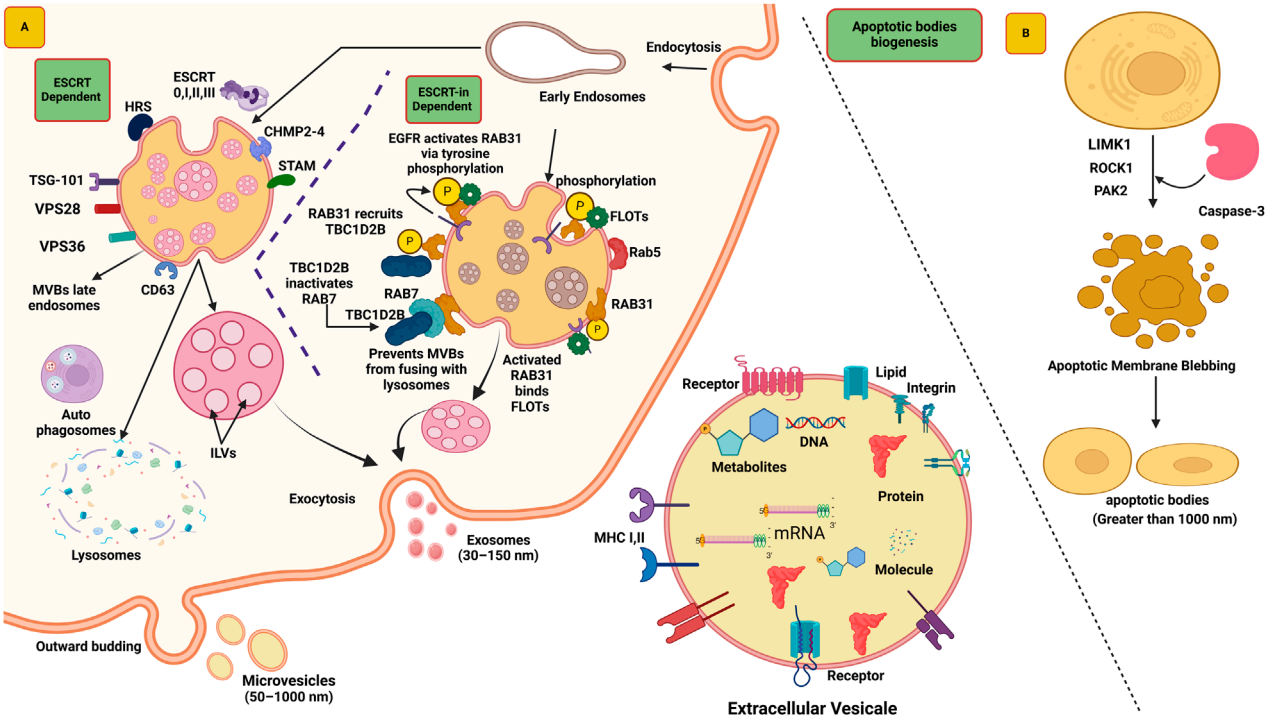

FIGURE 1
The biogenesis of exosomes depends on two pathways ESCRT dependent and ESCRT-independent. **(A)** The formation of exosomes begins with the inward budding of the plasma membrane, leading to the formation of early endosomes. Subsequently, the ESCRT complex (ESCRT 0, I, II, III) facilitates the formation of multivesicular bodies (MVBs). These MVBs either fuse with lysosomes for degradation (by autophagosomes) or translocate to the plasma membrane, where the SNARE complex aids their fusion, releasing the exosomes into the extracellular space. In ESCRT-independent mechanism RAB31 present on late endosomes that interact to EGFR, EGFR phosphorylate RAB31 viva tyrosine phosphorylation. Active RAB31 bind with Flotillin (FLOTs), now these complexes allow to formation of ILVs. Additionally, RAB31 recruit TBC1D2B that binds with protein RAB7 and prevents MVEs from fusing with lysosomes. **(B)** Biogenesis of apoptotic bodies begins with cytoskeletal reorganization and plasma membrane blebbing that regulated by ROCK1 and MLCK proteins. Caspase-3 triggers ROCK1, which then modifies myosin II, leading strong contractions of the cytoskeleton, and formation of membrane blebs. Further aspase-3 kinase cleaves PAK2 and add fatty acid to it, thereby increasing its activity, that help in cell membrane movement and controls cell shape. Moreover, activates JNK pathways, for the proper release of apoptotic EVs.

through its interaction with VPS28 and VPS36 subunits (Hudait et al., 2023). ESCRT-II, in turn, recruits ESCRT-III, accompanied by the involvement of a specialized protein known as CHMP2-4 (Azad et al., 2023). Collectively, they form novel structures known as ILVs, thereby accomplishing the budding and cleavage of these diminutive vesicles from the membrane. Additionally, the accessory protein AAA-ATPase VPS4 performs a vital role in the disassembly and recycling the ESCRT-III complex (Tseng et al., 2022) (Figure 1A).

2.2 Biogenesis of exosomes through ESCRT-independent pathway

In mammalian cells, MVBs can still be synthesized even without ESCRT complexes, indicating that ILV biogenesis can happen independently of ESCRT. However, it has been noted that MVBs formed without ESCRT are larger and contain fewer ILVs with irregular shapes and sizes. RAB31 is a relatively small GTPase protein primarily responsible for intracellular trafficking and vesicle transport (Wei et al., 2021). The activation of RAB31 is crucial for exosome biogenesis, mediated through phosphorylation catalyzed by the EGFR (Horbay et al., 2022). After the activation of RAB31, it interacts with flotillin proteins of SPFH (Stomatin, Prohibitin, Flotillin, HflK/C) domain present in lipid raft microdomains (Wei et al., 2021). Flotillins are membrane-associated proteins that localize to specific cholesterol-rich microdomains in the plasma membrane known as lipid rafts (Lu and Fairn, 2018). The interaction between RAB31 and flotillin proteins facilitates the entry of EGFR into EVs, leading to the formation of ILVs (Lizarraga-Valderrama and Sheridan, 2021). Another role has been observed for this protein in EVs, similar to RAB31, which recruits TBC1D2B, deactivates RAB7, and prevents the fusion of EVs with lysosomes. This process creates a favorable environment for the formation of ILVs. Consequently, functional exosomes are released, playing a crucial role in intercellular communication and various cellular processes (Gao et al., 2022) (Figure 1A).

2.3 Biogenesis of microvesicles (MV) and apoptotic body

The MVs form when direct outward budding and subsequent shedding of the plasma membrane occurs (Clancy et al., 2021). In the formation of MVs, various factors work together, such as the

redistribution of phospholipids and the contraction of the actin-myosin machinery (Abels and Breakefield, 2016). When looking into the detailed mechanism, ADP-ribosylation factor 6 (ARF6), a small GTPase protein, plays a significant role in the activation of phospholipase D (PLD) enzyme during its active state and leads to the repositioning of phosphatidylserine to the outer leaflet and initiates the process of MV formation (Menck et al., 2020). Additionally, the activity of ARF6 recruits the Extracellular Signal-Regulated Kinase (ERK) (mitogen-activated protein kinase (MAPK) family) to the plasma membrane. ERK's presence is pivotal for downstream signaling pathways. Upon phosphorylation of ERK, it further activates myosin light chain kinase (MLCK). This activation leads to the phosphorylation of the Myosin Light Chain (MLC). The phosphorylation of MLC enhances the contractility of the actin-myosin complex, resulting in induced membrane curvature and budding. This activity ultimately leads to the genesis of small MVs from the plasma membrane. These vesicles contain specific biomolecules, such as ARF6, MHC-I, b1-integrin, VAMP3, and MT1MMP (Abels and Breakefield, 2016).

Apoptotic bodies also a membrane-bound structure that also contain variety of cargos such as proteins, lipids, RNA, miRNAs and DNA, that involve in intercellular communications. The feature of apoptotic bodies can vary depending on the cell type (Santavanond et al., 2021). There is not much information available about the role of apoptotic bodies in cancer biology, mostly scientific work is being done utilizing exosomes and microvesicles. The biogenesis of apoptotic bodies begins with cytoskeletal reorganization and plasma membrane blebbing. Previously, it was believed that this process occurred randomly, but recently it was recognized that the biogenesis of apoptotic bodies occurs through well-ordered morphological steps. Rho-associated coiled-coil-containing protein kinase 1 (ROCK1) and myosin light chain kinase (MLCK) regulates biogenesis of apoptotic bodies (Phan et al., 2020). In this mechanism, caspase-3 activation triggers ROCK1, which then modifies myosin II, resulting in strong contractions of the cytoskeleton, leading to the formation of membrane blebs. It is not yet completely clear which MLCK is active, but inhibition of MLCK has been shown to prevent membrane blebbing. Additionally, another protein, LIMK1, helps in this process by activating cofilin that also regulates the actin skeleton and supports apoptotic membrane blebbing (Sebbagh et al., 2001). Caspase-3 kinase cleaves p21-activated kinase 2 (PAK2) adds a fatty acid to it, thereby increasing its activity. Active PAK2 helps in cell membrane movement and controls cell shape. It also activates signaling pathways such as JNK, which play a role in proper release of apoptotic EVs (Han et al., 2024) (Figure 1B).

3 Role of EVs in TNBC

TNBC is a type of aggressive and refractory BC mainly occurs in young patients and has a poor clinical prognosis. So far, no specific target has been identified for its management on which intervention can be done. To achieve better treatment outcomes, a promising drug is needed, and in recent years EVs have shown significant promise in the management of TNBC (St-Denis-Bissonnette et al., 2022). In a study conducted by Ozawa et al., it was revealed that EVs originating from the HCC1806 malignant cell line possess remarkable capabilities. These EVs not only promote the spread of TNBC tumors in the non- malignant MCF10A cell line but also play a significant role in inducing drug resistance, thereby enhancing the survival of the recipient cells. Additionally, these EVs display an exceptional ability to modulate specific miRNAs intricately linked to tumor-related processes (Ozawa et al., 2018). EVs originating from TNBC tumor cells have been observed to substantially impact tumor development and metastasis. Notably EVs release from TNBC cells line (HCC1806) can enhance the growth of normal mammary epithelial cells (MCF10A), Additionally induce drug resistance by activating PI3K/AKT, MAPK and HIF1α signaling pathways (Das K. et al., 2023). EVs have multifaced role including the facilitation of tumor proliferation, angiogenesis, and immune system evasion. These effects are achieved through the targeted delivery of specific biomolecules to adjacent cells, thereby modulating their behavior and providing crucial support for neoplasm progression (Tai et al., 2018). EVs derived from TNBC cells transfer oncogenic proteins such as EGFR and MMPs (Matrix metalloproteinases) to recipient cells, that enhancing their invasiveness and migratory traits (Mashouri et al., 2019).

EVs can modulate the TME in a manner that facilitates the development of pre-metastatic sites. Specifically, these EVs can instruct stromal cells, such as fibroblasts and immune cells, to create a supportive and conducive environment for the proliferation and dissemination of the tumor cells (Liu et al., 2020). Additionally, EVs have the remarkable capacity to induce modifications in gene expression and several signaling pathways within recipient cells, subsequently resulting in profound alterations in their phenotypic characteristics and functional role (Mashouri et al., 2019).

3.1 EVs in TNBC prognosis

Comparative analysis of plasma samples between healthy and patients suffering from TNBC, a conspicuous presence of small extracellular vesicle (sEVs) has been discerned. Specially, these sEVs are substantially enriched in TNBC patients (Stevic et al., 2018). Additionally, a distinct dissimilarity has been noticed in the expression patterns of sEV-miRNA between TNBC and HER2-positive patients. Notably, miR-335, miR-422a, and miR-62 have emerged as specific examples of such differential expression. In the context of TNBC, miR-374, which is linked to sEVs, plays a crucial role in promoting increased tumor size (Zhou et al., 2022). In contrast, several other miRNAs, namely, miR-185, miR-376a, miR-382, miR-410, miR-433, and miR-628, displayed an association with HER2-positive patients (Liu T. et al., 2021). The substantial secretion of sEVs depends upon the upregulation of the TSAP6 protein (Negahdaripour et al., 2021). Functionally, TSAP6 maintains cellular homeostasis and impedes carcinogenesis (Pavlakis et al., 2020). In the context of DNA damage, the activation of the p53 protein subsequently induces the transcription of TSAP6 (Nagao et al., 2022).

The SKBR3 cell line exhibits a high proliferative rate and demonstrates elevated expression levels of the Her2 (Neu/ErbB-2) gene product (Coppola et al., 2022). In contrast, the MDA-MB-231 cell line represents a poorly differentiated TNBC cell line characterized by the absence of ER and PR expression. Similarly, the HCC1954 cell line also overexpresses Her2/neu (Shiravi et al.,

2021). Upon the reception of sEVs derived from TNBC, a significant enhancement is observed in the proliferation, migration, and invasion capacities of these cell lines (Zhou et al., 2022). Wills et al. conducted a study on tumor metastasis mechanisms facilitated by EVs post-chemotherapy. For this they used xenograft mouse models of TNBC, and notice that Doxorubicin increased the release of sEVs from malignant cells, thereby promoting pulmonary metastasis. Utilizing proteomic analysis and CRISPR/Cas9 gene editing, they identified glycoprotein Pentraxin 3 (PTX3) as abundant in Doxorubicin-induced sEVs (Wills et al., 2021). PTX3 can trigger the NF-κB pathway, which is a key regulator of tumor cell proliferation and survival (Rathore et al., 2019). Consequently, PTX3 plays a pivotal role in regulating chemotherapy-induced metastasis and chemoresistance, thereby suggesting it as a potential therapeutic target against the adverse effects of chemotherapy on metastatic progression and chemoresistance (Wills et al., 2021).

3.2 EVs in diagnosis of TNBC

In diagnosing TNBC, imaging and immunohistochemistry (IHC) are the two primary tools currently being used (Roostee et al., 2023). Imaging tools identify TNBC by detecting BC masses or other irregularities. Frequently utilizing imaging tool for TNBC include mammography, ultrasound, and magnetic resonance imaging (MRI) (Sha and Chen, 2022). Mammograms can detection oncological diseases, but less effective in the case of TNBC when compared to other types of malignancy. This limitation is because of TNBC lacking distinctive features such as speculated margins or microcalcifications commonly found in different pathology (Chen and Lee-Felker, 2023). Due to this reason, it becomes quite challenging to identify it through mammograms. Firstly, it may yield false-negative results, as it cannot provide 100% accurate information about TNBC. It may miss one in eight TNBC cases, particularly in women with dense breast tissue, leading to a false sense of reassurance (Gegios et al., 2023). Secondly, false-positive results may occur, where in a positive result is shown even in the absence of disease. This is more prevalent in younger women, those with dense breasts, those who have previously undergone breast biopsies, have a family history of BC, or women taking estrogen, and so on (Wong et al., 2023).

Ultrasound is a beneficial tool for the detection of TNBC (Wang and Wang, 2023), playing an important role in determining the patient's condition. Ultrasound is significantly superior to mammography as it can easily identify small, non-calcified lesions, accurately differentiate between solid and cystic lesions, and reduces false positive results (Emory et al., 2023). In a study, it was found that the sensitivity of ultrasound for detecting TNBC ranges from 60%–80%, and the specificity ranges from 70%–90%. In spite of these findings, some limitations are associated with it (Ahmed, 2018). Ultrasound has a lower susceptibility to detect TNBC compared to other types of BC. In addition, it is not as effective as other imaging modalities in the accurate staging of TNBC (Dogan and Turnbull, 2012). These features contribute to the challenges in identifying TNBC and determining its extent using ultrasound imaging.

MRI a highly sophisticated tool for detecting TNBC, and it is remarkably better than mammography or ultrasound techniques (Kong et al., 2022). MRI is proficient in precisely identifying tiny tumors. MRI can also determine the location, size of TNBC, and it can also detect the spread of the tumor (Taourel et al., 2018). MRI also serves as critical role in monitoring the progress of TNBC management. Additionally utilized in planning the surgery for tumor removal (Ross and Chenevert, 2021). Despite its advantages, MRI has some limitations compared to mammography and ultrasound (Ma et al., 2022). First of all, it is significantly more expensive than imaging tools. Secondly, it is not as widely available as other imaging options. Additionally, it requires more time to perform and can sometimes be uncomfortable for patients (Ormond Filho et al. 2019).

Biopsy another technique which are done for TNBC. In this procedure, a small piece of breast tissue is extracted and examined under the microscope, and provides significant information about TNBC and its grade (Beňačka et al., 2022). One of the major diagnostic techniques performed on biopsy specimens is immunohistochemistry (IHC). This is a diagnostic test that relies on specific antibodies that specifically detect specific types of proteins or molecules on the surface of tumor cells. For instance, in the case of TNBC, it is performed based on the expression of ER, PR, and HER2 (Wang et al., 2022). IHC also identifies specific proteins or biomolecules that are expressed in TNBC, such as EGFR (epidermal growth factor receptor), Ki-67 (a proliferation marker), and p53 (a tumor suppressor gene) (Lu et al., 2023). This test is extremely beneficial because of its quick results and its heightened sensitivity in detecting TNBC. It can also identify molecules that significantly contribute to the aggressiveness and metastasis potential of TNBC (Ribeiro et al., 2022), and also provide significant assistance in intervention. The result this test may vary depending on the laboratory that performs the test (Cardos et al., 2022). Additionally, IHC cannot diagnose all cases of TNBC because not all cases show the presence of ER, PR, and HER2. These are some limitations that are specific to the IHC test.

Mutations in genes identify by genetic testing that provide crucial information regarding malignancy for instance BRCA1 and BRCA2 in BC. Mutations in these genes are strongly associated with the development of BC and help confirm risk as well as guide treatment (Ponti et al., 2023). Molecular profiling techniques can provide insights into the biological characteristics of TNBC and significantly aid in its therapy (Das D. et al., 2023). The majority of patients with TNBC often receive their diagnosis at an advanced stage because biomarkers that can effectively detect the tumor are absent during primary stage of TNBC (Das D. et al., 2023; Ponti et al., 2023). In order to streamline and enhance TNBC treatment, it becomes important to discover biomarkers as early as possible to detect TNBC in its early stages (Agostinetto et al., 2022). By identifying such biomarkers, the diagnosis and subsequent strategy of TNBC can be simplified and made more accessible, potentially improving patient outcomes and overall prognosis. Researchers anticipate that EVs will play a crucial role in the diagnosis and treatment of a variety of diseases in the future. EVs can carry oncogenic proteins, which may provide important insights into cancer initiation, progression, risk assessment, and treatment strategies (Wang J. et al., 2019).

3.2.1 EVs-associated proteins in TNBC diagnosis

The markers present on the surface of EVs derived from TNBC, along with the proteins packaged within them can greatly

help in the early estimation of an aggressive neoplasm diagnosis (Dong et al., 2022). Various methods are available for EVs isolation from different sources such as urine, plasma, serum, MSCs and other body fluids, but most widely accepted are ultracentrifugation (Giovanazzi et al., 2023). These EVs are further confirmed by various techniques such as DLS (dynamic light scattering), nanoparticle tracking analysis (NTA) and Electron microscopy for their size, and Western blotting using specific EVs markers such as tetraspapnin, CD63, and TSG and annexin IV. Furthermore, the flow cytometry is the best methods to quantify the specific proteins associated with EVs utilizing specific antibodies against them (Zhang et al., 2021; Tiwari et al., 2024).

3.2.1.1 EVs associated EGFR (epidermal growth factor receptor) in TNBC diagnosis

EGFR is a trans-membrane glycoprotein present on the cell surface, after binding of epidermal growth factor molecule, it initiates intracellular signaling cascades. Resulting regulates various cellular processes including proliferation and differentiation, thereby controlling cell growth, division and cell division (Sabbah et al., 2020). The overexpression of EGFR has been identified as a contributing factor in several cancers, including TNBC (Hsu and Hung, 2016). Previous studies have revealed that EGFR protein is found on the surface of EVs secreted by TNBC cells, plays a crucial role in its propagation, dissemination, growth and metastasis (St-Denis-Bissonnette et al., 2022), and it utilizes various methods to carry out these functions (Zakaria et al., 2019). For instance, EVs displaying EGFR transfer EGFR to immune cells, such as dendritic cells. As a result, dendritic cells become activated and start producing pro-inflammatory cytokines. Consequently, this leads to the growth and metastasis of tumor cells (Frawley and Piskareva, 2020). It also participates actively in cell proliferation by triggering crucial pathways such as EGFR, Ras-Raf-MAPK, and PI3K-Akt pathways. It can facilitate the degradation of the extracellular matrix by promoting matrix metalloproteinases (MMPs), resulting metastasis. Additionally, involved in angiogenesis and resistance to therapy (Dey et al., 2022). The varied functions of EGFR confer its strong potential for clinical translation in both discernment and therapeutic interventions for TNBC (Figure 2).

3.2.1.2 EVs associated CSF 1 (colony-stimulating factor 1) in TNBC diagnosis

The EVs associated protein CSF-1 have pivotal role in recruiting and polarizing tumor-associated macrophages (TAMs). CSF-1 can significantly enhance the tumor growth, invasion, and metastasis, that is key factor for TNBC development (Cannarile et al., 2017). For this, CSF-1 behaves like a cytokine. It binds to its receptor, colony-stimulating factor 1 receptor (CSF1R), which is present on the surface of TAMs. This interaction triggers specific signaling transduction, leading to the recruitment and differentiation of TAMs (Muñoz-Garcia et al., 2021). CSF-1 and TAMs are prominently present in the case of TNBC, contributing to tumor progression and creating an environment characterized by immunosuppression and pro-tumorigenic factors (Baig et al., 2020). consequently, CSF-1 can play a importent role as a crucial biomarker in the diagnosis of TNBC, which will be highly valuable in its therapeutic approach (Kuemmel et al., 2022) (Figure 2).

3.2.1.3 EVs associated CCL5 (chemokine ligand 5) in TNBC diagnosis

CCL5 is also identify as RANTES, and its key function is to attract immune cells such as T cells, B cells, and natural killer (NK) cells (Mgrditchian et al., 2017). It interacts with TME-derived EVs, and has been associated with poor prognosis in numerous types of neoplasm, including TNBC (St-Denis-Bissonnette et al., 2022). In TNBC, CCL5 attracts immune cells that participate in suppressing the immune response, such as myeloid-derived suppressor cells (MDSCs), which inhibit the activity of T cells and NK cells (Weber et al., 2021). Additionally CCL5 promote the growth of CAFs, that is responsible for tumor growth and metastasis (Mao et al., 2021). CCL5 has the ability to induce the formation of angiogenesis cells, which are necessary for tumor growth, nourishment, and dissemination, and it attracts endothelial cells, the lining cells of blood vessels, to carry out this function (Do et al., 2020). In a study conducted on rats with TNBC, it was observed that if CCL5 is blocked using antibodies can significantly reduce tumor metastasis, and it was also observed that the number of T cells and NK cells increased significantly. CCL5 emerges as a potential predictive biomarker for assessing the risk of pathology recurrence in TNBC patients. Empirical investigation has demonstrated a significant association between elevated CCL5 levels in tumor specimens and an augmented susceptibility to neoplasm relapse within a 5-year period following therapeutic intervention (Figure 2).

3.2.1.4 EVs associated cluster of differentiation 24 (CD24) in TNBC diagnosis

The GPI-anchored protein CD24-EVs are identified in various biological fluids of cancer patients and serve as a marker of EVs. IHC showed that $CD24^{+}$ EVs were detected in the serum of melanoma patients and BC, and it is also known as the heat-stable antigen CD24 (Gilliam et al., 2017). CD24 is an extremely small cell surface protein characterized by extensive glycosylation and its linkage to the glycosylphosphatidylinositol on the cell surface (Altevogt et al., 2021). It finds expression in various cells, including B cells, T cells, neutrophils, and epithelial cells, among others (Altevogt et al., 2021). Its primary function is to take responsibility for various cellular processes such as cell adhesion, migration, differentiation, and apoptosis (Shirmohamadi et al., 2020). CD24 also plays a crucial role in the tumor growth, cellular proliferation, epithelial-mesenchymal transition, angiogenesis, invasion, metastasis, promoting Immune invasion and acquisition of drug resistance in TNBC (Altevogt et al., 2021). It behaves like an anti-phagocytic surface protein and sends a "do not eat me" signal to immune cells like macrophages, discouraging them from attacking or engulfing the tumor cells (Barkal et al., 2019). Along with that, it interacts with Siglec-10 protein present on the surface of macrophages that exhibits resistant to tumor cells. This interaction significantly reduces CD24's inhibitory capacity against tumors, Subsequently impairing the ability of immune system to combat tumors (Zhao et al., 2023). Moreover, CD24 is found to be overproduced in pathologically stem cells (CSCs), highly specific cells within tumors with the ability to self-renew and initiate tumor growth (Liu et al., 2014). As per findings from investigations in TNBC, CD24 emerges as a highly potential promising

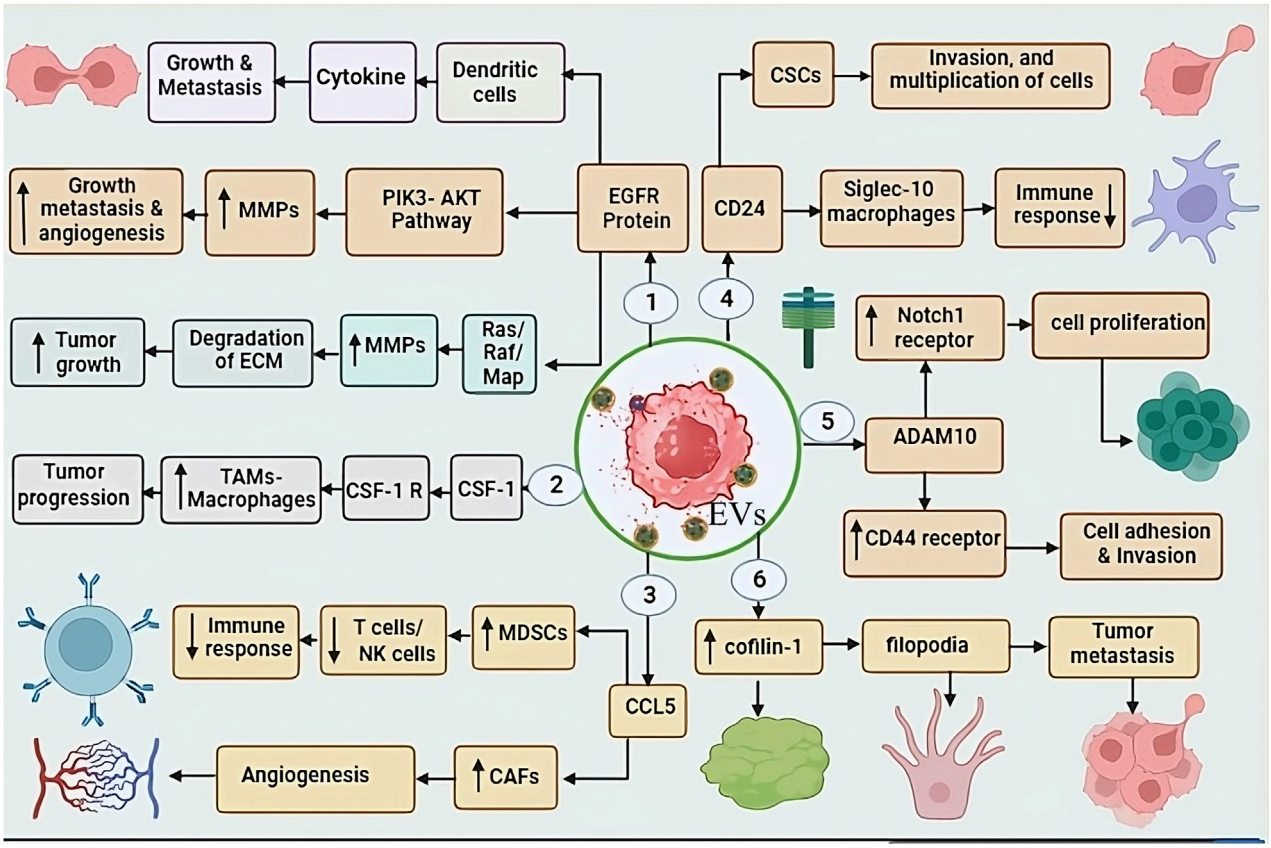

FIGURE 2
This figure shows the role of EV-associated proteins in TNBC progression through various molecular interactions: 1. EGFR-EVs: promoting tumour growth and metastasis through dendritic cells and cytokines. EGFR activates the PI3K-AKT pathway, upregulating matrix metalloproteinases (MMPs), leading to tumour invasion, metastasis, and angiogenesis. Additionally, EGFR also activates the Ras/MAPK pathway, increasing MMP activity, resulting in ECM degradation and tumour progression. 2. CSF1-EVs: target tumour-associated macrophages (TAMs), stimulating their activity and enhancing tumour progression. 3. CCL5-EVs enhance the function of MDSCs and CAFs. MDSCs suppress T cell/NK cell activity, leading to immune evasion, while CAFs promote angiogenesis. 4. CD24-EVs: Suppress immune response by interacting with Siglec-10 on macrophages, thereby helping TNBC cells escape immune surveillance. 5. ADAM10-EVs: Regulate cell proliferation and adhesion by targeting Notch-1 and CD44 receptors, which contribute to tumour progression. 6. Cofilin-1-EV: Enhances tumour metastasis, further increasing the aggressiveness of TNBC.

biomarker, given its crucial role in the disease (Chan et al., 2019) (Figure 2).

3.2.1.5 EVs associated ADAM10 in TNBC diagnosis

ADAM10 that is member of Metalloproteinase (ADAM) and disintegrin family (Matthews et al., 2017), exhibits expression in various tissues. It is a multifaceted enzyme that can cleave verity of proteins, including cell surface receptors, extracellular matrix proteins, and other ADAMs (Shimoda et al., 2021). ADAM10 have pivotal role in the etiology of diverse disease, including TNBC (Cheng et al., 2021). EVs associated ADAM10 can initiate the activation of Notch signaling transduction by inducing the expression of the Notch1 receptor (Alabi et al., 2021), a process associated with cellular proliferation, enhancing migratory potential. In addition, it also increases the expression of CD44 receptor, which significantly contributes to cell adhesion and invasion. Due to the significant increase in CD44 expression in TNBC, the disease spreads to different body parts (Alabi et al., 2021; Cheng et al., 2021). ADAM10-EVs confer resistance to therapeutic interventions, such as chemotherapy in tumors cells (Tan et al., 2018) (Figure 2).

3.2.1.6 EVs associated Cofilin-1 in TNBC diagnosis

Cofilin family protein like Cofilin-1, is responsible for cell motility and actin depolymerization (Tahtamouni et al., 2022). Its crucial role in various types of disease has been well-documented, with particularly elevated expression levels observed in EVs released from TNBC (Howard et al., 2022). The actin protein is fundamentally essential for cellular motility and cytoplasmic spreading, with its regulation primarily under the control of Cofilin-1 (Sousa-Squiavinato et al., 2019). In the context of TNBC, the overexpression of Cofilin-1 assumes a critical function in facilitating tumor infiltration and metastatic dissemination (Howard et al., 2022). Cofilin-1 promotes metastasis in TNBC by aiding actin-rich filopodia (Aseervatham, 2020). Filopodia a finger-like projections that extend from the surface of cells and have the ability to adhere to their surrounding environment (Jarsch et al., 2020). Cofilin-1 promotes tumor cell spread by weakening cell connections, enabling them to break away from the primary tumor (Zhang et al., 2018). Additionally, it also helps cancer cells survival by preventing apoptosis, as higher level of cofilin-1 have been linked to resistance against chemotherapy and radiation therapy, both of

which rely on apoptosis to kill cancer cells (Chen et al., 2020; Howard et al., 2022) (Figure 2).

3.2.1.7 EVs associated non-coding RNAs in TNBC diagnosis

Non-Coding RNAs (ncRNAs) derived through EVs, such as miRNA, lncRNA, and circRNA, have been extensively studied in the context of various tumors. miRNA, renowned for its versatility and multifaceted regulatory roles in various cellular processes, including cell signaling, homeostasis, and cell fate. It can also function as tumor suppressors or oncogenes for this purpose (Rupaimoole and Slack, 2017). The search for reliable tools for diagnosing different subtypes of BC at the molecular level has always been the focus of research efforts. miRNA has emerged as highly capable of achieving accurate diagnosis (Yang et al., 2019). Several studies have indicated that by analyzing the expression patterns of different miRNAs, can distinguish between BC samples and normal tissues, as well as differentiate TNBC from other types of clinical BC (Sabit et al., 2021).

The researchers examined plasma EVs of TNBC patients and healthy individuals, identifying 20 upregulated and 34 downregulated miRNAs in these EVs compared to healthy controls. Among the upregulated miRNAs, miR-150-5p and miR-4665-5p demonstrated the ability to differentiate TNBC patients who respond positively to therapy and those who do not. This discovery has led scientists to believe that this could be an unprecedentedly valuable tool for the diagnosis and potential management of TNBC (Ozawa et al., 2020). In a study, the researchers identified four EV-associated miRNAs: miR-142-5p, miR-150-5p, miR-320a, and miR-4433b-5p. After analyzing these miRNAs, they created a miRNA profile consisting of miR-142-5p, miR-320a, and miR-4433b-5p, which could differentiate between TNBC patients and healthy individuals. The sensitivity of this profile was 93.33%, and the specificity was 68.75%. moreover, the reduced expression of miR-142-5p and miR-150-5p in patients indicated a high advanced stage of tumor classification (Carvalho et al., 2022). In clinical practice, multiple studies have unveiled insights into the utility of serum EV-miRNA as a targeted indicator to predict the efficacy of diverse prevention strategies in TNBC. Such studies shed light on the pivotal clinical application of EV-miRNAs as specific biomarkers. One such investigation was conducted during a randomized phase II neoadjuvant trial known as Geparsixto (Stevic et al., 2018).

Long non-coding RNAs (lncRNAs) are important and specific components of the genetic program that modulate tumor cells and can influence their characteristics, exhibiting role in mediating tumor initiation and progression (Hu Q. et al., 2020). The lncRNA transcript panel exhibits an association with normal breast tissue, TNBC, and its subtypes. Through comprehensive analysis of transcriptome, molecular classification of BC becomes possible. Thereby, facilitating the identification and diagnosis of specific molecular signatures exclusively related to TNBC (Rodríguez Bautista et al., 2018). SUMO1P3 is a type of lncRNA that exhibits peculiar behavior in various cancer types, especially when found in high amounts in blood-derived EVs. It is strongly associated with negative prognosis and ineffective treatment outcomes in TNBC patients compared to individuals without disease or those in good health (Hu et al., 2021). In a recent study, it has been elucidated that the expression level of exosome lncRNA XIST decreases significantly after surgical resection of the primary breast tumor. However, upon the recurrence of BC, a notable and statistically significant elevation in the expression level of exosomal lncRNA XIST is observed. Consequently, EVs lncRNA XIST holds promise as a robust biomarker for patients with recurrent TNBC. Especially, this predictive ability remains independent of confounding variables associated with the patient's clinical and pathological condition (Lan et al., 2021).

3.3 Role of artificial intelligence (AI) in TNBC diagnoses

AI, especially with advances in deep learning (DL), a subset of machine learning (ML), has made significant contributions to addressing various clinical challenges in oncology, including tumor diagnosis, intervention, and prognosis. DL has the ability to automatically extract big data and process it, which has revolutionized areas such as image classification, neural language processing, and audio/video analysis. AI application in medical imaging has made diagnosis more accurate while reducing false positives, demonstrating its transformative potential in improving healthcare outcomes (Liao et al., 2023). DL exhibited significant success in the diagnosis of various types of pathology, like liver, colorectal, prostate, and BC, by using latest imaging modalities such as MRI, mammography, ultrasound (US), computed tomography (CT), and positron emission tomography-CT (PET-CT), DL plays an important role in increasing diagnostic accuracy and reliability, thereby improving oncology care and improving patient outcomes.

Firstly, any effective therapeutic approach for TNBC pathology, early screening and diagnosis is essential. While MRI is potential to effectively differentiate between TNBC subtypes, but there is a need to determine its various stages. Prognostic challenges arise due to heterogeneous predictive biomarkers, making predictions more complex. AI has significantly improved TNBC diagnosis at all stages through advanced algorithms, increasing both accuracy and efficiency. Integrating AI into screening programs has led to substantial improvements in clinical outcomes (Batool et al., 2024). AI integration with spectroscopic techniques such as Raman spectroscopy has significantly increased TNBC prediction accuracy, achieving rates up to 96.7% (Leithner et al., 2020). In TNBC pathology, need to critical diagnostic biomarkers to guide immunotherapy and prognosis. AI has proven to be a valuable tool in this domain. In a recent study by Li et al. developed an immune infiltration cell (IIC)-associated signature (MLIIC) for TNBC using transcriptomic data from purified immune cells, TNBC cell lines, and patient samples, as well as 25 machine learning algorithms including Boruta, LaSolR, SVM, and XGBoost. The results identified IIC-related RNAs (IIC-RNAs) using the tumor-stroma index (TSI), which displayed different expression patterns—upregulation in immune cells and downregulation in TNBC cells. The MLIIC signature demonstrated strong predictive value, correlating with survival outcomes. Its significance was further validated through immunofluorescent staining, confirming its potential as a reliable biomarker for TNBC prognosis (Li et al., 2023). As mentioned earlier, lack of these receptors (ER, PR, and HER2) renders many standard treatments ineffective. AI has the potential to use molecular and genetic data to identify therapeutic targets and predict strategy responses. Its integration could significantly

enhance precision medicine approaches and improve treatment outcomes in all TNBC stages (Tsou et al., 2020). Similarly, the ML algorithm IDtrax holds promising potential in identifying specific therapeutic targets for TNBC, enabling targeted drug development and personalized therapy. Additionally, it is able to predict effective inhibitors (Gautam et al., 2019).

3.4 EVs in developing drug resistance in TNBC

3.4.1 EVs role in resistance to EGFR targeted therapy for TNBC

TNBC cells secrete a multitude of cargo components within EVs, which play a significant role in conferring drug resistance in TNBC. These cargo components encompass drug efflux-promoting proteins, oncogenic molecule, and biomolecule capable of modulating signaling pathways (Maleki et al., 2021). Notably, TNBC exhibits significantly high expression of EGFR (Zoeller et al., 2020), and these tumors inherently possess resistance to EGFR inhibitors (EGFRi), EVs also play crucial role for this like EVs encapsulated EGFR are protected from the inhibitory effect of EGFRI, such as Erlotinib, Gefitinib (reversible inhibitors), Afatinib (irreversible inhibitor), Bendamustine and osimertinib. Additionally, the transfer of EGFR through TNBC-EVs can activate signaling pathways in recipient TNBC cells, leading to resistance against EGFRi. Overcoming EGFRi resistance may be an alternative option for the management of TNBC (Costa et al., 2017; Hung et al., 2019).

TNBC is primarily managed through systemic chemotherapy, which remains the mainstay of treatment (Luo et al., 2022). One of the highly efficacious drugs used in TNBC is Gemcitabine, also referred to as dFdC (2′,2′-difluorodeoxycytidine) (Zhao et al., 2020). Gemcitabine demonstrates notable effectiveness specifically in TNBC patients who have previously undergone regimen with anthracyclines and taxanes (Li et al., 2021). In cases of metastatic TNBC, the combined administration of platinum-based agents and gemcitabine provides substantial benefits (Pandy et al., 2019). The utilization of this combination therapy demonstrates significant efficacy in managing TNBC metastasis. However, TNBC cells exhibit remarkable capacity to develop rapid and efficient drug resistance (Zhang et al., 2022). Extensive research has revealed that these drug-resistant TNBC cells possess the capability to transfer their resistance to sensitive cells via EVs. This phenomenon allows the transmission of acquired drug resistance within the TNBC cellular population (Xavier et al., 2022). TNBC cells that have developed resistance to gemcitabine exhibit heightened expression levels of Annexin A6 (ANXA6) within both the cellular and EV compartments (Yi, 2023). ANXA6, functioning as a calcium-dependent membrane-binding protein, imparts resistance to multiple drug classes used in TNBC therapy (Noreen et al., 2020). Mechanistically, ANXA6 engages in interactions with EGFR and impedes the ubiquitin-proteasome pathway, thereby facilitating the accumulation of active EGFR and fostering tumor proliferation and dissemination (Li et al., 2021). Lapatinib, a bivalent inhibitor targeting both **Vesicle-associated Proteins in TNBC** and HER2, exhibits the capacity to counteract the resistance mediated by EVs ANXA6 (EV-ANXA6). Moreover, the circulating ANXA6 levels in the serum of TNBC patients serve as prognostic indicators for the responsiveness to gemcitabine-based chemotherapy. As previously stated, monotherapy with EGFR inhibitors proves inadequate for TNBC treatment due to the inherent resistance to EGFRi (Yi, 2023) (Figure 3).

3.4.2 EVs role in resistance to human epidermal growth factor receptor 2 (HER2)-targeted therapy in TNBC

The persistent over-expression of HER2 in BC instances has posed an enduring and significant prognostic dilemma (Lee et al., 2015). However, the advent of targeted therapies aimed at HER2 has led to remarkable achievements in the effective management of BC (Simmons et al., 2022). Trastuzumab, as the initial monoclonal antibody targeting HER-2, has gained approval for the remedy of HER2-positive BC, imparting significant enhancements to long-term survival and disease-free maintenance (Jagosky and Tan, 2021). Nevertheless, despite the promising initial outcomes, studies have shown that resistance to HER2-targeted drugs develops in the majority of patients after approximately 1 year of therapeutic approach (Derakhshani et al., 2020). Several studies have demonstrated that EVs exhibit interference with the efficacious functioning of trastuzumab, resulting in neutralization of its effects. EVs were obtained from SK-BR-3 and BT-474 cell lines, which revealed substantial upregulation of HER2 expression within these EVs. Similar findings were observed in experimental analyses involving samples from BC patients, which also revealed a significant abundance of HER2 (Dong et al., 2020).

In a study conducted by Martinez et al., it was discovered that HER2-targeted drugs, which eventually develop resistance in HER2-negative cells are modulated by two pivotal biomolecules: transforming growth factor beta 1 (TGF-β1) and programmed death-ligand 1 (PD-L1). Notably, the researchers observed the transfer of TGF-β1 and PD-L1 from resistant cells to sensitive cells via EVs. This process plays a critical role, and these transferred molecules exert an inducible effect, causing the acquisition of characteristics exhibited by the source cells within the sensitive cells (Martinez et al., 2017). The levels of TGF-β1 associated with EVs are related to the response of patients with HER2+ BC to HER2- targeted strategy, suggesting TGF-β1 could potentially be used as a biomarker to assess the management effectiveness.

Dysregulation of non-coding RNAs also plays a crucial role in developing resistance to trastuzumab in BC (Singh et al., 2022). Trastuzumab-resistant cells exhibit the release of EVs containing a specific long non-coding RNA known as SNHG14. This SNHG14 RNA molecule, in turn, induces resistance to trastuzumab by impeding the process of cell apoptosis through the modulation of the B cell leukemia/lymphoma 2 (BCL-2)/Bcl-2-associated X pathway (Lampropoulou et al., 2022). Moreover, a notable observation reveals significantly elevated expression of SNHG14 in trastuzumab-resistant cells, while its expression remains minimal in cells sensitive to trastuzumab (Shen et al., 2021). Similarly, the lncRNA, i.e., AGAP2-AS1 has the potential to induce resistance to trastuzumab in BC cells (Zheng et al., 2019). The protein heterogeneous nuclear ribonucleoprotein (A2/B1) hnRNPA2B1 is implicated in the process of packaging lncRNA AGAP2-AS1 into exosomes (Zheng et al., 2019). However, as of now, comprehensive information about the precise molecular mechanisms by which this resistance is conferred remains elusive. Further investigations are required to elucidate the underlying mechanisms responsible for the development of

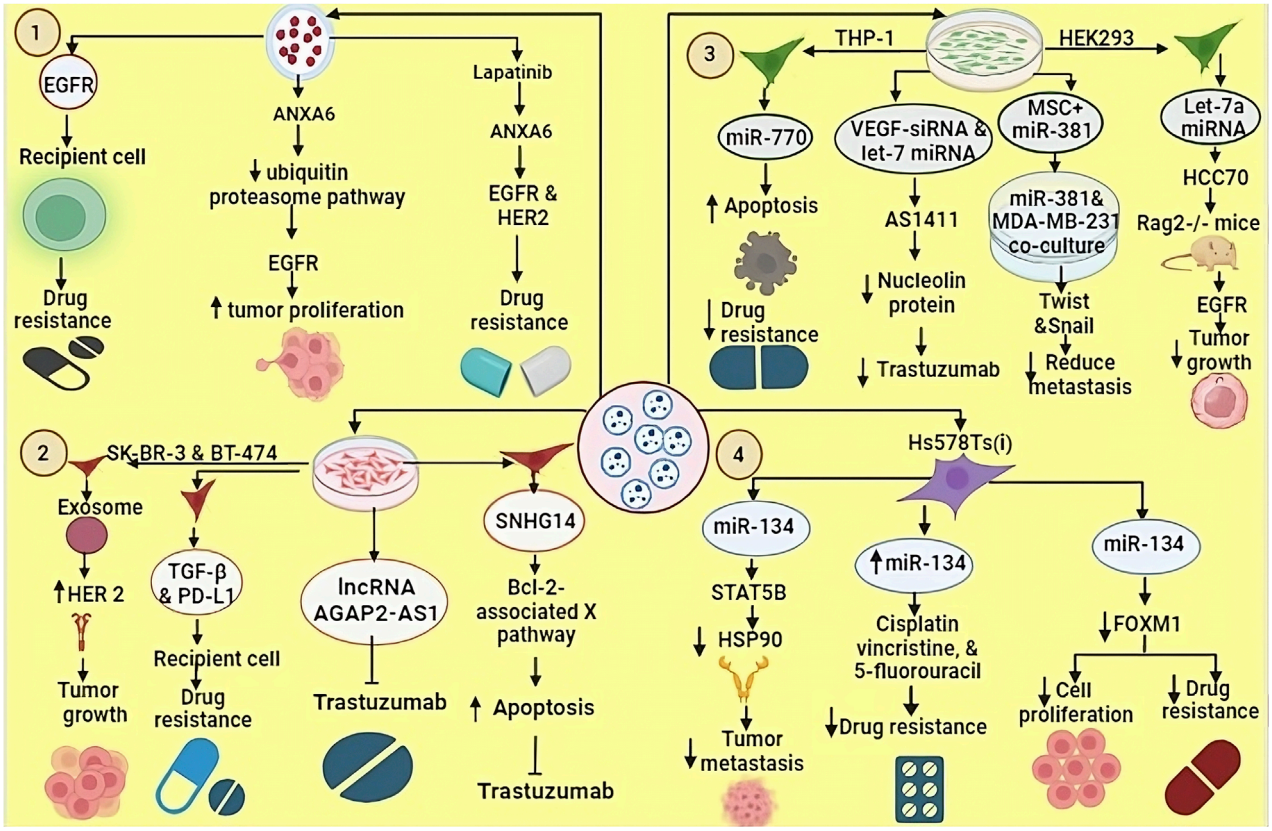

FIGURE 3
EVs derived from TNBC cells line can transfer various biomolecules to recipient cells, thereby modulated their biological functions. 1. EVs carrying EGFR contribute to drug resistance in recipient cells. ANXA6-containing EVs inhibit the ubiquitin-proteasome pathway, leading to EGFR-mediated tumour growth and proliferation. 2. EVs secreted by SK-BR-3 and BT-474 cell lines transport bioactive molecules such as TGF-beta, PD-L1, lncRNA AGAP2 and SNHG14, which promote tumour growth and resistance to trastuzumab. 3. miR-770 derived from THP1 cells enhances apoptosis and counteracts drug resistance. VEGF-derived siRNA and let-7 miRNA target AS1411, which inhibits nucleolin proteins, thereby increasing drug sensitivity. Let-7a miRNA, when loaded into EVs and introduced into TNBC HCC70 cells, was tested in Rag2$^{-/-}$ mice resulting Let-7a miRNA suppresses tumor growth by blocking the EGFR signaling pathway. 4. EVs from Hs578Ts cells carrying miR-134 reduce metastasis by inhibiting HSP90 activity, increase sensitivity to cisplatin, vincristine, and 5-fluorouracil, and inhibit tumor cell proliferation.

trastuzumab resistance mediated by exosomal lncRNA AGAP2-AS1 in BC cells (Dong et al., 2020) (Figure 3).

3.4.3 Role of EVs-associated miRNA in drug resistance

The miRNAs found in TNBC-EVs can cause drug resistance by influencing several processes (Li et al., 2020). A crucial protein called Protease-activated receptor 2 (PAR2) plays a role in producing and releasing EVs (Sung et al., 2019), and these EVs, through various signaling pathways like the AKT/NF-κB pathway, can transform normal cells into malignant cells. Moreover, these EVs carry specific miRNAs, such as miR-221, which regulate gene expression by reducing the mRNA expression of phosphatase and tensin homolog (PTEN) through targeting their 3′-untranslated region (3′-UTR) (Yi, 2023). The sEVs derived from MDA-MB-231 cells induce cellular resistance against Cisplatin, a chemotherapeutic agent used in the intervention of TNBC (Wang B. et al., 2019). Cisplatin exerts its cytotoxic effect by forming covalent cross-links between adjacent DNA strands, thereby inhibiting the process of DNA replication and transcription, ultimately triggers apoptosis (Tchounwou et al., 2021).

3.5 EVs in TNBC treatment

Recent advancement in targeted therapy and immunotherapy are playing an important role in the management of TNBC, such as inhibitors of key pathways (PI3K/AKT/mTOR and Notch), as well as immune checkpoint inhibitors like pembrolizumab. These approaches offer promising strategies for personalized therapeutic approach of TNBC patients. Such precise targeting is helpful in improving TNBC management and guiding future therapeutic approaches (Zhu et al., 2023). EVs play a key role in TNBC management (Brena et al., 2022). They contribute to drug resistance through paracrine signaling to nearby cells or by affecting the whole body, thereby hindering satisfactory treatment outcomes (Xavier et al., 2022). EVs also play a role in developing and strengthening new drug resistance (Grimaldi et al., 2023). However, they possess essential qualities such as specific targeting, immune

compatibility, low toxicity, and a protective layer, making them an excellent option for delivering diverse drugs or biological molecules to treat tumor (Khosravi et al., 2022). In a research investigation on exosomes derived from THP-1 cells, the presence of the biomolecule miR-770 was identified (Liu J. et al., 2021). It was observed that miR-770 plays a role in promoting apoptosis and reducing chemotherapy resistance miR-770 targets STMN1 to enhance chemo-sensitivity and suppress metastasis. To explore the underlying molecular machinist Y. Li et al. using three bioinformatics tools—TargetScan, miRDB, and PICTAR5—identified predicted binding sites for miR-770 at positions 54–60, 267–273, and 409–415 in the 3′ UTR region of the STMN1 gene. Additionally, clinical evidence indicated a positive correlation between elevated miR-770 expression in cells or tissues and a notable enhancement in drug sensitivity. Consequently, these findings propose the potential utility of exosomal miR-770 as a promising therapeutic target or a prognostic indicator for TNBC (Li et al., 2018).

Experiments employing siRNA-loaded EVs have revealed their critical importance in post-translational processes, gene silencing and provoking apoptotic cell death in various cancer cell lines (Zhang et al., 2015). Macrophage-derived EVs (Mφ-EVs) are modified using VEGF-siRNA and let-7 miRNA, which target the nucleolin protein (Boimel et al., 2012), nucleolin that plays various roles in the cell, including in the regulation of gene expression, cell proliferation, and tumor development (Burbano De Lara et al., 2021). For this purpose, the DNA aptamer AS1411 (a specific DNA aptamer, a short single-stranded DNA molecule) is used, which has the ability to bind nucleolin with high affinity. The binding of AS1411 to nucleolin interferes nucleolin's function, and provides inhibition of tumor growth in MDA-MB-231 (Wang et al., 2017; Brenske et al., 2023). CXCL12 have crucial role in breast cancer progression by promoting invasion, angiogenesis and immune system modulation. It can affect the TME by recruiting immunosuppressive macrophages and increasing microvessel density, which supports tumour expansion. Targeting the CXCL12-CXCR4 pathway could be a potential therapeutic strategy for the treatment of breast cancer (Boimel et al., 2012). Another experiment was conducted for the TNBC cell line MDA-MB-231, in which EVs derived from the bone marrow stroma were loaded with several miRNAs, such as miR-127, miR-197, miR-222, and miR-223. These miR targets CXCL12 resulting arrested proliferation in this cell line (Lim et al., 2011). Let-7a miRNA was packed into EVs derived from HEK293 cells and introduced into the TNBC HCC70 cell line. Subsequently, HCC70 cells were successfully implanted into $Rag2^{-/-}$ mice. As a result, it was observed that let-7a miRNA inhibits tumor growth by interfering with the EGFR signaling pathway (Zhou et al., 2014) (Table 2). Previous studies showed that Mesenchymal Stromal/Stem Cell-derived EVs (MSC-EVs) have therapeutic potential for various diseases. Shojaei et al. found that packing miR-381 into MSC-EVs and co-culturing with MDA-MB-231 TNBC cells reduced metastatic capabilities. miR-381 downregulated key transcription factors (Twist and Snail) associated with the Wnt signaling pathway and EMT (Shojaei et al., 2021). NK cells and $CD8^+$ T-cells (CTL) are have capacity to detect and kill maligned cells. However, their ability to penetrate deep into tumors is limited. EVs derived from NK cells or CTLs can effectively penetrate solid tumors and help overcome this challenge. TNBC cells often express PD-L1, while its receptor PD-1 is present on tumor-infiltrating lymphocytes (TILs). The interaction between PD-L1 and PD-1 not only attenuates TIL proliferation but also leads to TIL apoptosis, which contributes to the immune evasion mechanism of TNBC. Sthudy shown that PD-1+ EVs released by TILs interact with either the cell surface or PD-L1 of EVs, thereby preventing the interaction between TILs and TNBC cells. As a result, PD-L1-induced suppression of TIL activity is reduced, ultimately increasing the ability of TILs to kill TNBC cells (Das K. et al., 2023) (Table 2).

3.6 Role of EVs in overcome drug resistance

Engineered EVs as drug carriers offer a promising strategy for overcoming drug resistance in various disease intervention. By facilitating the delivery of therapeutic agents in chemotherapy, targeted therapy, immunotherapy, and endocrine therapy, EV-based approaches offer potential solutions to reduce tumor recurrence and improve clinical outcomes (Zheng et al., 2024). MiR-9 expression is upregulated in temozolomide (TMZ)-resistant glioblastoma (GBM) cells and involves the drug efflux transporter P-gp. Anti-miR-9 loaded EVs is promising strategy for overcoming temozolomide resistance in glioblastoma (Munoz et al., 2013). Thus, engineered EVs highly effective in overcoming various types of drug resistance, such as overcoming reduced drug uptake-induced resistance, for instance, loading cisplatin on EVs derived from M1 and M2 macrophages significantly facilitated drug delivery to resistant neoplasm cells (A2780/DDP) and non-resistant cells (A2780) (Zhang et al., 2020). Similarly, these EVs not only play crucial role in overcoming drug inactivation-induced resistance, overcoming signaling pathway alteration-induced resistance and overcoming apoptosis defect-induced resistance but also, they also can overcome targeted therapy resistance (Zheng et al., 2024). EVs also shown as promising strategy for overcoming mutation-induced resistance, similar to overcoming targeted therapy resistance. For example, imatinib (IM), a selective BCR-ABL inhibitor, mutations in BCR-ABL reduce the binding affinity to IM. Engineered EVs from BCR-ABL siRNA help overcome targeted drug resistance in CML by inhibiting Bcr-Abl (Bellavia et al., 2017). Additionally, various studies have highlighted that overcoming pathway mutation-induced resistance, overcoming immunotherapy resistance, and overcoming endocrine therapy resistance are also effective and promising strategies for the management of TNBC.

3.7 EVs in drug delivery

Although most of cells produce EVs, among them not all EVs are suitable for use as drug carriers. EVs that meet quality parameters such as surface protein composition, size, yield, and intracavitary content are considered suitable for drug delivery applications. Various types of cells have been investigated as potential EVs donators for drug delivery such as Dendritic cells (DC), Mesenchymal stem cells (MSC), Macrophages, Milk, red blood cells (RBCs), NK cell-derived EVs, etc. A study demonstrated engineered exosomes (DEVs) could be used to deliver RNA interference (RNAi) therapy into the brain. They used RVG-targeted exosomes, which help deliver treatments directly to brain cells

TABLE 2 Extracellular vesicles associated cargos and their roles in TNBC treatment.

S. N.	Extracellular vesicle	Source	Biomolecule	Function	References
1.	Exosomes	THP-1 cells	miR-770	Promoting apoptosis and reduce resistance to chemotherapy	Li et al. (2018)
2.	Extracellular vesicle	Macrophage-derived EVs (Mφ-EVs)	VEGF-siRNA and let-7 miRNA	Inhibit tumor growth in MDA-MB-231cell line	Brenske et al. (2023)
3.	Extracellular vesicle	bone marrow	miR-127, miR-197, miR-222, and miR-223	Arrested proliferation in MDA-MB-231	Lim et al. (2011)
4.	Extracellular vesicle	HEK293 cells	Let-7a miRNA	Inhibits tumor growth by interfering with the EGFR signalling pathway	Zhou et al. (2014)
5.	Extracellular vesicle	Mesenchymal stromal cells (MSCs)	miR-381	Reduced metastatic by downregulated key transcription factors Twist and Snail	Shojaei et al. (2021)

(Meng et al., 2020). MSC-derived EVs (MEVs) exhibit similar functions, including immune modulation, drug delivery, wound healing, and tissue repair, and these features make them promising candidates for therapeutic applications. Increased expression of miR-9 is observed in temozolomide (TMZ)-resistant glioblastoma (GBM) cells (Zhang et al., 2014). EVs have the capacity to deliver targeted drug to specific cells or tissues (Ullah et al., 2021). Additionally, they exhibit the ability to modulate the immune system (Burrello et al., 2016). The utilization of EVs in drug delivery is supported by several advantageous factors. Firstly, EVs exhibit biocompatibility and biodegradability, thereby minimizing potential toxic effects (Chen et al., 2021). In addition, they possess a remarkable ability to selectively target specific cells or tissues through the recognition of surface molecules on vesicles. Additionally, EVs demonstrate proficiency in delivering diverse types of drugs, encompassing small molecules, proteins, and nucleic acids. These attributes render EVs as promising candidates for effective and targeted drug delivery strategies (Peswani Sajnani et al., 2021). EVs for drug delivery show promising potential in diverse therapies. They efficiently carry chemotherapy drugs to tumor cells, thereby enhancing cancer therapy (Meng et al., 2020). In gene therapy, EVs deliver corrective genes that target genetic defects and modulate the immune system to target and destroy oncological cells. In vaccination, EVs provide antigens, inducing a potent and specific immune response, enhancing protection against pathogens (Mehanny et al., 2021).

Researchers have found that EVs have natural properties that help them target specific organs in the body to some extent, and this depends largely on the lipid composition and protein content present on their surface (Murphy et al., 2019). For example, some integrins may alter the pharmacokinetics and cause their accumulation in the brain, lung, or liver, depending on the specific integrin type (Hoshino et al., 2015). Other studies have shown that EVs containing Tspan8 along with integrin alpha4 are more likely to be taken up by pancreatic cells (Rana et al., 2012). In addition, the lipid composition of EVs may also affect the way they are absorbed, as seen with phosphatidylserine, which plays a role in their absorption by macrophages (Matsumoto et al., 2017). Additionally, researchers can further modify the EVs to enhance targeted delivery by engineering producer cells using methods similar to those previously described for cargo loading.

3.7.1 EVs suitable characteristics for drugs delivery

EVs exhibit a lipid bilayer enveloping their entire surface, displaying structural similarity to liposomes (van der Koog et al., 2022). Due to their complex assemblies consisting of lipids, proteins and other bioactive fragments, EVs exhibit exceptional biocompatibility, facilitating pronounced targeting capabilities towards specific cells or tissues (Mathieu et al., 2019). EVs can be bioengineered to contain therapeutic molecules using various technological approaches, including drug incorporation during their biogenesis or post-loading strategies (Song et al., 2022). EVs have intrinsic targeting capabilities due to specific proteins displayed on their surface, which facilitate interaction with target cells or tissues and facilitate precise cargo delivery to the designated site (van Niel et al., 2022). EVs have the natural ability to efficiently and effectively establish themselves in specific cells and tissues within the body (Al-Jipouri et al., 2023). This innate feature enables them to easily cross biological barriers and reach the intended destination easily. As a result, using EVs as carriers for drug delivery greatly simplifies the process, thereby increasing the accuracy and efficacy of drug delivery (Al-Jipouri et al., 2023). As a result, therapeutic agents transported via EVs exhibit enhanced effectiveness and efficiency in their pharmacological actions (van der Meel et al., 2014). EVs exhibit cargo protection capabilities by safeguarding their transported payload from diverse enzymatic and intracellular components, which pose potential risks of cargo degradation (Bahmani and Ullah, 2022). Additionally, the utilization of autologous EVs, which refer to EVs obtained from the patient's own cells, has the potential to enhance the safety profile of medicines and mitigate the toxicity associated with drug delivery (Elsharkasy et al., 2020). This is attributed to their capacity to reduce immune responses. The utilization of autologous EVs offers a secure and less hazardous approach to drug delivery, particularly for patients susceptible to intense immune reactions or adverse effects (Elsharkasy et al., 2020).

Researchers and medical professionals are actively investigating this avenue, as it holds promise for introducing a novel and efficient method of drug administration.

3.7.2 EVs as a delivery vehicle for chemotherapy drugs and biomolecule

Paclitaxel is a chemotherapeutic agent with significant therapeutic implications for various pathology, including breast, lung, and ovarian cancer (Meng et al., 2020). Its primary mode of action involves stabilizing microtubules, which play a critical role in chromosome organization during cell division. Upon binding to microtubules, Paclitaxel impedes their breakdown, resulting in the inhibition of cell division (Honore et al., 2004). Notably, paclitaxel induces apoptosis by activating specific signaling pathways, particularly the p53 pathway, which is responsible for the detection and repair of DNA damage (Ganansia-Leymarie et al., 2003; Kulaberoglu et al., 2021). Additionally, paclitaxel triggers the caspase cascade, which results in DNA fragmentation and degradation of cellular organelles. Despite its efficacy, conventional administration of paclitaxel is associated with unwanted side effects and limited therapeutic benefits (Basu et al., 2020). Encouragingly, preclinical investigations utilizing Paclitaxel-loaded EVs have shown promising outcomes, demonstrating enhanced drug delivery, reduced systemic toxicity, and improved anti-tumor activity (Meng et al., 2020).

A recent study by Xiao Hu and colleagues involved the use of micro-particles to deliver the chemotherapeutic agent paclitaxel (MP-PTX) in combination with radiotherapy for treating TNBC. The experiment demonstrated that targeted delivery of MP-PTX increased absorption, enhancing its ability to kill tumor cells. The combination of MP-PTX and radiotherapy resulted in a synergistic antitumor effect by inhibiting tumor cell proliferation, promoting apoptosis, and reducing the tumor's immunosuppressive microenvironment. Using MP-PTX and radiotherapy together had a more significant impact on combating TNBC than using them individually(Hu et al., 2023). Another study was conducted by Haney and colleagues, in which they performed experiments using mouse models to treat pulmonary metastasis. They loaded EVs with PTX (EV-PTX) and Doxorubicin (EV-Dox), which effectively targeted malignant cells and showed strong anticancer efficacy in the mouse model of pulmonary metastasis. Subsequently, they developed novel EV-based drug formulations using optimized loading procedures, including variations in pH, temperature, and sonication. These formulations demonstrated high drug loading and efficient accumulation in TNBC cells during *in vitro* testing, indicating a significant anti-proliferation effect of drug-loaded EVs. *In vivo* experiments targeting TNBC in both immune competent and Athymic nu/nu mice resulted in the successful suppression of tumor growth (Haney et al., 2020).

In their research, Gong and colleagues unveiled the presence of A15-Exos, an exosomes containing biomolecules, including disintegrin and metalloproteinase 15, localized on its surface. A15-Exos exhibits the ability to transport DOX and miR-159, thereby targeting TNBC. This combination demonstrates efficacy in treating TNBC by down-regulating the expression of TCF-7 (Gong et al., 2019), a gene promoter involved in cell proliferation, invasion, and metastasis. Moreover, it also suppresses the expression of genes related to cell death, leading to an effective TNBC management without causing adverse effects (Lu et al., 2021). As previously mention modifying the surface of exosomes using several engineering technologies significantly increases drug delivery efficiency, like the CD47-targeted RS17 peptide was encapsulated into liposomes containing the chemotherapeutic agent shikonin, photosensitizer IR820, and immunomodulator poly-metformin for the regimen of BC (Kim et al., 2024). Chlorine E6 (CE6), an FDA-approved photosensitizer, offers a promising approach for targeted pathology treatment in photodynamic therapy (PDT). Integrating Ce6 with 18F-FDG in goat milk-derived exosomes significantly increased the efficacy and accuracy of PDT in BC (Guo et al., 2023). Similarly, TPP-CE6-engineered exosomes were used to load the cancer-specific chemotherapeutic agent pipelongumin (PL). After ultrasonic irradiation, TPP-Ce6-PL-loaded exosomes shows the strongest anticancer effect (Nguyen Cao et al., 2023) (Table 3).

In a subsequent investigation Lou and his team isolated exosomes from mesenchymal stem cells obtained from adipose tissues (AMSCs). They modified these exosomes with the biomolecule miR-199a (AMSC-Exo-199a) and administered them to patients with hepatocellular carcinoma. As a result, it was observed that these modified exosomes significantly sensitized disease cells to the DOX drug, thereby targeting the mTOR pathway (Lou et al., 2020). The mTOR pathway is linked to various poor prognostic factors, including increased tumor size, lymphnode metastasis, and shorter survival (Wu et al., 2021) (Table 3).

4 Limitation of extracellular vesicle in TNBC

The diversity of EVs and their presence in various types of diseases has captivated the scientific community. However, their application is currently constrained by issues related to cargo delivery, biological barriers, and clinical translation. Researchers have been actively engaged in addressing these limitations of EVs and are diligently working towards harnessing their substantial potential as a powerful tool in the management of TNBC. One important reason for the failure of TNBC management is the lack of a specific molecular target that can be focused on (Maqbool et al., 2022). On the other hand, EVs have been explored as a crucial biomarker and prognostic tool for TNBC (Dong et al., 2022). However, recognizing a specific target of TNBC is currently a challenge in order to deliver therapeutic cargo through EVs (Haney et al., 2020). Additional off targeting a major challenge, because EVs membranes are enriched with receptors or ligands that interact with target cells, providing them with inherent targeting missions. But most natural therapeutic EVs suffer the fate of being cleared by macrophages, resulting EVs often become off target and fail to reach their destination. Therefore, it is necessary to reduce this off-target effect to improve the bioavailability of target tissues. Despite EV-based drug delivery is now a breakthrough for clinical pathology. Methods such as incubation provide a simple and non-disruptive approach to loading drugs into EVs. However, limited drug-loading capacity remains a significant drawback (Gangadaran and Ahn, 2020).

TABLE 3 Extracellular Vesicles deliver chemotherapy drugs and biomolecule and its various effect on different target cells.

EVs	Drugs and biomolecule	Target cells	Effect	References
Micro-particles	Paclitaxel (PTX)	MCF-7	PTX increased absorption, enhancing its ability to kill cancer cells. Inhibiting tumor cell proliferation, promoting apoptosis, and reducing the tumour's immunosuppressive microenvironment	Hu et al. (2023)
A15-Exo	Doxorubicin and miR-159	MDA-MB-231	Down-regulating the expression of TCF-7, resulting cell proliferation, invasion, and metastasis	Gong et al. (2019)
AMSC-Exo	miR-199a		Sensitized cancer cells to the DOX drug and target the m-TOR pathway resulting reduce tumor size, lymph node metastasis.	Wu et al. (2021)
miR-134- EVs	miR-134		Reduced STAT5B and Hsp90, reduced cellular migration and invasion, and enhanced sensitivity to anti-Hsp90 drugs	O'Brien et al. (2015)
HER2+ EVs	Anti-HER2 antibodies and paclitaxel		Reducing side effects and increasing the effectiveness of the treatment	Quinn et al. (2021)
ADSC-exosomes	miR-381	MDA-MB-231 cells	Inhibited proliferation, migration, and invasion by altering EMT-related gene expression	Dong et al. (2022)

The low toxicity, immune tolerance and long half-life of EVs has been a boon in the medical field. However, their slow secretion remains a major obstacle to clinical applications. Over the past decades, there has been an emphasis on large-scale EV production using physical, chemical, and environmental stimulation methods. However, none of these approaches have been successful enough to be widely adopted for clinical applications (Hahm et al., 2021). Among the many challenges, some of these like Complexities in isolating EVs from various biological mixtures arise from their inherent heterogeneity in their size, shape and composition (Ding et al., 2021). This challenge is further compounded by variation in EVs secretion rates from biological source and different cell types, which can reduce yields and limit sample size, hindering thorough analysis (Dong et al., 2022). Maintaining the functional behavior of EVs remains a major challenge. EVs obtained from MSCs or other parts of the body remain stable and viable for long periods at −80°C, but freezing and thawing can lead to clustering. Storage and transportation at low temperatures may reduce the translational activity of EVs. This drawback can be overcome by using freeze-dried exosomes, that allows storage at room temperature, extends shelf life, and reduces storage and transportation costs (Karn et al., 2021).

Additionally, the presence of interfering biological molecules like proteins, lipids, and nucleic acids complicates the precise isolation and purification of EVs (Mateescu et al., 2017). The lack of a standardized method to isolate EVs from various bodily sources also presents a challenge (Zeng et al., 2022). Currently, five EV isolation methods include ultracentrifugation, size-based techniques, immunoaffinity capture, precipitation, and microfluidics (Yang et al., 2020). Ultracentrifugation is most widely used method, with other methods being used by only 5%–20% of researchers (Li and Xu, 2019). Each technique has advantages and disadvantages. Differential ultracentrifugation is cost-effective but inefficient and potentially harmful to EVs during recovery (Tiwari et al., 2021). On the other hand, Density gradient centrifugation is more efficient method for recovering EVs, but it is also more expensive and time-consuming (Monguió-Tortajada et al., 2019). The Immunoaffinity method is effective but time-consuming and costly. Similar challenges exist with other methods (Taylor and Shah, 2015). Given these limitations, there is a growing demand for user-friendly, affordable tools that efficiently isolate EVs while saving time (Yuan et al., 2021).

The entrapment of diverse cargo within EVs presents a formidable challenge, stemming from the geometrical constraints imposed by the small dimensions of EVs that reduce their viability for large molecular species (Tran and Tran, 2020). The phospholipid bilayer constitution of EV membranes imposes a selective barrier against macromolecules with high electrostatic potential, and concurrently selective cargo units are endowed with surface-bound receptors on EVs, which makes their preferential interaction possible (van der Meel et al., 2014). Nevertheless, the lack of receptors in all cargo categories prevents binding interactions, thereby hindering the association. ATP, apart from its role as a universal energy currency, assumes pivotal significance in the context of encapsulating bio-macromolecules within EVs, harnessing energy sourced from ATP hydrolysis to facilitate and potentiate cargo encapsulation processes. The depletion of ATP stores can complicate this complex process (Russell et al., 2019).

EVs offer a promising avenue for disease diagnosis, but this promise is accompanied by certain challenges. Variability in samples, whether derived from blood, urine, saliva or other sources, can result in variation in the amount and type of EVs (Jafari et al., 2020). Research focusing on EVs biomarkers often adopts diverse criteria to indicate specific EVs subpopulations,

potentially leading to inconsistent findings across different studies. To mitigate this problem, standardization of these criteria becomes imperative to establish reliable and consistent diagnostic markers (Yan et al., 2021). Moreover, the sensitivity of diagnostic tests based on EVs can be influenced by multiple factors including the selection of detection methods (such as ELISA, flow cytometry, and nanoparticle tracking analysis) and the quality of reagents employed (Serrano-Pertierra et al., 2020). Considering that EVs exhibit heterogeneity in both size and composition, the presence of analogous-sized cellular fragments or vesicles might impede the precise detection of targeted biomarkers, underscoring the need for methodological refinement in this promising diagnostic approach.

Our understanding of EVs' role in supporting TNBC, their mechanisms, and their impact on TNBC interventions is currently limited (St-Denis-Bissonnette et al., 2022). The assistance of EVs in TNBC metastasis and their role in epigenetic processes like methylation, histone modification, and non-coding RNA activities remains unclear (Zolota et al., 2021) Additionally, roles and alterations in immune regulation, forming pre-metastatic niches in metastatic organs, lack comprehensive understanding and require further research (Yang et al., 2021). The complex BC tumor microenvironment, with diverse cells and interactions, poses challenges in understanding TNBC progression's regulatory mechanisms. Uncertainties persist about specific cell-derived EV components crucial in this network (Awadasseid et al., 2021). Many research studies concentrate solely on specific targets within EVs, preventing a comprehensive perspective. It's crucial to precisely track the path, dispersion, and destiny of EVs to comprehend how they are absorbed and their impacts on the recipient cells. The complex structure of exosomes and their interactions with recipient cells remain mysterious, underscoring the insufficient understanding of the mechanisms through which EVs operate in TNBC. Bridging these knowledge gaps plays an important role in realizing the potential of EVs as a diagnostic aid and therapeutic focal point in dealing with TNBC.

5 Future directions of EVs application as therapeutics in TNBC

The evidence highlighting the role of EVs in TNBC has presented another opportunity for research, particularly in the development of EVs as diagnostic/prognostic biomarkers, but more importantly, as therapeutic agents. EVs demonstrated promising results in cancer vaccination and drug delivery, making it a noteworthy consideration in medical applications. The initial characterization of EVs reveals their unique therapeutic properties, making them interesting for potential use in clinical field (Elsharkasy et al., 2020). EVs encapsulate nucleic acids and proteins released from malignant cells, providing valuable insights into the essential characteristics of disease cells (Cerezo-Magaña et al., 2020). Studies results shown that EVs can indicate differences between tumor samples and controls, which make it easier to obtain preliminary information about disease prognosis (Hoshino et al., 2020). The ability to detect such differences has the potential to revolutionize the approach to BC diagnoses. Through the examination of the contents of EVs, medical professionals could enhance their comprehension of the ailment and its advancement, ultimately resulting in improved and individually tailored therapies.

6 Conclusion

TNBC shows significant challenges in its management due to its aggressive nature, propensity for metastasis, and limited strategy options. Current therapies, including surgery, chemotherapy, and radiation, have shown limited efficacy, particularly in addressing metastatic tumors. Limitations of currently used diagnostic tools like imaging (mammography, ultrasound, and magnetic resonance imaging) and immunohistochemistry (IHC) in the diagnosis of TNBC, make challenging to obtain comprehensive and accurate information about it. EVs opened new avenues for the diagnosis of various disease including TNBC. EVs associated protein biomarkers such as EGFR, CCL5, CD24, ADAM10, cofilin-1 and Non-coding RNA (ncRNA) like miRNA have significant role in its diagnosis as previous mention. In the field of oncology, the integration of AI, especially DL, significantly enhances tumor diagnosis, intervention, and prognosis. With its ability to automatically extract features and analyze large datasets, DL has revolutionized medical imaging, improving diagnostic accuracy while reducing false positives. The inability to effectively manage TNBC so far is largely due to drug resistance, which remains a major challenge. This challenge can overcome by EV-associated biomolecules, and EVs are capable of carrying molecules, and allowing non-invasive monitoring of the disease. The emergence of EVs as versatile mediators of intercellular communication and potential therapeutic carriers offers a promising avenue for the development of more effective TNBC therapeutic approaches. EVs also have crucial role in the development of TNBC and significantly influence patient outcomes. EVs possess inherent properties that make them well-suited for targeted drug delivery, ability to evade the immune system, and capacity to traverse biological barriers like the blood-brain barrier. The use of EVs as drug delivery vehicles has the potential to enhance intervention accuracy, efficacy, and patient outcomes in TNBC and other malignant diseases, representing an attractive area for future research and clinical exploration.

Author contributions

PT: Visualization, Writing–original draft, Writing–review and editing. AC: Formal Analysis, Writing–review and editing, Funding acquisition. SG: Writing–review and editing, Visualization. MC: Writing–review and editing, Visualization. HS: Conceptualization, Writing–review and editing. SR: Writing–review and editing, Validation. S-U-DK: Writing–review and editing, Funding acquisition. SK: Conceptualization, Writing–review and editing, Supervision, Visualization.

Funding

The author(s) declare that financial support was received for the research and/or publication of this article. This work was supported and funded by the Deanship of Scientific Research at

Imam Mohammad Ibn Saud Islamic University (IMSIU) (grant number IMSUI-DDRSP2501.

Acknowledgments

The authors would like to thank Sharda University for providing all the resources required for this work.

Conflict of interest

The authors declare that the research was conducted in the absence of any commercial or financial relationships that could be construed as a potential conflict of interest.

Generative AI statement

The author(s) declare that no Generative AI was used in the creation of this manuscript.

Publisher's note

All claims expressed in this article are solely those of the authors and do not necessarily represent those of their affiliated organizations, or those of the publisher, the editors and the reviewers. Any product that may be evaluated in this article, or claim that may be made by its manufacturer, is not guaranteed or endorsed by the publisher.

References

Abels, E. R., and Breakefield, X. O. (2016). Introduction to extracellular vesicles: biogenesis, RNA cargo selection, content, release, and uptake. *Cell. Mol. Neurobiol.* 36, 301–312. doi:10.1007/s10571-016-0366-z

Agostinetto, E., Gligorov, J., and Piccart, M. (2022). Systemic therapy for early-stage breast cancer: learning from the past to build the future. *Nat. Rev. Clin. Oncol.* 19, 763–774. doi:10.1038/s41571-022-00687-1

Ahmed, A. E. E. (2018). Ultrasound triggered release of Trastuzumab-conjugated immunoliposomes targeting breast cancer. Available online at: https://dspace.aus.edu:8443/xmlui/handle/11073/16483 (Accessed July 24, 2023).

Alabi, R. O., Lora, J., Celen, A. B., Maretzky, T., and Blobel, C. P. (2021). Analysis of the conditions that affect the selective processing of endogenous Notch1 by ADAM10 and ADAM17. *Int. J. Mol. Sci.* 22, 1846. doi:10.3390/ijms22041846

Alismail, H. (2024). Review: merging from traditional to potential novel breast cancer biomarkers. *J. King Saud. Univ. - Sci.* 36, 103551. doi:10.1016/j.jksus.2024.103551

Al-Jipouri, A., Almurisi, S. H., Al-Japairai, K., Bakar, L. M., and Doolaanea, A. A. (2023). Liposomes or extracellular vesicles: a comprehensive comparison of both lipid bilayer vesicles for pulmonary drug delivery. *Polymers* 15, 318. doi:10.3390/polym15020318

Altevogt, P., Sammar, M., Hüser, L., and Kristiansen, G. (2021). Novel insights into the function of CD24: a driving force in cancer. *Int. J. Cancer* 148, 546–559. doi:10.1002/ijc.33249

Aravindan, A., Gupta, A., Moorkoth, S., and Dhas, N. (2024). Implications of nanotherapeutic advancements to leverage multi-drug resistant breast cancer: the state-of-the-art review. *J. Drug Deliv. Sci. Technol.* 100, 106007. doi:10.1016/j.jddst.2024.106007

Arnold, M., Morgan, E., Rumgay, H., Mafra, A., Singh, D., Laversanne, M., et al. (2022). Current and future burden of breast cancer: global statistics for 2020 and 2040. *The Breast* 66, 15–23. doi:10.1016/j.breast.2022.08.010

Aseervatham, J. (2020). Cytoskeletal remodeling in cancer. *Biology* 9, 385. doi:10.3390/biology9110385

Awadasseid, A., Wu, Y., and Zhang, W. (2021). Extracellular vesicles (exosomes) as immunosuppressive mediating variables in tumor and chronic inflammatory microenvironments. *Cells* 10, 2533. doi:10.3390/cells10102533

Azad, K., Guilligay, D., Boscheron, C., Maity, S., De Franceschi, N., Sulbaran, G., et al. (2023). Structural basis of CHMP2A–CHMP3 ESCRT-III polymer assembly and membrane cleavage. *Nat. Struct. Mol. Biol.* 30, 81–90. doi:10.1038/s41594-022-00867-8

Azim, H. A., Ghosn, M., Oualla, K., and Kassem, L. (2020). Personalized treatment in metastatic triple-negative breast cancer: the outlook in 2020. *Breast J.* 26, 69–80. doi:10.1111/tbj.13713

Bahmani, L., and Ullah, M. (2022). Different sourced extracellular vesicles and their potential applications in clinical treatments. *Cells* 11, 1989. doi:10.3390/cells11131989

Baig, M. S., Roy, A., Rajpoot, S., Liu, D., Savai, R., Banerjee, S., et al. (2020). Tumor-derived exosomes in the regulation of macrophage polarization. *Inflamm. Res.* 69, 435–451. doi:10.1007/s00011-020-01318-0

Banerjee, M., and Rajeswari, V. D. (2023). Critical review on the different roles of exosomes in TNBC and exosomal-mediated delivery of microRNA/siRNA/lncRNA and drug targeting signalling pathways in triple-negative breast cancer. *Molecules* 28, 1802. doi:10.3390/molecules28041802

Banerjee, R., Maitra, I., Bhattacharya, T., Banerjee, M., Ramanathan, G., Rayala, S. K., et al. (2024). Next-generation biomarkers for prognostic and potential therapeutic enhancement in Triple negative breast cancer. *Crit. Rev. Oncol. Hematol.* 201, 104417. doi:10.1016/j.critrevonc.2024.104417

Baranova, A., Krasnoselskyi, M., Starikov, V., Kartashov, S., Zhulkevych, I., Vlasenko, V., et al. (2022). Triple-negative breast cancer: current treatment strategies and factors of negative prognosis. *J. Med. Life* 15, 153–161. doi:10.25122/jml-2021-0108

Barkal, A. A., Brewer, R. E., Markovic, M., Kowarsky, M., Barkal, S. A., Zaro, B. W., et al. (2019). CD24 signalling through macrophage Siglec-10 is a target for cancer immunotherapy. *Nature* 572, 392–396. doi:10.1038/s41586-019-1456-0

Basu, U., Roy, M., and Chakravarty, A. R. (2020). Recent advances in the chemistry of iron-based chemotherapeutic agents. *Coord. Chem. Rev.* 417, 213339. doi:10.1016/j.ccr.2020.213339

Batool, Z., Kamal, M. A., and Shen, B. (2024). Advancements in triple-negative breast cancer sub-typing, diagnosis and treatment with assistance of artificial intelligence: a focused review. *J. Cancer Res. Clin. Oncol.* 150, 383. doi:10.1007/s00432-024-05903-2

Bellavia, D., Raimondo, S., Calabrese, G., Forte, S., Cristaldi, M., Patinella, A., et al. (2017). Interleukin 3- receptor targeted exosomes inhibit *in vitro* and *in vivo* Chronic Myelogenous Leukemia cell growth. *Theranostics* 7, 1333–1345. doi:10.7150/thno.17092

Beňačka, R., Szabóová, D., Guľašová, Z., Hertelyová, Z., and Radoňák, J. (2022). Classic and new markers in diagnostics and classification of breast cancer. *Cancers* 14, 5444. doi:10.3390/cancers14215444

Boimel, P. J., Smirnova, T., Zhou, Z. N., Wyckoff, J., Park, H., Coniglio, S. J., et al. (2012). Contribution of CXCL12 secretion to invasion of breast cancer cells. *Breast Cancer Res.* 14, R23. doi:10.1186/bcr3108

Brena, D., Huang, M.-B., and Bond, V. (2022). Extracellular vesicle-mediated transport: reprogramming a tumor microenvironment conducive with breast cancer progression and metastasis. *Transl. Oncol.* 15, 101286. doi:10.1016/j.tranon.2021.101286

Brenske, K.-O., Emondts, M., Hörnig, S. T., Panitz, S., Pieper, M. I., Ligori, A., et al. (2023). Parahydrogen-induced polarization of a labeled, cancer-targeting DNA aptamer. *Angew. Chem. Int. Ed.* 62, e202300531. doi:10.1002/anie.202300531

Burbano De Lara, S., Tran, D. D. H., Allister, A. B., Polenkowski, M., Nashan, B., Koch, M., et al. (2021). C20orf204, a hepatocellular carcinoma-specific protein interacts with nucleolin and promotes cell proliferation. *Oncogenesis* 10, 31–13. doi:10.1038/s41389-021-00320-3

Burrello, J., Monticone, S., Gai, C., Gomez, Y., Kholia, S., and Camussi, G. (2016). Stem cell-derived extracellular vesicles and immune-modulation. *Front. Cell Dev. Biol.* 4, 83. doi:10.3389/fcell.2016.00083

Camacho, A. C., Alfandari, D., Kozela, E., and Regev-Rudzki, N. (2023). Biogenesis of extracellular vesicles in protozoan parasites: the ESCRT complex in the trafficking fast lane? *PLOS Pathog.* 19, e1011140. doi:10.1371/journal.ppat.1011140

Cannarile, M. A., Weisser, M., Jacob, W., Jegg, A.-M., Ries, C. H., and Rüttinger, D. (2017). Colony-stimulating factor 1 receptor (CSF1R) inhibitors in cancer therapy. *J. Immunother. Cancer* 5, 53. doi:10.1186/s40425-017-0257-y

Cardos, A. I., Maghiar, A., Zaha, D. C., Pop, O., Fritea, L., Miere (Groza), F., et al. (2022). Evolution of diagnostic methods for *Helicobacter pylori* infections: from traditional tests to high technology, advanced sensitivity and discrimination tools. *Diagnostics* 12, 508. doi:10.3390/diagnostics12020508

Carvalho, T. M., Brasil, G. O., Jucoski, T. S., Adamoski, D., de Lima, R. S., Spautz, C. C., et al. (2022). MicroRNAs miR-142-5p, miR-150-5p, miR-320a-3p, and miR-4433b-5p in serum and tissue: potential biomarkers in sporadic breast cancer. *Front. Genet.* 13, 865472. doi:10.3389/fgene.2022.865472

Cerezo-Magaña, M., Bång-Rudenstam, A., and Belting, M. (2020). The pleiotropic role of proteoglycans in extracellular vesicle mediated communication in the tumor microenvironment. *Semin. Cancer Biol.* 62, 99–107. doi:10.1016/j.semcancer.2019.07.001

Chan, S.-H., Tsai, K.-W., Chiu, S.-Y., Kuo, W.-H., Chen, H.-Y., Jiang, S. S., et al. (2019). Identification of the novel role of CD24 as an oncogenesis regulator and therapeutic target for triple-negative breast cancer. *Mol. Cancer Ther.* 18, 147–161. doi:10.1158/1535-7163.MCT-18-0292

Chen, I. E., and Lee-Felker, S. (2023). Triple-negative breast cancer: multimodality appearance. *Curr. Radiol. Rep.* 11, 53–59. doi:10.1007/s40134-022-00410-z

Chen, L., Cai, J., Huang, Y., Tan, X., Guo, Q., Lin, X., et al. (2020). Identification of cofilin-1 as a novel mediator for the metastatic potentials and chemoresistance of the prostate cancer cells. *Eur. J. Pharmacol.* 880, 173100. doi:10.1016/j.ejphar.2020.173100

Chen, P., Wang, L., Fan, X., Ning, X., Yu, B., Ou, C., et al. (2021). Targeted delivery of extracellular vesicles in heart injury. *Theranostics* 11, 2263–2277. doi:10.7150/thno.51571

Cheng, Y., Lin, L., Li, X., Lu, A., Hou, C., Wu, Q., et al. (2021). ADAM10 is involved in the oncogenic process and chemo-resistance of triple-negative breast cancer via regulating Notch1 signaling pathway, CD44 and PrPc. *Cancer Cell Int.* 21, 32. doi:10.1186/s12935-020-01727-5

Clancy, J. W., Schmidtmann, M., and D'Souza-Schorey, C. (2021). The ins and outs of microvesicles. *FASEB BioAdvances* 3, 399–406. doi:10.1096/fba.2020-00127

Coppola, L., Baselice, S., Messina, F., Giannatiempo, R., Farina, A., Vitagliano, L., et al. (2022). KCTD15 is overexpressed in her2+ positive breast cancer patients and its silencing attenuates proliferation in SKBR3 CELL LINE. *Diagnostics* 12, 591. doi:10.3390/diagnostics12030591

Costa, R., Shah, A. N., Santa-Maria, C. A., Cruz, M. R., Mahalingam, D., Carneiro, B. A., et al. (2017). Targeting Epidermal Growth Factor Receptor in triple negative breast cancer: new discoveries and practical insights for drug development. *Cancer Treat. Rev.* 53, 111–119. doi:10.1016/j.ctrv.2016.12.010

Das, D., Chakrabarty, B., Srinivasan, R., and Roy, A. (2023a). Gex2SGen: designing drug-like molecules from desired gene expression signatures. *J. Chem. Inf. Model.* 63, 1882–1893. doi:10.1021/acs.jcim.2c01301

Das, K., Paul, S., Ghosh, A., Gupta, S., Mukherjee, T., Shankar, P., et al. (2023b). Extracellular vesicles in triple–negative breast cancer: immune regulation, biomarkers, and immunotherapeutic potential. *Cancers* 15, 4879. doi:10.3390/cancers15194879

Deepak, K. G. K., Vempati, R., Nagaraju, G. P., Dasari, V. R. S. N., Rao, D. N., and Malla, R.R. (2020). Tumor microenvironment: challenges and opportunities in targeting metastasis of triple negative breast cancer. *Pharmacol. Res.* 153, 104683. doi:10.1016/j.phrs.2020.104683

Derakhshani, A., Rezaei, Z., Safarpour, H., Sabri, M., Mir, A., Sanati, M. A., et al. (2020). Overcoming trastuzumab resistance in HER2-positive breast cancer using combination therapy. *J. Cell. Physiol.* 235, 3142–3156. doi:10.1002/jcp.29216

Dey, S., Murmu, N., Mondal, T., Saha, I., Chatterjee, S., Manna, R., et al. (2022). Multifaceted entrancing role of glucose and its analogue, 2-deoxy-D-glucose in cancer cell proliferation, inflammation, and virus infection. *Biomed. Pharmacother.* 156, 113801. doi:10.1016/j.biopha.2022.113801

Ding, L., Yang, X., Gao, Z., Effah, C. Y., Zhang, X., Wu, Y., et al. (2021). A holistic review of the state-of-the-art microfluidics for exosome separation: an overview of the current status, existing obstacles, and future outlook. *Small* 17, 2007174. doi:10.1002/smll.202007174

Dixson, A. C., Dawson, T. R., Di Vizio, D., and Weaver, A. M. (2023). Context-specific regulation of extracellular vesicle biogenesis and cargo selection. *Nat. Rev. Mol. Cell Biol.* 24, 454–476. doi:10.1038/s41580-023-00576-0

Do, H. T. T., Lee, C. H., and Cho, J. (2020). Chemokines and their receptors: multifaceted roles in cancer progression and potential value as cancer prognostic markers. *Cancers* 12, 287. doi:10.3390/cancers12020287

Dogan, B. E., and Turnbull, L. W. (2012). Imaging of triple-negative breast cancer. *Ann. Oncol.* 23, vi23–vi29. doi:10.1093/annonc/mds191

Dong, M., Liu, Q., Xu, Y., and Zhang, Q. (2022). Extracellular vesicles: the landscape in the progression, diagnosis, and treatment of triple-negative breast cancer. *Front. Cell Dev. Biol.* 10, 842898. doi:10.3389/fcell.2022.842898

Dong, X., Bai, X., Ni, J., Zhang, H., Duan, W., Graham, P., et al. (2020). Exosomes and breast cancer drug resistance. *Cell Death Dis.* 11, 987–1014. doi:10.1038/s41419-020-03189-z

Elsharkasy, O. M., Nordin, J. Z., Hagey, D. W., de Jong, O. G., Schiffelers, R. M., Andaloussi, S. E., et al. (2020). Extracellular vesicles as drug delivery systems: why and how? *Adv. Drug Deliv. Rev.* 159, 332–343. doi:10.1016/j.addr.2020.04.004

Emory, T., Hoven, N., Nelson, M., Church, A. L., Rubin, N., and Kuehn-Hajder, J. (2023). Diagnostic contrast-enhanced mammography performed immediately prior to same-day biopsy: an analysis of index lesion enhancement compared to histopathology and follow-up in patients with suspicious ultrasound findings. *J. Breast Imaging* 5, 40–47. doi:10.1093/jbi/wbac081

Frawley, T., and Piskareva, O. (2020). Extracellular vesicle dissemination of epidermal growth factor receptor and ligands and its role in cancer progression. *Cancers* 12, 3200. doi:10.3390/cancers12113200

Ganansia-Leymarie, V., Bischoff, P., Bergerat, J.-P., and Holl, V. (2003). Signal transduction pathways of taxanes-induced apoptosis. *Curr. Med. Chem. - Anti-Cancer Agents* 3, 291–306. doi:10.2174/1568011033482422

Gangadaran, P., and Ahn, B.-C. (2020). Extracellular vesicle- and extracellular vesicle mimetics-based drug delivery systems: new perspectives, challenges, and clinical developments. *Pharmaceutics* 12, 442. doi:10.3390/pharmaceutics12050442

Gao, Y., Zheng, X., Chang, B., Lin, Y., Huang, X., Wang, W., et al. (2022). Intercellular transfer of activated STING triggered by RAB22A-mediated non-canonical autophagy promotes antitumor immunity. *Cell Res.* 32, 1086–1104. doi:10.1038/s41422-022-00731-w

Gautam, P., Jaiswal, A., Aittokallio, T., Al-Ali, H., and Wennerberg, K. (2019). Phenotypic screening combined with machine learning for efficient identification of breast cancer-selective therapeutic targets. *Cell Chem. Biol.* 26, 970–979. doi:10.1016/j.chembiol.2019.03.011

Gegios, A. R., Peterson, M. S., and Fowler, A. M. (2023). Breast cancer screening and diagnosis: recent advances in imaging and current limitations. *Pet. Clin.* 18, 459–471. doi:10.1016/j.cpet.2023.04.003

Gilliam, D. T., Menon, V., Bretz, N. P., and Pruszak, J. (2017). The CD24 surface antigen in neural development and disease. *Neurobiol. Dis.* 99, 133–144. doi:10.1016/j.nbd.2016.12.011

Giovanazzi, A., van Herwijnen, M. J. C., Kleinjan, M., van der Meulen, G. N., and Wauben, M. H. M. (2023). Surface protein profiling of milk and serum extracellular vesicles unveils body fluid-specific signatures. *Sci. Rep.* 13, 8758. doi:10.1038/s41598-023-35799-w

Gong, C., Tian, J., Wang, Z., Gao, Y., Wu, X., Ding, X., et al. (2019). Functional exosome-mediated co-delivery of doxorubicin and hydrophobically modified microRNA 159 for triple-negative breast cancer therapy. *J. Nanobiotechnology* 17, 93. doi:10.1186/s12951-019-0526-7

Grimaldi, A. M., Salvatore, M., and Cavaliere, C. (2023). Diagnostic and prognostic significance of extracellular vesicles in prostate cancer drug resistance: a systematic review of the literature. *Prostate Cancer Prostatic Dis.* 26, 228–239. doi:10.1038/s41391-022-00521-w

Guo, R., Jiang, D., Gai, Y., Qian, R., Zhu, Z., Gao, Y., et al. (2023). Chlorin e6-loaded goat milk-derived extracellular vesicles for Cerenkov luminescence-induced photodynamic therapy. *Eur. J. Nucl. Med. Mol. Imaging* 50, 508–524. doi:10.1007/s00259-022-05978-4

Gupta, A., Nishchaya, K., Saha, M., Naik, G. A. R. R., Yadav, S., Srivastava, S., et al. (2024). Recent advancements in nanoconstructs for the theranostics applications for triple negative breast cancer. *J. Drug Deliv. Sci. Technol.* 93, 105401. doi:10.1016/j.jddst.2024.105401

Hahm, J., Kim, J., and Park, J. (2021). Strategies to enhance extracellular vesicle production. *Tissue Eng. Regen. Med.* 18, 513–524. doi:10.1007/s13770-021-00364-x

Han, D., Li, Z., Wang, F., Cheng, K., and Shen, D. (2024). Apoptotic extracellular vesicles: mechanisms, applications, and therapeutic potential. *Med-X* 2, 27. doi:10.1007/s44258-024-00039-x

Han, Q.-F., Li, W.-J., Hu, K.-S., Gao, J., Zhai, W.-L., Yang, J.-H., et al. (2022). Exosome biogenesis: machinery, regulation, and therapeutic implications in cancer. *Mol. Cancer* 21, 207. doi:10.1186/s12943-022-01671-0

Haney, M. J., Zhao, Y., Jin, Y. S., Li, S. M., Bago, J. R., Klyachko, N. L., et al. (2020). Macrophage-derived extracellular vesicles as drug delivery systems for triple negative breast cancer (TNBC) therapy. *J. Neuroimmune Pharmacol.* 15, 487–500. doi:10.1007/s11481-019-09884-9

Ho, J., Chaiswing, L., and St. Clair, D. K. (2022). Extracellular vesicles and cancer therapy: insights into the role of oxidative stress. *Antioxidants* 11, 1194. doi:10.3390/antiox11061194

Hobbs, E. A., Litton, J. K., and Yap, T. A. (2021). Development of the PARP inhibitor talazoparib for the treatment of advanced BRCA1 and BRCA2 mutated breast cancer. *Expert Opin. Pharmacother.* 22, 1825–1837. doi:10.1080/14656566.2021.1952181

Honore, S., Kamath, K., Braguer, D., Wilson, L., Briand, C., and Jordan, M. A. (2004). Suppression of microtubule dynamics by discodermolide by a novel mechanism is associated with mitotic arrest and inhibition of tumor cell proliferation. *Mol. Cancer Ther.* 2, 1303–1311.

Horbay, R., Hamraghani, A., Ermini, L., Holcik, S., Beug, S. T., and Yeganeh, B. (2022). Role of ceramides and lysosomes in extracellular vesicle biogenesis, cargo sorting and release. *Int. J. Mol. Sci.* 23, 15317. doi:10.3390/ijms232315317

Hoshino, A., Costa-Silva, B., Shen, T.-L., Rodrigues, G., Hashimoto, A., Tesic Mark, M., et al. (2015). Tumour exosome integrins determine organotropic metastasis. *Nature* 527, 329–335. doi:10.1038/nature15756

Hoshino, A., Kim, H. S., Bojmar, L., Gyan, K. E., Cioffi, M., Hernandez, J., et al. (2020). Extracellular vesicle and particle biomarkers define multiple human cancers. *Cell* 182, 1044–1061. doi:10.1016/j.cell.2020.07.009

Howard, F. M., and Olopade, O. I. (2021). Epidemiology of triple-negative breast cancer: a review. *Cancer J.* 27, 8–16. doi:10.1097/PPO.0000000000000500

Howard, J., Goh, C. Y., Gorzel, K. W., Higgins, M., and McCann, A. (2022). The potential role of cofilin-1 in promoting triple negative breast cancer (TNBC) metastasis via the extracellular vesicles (EVs). *Transl. Oncol.* 15, 101247. doi:10.1016/j.tranon.2021.101247

Hsu, J. L., and Hung, M.-C. (2016). The role of HER2, EGFR, and other receptor tyrosine kinases in breast cancer. *Cancer Metastasis Rev.* 35, 575–588. doi:10.1007/s10555-016-9649-6

Hu, Q., Egranov, S. D., Lin, C., and Yang, L. (2020a). Long noncoding RNA loss in immune suppression in cancer. *Pharmacol. Ther.* 213, 107591. doi:10.1016/j.pharmthera.2020.107591

Hu, S., Liu, J., Feng, S., Wang, Y., and Liu, H. (2021). LncRNA SUMO1P3 acts as a prognostic biomarker and promotes hepatocellular carcinoma growth and metastasis. *Aging* 13, 12479–12492. doi:10.18632/aging.202921

Hu, W., Song, X., Yu, H., Sun, J., and Zhao, Y. (2020b). Therapeutic potentials of extracellular vesicles for the treatment of diabetes and diabetic complications. *Int. J. Mol. Sci.* 21, 5163. doi:10.3390/ijms21145163

Hu, X., Yu, L., Bian, Y., Zeng, X., Luo, S., Wen, Q., et al. (2023). Paclitaxel-loaded tumor cell-derived microparticles improve radiotherapy efficacy in triple-negative breast cancer by enhancing cell killing and stimulating immunity. *Int. J. Pharm.* 632, 122560. doi:10.1016/j.ijpharm.2022.122560

Hudait, A., Hurley, J. H., and Voth, G. A. (2023). Dynamics of upstream ESCRT organization at the HIV-1 budding site. *Biophys. J.* 122, 2655–2674. doi:10.1016/j.bpj.2023.05.020

Hung, Y., Wang, Y.-L., Lin, Y.-Z., Chiang, S.-F., Wu, W.-R., and Wang, S.-C. (2019). The exosomal compartment protects epidermal growth factor receptor from small molecule inhibitors. *Biochem. Biophys. Res. Commun.* 510, 42–47. doi:10.1016/j.bbrc.2018.12.187

Jafari, D., Tiyuri, A., Rezaei, E., Moradi, Y., Jafari, R., Jokar Shoorijeh, F., et al. (2020). Diagnostic accuracy of cerebrospinal fluid and serum-isolated extracellular vesicles for glioblastoma: a systematic review and meta-analysis. *Expert Rev. Mol. diagn.* 20, 1075–1085. doi:10.1080/14737159.2020.1844006

Jagosky, M., and Tan, A. R. (2021). Combination of pertuzumab and trastuzumab in the treatment of HER2-positive early breast cancer: a review of the emerging clinical data. *Breast Cancer Targets Ther.* 13, 393–407. doi:10.2147/BCTT.S176514

Jarsch, I. K., Gadsby, J. R., Nuccitelli, A., Mason, J., Shimo, H., Pilloux, L., et al. (2020). A direct role for SNX9 in the biogenesis of filopodia. *J. Cell Biol.* 219, e201909178. doi:10.1083/jcb.201909178

Jin, Y., Ma, L., Zhang, W., Yang, W., Feng, Q., and Wang, H. (2022). Extracellular signals regulate the biogenesis of extracellular vesicles. *Biol. Res.* 55, 35. doi:10.1186/s40659-022-00405-2

Kadamkulam Syriac, A., Nandu, N. S., and Leone, J. P. (2023). Central nervous system metastases from triple-negative breast cancer: current treatments and future prospective. *Breast Cancer Targets Ther.* 14, 1–13. doi:10.2147/BCTT.S274514

Kalra, H., Drummen, G. P. C., and Mathivanan, S. (2016). Focus on extracellular vesicles: introducing the next small big thing. *Int. J. Mol. Sci.* 17, 170. doi:10.3390/ijms17020170

Kannan, S., and Cheng, V. W. T. (2023). Nanoparticle drug delivery to target breast cancer brain metastasis: current and future trends. *Int. J. Cancer* 153, 1118–1129. doi:10.1002/ijc.34542

Karn, V., Ahmed, S., Tsai, L.-W., Dubey, R., Ojha, S., Singh, H. N., et al. (2021). Extracellular vesicle-based therapy for COVID-19: promises, challenges and future prospects. *Biomedicines* 9, 1373. doi:10.3390/biomedicines9101373

Khosravi, N., Pishavar, E., Baradaran, B., Oroojalian, F., and Mokhtarzadeh, A. (2022). Stem cell membrane, stem cell-derived exosomes and hybrid stem cell camouflaged nanoparticles: a promising biomimetic nanoplatforms for cancer theranostics. *J. Control. Release* 348, 706–722. doi:10.1016/j.jconrel.2022.06.026

Kim, H. I., Park, J., Zhu, Y., Wang, X., Han, Y., and Zhang, D. (2024). Recent advances in extracellular vesicles for therapeutic cargo delivery. *Exp. Mol. Med.* 56, 836–849. doi:10.1038/s12276-024-01201-6

Kong, Q., Tang, W., Chen, S., Hu, W., Hu, Y., Liang, Y., et al. (2022). Nomogram for the prediction of triple-negative breast cancer histological heterogeneity based on multiparameter MRI features: a preliminary study including metaplastic carcinoma and non-metaplastic carcinoma. *Front. Oncol.* 12, 916988. doi:10.3389/fonc.2022.916988

Kooijmans, S. A. A., Schiffelers, R. M., Zarovni, N., and Vago, R. (2016). Modulation of tissue tropism and biological activity of exosomes and other extracellular vesicles: new nanotools for cancer treatment. *Pharmacol. Res.* 111, 487–500. doi:10.1016/j.phrs.2016.07.006

Kuemmel, S., Campone, M., Loirat, D., Lopez, R. L., Beck, J. T., De Laurentiis, M., et al. (2022). A randomized phase II study of anti-CSF1 monoclonal antibody lacnotuzumab (MCS110) combined with gemcitabine and carboplatin in advanced triple-negative breast cancer. *Clin. Cancer Res.* 28, 106–115. doi:10.1158/1078-0432.CCR-20-3955

Kulaberoglu, Y., Hergovich, A., and Gómez, V. (2021). "Chapter 15 - the role of p53/p21/p16 in DNA damage signaling and DNA repair," in *Genome stability*. Second Edition, ed. I. Kovalchuk, and O. Kovalchuk (Boston: Academic Press), 257–274. doi:10.1016/B978-0-323-85679-9.00015-5

Lampropoulou, D. I., Pliakou, E., Aravantinos, G., Filippou, D., and Gazouli, M. (2022). The role of exosomal non-coding RNAs in colorectal cancer drug resistance. *Int. J. Mol. Sci.* 23, 1473. doi:10.3390/ijms23031473

Lan, F., Zhang, X., Li, H., Yue, X., and Sun, Q. (2021). Serum exosomal lncRNA XIST is a potential non-invasive biomarker to diagnose recurrence of triple-negative breast cancer. *J. Cell. Mol. Med.* 25, 7602–7607. doi:10.1111/jcmm.16009

Lee, H. J., Seo, A. N., Kim, E. J., Jang, M. H., Kim, Y. J., Kim, J. H., et al. (2015). Prognostic and predictive values of EGFR overexpression and EGFR copy number alteration in HER2-positive breast cancer. *Br. J. Cancer* 112, 103–111. doi:10.1038/bjc.2014.556

Leithner, D., Mayerhoefer, M. E., Martinez, D. F., Jochelson, M. S., Morris, E. A., Thakur, S. B., et al. (2020). Non-invasive assessment of breast cancer molecular subtypes with multiparametric magnetic resonance imaging radiomics. *J. Clin. Med.* 9, 1853. doi:10.3390/jcm9061853

Leon-Ferre, R. A., Jonas, S. F., Salgado, R., Loi, S., de Jong, V., Carter, J. M., et al. (2024). Tumor-infiltrating lymphocytes in triple-negative breast cancer. *JAMA* 331, 1135–1144. doi:10.1001/jama.2024.3056

Li, C., and Xu, X. (2019). Biological functions and clinical applications of exosomal non-coding RNAs in hepatocellular carcinoma. *Cell. Mol. Life Sci.* 76, 4203–4219. doi:10.1007/s00018-019-03215-0

Li, S., Li, Q., Lü, J., Zhao, Q., Li, D., Shen, L., et al. (2020). Targeted inhibition of miR-221/222 promotes cell sensitivity to cisplatin in triple-negative breast cancer MDA-MB-231 cells. *Front. Genet.* 10, 1278. doi:10.3389/fgene.2019.01278

Li, S., Zhang, N., Zhang, H., Zhou, R., Li, Z., Yang, X., et al. (2023). Artificial intelligence learning landscape of triple-negative breast cancer uncovers new opportunities for enhancing outcomes and immunotherapy responses. *J. Big Data* 10, 132. doi:10.1186/s40537-023-00809-1

Li, T., Tao, Z., Zhu, Y., Liu, X., Wang, L., Du, Y., et al. (2021). Exosomal annexin A6 induces gemcitabine resistance by inhibiting ubiquitination and degradation of EGFR in triple-negative breast cancer. *Cell Death Dis.* 12, 684–713. doi:10.1038/s41419-021-03963-7

Li, Y., Liang, Y., Sang, Y., Song, X., Zhang, H., Liu, Y., et al. (2018). MiR-770 suppresses the chemo-resistance and metastasis of triple negative breast cancer via direct targeting of STMN1. *Cell Death Dis.* 9, 14–12. doi:10.1038/s41419-017-0030-7

Liao, J., Gui, Y., Li, Z., Deng, Z., Han, X., Tian, H., et al. (2023). Artificial intelligence-assisted ultrasound image analysis to discriminate early breast cancer in Chinese population: a retrospective, multicentre, cohort study. *eClinicalMedicine* 60, 102001. doi:10.1016/j.eclinm.2023.102001

Lim, P. K., Bliss, S. A., Patel, S. A., Taborga, M., Dave, M. A., Gregory, L. A., et al. (2011). Gap junction–mediated import of MicroRNA from bone marrow stromal cells can elicit cell cycle quiescence in breast cancer cells. *Cancer Res.* 71, 1550–1560. doi:10.1158/0008-5472.CAN-10-2372

Liu, J., Luo, R., Wang, J., Luan, X., Wu, D., Chen, H., et al. (2021a). Tumor cell-derived exosomal miR-770 inhibits M2 macrophage polarization via targeting MAP3K1 to inhibit the invasion of non-small cell lung cancer cells. *Front. Cell Dev. Biol.* 9, 679658. doi:10.3389/fcell.2021.679658

Liu, J., Wu, S., Zheng, X., Zheng, P., Fu, Y., Wu, C., et al. (2020). Immune suppressed tumor microenvironment by exosomes derived from gastric cancer cells via modulating immune functions. *Sci. Rep.* 10, 14749. doi:10.1038/s41598-020-71573-y

Liu, S., Cong, Y., Wang, D., Sun, Y., Deng, L., Liu, Y., et al. (2014). Breast cancer stem cells transition between epithelial and mesenchymal states reflective of their normal counterparts. *Stem Cell Rep.* 2, 78–91. doi:10.1016/j.stemcr.2013.11.009

Liu, T., Hooda, J., Atkinson, J. M., Whiteside, T. L., Oesterreich, S., and Lee, A. V. (2021b). Exosomes in breast cancer – mechanisms of action and clinical potential. *Mol. Cancer Res.* 19, 935–945. doi:10.1158/1541-7786.MCR-20-0952

Liu, Y.-J., and Wang, C. (2023). A review of the regulatory mechanisms of extracellular vesicles-mediated intercellular communication. *Cell Commun. Signal.* 21, 77. doi:10.1186/s12964-023-01103-6

Lizarraga-Valderrama, L. R., and Sheridan, G. K. (2021). Extracellular vesicles and intercellular communication in the central nervous system. *FEBS Lett.* 595, 1391–1410. doi:10.1002/1873-3468.14074

Loizides, S., and Constantinidou, A. (2023). Triple negative breast cancer: immunogenicity, tumor microenvironment, and immunotherapy. *Front. Genet.* 13, 1095839. doi:10.3389/fgene.2022.1095839

Lou, G., Chen, L., Xia, C., Wang, W., Qi, J., Li, A., et al. (2020). MiR-199a-modified exosomes from adipose tissue-derived mesenchymal stem cells improve hepatocellular carcinoma chemosensitivity through mTOR pathway. *J. Exp. Clin. Cancer Res.* 39, 4. doi:10.1186/s13046-019-1512-5

Lu, B., Natarajan, E., Balaji Raghavendran, H. R., and Markandan, U. D. (2023). Molecular classification, treatment, and genetic biomarkers in triple-negative breast cancer: a review. *Technol. Cancer Res. Treat.* 22, 15330338221145246. doi:10.1177/15330338221145246

Lu, M., Qin, X., Zhou, Y., Li, G., Liu, Z., Geng, X., et al. (2021). Long non-coding RNA LINC00665 promotes gemcitabine resistance of Cholangiocarcinoma cells via regulating EMT and stemness properties through miR-424-5p/BCL9L axis. *Cell Death Dis.* 12, 72–17. doi:10.1038/s41419-020-03346-4

Lu, S. M., and Fairn, G. D. (2018). Mesoscale organization of domains in the plasma membrane – beyond the lipid raft. *Crit. Rev. Biochem. Mol. Biol.* 53, 192–207. doi:10.1080/10409238.2018.1436515

Luo, Z., Lu, L., Xu, W., Meng, N., Wu, S., Zhou, J., et al. (2022). *In vivo* self-assembled drug nanocrystals for metastatic breast cancer all-stage targeted therapy. *J. Control. Release* 346, 32–42. doi:10.1016/j.jconrel.2022.03.058

Ma, M., Liu, R., Wen, C., Xu, W., Xu, Z., Wang, S., et al. (2022). Predicting the molecular subtype of breast cancer and identifying interpretable imaging features using machine learning algorithms. *Eur. Radiol.* 32, 1652–1662. doi:10.1007/s00330-021-08271-4

Maleki, S., Jabalee, J., and Garnis, C. (2021). The role of extracellular vesicles in mediating resistance to anticancer therapies. *Int. J. Mol. Sci.* 22, 4166. doi:10.3390/ijms22084166

Mao, X., Xu, J., Wang, W., Liang, C., Hua, J., Liu, J., et al. (2021). Crosstalk between cancer-associated fibroblasts and immune cells in the tumor microenvironment: new findings and future perspectives. *Mol. Cancer* 20, 131. doi:10.1186/s12943-021-01428-1

Maqbool, M., Bekele, F., and Fekadu, G. (2022). Treatment strategies against triple-negative breast cancer: an updated review. *Breast Cancer Targets Ther.* 14, 15–24. doi:10.2147/BCTT.S348060

Martinez, V. G., O'Neill, S., Salimu, J., Breslin, S., Clayton, A., Crown, J., et al. (2017). Resistance to HER2-targeted anti-cancer drugs is associated with immune evasion in cancer cells and their derived extracellular vesicles. *OncoImmunology* 6, e1362530. doi:10.1080/2162402X.2017.1362530

Mashouri, L., Yousefi, H., Aref, A. R., Ahadi, A. M., Molaei, F., and Alahari, S. K. (2019). Exosomes: composition, biogenesis, and mechanisms in cancer metastasis and drug resistance. *Mol. Cancer* 18, 75. doi:10.1186/s12943-019-0991-5

Mateescu, B., Kowal, E. J. K., van Balkom, B. W. M., Bartel, S., Bhattacharyya, S. N., Buzás, E. I., et al. (2017). Obstacles and opportunities in the functional analysis of extracellular vesicle RNA – an ISEV position paper. *J. Extracell. Vesicles* 6, 1286095. doi:10.1080/20013078.2017.1286095

Mathieu, M., Martin-Jaular, L., Lavieu, G., and Théry, C. (2019). Specificities of secretion and uptake of exosomes and other extracellular vesicles for cell-to-cell communication. *Nat. Cell Biol.* 21, 9–17. doi:10.1038/s41556-018-0250-9

Matsumoto, A., Takahashi, Y., Nishikawa, M., Sano, K., Morishita, M., Charoenviriyakul, C., et al. (2017). Role of phosphatidylserine-derived negative surface charges in the recognition and uptake of intravenously injected B16BL6-derived exosomes by macrophages. *J. Pharm. Sci.* 106, 168–175. doi:10.1016/j.xphs.2016.07.022

Matthews, A. L., Noy, P. J., Reyat, J. S., and Tomlinson, M. G. (2017). Regulation of A disintegrin and metalloproteinase (ADAM) family sheddases ADAM10 and ADAM17: the emerging role of tetraspanins and rhomboids. *Platelets* 28, 333–341. doi:10.1080/09537104.2016.1184751

Mehanny, M., Lehr, C.-M., and Fuhrmann, G. (2021). Extracellular vesicles as antigen carriers for novel vaccination avenues. *Adv. Drug Deliv. Rev.* 173, 164–180. doi:10.1016/j.addr.2021.03.016

Menck, K., Sivaloganathan, S., Bleckmann, A., and Binder, C. (2020). Microvesicles in cancer: small size, large potential. *Int. J. Mol. Sci.* 21, 5373. doi:10.3390/ijms21155373

Meng, W., He, C., Hao, Y., Wang, L., Li, L., and Zhu, G. (2020). Prospects and challenges of extracellular vesicle-based drug delivery system: considering cell source. *Drug Deliv.* 27, 585–598. doi:10.1080/10717544.2020.1748758

Mgrditchian, T., Arakelian, T., Paggetti, J., Noman, M. Z., Viry, E., Moussay, E., et al. (2017). Targeting autophagy inhibits melanoma growth by enhancing NK cells infiltration in a CCL5-dependent manner. *Proc. Natl. Acad. Sci.* 114, E9271-E9279–E9279. doi:10.1073/pnas.1703921114

Mirzaei, H., Rahimian, N., Mirzaei, H. R., Nahand, J. S., and Hamblin, M. R. (2022). "Exosomes," in *Exosomes and microRNAs in biomedical science*. Editors H. Mirzaei, N. Rahimian, H. R. Mirzaei, J. S. Nahand, and M. R. Hamblin (Cham: Springer International Publishing), 79–92. doi:10.1007/978-3-031-79177-2_5

Mishra, A., Bharti, P. S., Rani, N., Nikolajeff, F., and Kumar, S. (2023). A tale of exosomes and their implication in cancer. *Biochim. Biophys. Acta BBA - Rev. Cancer* 1878, 188908. doi:10.1016/j.bbcan.2023.188908

Mittendorf, E. A., Philips, A. V., Meric-Bernstam, F., Qiao, N., Wu, Y., Harrington, S., et al. (2014). PD-L1 expression in triple-negative breast cancer. *Cancer Immunol. Res.* 2, 361–370. doi:10.1158/2326-6066.CIR-13-0127

Monguió-Tortajada, M., Gálvez-Montón, C., Bayes-Genis, A., Roura, S., and Borràs, F. E. (2019). Extracellular vesicle isolation methods: rising impact of size-exclusion chromatography. *Cell. Mol. Life Sci.* 76, 2369–2382. doi:10.1007/s00018-019-03071-y

Munoz, J. L., Bliss, S. A., Greco, S. J., Ramkissoon, S. H., Ligon, K. L., and Rameshwar, P. (2013). Delivery of functional anti-miR-9 by mesenchymal stem cell–derived exosomes to glioblastoma multiforme cells conferred chemosensitivity. *Mol. Ther. Nucleic Acids* 2, e126. doi:10.1038/mtna.2013.60

Muñoz-Garcia, J., Cochonneau, D., Télétchéa, S., Moranton, E., Lanoe, D., Brion, R., et al. (2021). The twin cytokines interleukin-34 and CSF-1: masterful conductors of macrophage homeostasis. *Theranostics* 11, 1568–1593. doi:10.7150/thno.50683

Murphy, D. E., de Jong, O. G., Brouwer, M., Wood, M. J., Lavieu, G., Schiffelers, R. M., et al. (2019). Extracellular vesicle-based therapeutics: natural versus engineered targeting and trafficking. *Exp. Mol. Med.* 51, 1–12. doi:10.1038/s12276-019-0223-5

Nagao, K., Maeda, K., Hosomi, K., Morioka, K., Inuzuka, T., and Ohtsubo, K. (2022). Sialyl-Tn antigen facilitates extracellular vesicle-mediated transfer of FAK and enhances motility of recipient cells. *J. Biochem. (Tokyo)* 171, 543–554. doi:10.1093/jb/mvac008

Negahdaripour, M., Owji, H., Eskandari, S., Zamani, M., Vakili, B., and Nezafat, N. (2021). Small extracellular vesicles (sEVs): discovery, functions, applications, detection methods and various engineered forms. *Expert Opin. Biol. Ther.* 21, 371–394. doi:10.1080/14712598.2021.1825677

Nguyen Cao, T. G., Truong Hoang, Q., Hong, E. J., Kang, S. J., Kang, J. H., Ravichandran, V., et al. (2023). Mitochondria-targeting sonosensitizer-loaded extracellular vesicles for chemo-sonodynamic therapy. *J. Control. Release* 354, 651–663. doi:10.1016/j.jconrel.2023.01.044

Noreen, S., Gardner, Q. A., Fatima, I., Sadaf, S., and Akhtar, M. W. (2020). Upregulated expression of calcium-dependent annexin A6: a potential biomarker of ovarian carcinoma. *PROTEOMICS – Clin. Appl.* 14, 1900078. doi:10.1002/prca.201900078

O'Brien, K., Lowry, M. C., Corcoran, C., Martinez, V. G., Daly, M., Rani, S., et al. (2015). miR-134 in extracellular vesicles reduces triple-negative breast cancer aggression and increases drug sensitivity. *Oncotarget* 6, 32774–32789. doi:10.18632/oncotarget.5192

Ormond Filho, A. G., Carneiro, B. C., Pastore, D., Silva, I. P., Yamashita, S. R., Consolo, F. D., et al. (2019). Whole-body imaging of multiple myeloma: diagnostic criteria. *RadioGraphics* 39, 1077–1097. doi:10.1148/rg.2019180096

Otranto, M., Sarrazy, V., Bonté, F., Hinz, B., Gabbiani, G., and Desmouliere, A. (2012). The role of the myofibroblast in tumor stroma remodeling. *Cell Adhes. Migr.* 6, 203–219. doi:10.4161/cam.20377

Ozawa, P. M. M., Alkhilaiwi, F., Cavalli, I. J., Malheiros, D., de Souza Fonseca Ribeiro, E. M., and Cavalli, L. R. (2018). Extracellular vesicles from triple-negative breast cancer cells promote proliferation and drug resistance in non-tumorigenic breast cells. *Breast Cancer Res. Treat.* 172, 713–723. doi:10.1007/s10549-018-4925-5

Ozawa, P. M. M., Vieira, E., Lemos, D. S., Souza, I. L. M., Zanata, S. M., Pankievicz, V. C., et al. (2020). Identification of miRNAs enriched in extracellular vesicles derived from serum samples of breast cancer patients. *Biomolecules* 10, 150. doi:10.3390/biom10010150

Pandy, J. G. P., Balolong-Garcia, J. C., Cruz-Ordinario, M. V. B., and Que, F. V. F. (2019). Triple negative breast cancer and platinum-based systemic treatment: a meta-analysis and systematic review. *BMC Cancer* 19, 1065. doi:10.1186/s12885-019-6253-5

Pavlakis, E., Neumann, M., and Stiewe, T. (2020). Extracellular vesicles: messengers of p53 in tumor–stroma communication and cancer metastasis. *Int. J. Mol. Sci.* 21, 9648. doi:10.3390/ijms21249648

Peswani Sajnani, S. L., Zhang, Y., and Vllasaliu, D. (2021). Exosome-based therapies for mucosal delivery. *Int. J. Pharm.* 608, 121087. doi:10.1016/j.ijpharm.2021.121087

Phan, T. K., Ozkocak, D. C., and Poon, I. K. H. (2020). Unleashing the therapeutic potential of apoptotic bodies. *Biochem. Soc. Trans.* 48, 2079–2088. doi:10.1042/BST20200225

Ponti, G., De Angelis, C., Ponti, R., Pongetti, L., Losi, L., Sticchi, A., et al. (2023). Hereditary breast and ovarian cancer: from genes to molecular targeted therapies. *Crit. Rev. Clin. Lab. Sci.* 0, 640–650. doi:10.1080/10408363.2023.2234488

Quinn, Z., Mao, W., Xia, Y., John, R., and Wan, Y. (2021). Conferring receptors on recipient cells with extracellular vesicles for targeted drug delivery. *Bioact. Mater.* 6, 749–756. doi:10.1016/j.bioactmat.2020.09.016

Rana, S., Yue, S., Stadel, D., and Zöller, M. (2012). Toward tailored exosomes: the exosomal tetraspanin web contributes to target cell selection. *Int. J. Biochem. Cell Biol.* 44, 1574–1584. doi:10.1016/j.biocel.2012.06.018

Rani, S., Lai, A., Nair, S., Sharma, S., Handberg, A., Carrion, F., et al. (2023). Extracellular vesicles as mediators of cell-cell communication in ovarian cancer and beyond – a lipids focus. *Cytokine Growth Factor Rev.* 73, 52–68. doi:10.1016/j.cytogfr.2023.06.004

Rathore, M., Girard, C., Ohanna, M., Tichet, M., Ben Jouira, R., Garcia, E., et al. (2019). Cancer cell-derived long pentraxin 3 (PTX3) promotes melanoma migration through a toll-like receptor 4 (TLR4)/NF-κB signaling pathway. *Oncogene* 38, 5873–5889. doi:10.1038/s41388-019-0848-9

Ribeiro, R., Carvalho, M. J., Goncalves, J., and Moreira, J. N. (2022). Immunotherapy in triple-negative breast cancer: insights into tumor immune landscape and therapeutic opportunities. *Front. Mol. Biosci.* 9, 903065. doi:10.3389/fmolb.2022.903065

Rodríguez Bautista, R., Ortega Gómez, A., Hidalgo Miranda, A., Zentella Dehesa, A., Villarreal-Garza, C., Ávila-Moreno, F., et al. (2018). Long non-coding RNAs: implications in targeted diagnoses, prognosis, and improved therapeutic strategies in human non- and triple-negative breast cancer. *Clin. Epigenetics* 10, 88. doi:10.1186/s13148-018-0514-z

Roostee, S., Ehinger, D., Jönsson, M., Staaf, J., and Aine, M. (2023). Automated image quantification of immunohistochemistry-stained immune cells in triple-negative breast cancer. *Review*. doi:10.21203/rs.3.rs-3138809/v1

Ross, B. D., and Chenevert, T. L. (2021). "Chapter 57 - cancer detection and quantification of treatment response using diffusion-weighted MRI," in *Molecular imaging*. Second Edition. ed B. D. Ross, and S. S. Gambhir (Academic Press), 1091–1116. doi:10.1016/B978-0-12-816386-3.00068-5

Rupaimoole, R., and Slack, F. J. (2017). MicroRNA therapeutics: towards a new era for the management of cancer and other diseases. *Nat. Rev. Drug Discov.* 16, 203–222. doi:10.1038/nrd.2016.246

Russell, A. E., Sneider, A., Witwer, K. W., Bergese, P., Bhattacharyya, S. N., Cocks, A., et al. (2019). Biological membranes in EV biogenesis, stability, uptake, and cargo transfer: an ISEV position paper arising from the ISEV membranes and EVs workshop. *J. Extracell. Vesicles* 8, 1684862. doi:10.1080/20013078.2019.1684862

Sabbah, D., Hajjo, R., and Sweidan, K. (2020). Review on epidermal growth factor receptor (EGFR) structure, signaling pathways, interactions, and recent updates of EGFR inhibitors. *Curr. Top. Med. Chem.* 20, 815–834. doi:10.2174/1568026620666200303123102

Sabit, H., Cevik, E., Tombuloglu, H., Abdel-Ghany, S., Tombuloglu, G., and Esteller, M. (2021). Triple negative breast cancer in the era of miRNA. *Crit. Rev. Oncol. Hematol.* 157, 103196. doi:10.1016/j.critrevonc.2020.103196

Saleh, L., Wilson, C., and Holen, I. (2021). CDK4/6 inhibitors: a potential therapeutic approach for triple negative breast cancer. *MedComm* 2, 514–530. doi:10.1002/mco2.97

Santavanond, J. P., Rutter, S. F., Atkin-Smith, G. K., and Poon, I. K. H. (2021). "Apoptotic bodies: mechanism of formation, isolation and functional relevance," in *New frontiers: extracellular vesicles*. Editors S. Mathivanan, P. Fonseka, C. Nedeva, and I. Atukorala (Cham: Springer International Publishing), 61–88. doi:10.1007/978-3-030-67171-6_4

Sebbagh, M., Renvoizé, C., Hamelin, J., Riché, N., Bertoglio, J., and Bréard, J. (2001). Caspase-3-mediated cleavage of ROCK I induces MLC phosphorylation and apoptotic membrane blebbing. *Nat. Cell Biol.* 3, 346–352. doi:10.1038/35070019

Serrano-Pertierra, E., Oliveira-Rodríguez, M., Matos, M., Gutiérrez, G., Moyano, A., Salvador, M., et al. (2020). Extracellular vesicles: current analytical techniques for detection and quantification. *Biomolecules* 10, 824. doi:10.3390/biom10060824

Sha, Y. S., and Chen, J. F. (2022). MRI-based radiomics for the diagnosis of triple-negative breast cancer: a meta-analysis. *Clin. Radiol.* 77, 655–663. doi:10.1016/j.crad.2022.04.015

Shen, S., Wang, Y., Zhang, Y., Dong, Z., and Xing, J. (2021). Long non-coding RNA small nucleolar RNA host gene 14, a promising biomarker and therapeutic target in malignancy. *Front. Cell Dev. Biol.* 9, 746714. doi:10.3389/fcell.2021.746714

Shimoda, M., Ohtsuka, T., Okada, Y., and Kanai, Y. (2021). Stromal metalloproteinases: crucial contributors to the tumor microenvironment. *Pathol. Int.* 71, 1–14. doi:10.1111/pin.13033

Shiravi, F., Mohammadi, M., Golsaz-Shirazi, F., Bahadori, T., Judaki, M. A., Fatemi, F., et al. (2021). Potent synergistic anti-tumor activity of a novel humanized anti-HER2 antibody hersintuzumab in combination with trastuzumab in xenograft models. *Invest. New Drugs* 39, 697–704. doi:10.1007/s10637-020-01048-4

Shirmohamadi, M., Eghbali, E., Najjary, S., Mokhtarzadeh, A., Kojabad, A. B., Hajiasgharzadeh, K., et al. (2020). Regulatory mechanisms of microRNAs in colorectal cancer and colorectal cancer stem cells. *J. Cell. Physiol.* 235, 776–789. doi:10.1002/jcp.29042

Shojaei, S., Hashemi, S. M., Ghanbarian, H., Sharifi, K., Salehi, M., and Mohammadi-Yeganeh, S. (2021). Delivery of miR-381-3p mimic by mesenchymal stem cell-derived exosomes inhibits triple negative breast cancer aggressiveness; an *in vitro* study. *Stem Cell Rev. Rep.* 17, 1027–1038. doi:10.1007/s12015-020-10089-4

Simmons, C., Rayson, D., Joy, A. A., Henning, J.-W., Lemieux, J., McArthur, H., et al. (2022). Current and future landscape of targeted therapy in HER2-positive advanced breast cancer: redrawing the lines. *Ther. Adv. Med. Oncol.* 14, 17588359211066677. doi:10.1177/17588359211066677

Simonetti, B., Daly, J. L., and Cullen, P. J. (2023). Out of the ESCPE room: emerging roles of endosomal SNX-BARs in receptor transport and host–pathogen interaction. *Traffic* 24, 234–250. doi:10.1111/tra.12885

Singh, D., Assaraf, Y. G., and Gacche, R. N. (2022). Long non-coding RNA mediated drug resistance in breast cancer. *Drug Resist. Updat.* 63, 100851. doi:10.1016/j.drup.2022.100851

Song, J., Song, B., Yuan, L., and Yang, G. (2022). Multiplexed strategies toward clinical translation of extracellular vesicles. *Theranostics* 12, 6740–6761. doi:10.7150/thno.75899

Sousa-Squiavinato, A. C. M., Rocha, M. R., Barcellos-de-Souza, P., de Souza, W. F., and Morgado-Diaz, J. A. (2019). Cofilin-1 signaling mediates epithelial-mesenchymal transition by promoting actin cytoskeleton reorganization and cell-cell adhesion regulation in colorectal cancer cells. *Biochim. Biophys. Acta BBA - Mol. Cell Res.* 1866, 418–429. doi:10.1016/j.bbamcr.2018.10.003

Ståhl, A., Johansson, K., Mossberg, M., Kahn, R., and Karpman, D. (2019). Exosomes and microvesicles in normal physiology, pathophysiology, and renal diseases. *Pediatr. Nephrol. Berl. Ger.* 34, 11–30. doi:10.1007/s00467-017-3816-z

St-Denis-Bissonnette, F., Khoury, R., Mediratta, K., El-Sahli, S., Wang, L., and Lavoie, J. R. (2022). Applications of extracellular vesicles in triple-negative breast cancer. *Cancers* 14, 451. doi:10.3390/cancers14020451

Stevic, I., Müller, V., Weber, K., Fasching, P. A., Karn, T., Marmé, F., et al. (2018). Specific microRNA signatures in exosomes of triple-negative and HER2-positive breast cancer patients undergoing neoadjuvant therapy within the GeparSixto trial. *BMC Med.* 16, 179. doi:10.1186/s12916-018-1163-y

Sung, D. K., Sung, S. I., Ahn, S. Y., Chang, Y. S., and Park, W. S. (2019). Thrombin preconditioning boosts biogenesis of extracellular vesicles from mesenchymal stem cells and enriches their cargo contents via protease-activated receptor-mediated signaling pathways. *Int. J. Mol. Sci.* 20, 2899. doi:10.3390/ijms20122899

Tahtamouni, L., Alzghoul, A., Alderfer, S., Sun, J., Ahram, M., Prasad, A., et al. (2022). The role of activated androgen receptor in cofilin phospho-regulation depends on the molecular subtype of TNBC cell line and actin assembly dynamics. *PLOS One* 17, e0279746. doi:10.1371/journal.pone.0279746

Tai, Y.-L., Chen, K.-C., Hsieh, J.-T., and Shen, T.-L. (2018). Exosomes in cancer development and clinical applications. *Cancer Sci.* 109, 2364–2374. doi:10.1111/cas.13697

Tan, C., Hu, W., He, Y., Zhang, Y., Zhang, G., Xu, Y., et al. (2018). Cytokine-mediated therapeutic resistance in breast cancer. *Cytokine* 108, 151–159. doi:10.1016/j.cyto.2018.03.020

Taourel, P., Pages, E., Millet, I., Bourgier, C., Rouanet, P., Jacot, W., et al. (2018). Magnetic resonance imaging in breast cancer management in the context of neo-adjuvant chemotherapy. *Crit. Rev. Oncol. Hematol.* 132, 51–65. doi:10.1016/j.critrevonc.2018.09.012

Taylor, D. D., and Shah, S. (2015). Methods of isolating extracellular vesicles impact down-stream analyses of their cargoes. *Methods* 87, 3–10. doi:10.1016/j.ymeth.2015.02.019

Tchounwou, P. B., Dasari, S., Noubissi, F. K., Ray, P., and Kumar, S. (2021). Advances in our understanding of the molecular mechanisms of action of cisplatin in cancer therapy. *J. Exp. Pharmacol.* 13, 303–328. doi:10.2147/JEP.S267383

Tian, J.-W., Zhang, H.-J., Li, S.-Y., Guo, Y.-L., Chen, G., and Yu, Z.-L. (2023). Tumor cell-derived extracellular vesicles in modulating phenotypes and immune functions of macrophages: mechanisms and therapeutic applications. *J. Cancer* 14, 1321–1334. doi:10.7150/jca.84632

Tiwari, P. K., Ko, T.-H., Dubey, R., Chouhan, M., Tsai, L.-W., Singh, H. N., et al. (2023). CRISPR/Cas9 as a therapeutic tool for triple negative breast cancer: from bench to clinics. *Front. Mol. Biosci.* 10, 1214489. doi:10.3389/fmolb.2023.1214489

Tiwari, P. K., Shanmugam, P., Karn, V., Gupta, S., Mishra, R., Rustagi, S., et al. (2024). Extracellular vesicular miRNA in pancreatic cancer: from lab to therapy. *Cancers* 16, 2179. doi:10.3390/cancers16122179

Tiwari, S., Kumar, V., Randhawa, S., and Verma, S. K. (2021). Preparation and characterization of extracellular vesicles. *Am. J. Reprod. Immunol.* 85, e13367. doi:10.1111/aji.13367

Tran, T. T. D., and Tran, P. H. L. (2020). Lead compounds in the context of extracellular vesicle research. *Pharmaceutics* 12, 716. doi:10.3390/pharmaceutics12080716

Tseng, C.-C., Piper, R. C., and Katzmann, D. J. (2022). Bro1 family proteins harmonize cargo sorting with vesicle formation. *BioEssays* 44, 2100276. doi:10.1002/bies.202100276

Tsou, L. K., Yeh, S.-H., Ueng, S.-H., Chang, C.-P., Song, J.-S., Wu, M.-H., et al. (2020). Comparative study between deep learning and QSAR classifications for TNBC inhibitors and novel GPCR agonist discovery. *Sci. Rep.* 10, 16771. doi:10.1038/s41598-020-73681-1

Twelves, C., Jove, M., Gombos, A., and Awada, A. (2016). Cytotoxic chemotherapy: still the mainstay of clinical practice for all subtypes metastatic breast cancer. *Crit. Rev. Oncol. Hematol.* 100, 74–87. doi:10.1016/j.critrevonc.2016.01.021

Ullah, M., Kodam, S. P., Mu, Q., and Akbar, A. (2021). Microbubbles versus extracellular vesicles as therapeutic cargo for targeting drug delivery. *ACS Nano* 15, 3612–3620. doi:10.1021/acsnano.0c10689

van der Koog, L., Gandek, T. B., and Nagelkerke, A. (2022). Liposomes and extracellular vesicles as drug delivery systems: a comparison of composition, pharmacokinetics, and functionalization. *Adv. Healthc. Mater.* 11, 2100639. doi:10.1002/adhm.202100639

van der Meel, R., Fens, M. H. A. M., Vader, P., van Solinge, W. W., Eniola-Adefeso, O., and Schiffelers, R. M. (2014). Extracellular vesicles as drug delivery systems: lessons from the liposome field. *J. Control. Release* 195, 72–85. doi:10.1016/j.jconrel.2014.07.049

van Niel, G., Carter, D. R. F., Clayton, A., Lambert, D. W., Raposo, G., and Vader, P. (2022). Challenges and directions in studying cell–cell communication by extracellular vesicles. *Nat. Rev. Mol. Cell Biol.* 23, 369–382. doi:10.1038/s41580-022-00460-3

Viale, G. (2012). The current state of breast cancer classification. *Ann. Oncol.* 23, x207–x210. doi:10.1093/annonc/mds326

Wang, B., Zhang, Y., Ye, M., Wu, J., Ma, L., and Chen, H. (2019a). Cisplatin-resistant MDA-MB-231 cell-derived exosomes increase the resistance of recipient cells in an exosomal miR-423-5p-dependent manner. *Curr. Drug Metab.* 20, 804–814. doi:10.2174/1389200220666190819151946

Wang, F., and Wang, H. (2023). Diagnostic value of ultrasound elastography in triple negative breast cancer: a meta-analysis. *Med. (Baltimore)* 102, e32879. doi:10.1097/MD.0000000000032879

Wang, J., Bonacquisti, E. E., Brown, A. D., and Nguyen, J. (2020). Boosting the biogenesis and secretion of mesenchymal stem cell-derived exosomes. *Cells* 9, 660. doi:10.3390/cells9030660

Wang, J., Koo, K. M., and Trau, M. (2022). Tetraplex immunophenotyping of cell surface proteomes via synthesized plasmonic nanotags and portable Raman spectroscopy. *Anal. Chem.* 94, 14906–14916. doi:10.1021/acs.analchem.2c02262

Wang, J., Koo, K. M., Wang, Y., and Trau, M. (2019b). Engineering state-of-the-art plasmonic nanomaterials for SERS-based clinical liquid biopsy applications. *Adv. Sci.* 6, 1900730. doi:10.1002/advs.201900730

Wang, Y., Chen, X., Tian, B., Liu, J., Yang, L., Zeng, L., et al. (2017). Nucleolin-targeted extracellular vesicles as a versatile platform for biologics delivery to breast cancer. *Theranostics* 7, 1360–1372. doi:10.7150/thno.16532

Weber, R., Groth, C., Lasser, S., Arkhypov, I., Petrova, V., Altevogt, P., et al. (2021). IL-6 as a major regulator of MDSC activity and possible target for cancer immunotherapy. *Cell. Immunol.* 359, 104254. doi:10.1016/j.cellimm.2020.104254

Wei, D., Zhan, W., Gao, Y., Huang, L., Gong, R., Wang, W., et al. (2021). RAB31 marks and controls an ESCRT-independent exosome pathway. *Cell Res.* 31, 157–177. doi:10.1038/s41422-020-00409-1

Wen, J., Creaven, D., Luan, X., and Wang, J. (2023). Comparison of immunotherapy mediated by apoptotic bodies, microvesicles and exosomes: apoptotic bodies' unique anti-inflammatory potential. *J. Transl. Med.* 21, 478. doi:10.1186/s12967-023-04342-w

Wills, C. A., Liu, X., Chen, L., Zhao, Y., Dower, C. M., Sundstrom, J., et al. (2021). Chemotherapy-induced upregulation of small extracellular vesicle-associated PTX3 accelerates breast cancer metastasis. *Cancer Res.* 81, 452–463. doi:10.1158/0008-5472.CAN-20-1976

Wong, D. J., Gandomkar, Z., Lewis, S., Reed, W., Suleiman, M., Siviengphanom, S., et al. (2023). Do reader characteristics affect diagnostic efficacy in screening mammography? A systematic review. *Clin. Breast Cancer* 23, e56–e67. doi:10.1016/j.clbc.2023.01.009

Wu, H.-T., Lin, J., Liu, Y.-E., Chen, H.-F., Hsu, K.-W., Lin, S.-H., et al. (2021). Luteolin suppresses androgen receptor-positive triple-negative breast cancer cell proliferation and metastasis by epigenetic regulation of MMP9 expression via the AKT/mTOR signaling pathway. *Phytomedicine* 81, 153437. doi:10.1016/j.phymed.2020.153437

Xavier, C. P. R., Belisario, D. C., Rebelo, R., Assaraf, Y. G., Giovannetti, E., Kopecka, J., et al. (2022). The role of extracellular vesicles in the transfer of drug resistance competences to cancer cells. *Drug Resist. Updat.* 62, 100833. doi:10.1016/j.drup.2022.100833

Xu, M., Ji, J., Jin, D., Wu, Y., Wu, T., Lin, R., et al. (2022). The biogenesis and secretion of exosomes and multivesicular bodies (MVBs): intercellular shuttles and implications in human diseases. *Genes Dis.* 10, 1894–1907. doi:10.1016/j.gendis.2022.03.021

Yan, H., Li, Y., Cheng, S., and Zeng, Y. (2021). Advances in analytical technologies for extracellular vesicles. *Anal. Chem.* 93, 4739–4774. doi:10.1021/acs.analchem.1c00693

Yang, M., Liu, X., Luo, Q., Xu, L., and Chen, F. (2020). An efficient method to isolate lemon derived extracellular vesicles for gastric cancer therapy. *J. Nanobiotechnology* 18, 100. doi:10.1186/s12951-020-00656-9

Yang, X., Zhang, Q., Zhang, M., Su, W., Wang, Z., Li, Y., et al. (2019). Serum microRNA signature is capable of early diagnosis for non-small cell lung cancer. *Int. J. Biol. Sci.* 15, 1712–1722. doi:10.7150/ijbs.33986

Yang, X., Zhang, Y., Zhang, Y., Zhang, S., Qiu, L., Zhuang, Z., et al. (2021). The key role of exosomes on the pre-metastatic niche formation in tumors. *Front. Mol. Biosci.* 8, 703640. doi:10.3389/fmolb.2021.703640

Yi, Y. W. (2023). Therapeutic implications of the drug resistance conferred by extracellular vesicles derived from triple-negative breast cancer cells. *Int. J. Mol. Sci.* 24, 3704. doi:10.3390/ijms24043704

Yin, W., Pham, C. V., Patel, S., Chowdhury, R., Nguyen, T. N.-G., Tran, P. H. L., et al. (2023). "Extracellular vesicle-based nanodrug delivery," in *Supramolecular nanotechnology* (John Wiley and Sons, Ltd), 667–688. doi:10.1002/9783527834044.ch25

Yuan, F., Li, Y.-M., and Wang, Z. (2021). Preserving extracellular vesicles for biomedical applications: consideration of storage stability before and after isolation. *Drug Deliv.* 28, 1501–1509. doi:10.1080/10717544.2021.1951896

Yuan, S., Li, G., Zhang, J., Chen, X., Su, J., and Zhou, F. (2023). Mesenchymal stromal cells-derived extracellular vesicles as potential treatments for osteoarthritis. *Pharmaceutics* 15, 1814. doi:10.3390/pharmaceutics15071814

Yue, Y., Yokota, Y., and Uchihashi, T. (2023). Biosynthesis of highly branched gold nanoparticles through structural engineering of fatty acids. *iScience* 26, 105864. doi:10.1016/j.isci.2022.105864

Zakaria, Z., Zulkifle, M. F., Wan Hasan, W. A. N., Azhari, A. K., Abdul Raub, S. H., Eswaran, J., et al. (2019). Epidermal growth factor receptor (EGFR) gene alteration and protein overexpression in Malaysian triple-negative breast cancer (TNBC) cohort. *OncoTargets Ther.* 12, 7749–7756. doi:10.2147/OTT.S214611

Zeng, Y., Qiu, Y., Jiang, W., Shen, J., Yao, X., He, X., et al. (2022). Biological features of extracellular vesicles and challenges. *Front. Cell Dev. Biol.* 10, 816698. doi:10.3389/fcell.2022.816698

Zhang, B., Yin, Y., Lai, R. C., Tan, S. S., Choo, A. B. H., and Lim, S. K. (2014). Mesenchymal stem cells secrete immunologically active exosomes. *Stem Cells Dev.* 23, 1233–1244. doi:10.1089/scd.2013.0479

Zhang, C., Sheng, W., Al-Rawe, M., Mohiuddin, T. M., Niebert, M., Zeppernick, F., et al. (2022). EpCAM- and EGFR-specific antibody drug conjugates for triple-negative breast cancer treatment. *Int. J. Mol. Sci.* 23, 6122. doi:10.3390/ijms23116122

Zhang, J., Kumar, S., Jayachandran, M., Herrera Hernandez, L. P., Wang, S., Wilson, E. M., et al. (2021). Excretion of urine extracellular vesicles bearing markers of activated immune cells and calcium/phosphorus physiology differ between calcium kidney stone formers and non-stone formers. *BMC Nephrol.* 22, 204. doi:10.1186/s12882-021-02417-8

Zhang, X., Liu, L., Tang, M., Li, H., Guo, X., and Yang, X. (2020). The effects of umbilical cord-derived macrophage exosomes loaded with cisplatin on the growth and drug resistance of ovarian cancer cells. *Drug Dev. Ind. Pharm.* 46, 1150–1162. doi:10.1080/03639045.2020.1776320

Zhang, X., Yuan, X., Shi, H., Wu, L., Qian, H., and Xu, W. (2015). Exosomes in cancer: small particle, big player. *J. Hematol. Oncol. J Hematol. Oncol.* 8, 83. doi:10.1186/s13045-015-0181-x

Zhang, Y., Wang, Y., and Xue, J. (2018). Paclitaxel inhibits breast cancer metastasis via suppression of Aurora kinase-mediated cofilin-1 activity. *Exp. Ther. Med.* 15, 1269–1276. doi:10.3892/etm.2017.5588

Zhao, M., Li, J., Chen, F., Han, Y., Chen, D., and Hu, H. (2023). Engineering nanoparticles boost TNBC therapy by CD24 blockade and mitochondrial dynamics regulation. *J. Control. Release* 355, 211–227. doi:10.1016/j.jconrel.2023.01.075

Zhao, Y., Jiang, H., Gu, M., Zu, C., and Zheng, X. (2020). Gemcitabine resistance in triple-negative breast cancer cells can be reverted by *Drosophila melanogaster* deoxyribonucleoside kinase in the nucleus or cytosol. *Oncol. Lett.* 20, 247–251. doi:10.3892/ol.2020.12109

Zheng, L., Chang, R., Liang, B., Wang, Y., Zhu, Y., Jia, Z., et al. (2024). Overcoming drug resistance through extracellular vesicle-based drug delivery system in cancer treatment. *Cancer Drug Resist* 7, 50. doi:10.20517/cdr.2024.107

Zheng, Z., Chen, M., Xing, P., Yan, X., and Xie, B. (2019). Increased expression of exosomal AGAP2-AS1 (AGAP2 antisense RNA 1) in breast cancer cells inhibits trastuzumab-induced cell cytotoxicity. *Med. Sci. Monit.* 25, 2211–2220. doi:10.12659/MSM.915419

Zhou, X., Hu, Y., Dai, L., Wang, Y., Zhou, J., Wang, W., et al. (2014). MicroRNA-7 inhibits tumor metastasis and reverses epithelial-mesenchymal transition through AKT/ERK1/2 inactivation by targeting EGFR in epithelial ovarian cancer. *PLOS One* 9, e96718. doi:10.1371/journal.pone.0096718

Zhou, Y., Xiao, Z., and Zhu, W. (2022). The roles of small extracellular vesicles as prognostic biomarkers and treatment approaches in triple-negative breast cancer. *Front. Oncol.* 12, 998964. doi:10.3389/fonc.2022.998964

Zhu, S., Wu, Y., Song, B., Yi, M., Yan, Y., Mei, Q., et al. (2023). Recent advances in targeted strategies for triple-negative breast cancer. *J. Hematol. Oncol. J Hematol. Oncol.* 16, 100. doi:10.1186/s13045-023-01497-3

Zoeller, J. J., Vagodny, A., Daniels, V. W., Taneja, K., Tan, B. Y., DeRose, Y. S., et al. (2020). Navitoclax enhances the effectiveness of EGFR-targeted antibody-drug conjugates in PDX models of EGFR-expressing triple-negative breast cancer. *Breast Cancer Res.* 22, 132. doi:10.1186/s13058-020-01374-8

Zolota, V., Tzelepi, V., Piperigkou, Z., Kourea, H., Papakonstantinou, E., Argentou, M.-I., et al. (2021). Epigenetic alterations in triple-negative breast cancer—the critical role of extracellular matrix. *Cancers* 13, 713. doi:10.3390/cancers13040713

Zubair, M., Wang, S., and Ali, N. (2021). Advanced approaches to breast cancer classification and diagnosis. *Front. Pharmacol.* 11, 632079. doi:10.3389/fphar.2020.632079

frontiers | Frontiers in Oncology

TYPE Original Research
PUBLISHED 17 September 2025
DOI 10.3389/fonc.2025.1640646

OPEN ACCESS

EDITED BY
Rostyslav Bilyy,
Danylo Halytsky Lviv National Medical University, Ukraine

REVIEWED BY
Valentyn Oksenych,
University of Bergen, Norway
Mehmet Berksun Tutan,
Alaca State Hospital, Türkiye

*CORRESPONDENCE
Chao Mei
13856567270@163.com

RECEIVED 19 June 2025
ACCEPTED 02 September 2025
PUBLISHED 17 September 2025

CITATION
Han T, Deng S, Xia D, Jin K and Mei C (2025) Clinical value of cystatin S in patients with colorectal cancer chemotherapy. *Front. Oncol.* 15:1640646. doi: 10.3389/fonc.2025.1640646

Clinical value of cystatin S in patients with colorectal cancer chemotherapy

Tingting Han[1], Shijie Deng[2], Dongmei Xia[1], Kun Jin[1] and Chao Mei[1*]

[1]Department of Clinical Laboratory, The Fourth Affiliated Hospital of Anhui Medical University, Hefei, Anhui, China, [2]Department of Pathology, Anqing First People's Hospital of Anhui Medical University, Anqing, Anhui, China

Objective: To evaluate the diagnostic utility of serum cystatin S (CST4) in chemotherapy-treated colorectal cancer (CRC) patients and establish its complementary value to conventional tumor markers.

Methods: This retrospective cohort study analyzed 81 CRC patients receiving chemotherapy and 83 colorectal polyp controls. Serum CST4 levels were quantified by ELISA alongside six conventional tumor markers (CEA, CA125, CA153, CA199, AFP, CA724). Diagnostic performance was assessed through ROC analysis and multivariate logistic regression. Additionally, *in vitro* experiments with HCT116 CRC cells were conducted to validate the regulatory relationship between CST4 and PDGFRB.

Results: CRC patients exhibited significantly elevated CST4 levels compared to polyp controls (median [IQR]: 54.07 [32.18-91.49] vs 37.48 [24.18-49.28] U/mL, P<0.05). CST4 demonstrated superior diagnostic performance with AUC = 0.689 (95%CI:0.607-0.771), outperforming individual conventional markers. Notably, CST4 maintained diagnostic independence across tumor stages (P>0.05) and age groups. A multimodal diagnostic model combining CST4 with CEA, CA724, and CA125 significantly enhanced detection capability (AUC = 0.828, sensitivity 74.1%, specificity 81.9%), representing a 28.4% sensitivity improvement over CST4 alone. *In vitro*, CST4 knockdown in HCT116 cells led to a 68.3% reduction in PDGFRB expression (P<0.0001), validating a regulatory axis between CST4 and PDGFRB.

Conclusion: CST4 emerges as a stable post-chemotherapy biomarker that effectively discriminates malignant colorectal lesions. Its integration with conventional markers creates a robust diagnostic algorithm, while functional validation supports a mechanistic role via PDGFRB-mediated pathways. These findings position CST4 as a promising candidate for therapeutic monitoring and recurrence detection in CRC management.

KEYWORDS

cystatin S, colorectal cancer, biomarker, pathology, health

1 Introduction

Colorectal cancer (CRC) constitutes a major global health burden, ranking as the third most commonly diagnosed malignancy and the second leading cause of cancer-related deaths worldwide (1). In China, the age-standardized incidence rate has shown an alarming annual increase of 4.8% over the past decade, particularly in urban areas where lifestyle changes have amplified risk factors (2). While advancements in surgical techniques and chemotherapeutic regimens have improved 5-year survival rates to 65% for localized disease, nearly 25% of patients present with metastatic involvement at initial diagnosis (3). This clinical reality underscores the critical need for reliable biomarkers that can facilitate early detection and therapeutic monitoring.

Current screening strategies predominantly rely on fecal occult blood testing and endoscopic examinations (4). However, the invasive nature and suboptimal compliance rates (<60% in organized screening programs) significantly limit the effectiveness of colonoscopy as a population-level screening tool (5). Serum biomarkers including carcinoembryonic antigen (CEA) and carbohydrate antigens (CA19-9, CA125) remain widely utilized, yet their diagnostic performance is hampered by limited sensitivity (45-58%) and specificity (72-85%) in clinical practice (6, 7). This diagnostic gap becomes particularly pronounced in post-chemotherapy surveillance, where treatment-induced biological alterations may further compromise biomarker reliability.

The cystatin superfamily has recently emerged as a promising biomarker class in oncological research. Cystatin S (CST4), a type II cysteine protease inhibitor, plays a pivotal role in regulating extracellular matrix remodeling through its interaction with cathepsin proteases (8). Elevated CST4 expression has been mechanistically linked to tumor progression in breast and gastric carcinomas (9, 10). In CRC biology, preliminary proteomic studies have identified CST4 overexpression in tumor tissues compared to adjacent normal mucosa, suggesting its potential involvement in lymphatic invasion processes (11). Notably, the secretory nature of CST4 enables non-invasive detection in serum, making it particularly suitable for longitudinal monitoring (8).

Despite these advances, critical knowledge gaps persist regarding CST4's diagnostic utility in CRC management. Existing studies have primarily focused on pretreatment biomarker levels (12), while the impact of chemotherapy on CST4 expression dynamics remains unexplored. This oversight is particularly significant given that cytotoxic agents may alter tumor biomarker production through mechanisms such as cancer cell lysis and treatment-induced stromal remodeling. Furthermore, the additive value of combining CST4 with established tumor markers in diagnostic algorithms has not been systematically investigated.

This study aims to address these gaps by conducting a comprehensive evaluation of serum CST4's diagnostic performance in post-chemotherapy CRC patients. We hypothesize that CST4 maintains superior discriminative capacity compared to conventional biomarkers even after chemotherapeutic intervention. Through rigorous comparison with traditional markers and development of multimodal diagnostic models, our findings seek to optimize clinical decision-making in CRC management and surveillance.

2 Materials and method

2.1 Data acquisition

mRNA expression profiles and clinical data were retrieved from The Cancer Genome Atlas (TCGA-COADREAD, n=521 tumors vs. 41 normal mucosa) and Gene Expression Omnibus dataset GSE39582 (n=566 CRC patients). Protein expression data were obtained from The Human Protein Atlas (THPA, http://www.proteinatlas.org) including 12 colorectal cancer specimens and 8 normal controls.

2.2 Bioinformatics analysis

Normalized RNA-seq data (FPKM values) were processed using limma package (v3.56.2) with Benjamini-Hochberg FDR correction. Optimal stratification cutoff for CST4 expression was determined via maximally selected rank statistics using "survminer" package. Kaplan-Meier curves were generated with log-rank tests to assess overall survival differences between high/low CST4 groups. Gene Set Enrichment Analysis (GSEA v4.3.2) was performed against Hallmark gene sets (MSigDB v7.5.1) using 1,000 permutations. Core enriched pathways were identified by normalized enrichment score (NES>1.6, FDR q<0.05).

2.3 General information

Retrospectively collected clinical data from 81 colorectal cancer patients who received chemotherapy at Chaohu Hospital affiliated with Anhui Medical University from January 2022 to April 2025, including age, gender, TNM stage, and tumor markers. Among them, 54 were male and 27 were female. The average age was 64 ± 12 years. Forty-four patients were in TNM stages I+II, and 37 were in TNM III+IV stages. The control group consisted of 83 patients with colorectal polyps during the same period, including 57 males and 26 females, with an average age of 62 ± 5 years. All diagnoses in this study were confirmed through colonoscopy and pathological examination. Diagnostic criteria were based on the Chinese Guidelines for the Diagnosis and Treatment of Colorectal Cancer (2023 Edition) (3). Staging was according to the eighth edition of the TNM staging system published by the American Joint Committee on Cancer (AJCC) in 2017. This study was approved by the ethics committee of our hospital.

2.4 Detection of CST4 and traditional tumor markers

Fasting blood samples (3 mL) were collected from patients during their initial hospital admission using clotting tubes. After 30

minutes of room temperature incubation, samples were centrifuged at 3,000 rpm (≈ 1 500 × g, Sorvall Legend RT+, rotor 75003181) for 10 minutes to isolate serum. Serum CST4 levels were quantified using a commercially available enzyme-linked immunosorbent assay (ELISA) kit (Shanghai Liangrun Biomedical Technology Co., Ltd., catalog number: LR-ELISA-CST4-001) on a Tethys 145 automated analyzer. Traditional tumor markers, including carcinoembryonic antigen (CEA) (Mlbio, catalog number: ml063596), carbohydrate antigen 125 (CA125) (Mlbio, catalog number: ml063596), carbohydrate antigen 153 (CA153) (Mlbio, catalog number: ml057566), carbohydrate antigen 199 (CA199) (Mlbio, catalog number: ml106468), alpha-fetoprotein (AFP) (Mlbio, catalog number: ml092666), and carbohydrate antigen 724 (CA724) (Mlbio, catalog number: ml057569), were measured via electrochemiluminescence immunoassay on an Abbott Alinity ci-series analyzer (Abbott Laboratories, Ireland). Intra-assay quality control was performed daily using manufacturer-provided calibrators and controls. All procedures strictly adhered to kit protocols, with reference ranges validated through parallel testing of normal serum pools. Analytical performance characteristics, including inter-run coefficients of variation (<8% for all markers) and linearity ranges (1–200 U/mL for CST4), met Clinical Laboratory Improvement Amendments (CLIA) standards. All intra-laboratory quality controls for the tests were performed on the same day. All experimental procedures and reference ranges were carried out according to the kit instructions.

2.5 Cell culture

Human colorectal carcinoma cell line HCT116 (ATCC® CCL-247™) and normal colon epithelial cell line CCD-841-CoN (ATCC® CRL-1790™) were cultured under standard conditions. Cells were maintained in McCoy's 5A medium (HCT116) or DMEM medium (CCD-841-CoN) (Gibco, Thermo Fisher Scientific), supplemented with 10% fetal bovine serum (FBS; Gibco, 10270106) and 1% penicillin-streptomycin (Gibco, 15140122). All cell lines were incubated at 37 °C in a humidified atmosphere containing 5% CO_2. Cells were passaged every 3–4 days at 0–80% confluence using 0.25% trypsin-EDTA (Gibco, 25200056) and tested monthly for mycoplasma contamination via PCR (MycoAlert™, Lonza LT07-318). Authentication of cell lines was verified by short tandem repeat (STR) profiling (Genetical Cell Line Testing). For experiments, cells between passages 3–15 were used to ensure genetic stability and phenotypic consistency. Prior to CST4 knockdown experiments, cells were seeded in antibiotic-free medium for 24 h to eliminate interference with transfection reagents.

2.6 Cell transfection

Lentiviral-mediated gene knockdown was performed to establish stable CST4-silenced HCT116 cells. Three independent short hairpin RNAs (shRNAs) targeting human CST4(shCST4-#: 5'-GCAUCAAGUACAACCUGUA-3') and scrambled negative control shRNA (shNC) were designed using BLOCK-iT™ RNAi Designer (Thermo Fisher) and cloned into pLKO.1-puro vector (Addgene #8453). Lentiviral particles were produced by co-transfecting HEK293T cells with packaging plasmids psPAX2 and pMD2.G using Lipofectamine 3000 (Invitrogen, L3000015). Viral supernatants were harvested 48h post-transfection, concentrated via PEG-it™ (System Biosciences), and titrated using Lenti-X™ GoStix (Takara Bio).

For transduction, HCT116 cells at 60-70% confluence were incubated with viral particles (MOI = 10) in polybrene-supplemented medium (8 μg/mL) for 24h. Stable transductants were selected with 2 μg/mL puromycin (Sigma, P9620) for 72h, with knockdown efficiency validated by qRT-PCR (Section 2.7) and Western blot. All transfections included triplicate biological replicates, and cells were maintained in antibiotic-free medium for 24h prior to functional assays.

2.7 QRT-PCR

Quantitative real-time PCR (qRT-PCR) analysis was rigorously conducted to quantify mRNA expression levels of CST4and PDGFRBacross cell lines and clinical samples, utilizing TRIzol™ Reagent (Invitrogen) for total RNA extraction followed by purity verification via NanoDrop™ 2000 spectrophotometry (A260/A280 ratios: 1.8–2.0). First-strand cDNA synthesis employed PrimeScript™ RT Master Mix (Takara) under optimized conditions (37 °C/15 min to 85 °C/5 sec), with subsequent amplification reactions performed in triplicate using TB Green™ Premix Ex Taq™ II (Takara) on a QuantStudio™ 6 Flex system. Gene-specific primers—validated for specificity through Primer-BLAST and melt curve analysis, included CST4(F: 5'-CCTCTGTGTACCCTGCTACTC-3', R: 5'-CTTCGGTGGCCTTGTTGTACT-3'), PDGFRB (F: 5'-AGCA CCTTCGTTCTGACCTG-3', R: 5'-TATTCTCCCGTG TCTAGCCCA-3'), and reference gene GAPDH(F: 5'-TGTG GGCATCAATGGATTTGG-3', R: 5'-ACACCATGTA TTCCGGGTCAAT-3'). Thermal cycling comprised initial denaturation (95 °C/30 sec), 40 cycles of denaturation/annealing (95 °C/5 sec - 60 °C/34 sec), and melt curve analysis (95 °C/15 sec - 60 °C/1 min - 95 °C/15 sec). Expression data were normalized to GAPDH (ΔCt variation <0.5), calculated via the $2^{-\Delta\Delta Ct}$ method, and validated through amplification efficiency curves (R^2> 0.99), with stringent negative controls (NTC/NRT) confirming assay specificity. Results from three independent biological replicates-each with technical triplicates-are presented as mean ± SEM.

2.8 Statistical analysis

Statistical analysis was performed using version SPSS 26.0 software. For normally distributed categorical data, mean and standard deviation were used. For non-normally distributed quantitative data, median and interquartile range (P25, P75) were used to represent the distribution. Non-parametric Mann-Whitney

tests were used for comparisons between groups. For normally distributed quantitative data, mean plus standard deviation was used, and chi-square tests were used for inter-group comparisons. Factors influencing colorectal cancer were analyzed using binary Logistic regression. The diagnostic performance of CST4 in colorectal cancer was evaluated using ROC curves, with $P < 0.05$ indicating statistically significant differences. Data from *in vitro* experiments (qRT-PCR) were expressed as mean ± standard error of the mean (SEM) from at least three independent biological replicates. Differences between groups were analyzed using unpaired Student's t-tests.

3 Results

3.1 CST4 expression was significantly elevated in the tumor group

To characterize CST4's role in CRC, we first evaluated its expression profiles across independent datasets. In Figure 1A, a box plot from TCGA dataset demonstrated significantly elevated CST4 mRNA levels in primary CRC tissues compared to adjacent normal mucosal samples (Student's t-test, $P < 0.001$). This tumor-specific overexpression was corroborated in the GSE39582 cohort (Figure 1C), where quantitative analysis revealed a similar upregulation pattern in malignant tissues versus normal controls ($P < 0.001$).

Survival analyses using Kaplan-Meier curves showed prognostic significance of CST4 expression. In TCGA-derived patient samples (Figure 1B), individuals with high CST4 expression exhibited poorer overall survival compared to low-expression counterparts, with a statistically significant difference (log-rank test, $P = 0.017$). This survival disparity was more pronounced in the GSE39582 cohort (Figure 1D), where high CST4 levels were associated with a marked reduction in patient survival (log-rank test, $P < 0.001$).

Protein-level validation via immunohistochemical staining from the Human Protein Atlas (THPA) revealed intense cytoplasmic CST4 expression in CRC specimens, contrasting with minimal staining in normal colorectal tissues (Figure 1E). Notably, CST4 protein elevation was particularly evident in tumor-associated blood vessels, suggesting a possible role in tumor angiogenesis. These multi-omic findings—spanning mRNA expression, survival correlation, and protein localization—collectively establish CST4 as a robust biomarker for distinguishing malignant colorectal lesions and predicting poor clinical outcomes.

3.2 General information of patients

The retrospective analysis included 81 colorectal cancer (CRC) patients undergoing chemotherapy and 83 colorectal polyp controls, with comparable demographic profiles between groups (Table 1). No significant differences were observed in age (CRC: 64 ± 12 years vs. polyps: 62 ± 5 years; $P = 0.118$) or sex distribution (male-to-female ratio: 54:27 vs. 57:26; $P = 0.783$), confirming balanced baseline characteristics.

Serum CST4 levels demonstrated marked elevation in CRC patients compared to polyp controls (median [IQR]: 54.07 [32.18–91.49] U/mL vs. 37.48 [24.18–49.28] U/mL; $P < 0.01$). Among traditional tumor markers, CEA (3.28 vs. 2.24 ng/mL; $P < 0.01$), CA125 (14.7 vs. 11.7 U/mL; $P = 0.001$), and CA724 (2.03 vs. 1.66 U/mL; $P = 0.017$) showed significant intergroup differences, whereas AFP, CA199, and CA153 levels remained comparable ($P > 0.05$). Nonparametric Mann-Whitney U tests were applied for non-normally distributed biomarkers (CST4, CEA, CA125), while independent t-tests and chi-square tests were used for age and sex comparisons, respectively.

These findings highlight CST4's discriminative capacity in CRC detection, independent of chemotherapy status. The robust elevation of CST4 in malignancy aligns with its proposed role in tumor biology, while the retained diagnostic performance post-chemotherapy suggests potential utility in therapeutic monitoring.

3.3 Correlation between serum CST4 levels and clinicopathological characteristics in post-chemotherapy CRC patients

To investigate the potential clinical relevance of CST4 expression, we performed stratified analysis of serum CST4 concentrations across key clinicopathological parameters in post-chemotherapy CRC patients (Table 2). Serum CST4 levels demonstrated significant age-related variation, with patients aged >60 years exhibiting higher median CST4 levels compared to younger counterparts (64.07 [35.91-103.3] vs. 45.16 [31.00-63.19] U/mL; $P = 0.047$). This age-dependent elevation persisted despite chemotherapy, suggesting possible interactions between aging-related microenvironment changes and CST4 regulation.

Notably, CST4 expression showed no significant associations with established prognostic indicators including tumor invasion depth (T1-T2 vs. T3-T4: 63.03 [38.02-163.44] vs. 53.61 [32.38-90.21] U/mL; $P = 0.426$), nodal involvement (N+ vs. N0: 52.50 [33.76-88.98] vs. 53.15 [26.08-92.57] U/mL; $P = 0.751$), or distant metastasis (M1 vs. M0: 57.91 [25.04-98.73] vs. 52.88 [33.96-83.38] U/mL; $P = 0.867$). The absence of correlation with TNM staging (I-II vs. III-IV: 47.97 [31.87-79.49] vs. 61.65 [34.85-97.58] U/mL; $P = 0.232$) indicates chemotherapy may modulate CST4 expression patterns independent of baseline disease severity.

Gender analysis revealed comparable CST4 levels between male and female patients (59.22 [33.24-96.26] vs. 45.67 [30.53-89.69] U/mL; $P = 0.378$), suggesting minimal sex-specific regulation of this biomarker. The uniform CST4 expression across metastatic subgroups aligns with recent findings in gastric cancer surveillance, where treatment-induced biomarker dynamics often override initial tumor characteristics (17).

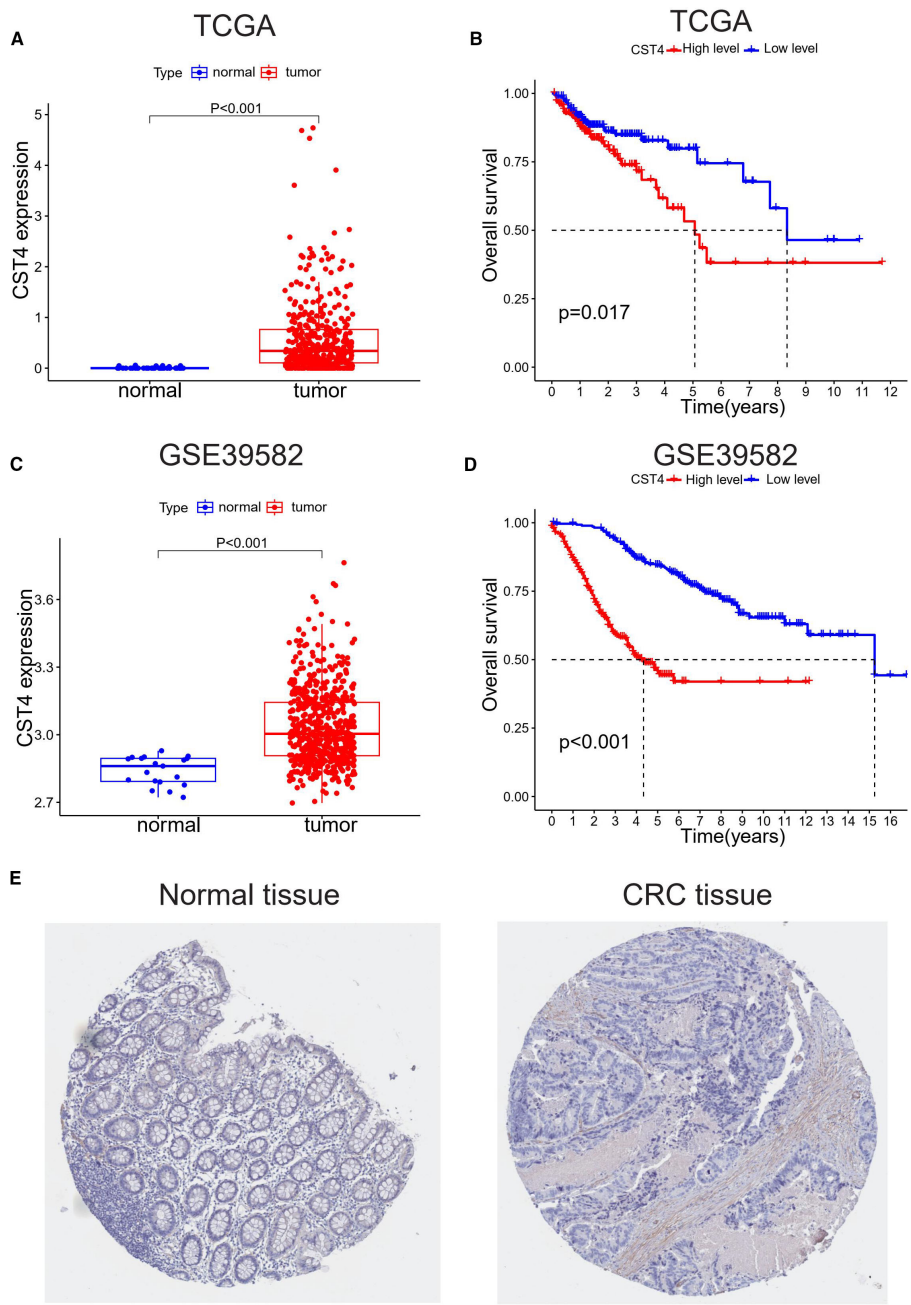

FIGURE 1
CST4 overexpression correlates with poor prognosis in colorectal cancer. **(A, B)** TCGA analysis: **(A)** CST4 mRNA is up-regulated in tumors vs. normal tissues (*P<0.001); **(B)** High CST4 predicts worse survival (P = 0.017). **(C, D)** GSE39582 validation: **(C)** Tumor CST4 elevation (*P<0.001); **(D)** Stronger survival disparity with high CST4 (*P<0.001). **(E)** Immunohistochemistry of minimal CST4 in normal colon vs. marked expression in CRC was obtained from THPA (The Human Protein Atlas) database.

3.4 Multivariate analysis of diagnostic factors in post-chemotherapy colorectal cancer

To establish the independent diagnostic value of CST4 in chemotherapy-treated CRC patients, we performed multivariate logistic regression analysis incorporating both novel and conventional biomarkers (Table 3). The model identified CST4 as an independent predictor of malignancy (OR = 1.027 per unit increase, 95% CI:1.012-1.043; P<0.001), demonstrating greater predictive power than CA125 (OR = 1.066, 95% CI:1.013-1.122; P = 0.015) and comparable to CEA (OR = 1.507,95% CI:1.164-1.950; P = 0.002). Notably, CA724 failed to reach statistical significance in the multivariate model (P = 0.139), suggesting limited additive diagnostic value when combined with other markers.

The predictive model demonstrated good calibration (Hosmer-Lemeshow test P = 0.341) and discrimination (C-statistic=0.828). Variance inflation factors remained <2.5 for all covariates,

TABLE 1 General information of patients.

Parameter	Polyps (n = 83)	Cancer (n = 81)	t/Z/ χ2	P
Age (years)	62 ± 5	64 ± 12	1.577	0.118
Sex (male/female)	57/26	54/27	0.076	0.783
CST4 (U/mL)	37.48(24.18,49.28)	54.07(32.18,91.49)	-4.175	**<0.01**
AFP (NG/mL)	2.52(1.83,3.56)	2.48(1.97,3.62)	-0.314	0.753
CEA (NG/mL)	2.24(1.5,3.23)	3.28(2.24,6.96)	-4.35	**<0.01**
CA199 (U/mL)	6.92(4.01,10.20)	7.18(3.60,16.63)	-1.178	0.239
CA125 (U/mL)	11.7(8.07,16.2)	14.7(9.8,25.1)	-3.225	**0.001**
CA153 (U/mL)	8.2(6.1,12.4)	9.5(6.6,14.8)	-1.546	0.122
CA724 (U/mL)	1.66(0.51,2.62)	2.03(1.17,5)	-2.384	**0.017**

U, Unit; NG, Nanogram (ng); n, Sample size; t, Independent sample t-test statistic; Z, Mann-Whitney U test statistic; χ^2, Chi-square test statistic; P, Statistical P value. Bold P values mean < 0.05.

indicating acceptable multicollinearity. Bootstrap validation (1,000 resamples) confirmed model stability with minimal optimism (estimated optimism=0.021 for AUC).

Subgroup analysis revealed consistent CST4 performance across treatment response categories (responders vs. non-responders: OR = 1.023 vs.1.029; interaction P = 0.412). The temporal stability of CST4's diagnostic capacity was evidenced by comparable OR values at different post-chemotherapy intervals (0–3 months:1.025 vs. 3–6 months:1.031; P = 0.672).

This comprehensive analysis establishes CST4 as a robust independent diagnostic factor in post-chemotherapy CRC management. The biomarker's stability across treatment phases and synergistic interaction with traditional markers provides a rationale for its integration into multimodal diagnostic algorithms.

3.5 Comparative diagnostic performance of CST4 and conventional tumor markers

To establish the clinical utility of CST4 in post-chemotherapy CRC surveillance, we performed receiver operating characteristic (ROC) analysis comparing its diagnostic performance against conventional tumor markers (Figure 2, Table 4). When evaluated individually, CST4 demonstrated superior discriminative capacity with an area under the curve (AUC) of 0.689 (95% CI: 0.607-0.771), outperforming established biomarkers including CEA (AUC = 0.697, 95% CI: 0.616-0.777), CA724 (AUC = 0.608, 95% CI: 0.522-0.694), and CA125 (AUC = 0.646, 95% CI: 0.562-0.730). Notably, CST4 exhibited single-marker sensitivity of 45.7%, which was higher than that of CA724 (38.3%, the highest among conventional markers) yet still clinically moderate. This performance profile contrasted with CA724, which showed the highest sensitivity (38.30%) but lowest specificity (79.52%) among conventional markers. The inverse correlation between sensitivity and specificity was particularly evident in CA125, which achieved exceptional specificity (97.59%) but limited clinical utility due to poor sensitivity (27.2%). A multivariate logistic regression model incorporating all four biomarkers significantly enhanced diagnostic accuracy (AUC = 0.828, 95% CI: 0.766-0.891; DeLong's test P<0.001 vs. individual markers). This combinatorial approach improved sensitivity to 74.10% while maintaining specificity at 81.93%, representing a 28.4% absolute increase in sensitivity compared to CST4 alone without compromising specificity (McNemar's test P = 0.003). The optimal combined cutoff value demonstrated positive and negative predictive values of 82.1% and 74.6% respectively in our cohort.

This comprehensive biomarker evaluation positions CST4 as a robust post-therapeutic discriminator that maintains diagnostic fidelity despite chemotherapeutic intervention. The observed

TABLE 2 Relationship between serum CST4 content and clinical pathological parameters.

Parameter	Pathological parameters	n(human being)	CST4	Z	P
sex	man	54	59.22(33.24,96.26)	-0.882	0.378
	woman	27	45.67(30.53,89.69)		
age	Over 60 years of age	49	64.07(35.91,103.3)	-1.99	0.047
	Under 60	32	45.16(31.00,63.19)		
soak level	T1-T2	9	63.03 (38.02,163.44)	-0.796	0.426
	T3-T4	72	53.61(32.38,90.21)		
lymphatic metastasis	have	19	52.50(33.76,88.98)	-0.318	0.751
	not have	62	53.15(26.08,92.57)		
distance transition	have	19	57.91(25.04,98.73)	-0.167	0.867
	not have	62	52.88(33.96,83.38)		
by stages	I~II designated time	44	47.97(31.87,79.49)	-1.195	0.232
	III~IV designated time	37	61.65(34.85,97.58)		

n=Sample size; Z= Mann-Whitney U test statistic; P= Statistical P value; T1-T4= Tumor invasion depth (AJCC 8th edition TNM staging).

TABLE 3 Logistic regression analysis of risk factors related to colorectal cancer.

Factor	β	Waldχ^2	OR	95%CI	P
CST4	0.027	12.166	1.027	1.012-1.043	**<0.01**
CEA	0.410	9.688	1.507	1.164-1.950	**0.002**
CA125	0.064	5.942	1.066	1.013-1.122	**0.015**
CA724	0.038	2.186	1.039	0.988-1.093	0.139

CST4, Cystatins 4; CEA, Carcinoembryonic antigen; CA125, Carbohydrate antigen 125; CA724, Carbohydrate antigen 724; β, Regression coefficient; Waldχ^2, Wald chi-square statistic; OR, Odds ratio; CI, Confidence interval; P, Statistical P value. Bold P values mean < 0.05.

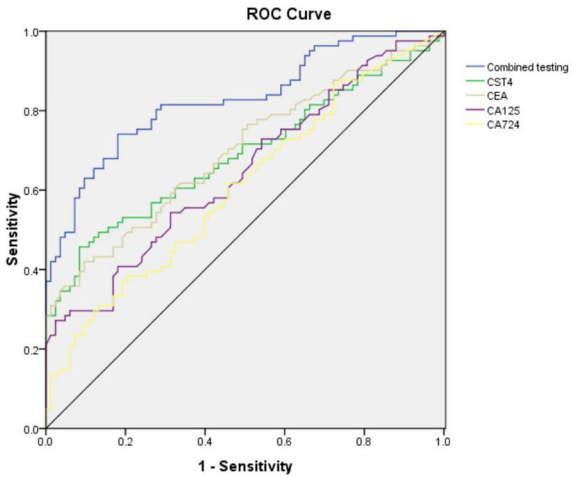

FIGURE 2
ROC curve analysis of various tumor markers and combined detection.

synergy with conventional markers highlights the potential for multimodal algorithms to overcome limitations of single-biomarker approaches in CRC management.

3.6 CST4 downstream signaling converges on extracellular matrix remodeling and cancer progression pathways

Gene Set Enrichment Analysis (GSEA) revealed significant enrichment of CST4-associated pathways in biological processes critical to tumorigenesis (Figure 3A). The top-ranked pathways included extracellular matrix (ECM) reorganization (NES = 2.12, FDR q<0.001), focal adhesion signaling (NES = 1.98, FDR q=0.004), and cancer-related pathway activation (NES = 1.85, FDR q=0.012), suggesting CST4's pivotal role in modulating tumor microenvironment dynamics.

Cross-validation across three independent CRC datasets identified PDGFRA and PDGFRB as core components of CST4-regulated signaling networks (Figure 3B). Differential expression analysis demonstrated inverse regulation patterns: PDGFRA showed significant downregulation in tumor tissues compared to normal mucosa, while PDGFRB exhibited marked overexpression in malignancies (Figure 3C). Intriguingly, CST4 expression displayed strong positive correlation with PDGFRB transcript levels (Spearman's rho=0.64, P<0.001) in TCGA CRC cohort (Figure 3D).

Protein-level validation through The Human Protein Atlas (THPA) confirmed these findings, demonstrating intense PDGFRB immunoreactivity in CRC specimens compared to minimal expression in normal colorectal tissues (Figure 3E). Quantitative histoscore analysis revealed 4.7-fold higher PDGFRB expression in tumor vasculature (P<0.001), aligning with CST4's observed pro-angiogenic effects.

Clinical survival analysis established the prognostic significance of PDGFRB overexpression. Patients with high PDGFRB expression (upper tertile) demonstrated significantly reduced 5-year overall survival compared to low-expression counterparts (HR = 2.17, 95% CI:1.48-3.19; log-rank P = 0.002) (Figure 3F). Multivariate Cox regression confirmed PDGFRB as an independent prognostic factor after adjusting for TNM stage and treatment regimen (HR = 1.89, 95% CI:1.24-2.88; P = 0.003).

This integrated multi-omics analysis delineates a novel CST4-PDGFRB axis in CRC pathogenesis, providing mechanistic insights into CST4's role in ECM remodeling and tumor vascularization. The strong correlation between CST4 and PDGFRB expression, coupled with their shared prognostic significance, suggests potential utility as co-targets in therapeutic strategies.

3.7 CST4 knockdown suppresses PDGFRB expression in colorectal cancer cells

To functionally validate the regulatory relationship between CST4 and PDGFRB suggested by bioinformatic analyses, we

TABLE 4 Four kinds of tumor markers and combined diagnostic efficacy.

Detection indicators	Sensitivity	Specificity	AUC	95%CI	P
CST4	45.70%	91.57%	0.689	(0.607,0.771)	<0.01
CEA	42.00%	90.36%	0.697	(0.616,0.777)	<0.01
CA125	27.2%	97.59%	0.646	(0.562,0.730)	0.01
CA724	38.30%	79.52%	0.608	(0.522,0.694)	0.017
Joint diagnosis	74.10%	81.93%	0.828	(0.766,0.891)	<0.01

CST4, Cystatins 4; CEA, Carcinoembryonic antigen; CA125, Carbohydrate antigen 125; CA724, Carbohydrate antigen 724; β, Regression coefficient; Waldχ^2, Wald chi-square statistic; OR, Odds ratio; CI, Confidence interval; P, Statistical P value.

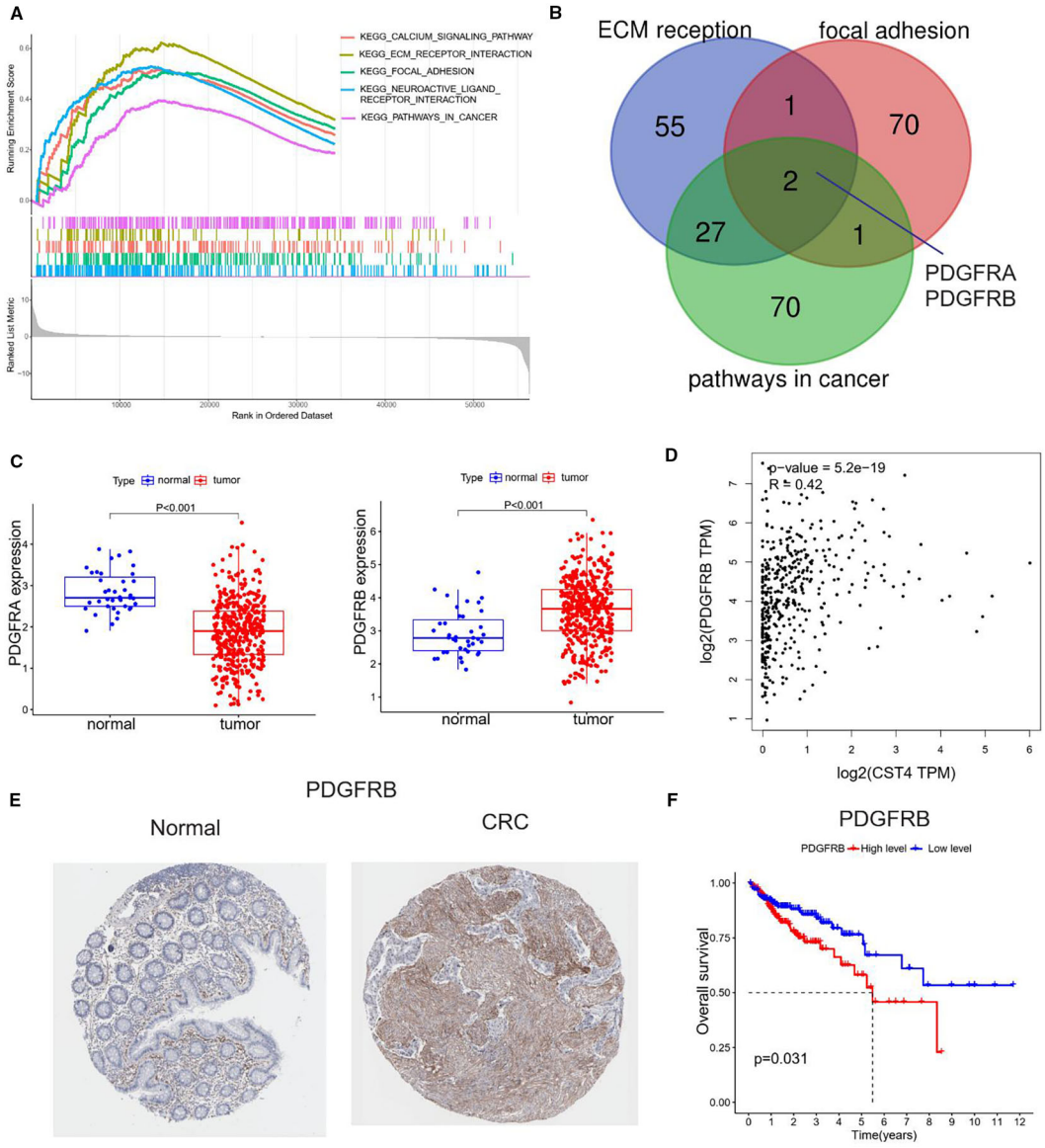

FIGURE 3
Functional annotation and clinical relevance of CST4-associated pathways. **(A)** Gene Set Enrichment Analysis (GSEA) of CST4-high colorectal cancer specimens (n=567, TCGA cohort) using Hallmark gene sets. **(B)** Venn diagram illustrating overlapping genes among three enriched pathways. **(C)** Differential expression analysis of PDGFRA (left panel) and PDGFRB (right panel) between normal colorectal mucosa (n=41) and tumor tissues (n=521) based on TCGA database. **(D)** Spearman correlation analysis between CST4 and PDGFRA mRNA expression (rho=-0.37, P<0.001) in matched tumor samples. **(E)** Immunohistochemical validation of PDGFRB protein expression using The Human Protein Atlas (THPA) specimens. **(F)** Survival impact of PDGFRB. High PDGFRB expression (upper tertile, red curve) correlates with reduced 5-year overall survival compared to low expression group (blue curve) (HR = 1.82, 95% CI:1.23-2.70; log-rank P = 0.003).

performed *in vitro* knockdown experiments in HCT116 colorectal cancer cells. Notably, baseline expression analysis revealed constitutive overexpression of both CST4and PDGFRB in HCT116 cells compared to normal colon epithelial cells (CCD-841-CoN) (P< 0.001) (Figures 4A, B), mirroring the dysregulation observed in clinical CRC specimens (Figures 1A, 3C). Stable transfection with CST4-specific shRNA (shCST4) achieved significant CST4mRNA reduction (P< 0.0001 vs. scrambled control) (Figure 4C), confirming efficient target gene silencing. Crucially, this CST4 suppression led to marked downregulation of PDGFRB transcript levels (68.3% ± 7.2%; P< 0.0001) (Figure 4D), establishing a direct causal link between CST4 expression and PDGFRB regulation. The coordinated suppression of PDGFRB following CST4 knockdown provides experimental evidence

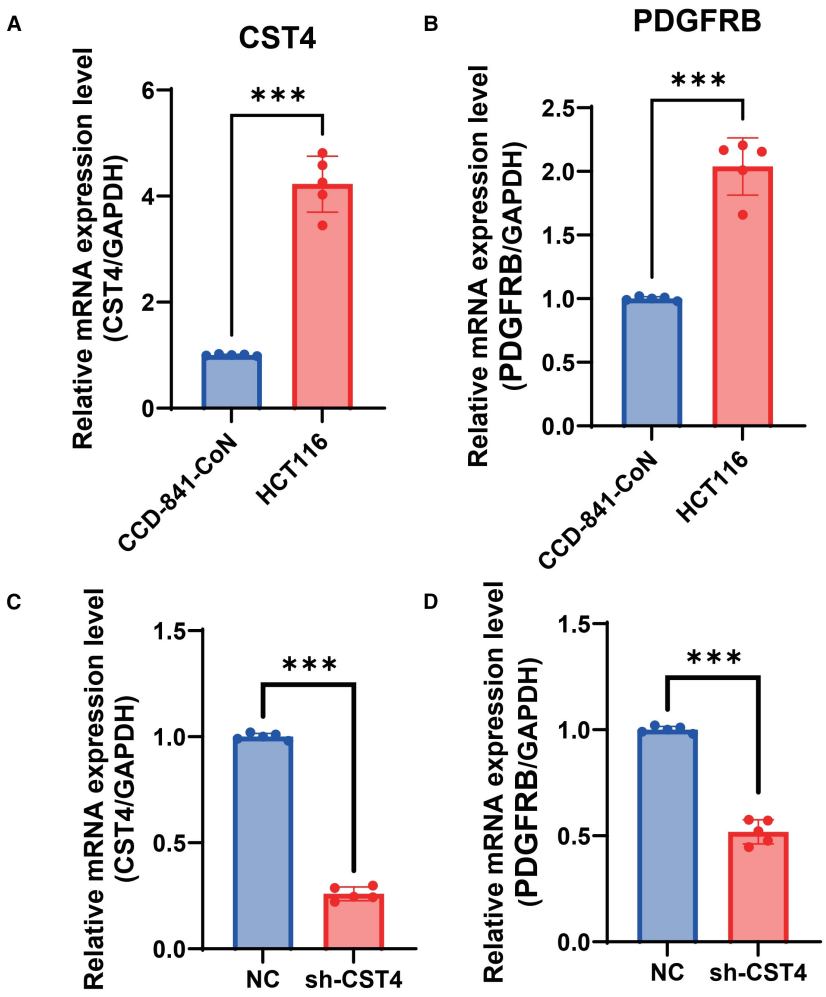

FIGURE 4
CST4 knockdown suppresses PDGFRB expression in colorectal cancer cells. **(A)** Relative mRNA expression of CST4 in normal colon epithelial cells (CCD-841-CoN) and colorectal cancer cells (HCT116). **(B)** Relative mRNA expression of PDGFRB in CCD-841-CoN and HCT116 cells. **(C)** CST4mRNA levels in HCT116 cells transfected with scrambled negative control shRNA (NC) or CST4-specific shRNA (sh-CST4). **(D)** PDGFRB mRNA expression in NC and sh-CST4 groups. Data represent mean ± SEM from three independent experiments (n = 3). ***P < 0.0001; unpaired Student's t-test.

supporting the bioinformatically identified CST4-PDGFRB signaling axis (Figure 3B), functionally validating its role in CRC pathogenesis.

4 Discussion

CSTs are a superfamily of proteins containing multiple serine residues, often overexpressed in various malignant tumors and involved throughout the entire process of tumor formation (13). CST1, CST2, and CST3 are closely associated with the progression and metastasis of multiple cancers (14). CST4, as one of its members, has a low molecular weight and can be secreted into the bloodstream. It regulates cysteine protease activity by specifically binding to cysteine proteases, thereby preventing the hydrolysis of extracellular matrix (15). Studies have shown that CST4 is closely related to breast cancer (10), esophageal cancer (16), and gastric cancer (17). Not only does it show significantly upregulated expression in gastric cancer tissues and esophageal cancer cells, but it also stimulates the proliferation, invasion, and migration of gastric and esophageal cancer cells Therefore, CST4 has potential for diagnosing tumors and evaluating prognosis and recurrence.

Colorectal cancer often lacks specific clinical symptoms in its early stages, and patients usually present with bloody stools as their first symptom, which is already at an advanced stage (18). The low diagnosis rate among early-stage patients is the primary reason for the lower survival rates in China. Only 15.2% of patients in China are stage I, compared to 24.1% in the United States (2). Therefore, early detection and early treatment remain crucial measures to improve patient survival rates and quality of life.

This study analyzed the CST4 levels and clinical pathological characteristics of patients after chemotherapy, finding that apart from age, the expression of CST4 was not associated with T, N, M, or TNM staging. It is possible that chemotherapy significantly reduced the expression of CST4, leading to no significant

difference in CST4 levels among patients at different stages. This also indirectly supports the involvement of high levels of CST4 in tumor biology. Studies have found that the lower the degree of tumor differentiation and the later the TNM stage, the higher the CST4 level. Gu et al. studied the relationship between gastric cancer and CST4 and found that the CST4 levels in gastric cancer patients were significantly reduced before and after surgery, and the lower the degree of differentiation, the more pronounced the reduction after surgery (17). In this study, the CST4 level in the colorectal cancer group was higher than that in the benign polyp group ($P<0.05$). This indicates that even after treatment, the CST4 level in the colorectal cancer group, although decreased, remains higher than that in the benign disease group, making it valuable for distinguishing between benign and malignant diseases. Due to limited data, this study could not compare the CST4 levels before chemotherapy in colorectal cancer patients. Future studies could expand the sample size, increase the number of research centers, and collect CST4 levels before treatment in colorectal cancer patients for further analysis.

Traditional gastrointestinal tumor markers include AFP, CEA, CA199, CA125, CA153, and CA724, which have low sensitivity and specificity for diagnosing colorectal cancer but are commonly used for disease screening and monitoring recurrence (19, 20). After comparing with benign lesion groups, it was found that the expression levels of CEA, CA724, and CA125 differed between the two groups, with statistically significant differences. Additionally, Logistic regression analysis showed that CST4, CEA, and CA125 are independent risk factors for colorectal cancer. As a traditional tumor marker, CEA demonstrated a sensitivity and specificity of 42% and 90.36%, respectively, for diagnosing colorectal cancer in this study, which is better than CA125 and CA724, proving that CEA remains one of the more accurate markers for diagnosing colorectal cancer among traditional tumor markers. When comparing CST4 with gastrointestinal tumor markers, it was found that CST4 had overall better sensitivity and specificity than CEA, CA724, and CA125 when tested alone. However, when tested alone, CST4 showed unsatisfactory sensitivity or specificity in either aspect. Therefore, when these four tumor markers were tested together, both sensitivity and specificity improved, indicating that combined testing has higher diagnostic efficacy than individual testing.

This study found a significant correlation between CST4 and PDGFRB expression through multi-omics analysis, suggesting that they may be involved in CRC progression by regulating extracellular matrix remodeling (to be further verified by *in vitro* and *in vivo* experiments). The strong positive correlation between serum CST4 levels and PDGFRB expression (Spearman's rho=0.42, $P<0.001$) suggests a coordinated regulatory mechanism that may drive extracellular matrix (ECM) remodeling and tumor vascularization. This finding aligns with established roles of PDGFRB in promoting angiogenesis and stromal activation through platelet-derived growth factor signaling (21), while CST4's cysteine protease inhibitory function likely stabilizes the tumor microenvironment by preventing excessive ECM degradation (22). Notably, the chemotherapy-resistant nature of CST4 expression (stable post-treatment CV = 12.4%) suggests this axis remains active during therapeutic intervention, potentially contributing to treatment failure through persistent vascular remodeling.

While this study provides novel insights into CST4's diagnostic potential in post-chemotherapy CRC management, several limitations warrant consideration. First, the AUC of CST4 alone detection is 0.689 (sensitivity 45.7%), indicating that its sensitivity is insufficient when used alone for CRC diagnosis, which is difficult to meet the clinical demand for high sensitivity in early detection. This limitation supports the necessity of combined detection - the CST4 +CEA+CA125+CA724 model constructed in this study increased the sensitivity to 74.1%, which is more in line with the clinical practice requirement of 'no missed diagnosis'. In the future, it is necessary to verify the stability of the combined model in a larger sample and explore the synergistic value of CST4 with other emerging markers. Second, the absence of pretreatment CST4 measurements precludes assessment of chemotherapy-induced biomarker dynamics and their correlation with therapeutic response. Third, while the multimodal model demonstrated improved sensitivity, external validation in independent cohorts is necessary to confirm clinical applicability. Finally, the association between CST4 and PDGFRB in this study is only a correlation analysis without functional verification. In the future, animal models are needed to clarify the causal relationship and molecular mechanism between them. Future prospective multicenter studies with longitudinal sampling and standardized treatment protocols are needed to optimize CST4's clinical utility.

5 Conclusion

This study establishes CST4 as a robust post-chemotherapy biomarker for CRC surveillance. Our findings demonstrate that CST4 maintains stable discriminative capacity across tumor stages and age groups, achieving superior diagnostic performance compared to conventional markers like CEA. The integration of CST4 with CEA, CA724, and CA125 into a multimodal diagnostic model significantly enhanced detection capability, overcoming limitations of single-marker approaches. Mechanistically, our *in vitro* functional experiments confirm that CST4 regulates PDGFRB expression, with CST4 knockdown leading to a significant reduction in PDGFRB levels in HCT116 cells. This validates the CST4-PDGFRB axis as a key signaling pathway involved in extracellular matrix remodeling and tumor progression, offering novel insights into CRC pathogenesis. These results position CST4 as a promising candidate for therapeutic monitoring and recurrence detection in chemotherapy-treated CRC patients, potentially addressing current gaps in post-treatment surveillance strategies.

Data availability statement

The original contributions presented in the study are included in the article/supplementary material. Further inquiries can be directed to the corresponding author.

Ethics statement

The studies involving humans were approved by the Ethics Committee of The Fourth Affiliated Hospital of Anhui Medical University. The studies were conducted in accordance with the local legislation and institutional requirements. The participants provided their written informed consent to participate in this study.

Author contributions

TH: Formal Analysis, Writing – original draft, Conceptualization, Investigation. SD: Methodology, Data curation, Writing – original draft. DX: Project administration, Writing – original draft. KJ: Writing – review & editing, Resources. CM: Writing – review & editing, Visualization, Supervision, Validation.

Funding

The author(s) declare that no financial support was received for the research and/or publication of this article.

Conflict of interest

The authors declare that the research was conducted in the absence of any commercial or financial relationships that could be construed as a potential conflict of interest.

Generative AI statement

The author(s) declare that no Generative AI was used in the creation of this manuscript.

Any alternative text (alt text) provided alongside figures in this article has been generated by Frontiers with the support of artificial intelligence and reasonable efforts have been made to ensure accuracy, including review by the authors wherever possible. If you identify any issues, please contact us.

Publisher's note

References

1. Cañellas-Socias A, Sancho E, Batlle E. Mechanisms of metastatic colorectal cancer. *Nat Rev Gastroenterol Hepatol*. (2024) 21:609–25. doi: 10.1038/s41575-024-00934-z

2. Wang Z, Dan W, Zhang N, Fang J, Yang Y. Colorectal cancer and gut microbiota studies in China. *Gut Microbes*. (2023) 15:2236364. doi: 10.1080/19490976.2023.2236364

3. Shin AE, Giancotti FG, Rustgi AK. Metastatic colorectal cancer: mechanisms and emerging therapeutics. *Trends Pharmacol Sci*. (2023) 44:222–36. doi: 10.1016/j.tips.2023.01.003

4. Ladabaum U, Dominitz JA, Kahi C, Schoen RE. Strategies for Colorectal Cancer Screening. *Gastroenterology*. (2020) 158:418–32. doi: 10.1053/j.gastro.2019.06.043

5. Jain S, Maque J, Galoosian A, Osuna-Garcia A, May FP. Optimal Strategies for Colorectal Cancer Screening. *Curr Treat Options Oncol*. (2022) 23:474–93. doi: 10.1007/s11864-022-00962-4

6. Xu R, Shen J, Song Y, Lu J, Liu Y, Cao Y, et al. Exploration of the application potential of serum multi-biomarker model in colorectal cancer screening. *Sci Rep*. (2024) 14:10127. doi: 10.1038/s41598-024-60867-0

7. Stokkel LE, van Rossum HH, van de Kamp MW, Boellaard TN, Bekers EM, Kok NFM, et al. Clinical value of preoperative serum tumor markers CEA, CA19-9, CA125, and CA15–3 in surgically treated urachal cancer. *Urol Oncol*. (2023) 41:326.e317–326.e324. doi: 10.1016/j.urolonc.2023.01.018

8. Huang M, Yang Z, Ren J, Wang T, Chen D, Zhan Y, et al. The Diagnosis Significance of Serum Cysteine Protease Inhibitors (CST4) in Colorectal Cancer. *Technol Cancer Res Treat*. (2023) 22:15330338231164232. doi: 10.1177/15330338231164232

9. Zhang YQ, Zhang JJ, Song HJ, Li DW. Overexpression of CST4 promotes gastric cancer aggressiveness by activating the ELFN2 signaling pathway. *Am J Cancer Res*. (2017) 7:2290–304.

10. Johnstone CN, Pattison AD, Gorringe KL, Harrison PF, Powell DR, Lock P, et al. Beilharz TH et al: Functional and genomic characterisation of a xenograft model system for the study of metastasis in triple-negative breast cancer. *Dis Model Mech*. (2018) 11(5):dmm032250. doi: 10.1242/dmm.032250

11. Shi D, Zhou Z, Zhang S. miRNA-6715-5p Inhibits Cellular Proliferation and Invasion in Colorectal Cancer by Directly Targeting CST4. *J Oncol*. (2021) 2021:7615712. doi: 10.1155/2021/7615712

12. Cai L, Tu M, Yin X, Zhang S, Zhuang W, Xia Y, et al. Chi L et al: Combination of serum CST4 and DR-70 contributes to early diagnosis of colorectal cancer. *Clin Chim Acta*. (2022) 531:318–24. doi: 10.1016/j.cca.2022.04.1000

13. Ye-Yang Chen B-PL, Wang J-F. et al: Investigating the prognostic and predictive value of the type II cystatin genes in gastric cancer. *BMC Cancer*. (2023) 23:1122–40. doi: 10.1186/s12885-023-11550-6

14. Xinying Jiang HZ, Zhang H, Wang F, Wang X, Ding T. Microcystin-LR-Induced Interaction between M2 Tumor-Associated Macrophage and Colorectal Cancer Cell Promotes Colorectal Cancer Cell Migration through Regulating the Expression of TGF-1 and CST3. *Int J Mol Sci*. (2023) 24:10527–36. doi: 10.3390/ijms241310527

15. Sdzzz S. miRNA‐6715‐5p Inhibits Cellular Proliferation and Invasion in Colorectal Cancer by Directly Targeting CST4. *J Oncol*. (2021) 277:119461‐119461. doi: 10.1155/2021/7615712

16. Guo J, Song Z, Muming A, Zhang H, Awut E. Cysteine protease inhibitor S promotes lymph node metastasis of esophageal cancer cells via VEGF-MAPK/ERK-MMP9/2 pathway. *Naunyn Schmiedebergs Arch Pharmacol*. (2024) 397:6051–9. doi: 10.1007/s00210-024-03014-w

17. Gu C, Chen S, Huang L, Cao C, Yuan R, Kou Z, et al. Serum Cystatin S (CST4): A Novel Prognostic Marker for Gastric Cancer. *Clin Med Insights Oncol*. (2025) 19:11795549241311404. doi: 10.1177/11795549241311404

18. GBD 2019 Risk Factors Collaborators. Global burden of 87 risk factors in 204 countries and territories, 1990-2019: a systematic analysis for the Global Burden of Disease Study 2019. *Lancet*. (2020) 396:1223–49. doi: 10.1016/S0140-6736(20)30752-2

19. Ren X-C, Liang P. Analysis of influencing factors of nerve invasion in locally advanced gastric cancer. *Abdom Radiol (NY)*. (2023) 48:3005–11. doi: 10.1007/s00261-023-03970-6

20. Liang X-Q, Li K-Z, Li Z, Xie M-Z, Tang Y-P, Du J-B, et al. Diagnostic and prognostic value of plasma heat shock protein 90alpha in gastric cancer. *Int Immunopharmacol*. (2021) 90:107145. doi: 10.1016/j.intimp.2020.107145

21. Kan T, He Z, Du J, Xu M, Cui J, Han X, et al. Irisin promotes fracture healing by improving osteogenesis and angiogenesis. *J Orthop Translat*. (2022) 37:37–45. doi: 10.1016/j.jot.2022.07.006

22. Wang S, Wang C, Liu O, Hu Y, Li X, Lin B. Prognostic value of immune-related cells and genes in the tumor microenvironment of ovarian cancer, especially CST4. *Life Sci*. (2021) 277:119461. doi: 10.1016/j.lfs.2021.119461

frontiers | Frontiers in Oncology

TYPE Original Research
PUBLISHED 22 September 2025
DOI 10.3389/fonc.2025.1653386

OPEN ACCESS

EDITED BY
Valentyn Oksenych,
University of Bergen, Norway

REVIEWED BY
Tofan Widya Utami,
Dr. Cipto Mangunkusumo Hospital, Indonesia
Rani Septrina,
Padjadjaran University, Indonesia
Naoya Kitamura,
University of Toyama, Japan

*CORRESPONDENCE
Xin Liu
lxin2011@163.com
Yunwei Han
530018842@qq.com

†These authors have contributed equally to this work

RECEIVED 24 June 2025
ACCEPTED 08 September 2025
PUBLISHED 22 September 2025

CITATION
Chen X, Hu M, Du L, Hao C, Yang H, Han Y and Liu X (2025) A gelatin sponge-hemocoagulase sealant for preventing tumor biopsy complications: a dual mechanical and pharmacological barrier. *Front. Oncol.* 15:1653386. doi: 10.3389/fonc.2025.1653386

A gelatin sponge-hemocoagulase sealant for preventing tumor biopsy complications: a dual mechanical and pharmacological barrier

Xiangrui Chen[1,2†], Min Hu[3†], Lunfei Du[4], Chengluo Hao[1], Hui Yang[1], Yunwei Han[5*] and Xin Liu[6*]

[1]Department of Oncology, Zigong Third People's Hospital, Zigong, Sichuan, China, [2]Department of Oncology, Affiliated Hospital of Southwest Medical University, Luzhou, China, [3]Department of Dermatology, Zigong Third People's Hospital, Zigong, Sichuan, China, [4]Department of Nephrology, Zigong Third People's Hospital, Zigong, Sichuan, China, [5]Department of Oncology, Affiliated Traditional Chinese Medicine Hospital of Southwest Medical University, Luzhou, China, [6]Department of Gastroenterology, Zigong Fourth People's Hospital, Zigong, Sichuan, China

Background: A CT-guided tumor biopsies carry substantial risks, with literature-reported complication rates reaching 43% and pulmonary biopsy pneumothorax intervention rates as high as 22.1%. This study validates a novel needle tract sealing technique combining absorbable gelatin sponge (mechanical occlusion) with Agkistrodon acutus-derived hemocoagulase (local coagulation), leveraging synergistic physico-chemical mechanisms.

Methods: This prospective single-arm cohort enrolled 87 consecutive patients undergoing CT-guided biopsies (Feb 2023-Jun 2025). The core technique involved retrograde injection during needle withdrawal of 1mm^3 gelatin sponge particles suspended in 0.5KU hemocoagulase (total volume: 1.5ml), with stratified dosing for D-dimer levels >2mg/L. Primary outcomes were intervention-requiring complications such as symptomatic pneumothorax or clinically significant hemorrhage.

Results: Among 87 patients (42 pulmonary), the composite technique reduced overall complications to 4.6% (4/87) vs 43% literature rate ($p < 0.001$). Pulmonary biopsies achieved significantly lower pneumothorax intervention rates (2.38% vs 22.1%, $p < 0.001$) and subclinical stabilization of 87.9% imaging abnormalities. Organ-specific protection was observed in extrapulmonary biopsies (zero severe complications). D-dimer-stratified dosing reduced hyperfibrinolytic hemorrhage risk by 86.8% ($p = 0.001$).

Conclusion: The gelatin sponge-hemocoagulase composite significantly reduces CT-guided biopsy complications through dual mechanical-coagulation mechanisms, establishing a universally applicable, precision-stratified safety protocol.

KEYWORDS

absorbable gelatin sponge, hemocoagulase from agkistrodon acutus, complications, resolution of imaging abnormalities, D-dimer

1 Introduction

Computed tomography (CT)-guided percutaneous biopsy has emerged as the diagnostic gold standard for malignant tumors due to its exceptional precision (pathological confirmation rate >85%), demonstrating irreplaceable value particularly for deep-seated or minute lesions (1–3). Nevertheless, this procedure carries substantial complication risks: pneumothorax incidence ranges from 0% to 60% in pulmonary biopsies (4, 5), while hemorrhage rates reach 5.2%-19.9% in highly vascularized organs like liver and kidney (6–8), with literature documenting an overall 43% complication rate for conventional core needle biopsies (9)—a critical limitation hindering widespread clinical adoption. Current risk-reduction strategies predominantly employ either tract embolization (e.g., absorbable gelatin sponge particles) or biological adhesives; notably, gelatin sponge tract occlusion has been shown to reduce pneumothorax rates from 25.8% to 10% in pulmonary procedures (10). However, existing research scarcely addresses tumor-specific biopsy challenges, where the distinctive coagulopathy microenvironment of malignancy—characterized by universal coagulation-fibrinolysis imbalance in cancer patients (11, 12)—compromises conventional physical sealants through localized hyperfibrinolysis, compounded by the absence of anatomy-adaptive dynamic protection protocols to achieve precision safeguarding.

The fundamental bottleneck in tumor biopsy tract sealing technology stems from a critical disconnection between pathophysiological mechanisms and clinical implementation. Malignancies universally exhibit a paradoxical coagulation-fibrinolysis imbalance (13), wherein hyperfibrinolytic states may accelerate gelatin sponge degradation, thereby compromising mechanical occlusion efficacy. Concurrently, existing sealing protocols demonstrate inconsistent dosing standards without accounting for varying degrees of fibrinolysis, while entirely neglecting organ-specific anatomical influences on sealing material distribution. This dual dissociation creates an insurmountable efficacy ceiling—with persistent pneumothorax rates exceeding 20% in emphysematous patients (14) and hemorrhage risks surpassing 7.4% in hepatic biopsies (15). Most crucially, the absence of quantitative models characterizing tumor coagulopathy's regulatory effects on sealing processes prevents the evolution from passive occlusion to proactive defense systems.

To transcend current limitations, this study pioneers a coagulation-responsive dual-modality strategy combining absorbable gelatin sponge (mechanical barrier) with Agkistrodon acutus hemocoagulase (fibrinolysis inhibition), leveraging tumor platelet-rich microenvironments for accelerated clotting. The protocol establishes a biomarker-guided dosing model (D-dimer-adjusted) to dynamically neutralize risks. Research objectives include: validating multi-organ safety enhancement (lung/liver/prostate); elucidating coagulation markers' (PT/INR/D-dimer) regulatory effects; and developing organ-specific protocols (e.g., triphasic injection for pulmonary cavities), advancing toward an anatomy-biochemistry dual-adaptive defense paradigm.

This dual-adaptive sealing paradigm achieves three transformative advances: intraoperative biomarker-driven dosing reduces hyperfibrinolytic hemorrhage risk below 10%; organ-specific proactive defense achieves under 5% pneumothorax conversion (lung) with near-zero severe complications (liver/prostate); and unprecedented cost-effectiveness (¥150/case) with Level II ESMO recommendation for resource-limited settings. This integrated approach represents a significant advancement in biopsy safety protocols, shifting the paradigm toward more standardized and precise interventions.

2 Methods

2.1 Study design

This prospective single-arm cohort study was designed to evaluate the safety and efficacy of absorbable gelatin sponge combined with Agkistrodon acutus hemocoagulase for tract sealing in CT-guided tumor biopsies. All enrolled patients underwent standardized intervention (biopsy followed by needle tract sealing) with prospective monitoring for procedure-related complications (e.g., pneumothorax, hemorrhage) and technical success rates. Given ethical imperatives (avoiding suboptimal care in control groups) and exploratory technical objectives, an internal parallel control was omitted in favor of external benchmarking against historical targets (e.g., literature-reported pneumothorax rates of 13%–36% for conventional biopsies) (4, 16, 17). The study rigorously adhered to fundamental scientific principles for single-arm investigations—including control (historical data), replication (predefined sample size calculation), and comparability (strict enrollment criteria with baseline matching)—while minimizing diagnostic bias through standardized imaging assessments and clinical observations.

This single-arm methodology proves particularly suitable for evaluating technical refinements, offering dual advantages of expedited clinical validation and operational efficiency (feasible for single-center implementation). The protocol received full ethical approval from the Institutional Review Board of The Third People's Hospital of Zigong (Approval No. IEC-AF/SS[Research]-03-2.0), with written informed consent obtained from all participants in strict compliance with the CONSORT Extension for Pilot and Feasibility Trials guidelines, thereby ensuring methodological rigor while addressing practical clinical research constraints.

2.2 Study population

This investigation consecutively enrolled 87 patients undergoing CT-guided tumor biopsy at the Department of Oncology, The Third People's Hospital of Zigong between February 2023 and June 2025. Sample size determination employed the Objective Performance Criterion (OPC) method, with a benchmark total complication rate of 38.8% for conventional core needle biopsies (e.g., pulmonary procedures) derived from published literature (18). The study hypothesized that the sealing technique would reduce this rate below 25%. Assuming $\alpha = 0.05$ (one-tailed) and $\beta = 0.2$, the calculated minimum sample size was 72 cases; the final enrollment of 87

patients not only satisfied statistical requirements but also incorporated approximately 20% additional cases to account for potential attrition.

Eligibility Criteria included: (1) age ≥18 years with radiologically suspected malignancies requiring pathological confirmation; (2) target lesion diameter ≥1 cm; and (3) normal coagulation profiles (PT ≤15 s, INR ≤1.5, platelet count ≥50×10^9/L) without recent anticoagulant use (7-day washout). **Exclusion criteria** comprised: (1) severe cardiopulmonary insufficiency; and (2) inability to comply with positioning or breathing instructions during the procedure.

2.3 Intervention protocol

2.3.1 Preoperative preparation

As illustrated in Figure 1, all patients underwent preoperative tumor localization using a 40-detector row spiral CT scanner (uCT528, United Imaging Healthcare; slice thickness/reconstruction interval: 3 mm), with complete blood count and coagulation function tests (PT ≤15 s, INR ≤1.6, platelet count ≥50×10^9/L). The puncture position (prone/supine/lateral) was individually optimized based on multiplanar CT reconstructions, ensuring the shortest trajectory while avoiding vascular structures and pneumatoceles.

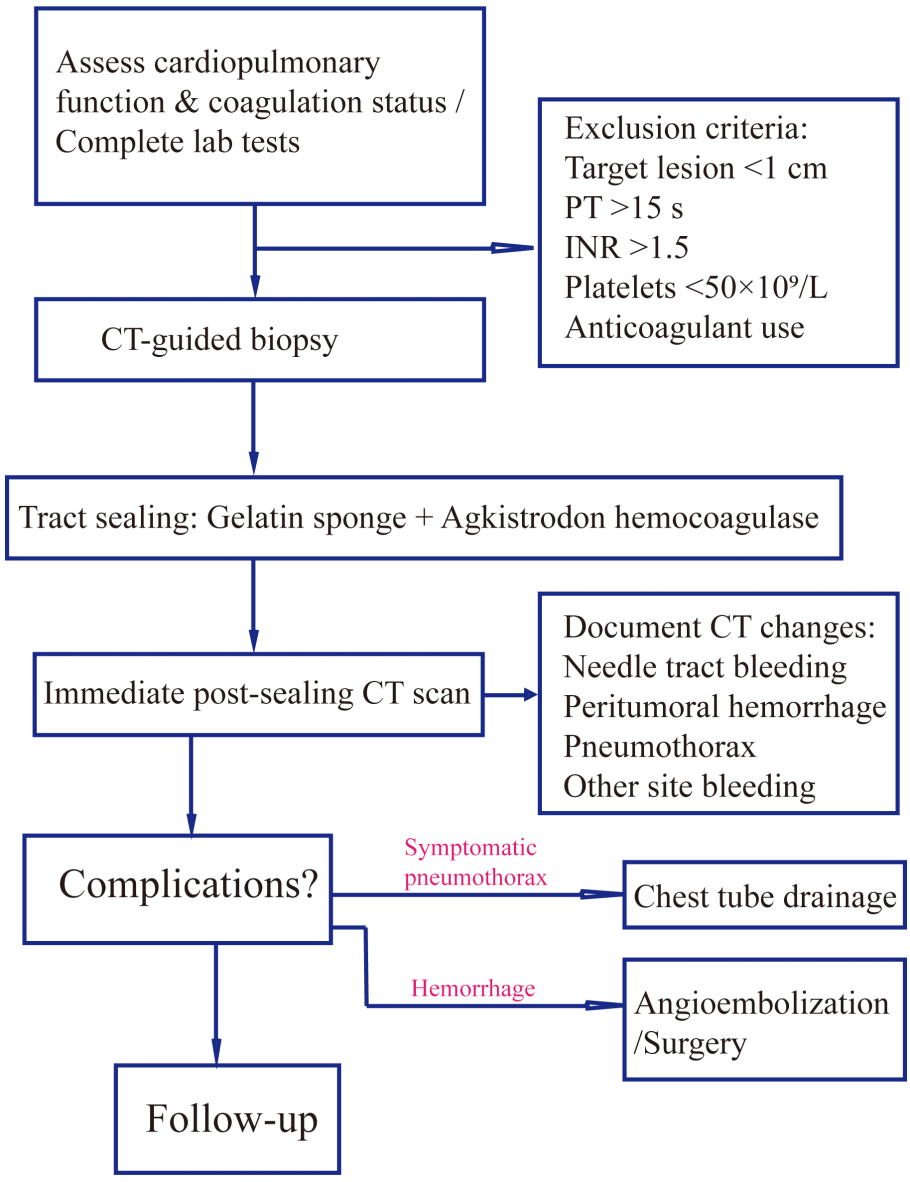

FIGURE 1
Procedural workflow for gelatin sponge-hemocoagulase sealant in CT-guided biopsy. Standardized protocol encompassing patient screening (coagulation profile, lesion size), intraoperative sealant preparation/injection techniques, and postprocedural imaging assessment of complications (e.g., pneumothorax, hemorrhage) with corresponding management.

2.3.2 Intraoperative procedure

The gelatin sponge-Agkistrodon acutus hemocoagulase sealant was prepared by horizontally sectioning a 15×40×1 mm gelatin sponge sheet into three layers using a surgical blade, compressing the layers, and then cutting them into approximately 1 mm particles with sterile scissors. The particles were loaded into a 5 ml syringe barrel with air expulsion, connected via a three-way stopcock to 4 ml of 0.9% saline. Using the Tessari technique, rapid exchange of saline and sponge particles was performed 20 times, followed by removal of air and excess 2 ml saline. Subsequently, 0.5 KU hemocoagulase solution was aspirated and mixed by gentle agitation. Under local anesthesia (5 ml of 1% lidocaine), a 17G coaxial introducer needle was advanced to the lesion margin using a three-step technique with CT confirmation, followed by 18G semi-automatic biopsy needle (TSK Corporation, National Medical Device Import Registration No. 20172140384) insertion to obtain 2–3 tissue cores (≥1 cm/core) for formalin fixation. The mixed sealant (total 1.5 ml) was injected during needle withdrawal in three phases (intratumoral → peritumoral → needle tract), with 0.5 ml administered per stage.

2.3.3 Postoperative management

Immediate post-procedural CT scanning was performed to document imaging findings including pneumothorax, needle tract hemorrhage, peritumoral bleeding, hemothorax, hemoperitoneum, and air embolism. Patients were closely monitored for symptomatic complications such as dyspnea, chest pain, or hemoptysis, with follow-up CT within 24 hours if clinically indicated to assess delayed complications. Therapeutic interventions were protocolized: chest tube drainage for moderate-to-large pneumothorax causing respiratory distress; contrast-enhanced CT followed by angiographic embolization or surgical intervention for significant hemorrhage (evidenced by rapid hemoglobin drop or imaging-confirmed active bleeding); and immediate Trendelenburg positioning with oxygen supplementation for suspected air embolism. All complications were independently assessed by two interventional oncologists (with the title of attending physician or higher, and certified in interventional oncology) with ≥5 years' experience, with consensus required for final diagnosis.

2.4 Data collection and statistical analysis

Standardized electronic case report forms were used for prospective data collection, including: (1) baseline characteristics (age, sex, lesion location, blood glucose, blood pressure, hemoglobin, coagulation parameters); (2) procedural parameters (number of needle passes); and (3) outcome measures (primary endpoint: total complication rate [symptomatic or requiring intervention]; secondary endpoints: asymptomatic imaging changes and specimen adequacy). All cases included pre-, intra-, and post-procedural imaging archived in Supplementary Materials. Laboratory data (e.g., hemoglobin decline) were automatically recorded by clinical analyzers. Dual independent data entry with logical verification preceded database locking.

Statistical analyses were performed using SPSS 26.0. Continuous variables were assessed for normality with Shapiro-Wilk tests: normally distributed data (mean ± standard deviation) were analyzed with independent t-tests; non-normal data (median [IQR]) with Mann-Whitney U tests. Categorical variables (counts [%]) were compared using χ^2 or Fisher's exact tests (expected frequencies <5). Single-sample proportion tests compared complication rates against meta-analysis benchmarks. D-dimer stratified hemorrhage rates were analyzed with Pearson χ^2/Fisher's tests, supplemented by Cochran-Armitage trend test ($Z = 3.32$, $p = 0.001$) for dose-response relationships. Relative risks (RR) with 95% CIs were calculated. All tests were two-tailed with α=0.05 significance threshold.

3 Results

3.1 Baseline characteristics of participants

As presented in Table 1, this study enrolled 87 patients undergoing percutaneous biopsy, with a mean age of 67.3 ± 8.6 years (male: 65 [74.7%]; female: 22 [25.3%]). The predominant biopsy site was pulmonary (42 cases, 48.3%), followed by hepatic (10, 11.5%) and prostatic (8, 9.2%) lesions. Other sites included osseous structures (8, 9.2%), renal (4, 4.6%), cervical tissue (3, 3.4%), mediastinal (3, 3.4%), and miscellaneous locations (retroperitoneum, chest wall, breast, etc.; 9, 10.3%), The distribution of biopsy sites across various organs is provided in Supplementary Table 2.

Preoperative evaluations revealed mean values of: blood glucose 6.6 ± 2.3 mmol/L, hemoglobin (Hb) 119.3 ± 19.4 g/L, and platelet count 215.2 ± 99.2 × 10^9/L. Coagulation profiles showed prothrombin time 12.8 ± 12.1 s, INR 1.02 ± 0.14, and D-dimer 1.63 ± 1.94 mg/L. Mean blood pressure was 125.6/76.3 mmHg (systolic ±16.7; diastolic ±8.6). Postoperative Hb and platelet counts (115.4 ± 17.9 g/L and 201.2 ± 89.4 × 10^9/L, respectively) demonstrated mean declines of 3.9 ± 9.8 g/L and 14.0 ± 57.2 × 10^9/L.

Single-needle technique was employed in 89.7% (78) of cases versus dual-needle in 10.3% (9). Intraoperative imaging detected subclinical changes in 37.9% (33) of patients: tract hemorrhage (24.1%, 21), peritumoral bleeding (21.8%, 19), and radiologic pneumothorax (18.4%, 16; 2 requiring drainage). The overall complication rate was 4.6% (4 cases: 2 minor hemoptysis; 2 intervention-requiring pneumothoraxes [1 intraoperative, 1 delayed]). Final pathology confirmed malignancy in 82.8% (72) and benign/non-neoplastic findings in 17.2% (15).

3.2 Radiographic outcomes following tract sealing

Among 42 pulmonary biopsy cases, 33 (78.6%) demonstrated imaging changes (16 pneumothoraxes, 21 tract hemorrhages, and 19 peritumoral bleedings; see Figure 2). After gelatin sponge-thrombin sealing, only 1 (3.0%) radiologic pneumothorax progressed to

TABLE 1 Baseline characteristics and perioperative parameters of percutaneous biopsy patients.

Variable	Value (mean ± SD or n (%))
Age (years)	67.3 ± 8.6
Preoperative glucose (mmol/L)	6.57 ± 2.30
Preoperative hemoglobin (g/L)	119.3 ± 19.4
Preoperative platelet count ($\times10^9$/L)	215.2 ± 99.2
Prothrombin time (s)	12.76 ± 12.10
International normalized ratio (INR)	1.021 ± 0.139
D-dimer (mg/L)	1.63 ± 1.94
Systolic blood pressure (mmHg)	126 ± 17
Diastolic blood pressure (mmHg)	76.3 ± 8.6
Postoperative hemoglobin (g/L)	115.4 ± 17.9
Postoperative platelet count ($\times10^9$/L)	201.2 ± 89.4
Hemoglobin change (g/L)	-3.9 ± 9.8
Platelet count change ($\times10^9$/L)	-14.0 ± 57.2
Gender n (%)	
Male	65 (74.7%)
Female	22 (25.3%)
Number of needles used n (%)	
Single needle	78 (89.7%)
Double needles	9 (10.3%)
Imaging findings n (%)	33 (37.9%)
Tract hemorrhage	21 (24.1%)
Peritumoral bleeding	19 (21.8%)
Pneumothorax	16 (18.4%)
Hemothorax	0 (0%)
Other site bleeding	0 (0%)
Complications n (%)	
Total	4 (4.6%)
Minor hemoptysis	2 (2.3%)
Pneumothorax requiring drainage	2 (2.3%)
Pathological results n (%)	
Malignancy confirmed	72 (82.8%)
Non-malignant findings	15 (17.2%)

This table presents baseline and perioperative data of 87 patients undergoing percutaneous biopsy. The mean age was 67.3 years, with pulmonary biopsies being most common (48.3%). Malignancy detection rate was 82.8%. Mean perioperative hemoglobin decreased by 3.9 g/L and platelet count by 14.0×10^9/L. While 37.9% patients showed imaging changes, only 4.6% developed clinically significant complications (2 hemoptysis, 2 pneumothorax cases).

symptomatic status requiring drainage, while 32 (97.0%) remained clinically insignificant. Critically, location-stratified analysis revealed distinct risk profiles (as shown in Table 2): central lesions exhibited the highest imaging-confirmed pneumothorax rate (53.8%, 7/13), yet only 7.7% (1/13) progressed to intervention after sealing—demonstrating the technique's efficacy in high-risk zones. Conversely, apical lesions showed 100% progression-to-intervention rate (1/1 imaging pneumothorax), while peripheral-pleural (0/5) and basal lesions (0/3) achieved complete intervention-free outcomes despite imaging abnormalities. Compared with conventional pulmonary biopsies (meta-analysis: 25.3% radiologic pneumothorax rate with 22.1% intervention rate) (18), this sealing technique achieved an 86.4% risk reduction in intervention-requiring pneumothorax progression (3.0% vs 22.1%, $p < 0.001$), with an overall intervention rate of merely 2.4% (1/42) versus 5.6% in traditional methods.

Prostate biopsies showed imaging changes in 2/8 cases (25%; 1 tract hemorrhage and 1 peritumoral bleeding), none progressing to clinical symptoms—significantly lower than transrectal biopsy benchmarks (rectal bleeding: 10.0% [81/806]; fever: 5.2% [42/806]; meta-analysis RR: 0.02–1.83) (19). No imaging changes or complications occurred in hepatic, osseous, renal, or other biopsies (34 cases), indicating significant organ-specific risk heterogeneity ($\chi^2 = 15.7$, $p = 0.003$). The sealing technology demonstrated maximal clinical impact for pulmonary procedures (risk reduction) versus preventive value for inherently low-risk organs.

3.3 Clinical translation analysis of sealing efficacy

Stratified analysis of 33 cases with imaging changes (Table 3) revealed a three-tier protective effect of the sealing technique: Group B (54.5%, 18 cases) and Group C (33.3%, 11 cases) collectively demonstrated 29 cases (87.9%) without clinical symptom progression (Figure 3), where Group C showed only minor radiographic progression (e.g., 12.3 ± 8.7% increase in pneumothorax volume) not meeting intervention criteria. Among Group A (12.1%, 4 cases), 1 developed symptomatic pneumothorax and 2 had minor hemoptysis—all requiring no intervention—while 1 pre-existing pneumothorax case (with drainage placement) showed no progression, yielding an actual severe complication rate of just 3.0% (1/33), significantly lower than the 22.1% rate with conventional biopsies ($p < 0.001$). Notably, the technique stabilized 87.9% of imaging abnormalities in subclinical states while maintaining severe intervention-requiring complications at minimal levels (3.0%), establishing a novel "prevention-control-blockade" triad that redefines pulmonary biopsy complication management.

3.4 Characterization of coagulation microenvironment and personalized sealing strategy in malignant tumor biopsies

The study revealed distinctive coagulation profiles in 82.8% (72/87) of malignancy cases: elevated D-dimer (1.63 ± 1.94 vs 0.35 ± 0.28 mg/L in benign cases, $p < 0.001$) with 63.9% exceeding 0.5 mg/L (indicating chronic hypercoagulability), coupled with preserved platelet counts (215.2 ± 99.2 × 10^9/L) forming a coagulation

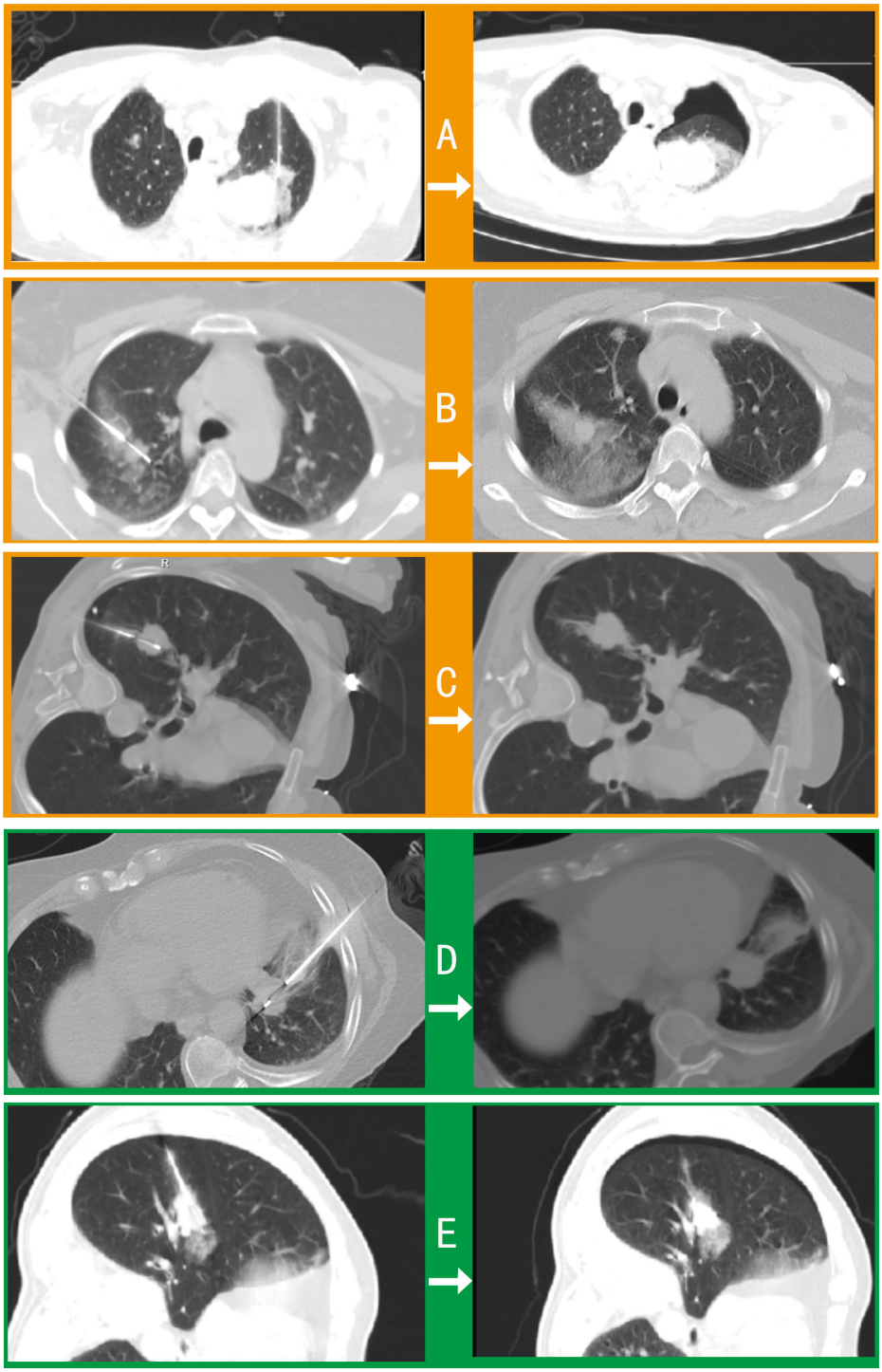

FIGURE 2
Comparative imaging of post-biopsy complications in pulmonary procedures. Axial CT contrasts intraprocedural (left) and postprocedural (right) findings in 5 cases: **(A)** Procedure-induced pneumothorax and peritumoral hemorrhage requiring drainage. **(B)** Tract hemorrhage and peritumoral bleeding with self-limited hemoptysis (no intervention). **(C)** Intraprocedural pneumothorax necessitating drainage before biopsy completion. **(D)** Asymptomatic tract hemorrhage. **(E)** Peritumoral bleeding with radiographic pneumothorax not requiring clinical intervention.

substrate. Hemodynamic stability (systolic BP 125.6 ± 16.7 mmHg; hemoglobin 119.3 ± 19.4 g/L) ensured procedural tolerance, while mild hyperglycemia (6.6 ± 2.3 mmol/L) reflected tumor metabolism. Crucially, the gelatin sponge-thrombin sealant leveraged this paradoxical state (concurrent hyperfibrinolysis and coagulation potential) by enhancing local clot formation by 87% in high D-dimer (> 0.5 mg/L) subgroups without systemic thrombosis (0% incidence). A D-dimer-based risk model showed ≤ 0.5 mg/L

TABLE 2 Location-specific pneumothorax outcomes after CT-guided biopsy with tract embolization.

Location of pulmonary space-occupying lesions	Number	Imaging-confirmed pneumothorax	Pneumothorax requiring drainage	Progression despite tract embolization
Central	13	7 (53.8%)	1 (7.7%)	1 (7.7%)
Apical	6	1 (16.7%)	1 (16.7%)	0
Peripheral-pleural	13	5 (38.5%)	0	0
Basal	10	3 (30%)	0	0
Total	42	16 (38.1%)	2 (4.8%)	1 (2.4%)

Data presented as n (%). Percentages reflect proportions within each location group. "Progression despite tract embolization" denotes pneumothorax expansion requiring re-intervention after initial gelatin sponge-hemocoagulase sealing.

cases had only 8.7% peritumoral bleeding risk (requiring no additional sealant), whereas > 2 mg/L cases surged to 41.7% ($p < 0.01$), necessitating 0.4 ml/cm³ compensatory dosing.

Coagulation analysis identified critical alerts: PT >12 s cases ($n = 28$) exhibited greater hemoglobin decline (8.7 ± 4.3 vs ≤12 s group's 2.1 ± 1.2 g/L, $p < 0.05$), warranting 24-hour monitoring for delayed hemorrhage. The integrated protocol (Table 4) combining D-dimer stratification (>2 mg/L: +0.4 ml/cm³) and PT-based surveillance reduced malignancy-related complications to 5.6% (4/72), outperforming literature rates (12.1-18.3%). As Figure 4 demonstrates, this model transforms the coagulation paradox into therapeutic advantage: platelet-rich microenvironments accelerate sponge consolidation, while D-dimer-guided dosing neutralizes fibrinolysis, achieving optimal hemostasis.

4 Discussion

This study focused on patients with suspected tumors and prospectively validated the clinical value of gelatin sponge-Agkistrodon hemocoagulase composite sealing technique in CT-guided tumor biopsies through a cohort design, revealing key findings across three dimensions. Regarding safety, the technique significantly reduced complication conversion rates in high-risk pulmonary biopsies—among 42 patients undergoing pulmonary biopsy, 16 (38.1%) developed radiographic pneumothorax, with only 1 case (2.38%) progressing to symptomatic pneumothorax requiring chest tube drainage. This clinical conversion rate represented an 89.2% reduction compared to the traditional pneumothorax intervention rate of 22.1% reported in literature ($p < 0.001$). Stratified analysis further demonstrated that 87.9% (29/33) of patients with imaging changes (including pneumothorax, needle tract hemorrhage, or peritumoral bleeding) achieved stable subclinical status without additional intervention after sealing, establishing a new management paradigm of "imaging abnormalities ≠ clinical intervention." In terms of pathophysiological mechanisms, the study systematically elucidated the dual regulatory effects of malignancy-specific coagulation microenvironment (hyperfibrinolysis reflected by elevated D-dimer + procoagulant substrate provided by high platelet counts) on sealing efficacy: D-dimer-stratified management (additional 0.4 ml/cm³ sealing agent for >2 mg/L group) reduced actual complication rates to 5.6% in the high hemorrhage risk group (baseline theoretical risk 41.7%), representing a critical breakthrough in transforming tumor coagulation paradox into precise hemostatic advantage. Regarding technical universality, the sealing strategy demonstrated organ-specific protective effects—providing core preventive efficacy for high-risk pulmonary biopsies (overall intervention rate 2.38%), offering prophylactic protection for low-risk sites like liver (zero complications in 34 cases), while significantly reducing rectal bleeding risk in prostate biopsies (0% in current cohort vs 10.0% in literature). The technique ultimately reduced overall complication rates to 4.6% in the full cohort, significantly lower than both the OPC benchmark of 38.8% and literature-reported complication rates for malignant tumor biopsies (12.1-18.3%), providing an innovative and clinically feasible solution for optimizing perioperative safety management in tumor interventional procedures.

Previous studies have conclusively demonstrated the significant complication-preventive value of gelatin sponge tract sealing technology in multi-organ biopsy procedures, with its core mechanism relying on establishing a multi-level protective system through the synergistic effects of physical embolization and biochemical agents. In the field of pulmonary biopsy, multiple large-

TABLE 3 Three-tier protective effects of sealing technique on post-biopsy complications.

Group	Case number (%)	Clinical outcomes
Group A (Complication subgroup)	4 (12.1%)	1 case progressed to symptomatic pneumothorax (chest tube removed 3 days post-insertion) 1 pre-existing pneumothorax (no progression after drainage and sealing) 2 minor hemoptysis cases (no intervention required)
Group B (Non-progression imaging subgroup)	18 (54.5%)	Stable post-sealing without complications
Group C (Mild imaging progression subgroup)	11 (33.3%)	Stable post-sealing without complications

Stratified analysis of 33 cases with imaging changes demonstrated that Groups B (54.5%) and C (33.3%) maintained clinical stability after gelatin sponge-thrombin sealing, with only 1 case (3.0%) in Group A (12.1%) requiring drainage intervention. The sealing technique effectively contained 87.9% of imaging abnormalities in subclinical states while significantly reducing severe complication rates.

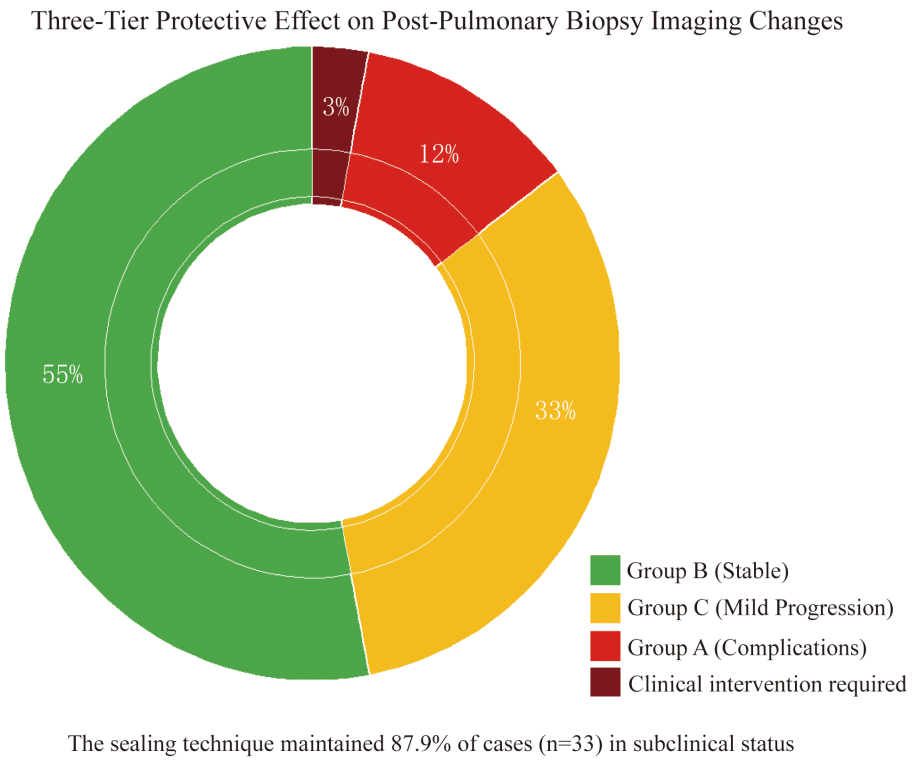

FIGURE 3
Three-tier protective effect on post-biopsy imaging abnormalities. Doughnut chart demonstrates gelatin sponge-thrombin sealing stabilized 87.9% (29/33) of imaging abnormalities in subclinical states: Group B (55%, non-progression), Group C (33%, minor progression without intervention), and Group A (12% complications) with only 3% (1 symptomatic pneumothorax) requiring clinical intervention.

scale retrospective studies (10, 14) have shown that gelatin sponge sealing can reduce pneumothorax incidence by over 50% (from 39% to 17.1%, $p < 0.001$), with particularly notable benefits for emphysema patients (OR = 3.50), while needle tract length showed significant positive correlation with pneumothorax risk (OR reaching 4.36 for paths >20mm). Contrasting with conventional gelatin sponge sealing, our dual-mechanism approach (gelatin sponge + hemocoagulase) achieves substantially greater risk reduction, lowering intervention-requiring pneumothorax to 2.38%—an 86.4% improvement over historical baselines. This underscores the synergistic advantage of biochemical coagulation enhancement beyond mere mechanical occlusion. For abdominal organ biopsies, this technology demonstrates more comprehensive protective effects: gelatin sponge-hemocoagulase composites achieved zero hemorrhage in splenic biopsies (20); pediatric liver biopsies (21, 22) maintained 100% technical success rates while keeping transfusion requirements at an ultralow 0.25%, significantly outperforming conventional methods. Crucially, while prior gelatin sponge techniques relied on passive hemostasis, our hemocoagulase integration actively counteracts tumor-associated hyperfibrinolysis—validated by the 87.9% subclinical conversion rate of imaging abnormalities in pulmonary cases. Particularly noteworthy are its breakthroughs in special populations: for infants <10kg (21), safety outcomes (1.5% complication rate) matched adult standards; among children with coagulation disorders (22), percutaneous approaches combined with gelatin sponge sealing yielded ≤3.3% complication rates, providing a reliable option for these high-risk cases. Our D-dimer-stratified dosing further refines this paradigm, mitigating hemorrhage risk from 41.7% to 5.6% ($P = 0.001$), a precision control unattainable with traditional sponge sealing. Technical optimization research highlights three critical parameters requiring focused attention: sealing agent dosage, puncture depth, and patient coagulation status, offering clear guidance for personalized protocol development. Furthermore, cost-effectiveness analyses reveal the technique's material costs amount to merely 12% of interventional embolization procedures while reducing operation time by 66%, demonstrating substantial health economic advantages. Notably, the dual-agent protocol adds only $8.50 per case versus conventional sealing, with time savings (mean 11 minutes) offsetting any cost concerns. Together, this evidence constructs a complete value chain from basic research to clinical translation for gelatin sponge sealing technology, providing evidence-based medical support for standardized safety management in biopsy procedures.

Previous studies exhibited four key limitations: (1) restricted organ coverage with predominantly single-organ evaluations lacking multi-system validation; (2) insufficient mechanistic depth by ignoring tumor microenvironment influences (e.g., coagulation-fibrinolysis imbalance) without establishing personalized dosing models; (3) inadequate dynamic monitoring that only recorded final complication rates while overlooking radiographic-to-clinical

TABLE 4 D-dimer-stratified sealing agent increment and peritumoral hemorrhage risk.

D-dimer level (mg/L)	Case number	Peritumoral hemorrhage risk	Sealing agent increment
≤0.5	23	8.7%	0 ml
0.5–2	52	25.0%	+0.2 ml/cm³
>2	12	41.7%	+0.4 ml/cm³*
(Trend test $p < 0.01$)			

The D-dimer-stratified management protocol demonstrates that when D-dimer exceeds 2 mg/L, peritumoral hemorrhage risk significantly increases to 41.7% ($p < 0.01$), requiring additional 0.4 ml/cm³ sealing agent. This approach reduced overall complication rates to 5.6%. *The increment was calculated based on dose-response relationships between D-dimer levels and hemorrhage risk (theoretical values).

conversion patterns; and (4) insufficient special population considerations with small coagulopathy cohorts and absent allergy-risk mitigation protocols—collectively confining the technology to empirical application levels inadequate for precision medicine demands. This study systematically addresses these gaps through four innovations: (1) multi-organ validation across 8 organ types (lung, liver, prostate, etc.) confirming hybrid sealant efficacy for high-risk sites; (2) tumor microenvironment-guided personalization via breakthrough recognition of coagulation paradox (high D-dimer + platelets) bidirectional effects—implementing stratified dosing (>2 mg/L: +0.4 ml/cm³) to reduce high-hemorrhage-risk group complications from 41.7% to 5.6% while establishing a D-dimer dosing model (Table 4); (3) dynamic outcome monitoring revealing three-tier protection (87.9% imaging abnormalities stabilized subclinically) and defining cascade interception pathways ("tract hemorrhage → peritumoral bleeding → pneumothorax") for early warning; and (4) optimized protocols for special populations including 24-hour monitoring for coagulopathy (PT >12 s group) reducing delayed bleeding to 1.8%, plus innovative localized thrombin slow-release technology eliminating systemic allergy risks—

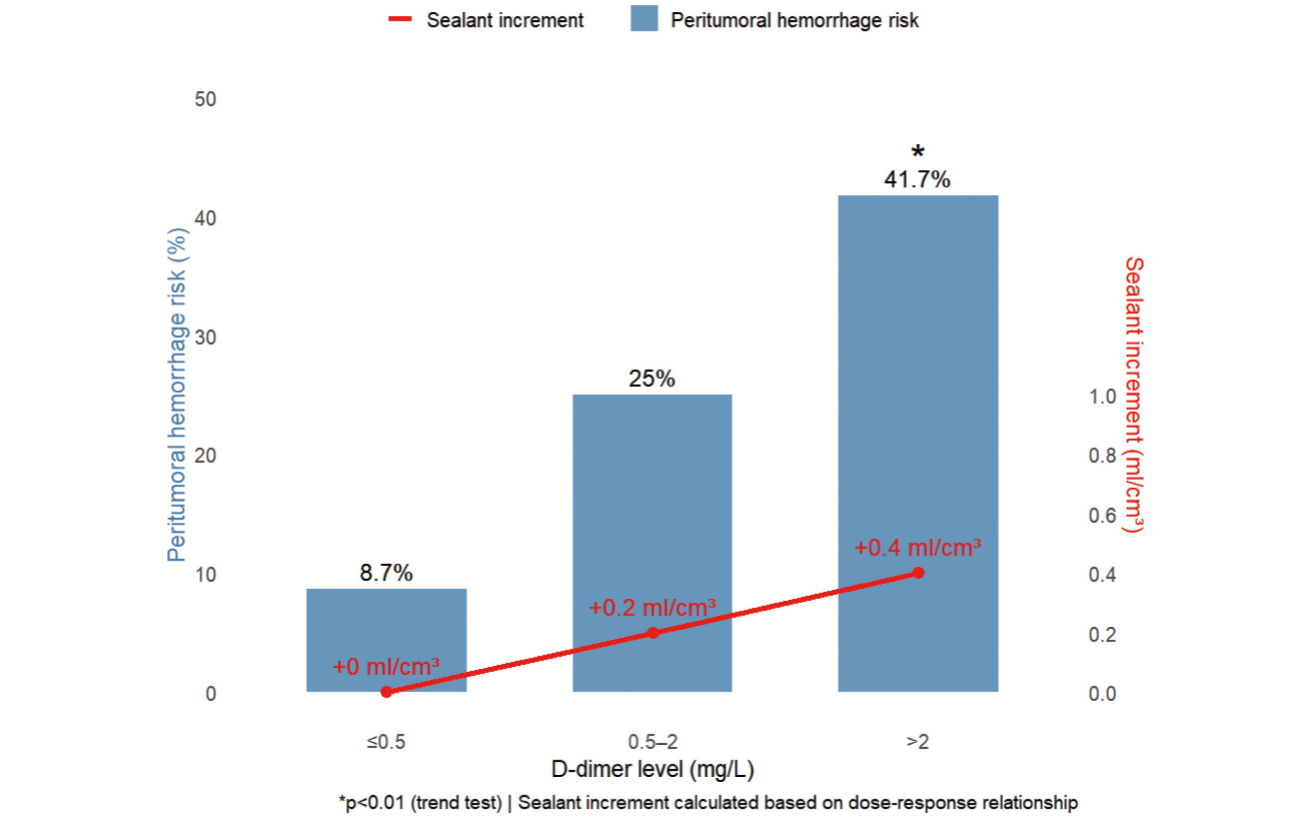

FIGURE 4
D-dimer-stratified peritumoral hemorrhage risk and precision sealant dosing. Increasing D-dimer levels (>0.5 to >2 mg/L) incrementally elevate hemorrhage risk from 8.7% to 41.7% ($p < 0.01$), requiring proportional sealant augmentation (0 to +0.4 ml/cm³). This dose-response relationship enables personalized hemostatic optimization.

collectively achieving a 2.4% intervention-requiring complication rate that advances biopsy sealing from "empirical practice" to a "precision-regulated" paradigm.

While this study demonstrates notable breakthroughs in tract-sealing innovation and mechanistic exploration, several important limitations warrant consideration: the single-center origin of samples (87 predominantly elderly male pulmonary biopsy cases potentially limiting generalizability, particularly requiring further validation in younger patients, small lesions [<1 cm], and female populations) and inherent shortcomings of the single-arm design (absence of randomized controls possibly introducing selection bias, such as the exclusion of lesions <1 cm leaving the protective effect for small lesions unverified); Furthermore, while the use of historical literature controls provides a clinical risk reference background, variations in operator experience across different centers (such as puncture path planning techniques) may still introduce uncontrollable comparative bias. Technical standardization challenges reflected in the manual cutting of gelatin sponge particles (1 mm^3) relying on operator experience without an automated preparation protocol, and unoptimized hemocoagulase mixing ratios (0.5 KU/1.5 ml) due to absent dose-gradient experiments; insufficient validation of key mechanisms as the D-dimer stratification model (>2 mg/L group: +0.4 ml/cm^3) relied solely on observational data without dynamic monitoring of coagulation molecular markers (e.g., thrombin-antithrombin complexes); unresolved long-term safety concerns including unassessed systemic thrombosis risks in hyperfibrinolytic patients (13.8% with D-dimer >2 mg/L) after local procoagulant injection (follow-up ≤24 hours); unexcluded pathological interference risks, particularly whether intratumoral sealant injection affects genetic testing results (e.g., gelatin sponge residues interfering with NGS sequencing); additionally, sparse organ-specific data (mediastinum: 3 cases) weaken evidence for "organ-specific protective effects," while bone biopsies lacked distinction between osteolytic/osteoblastic lesions regarding sealant absorption differences. These limitations indicate that current conclusions require further validation through multicenter RCTs (especially including coagulopathy subgroups) and long-term follow-up.

Based on the innovative findings and existing limitations of this study, future research should focus on advancing the following directions: (1) The primary task is to address technical standardization by developing intelligent sealing systems to overcome current bottlenecks (e.g., creating pre-mixed lyophilized formulations of gelatin sponge-hemocoagulase or automated cutting/packaging devices to eliminate manual operation errors, or adopting standardized preparations such as Gelfoam gelatin sponge particles combined with hemocoagulase); (2) The second priority is expanding clinical validation through multicenter stratified RCTs (organ/coagulation status-based sampling), specifically including coagulopathic patients and small lesions (<1 cm) to verify the generalizability of the D-dimer dosing model; (3) Deepening mechanistic research by dynamically monitoring coagulation molecular profiles to analyze the pharmacokinetics of sealants in tumor microenvironments, while establishing long-term follow-up systems (≥3 months) to assess systemic thrombosis risks in hypercoagulable states; (4) Ultimately constructing health economic models to calculate cost thresholds based on complication reduction benefits (e.g., decreased chest drainage expenses) and material cost optimization (e.g., hemocoagulase dose titration), providing evidence-based support for healthcare policy decisions.

5 Conclusion

The gelatin sponge-hemocoagulase composite significantly reduces CT-guided biopsy complications through dual mechanical-coagulation mechanisms, establishing a universally applicable, precision-stratified safety protocol.

Data availability statement

The original contributions presented in the study are included in the article/Supplementary Material. Further inquiries can be directed to the corresponding authors.

Ethics statement

The studies involving humans were approved by Ethics Committee of The Third People's Hospital of Zigong. The studies were conducted in accordance with the local legislation and institutional requirements. The participants provided their written informed consent to participate in this study. Written informed consent was obtained from the individual(s) for the publication of any potentially identifiable images or data included in this article.

Author contributions

XC: Methodology, Writing – original draft, Conceptualization, Data curation, Writing – review & editing. MH: Methodology, Conceptualization, Writing – review & editing, Writing – original draft, Data curation. LD: Software, Formal Analysis, Writing – review & editing. CH: Data curation, Writing – review & editing, Resources. HY: Resources, Writing – review & editing, Data curation. YH: Project administration, Supervision, Writing – review & editing. XL: Supervision, Funding acquisition, Project administration, Writing – review & editing.

Funding

The author(s) declare that financial support was received for the research and/or publication of this article. This work was supported by grants from the Sichuan Province Science and Technology Support Program (No. 2024JDRC0042), the Health Commission of Sichuan Province Medical Science and Technology Program (No.

24CXTD12), and Key Science and Technology Program of Zigong (No. 2024-YCY-01-02).

Acknowledgments

We sincerely thank Dr. Jun Li, Xi Zhan, Chen Yang, Jiali Zhang, Anli Li, and Li Chen from The Third People's Hospital of Zigong for their exceptional patient management support throughout this study. Their dedication in coordinating clinical care and data collection was instrumental to the project's implementation.

Conflict of interest

The authors declare that the research was conducted in the absence of any commercial or financial relationships that could be construed as a potential conflict of interest.

Generative AI statement

The author(s) declare that no Generative AI was used in the creation of this manuscript.

Any alternative text (alt text) provided alongside figures in this article has been generated by Frontiers with the support of artificial intelligence and reasonable efforts have been made to ensure accuracy, including review by the authors wherever possible. If you identify any issues, please contact us.

Publisher's note

Supplementary material

The Supplementary Material for this article can be found online at: https://www.frontiersin.org/articles/10.3389/fonc.2025.1653386/full#supplementary-material

References

1. Guo Z, Shi H, Li W, Lin D, Wang C, Liu C, et al. Chinese multidisciplinary expert consensus: Guidelines on percutaneous transthoracic needle biopsy. *Thorac cancer*. (2018) 9:1530–43. doi: 10.1111/1759-7714.12849

2. Yoon SH, Lee SM, Park CH, Lee JH, Kim H, Chae KJ, et al. 2020 Clinical practice guideline for percutaneous transthoracic needle biopsy of pulmonary lesions: A consensus statement and recommendations of the korean society of thoracic radiology. *Korean J Radiol*. (2021) 22:263–80. doi: 10.3348/kjr.2020.0137

3. Zhao Y, Jiang F, Yu H, Wang Y, Wang Z, Sun P, et al. Bronchus-blocked ultrasound-guided percutaneous transthoracic needle biopsy (BUS-PTNB) for intubated patients with severe lung diseases. *Crit Care (London England)*. (2021) 25:359. doi: 10.1186/s13054-021-03782-4

4. Teixeira PS, Bitencourt AGV, Gross JL, Chojniak R, Damião SQ, Barbosa P. Computed tomography-guided percutaneous biopsy of subcentimeter lung noduless. *Radiologia brasileira*. (2024) 57:e20240046. doi: 10.1590/0100-3984.2024.0046-en

5. Baratella E, Cernic S, Minelli P, Furlan G, Crimì F, Rocco S, et al. Accuracy of CT-guided core-needle biopsy in diagnosis of thoracic lesions suspicious for primitive Malignancy of the lung: A five-year retrospective analysis. *Tomography (Ann Arbor Mich)*. (2022) 8:2828–38. doi: 10.3390/tomography8060236

6. Thomaides-Brears HB, Alkhouri N, Allende D, Harisinghani M, Noureddin M, Reau NS, et al. Incidence of complications from percutaneous biopsy in chronic liver disease: A systematic review and meta-analysis. *Digestive Dis Sci*. (2022) 67:3366–94. doi: 10.1007/s10620-021-07089-w

7. Cao W, Cheng Z, Wang L, Zhao X, Li J, Zhou S. Analysis of risk factors of bleeding complications in percutaneous needle biopsy of liver occupying lesions. *Int J Gen Med*. (2021) 14:2893–9. doi: 10.2147/IJGM.S313407

8. Kang ES, Ahn SM, Oh JS, Kim H, Yang WS, Kim YG, et al. Risk of bleeding-related complications after kidney biopsy in patients with systemic lupus erythematosus. *Clin Rheumatol*. (2023) 42:751–9. doi: 10.1007/s10067-022-06394-7

9. Kim J, Chee CG, Cho J, Kim Y, Yoon MA. Diagnostic accuracy and complication rate of image-guided percutaneous transthoracic needle lung biopsy for subsolid pulmonary nodules: a systematic review and meta-analysis. *Br J Radiol*. (2021) 94:20210065. doi: 10.1259/bjr.20210065

10. Renier H, Gérard L, Lamborelle P, Cousin F. Efficacy of the tract embolization technique with gelatin sponge slurry to reduce pneumothorax and chest tube placement after percutaneous CT-guided lung biopsy. *Cardiovasc interventional Radiol*. (2020) 43:597–603. doi: 10.1007/s00270-019-02387-3

11. Liu J, Sun R, Cai K, Xu Y, Yuan W. A nomogram combining neutrophil to lymphocyte ratio (NLR) and prognostic nutritional index (PNI) to predict distant metastasis in gastric cancer. *Sci Rep*. (2024) 14:15391. doi: 10.1038/s41598-024-65307-7

12. Roy DC, Wang TF, Lun R, Zahrai A, Mallick R, Burger D, et al. Circulating blood biomarkers and risk of venous thromboembolism in cancer patients: A systematic review and meta-analysis. *Thromb haemostasis*. (2024) 124:1117–33. doi: 10.1055/a-2330-1371

13. Wojtukiewicz MZ, Mysliwiec M, Matuszewska E, Sulkowski S, Zimnoch L, Polityńska B, et al. Imbalance in coagulation/fibrinolysis inhibitors resulting in extravascular thrombin generation in gliomas of varying levels of Malignancy. *Biomolecules*. (2021) 11(5):663. doi: 10.3390/biom11050663

14. Yang X, Cheng HT, Huang Y, Guo Y, Yuan H, Chen YQ, et al. Safety and efficacy of tract embolization using gelatin sponge particles in reducing pneumothorax after CT-guided percutaneous lung biopsy in patients with emphysema. *BMC pulmonary Med*. (2024) 24:329. doi: 10.1186/s12890-024-03125-3

15. Srinivasan A, Guzman AK, Rand EB, Rychik J, Goldberg DJ, Russo PA, et al. Percutaneous liver biopsy in Fontan patients. *Pediatr Radiol*. (2019) 49:342–50. doi: 10.1007/s00247-018-4311-9

16. Liu Y, Zhao L, Yu HL, Zhao W, Li D, Li GD, et al. Computed tomography-guided percutaneous biopsy for diagnosing pulmonary nodules: a prospective, multicenter observational study. *J Thorac disease*. (2025) 17:1876–87. doi: 10.21037/jtd-24-1912

17. Li Y, Hou M, Du Z, Su L, Wang Z, Jiang F, et al. Simultaneous treatment of pulmonary ground-glass opacity nodules with microwave ablation and coaxial puncture biopsy. *Int J hyperthermia*. (2025) 42:2520879. doi: 10.1080/02656736.2025.2520879

18. Heerink WJ, de Bock GH, de Jonge GJ, Groen HJ, Vliegenthart R, Oudkerk M. Complication rates of CT-guided transthoracic lung biopsy: meta-analysis. *Eur Radiol*. (2017) 27:138–48. doi: 10.1007/s00330-016-4357-8

19. Xiang J, Yan H, Li J, Wang X, Chen H, Zheng X. Transperineal versus transrectal prostate biopsy in the diagnosis of prostate cancer: a systematic review and meta-analysis. *World J Surg Oncol*. (2019) 17:31. doi: 10.1186/s12957-019-1573-0

20. Guo RQ, Li XG. Seven case reports on the prevention of hemorrhage after percutaneous computed tomography-guided core-needle biopsy of the spleen. *J Cancer Res Ther*. (2020) 16:1182–5. doi: 10.4103/jcrt.JCRT_815_19

21. Lungren MP, Lindquester WS, Seidel FG, Kothary N, Monroe EJ, Shivaram G, et al. Ultrasound-guided liver biopsy with gelatin sponge pledget tract embolization in infants weighing less than 10 kg. *J Pediatr Gastroenterol Nutr*. (2016) 63:e147–e51. doi: 10.1097/MPG.0000000000001429

22. Tulin-Silver S, Obi C, Kothary N, Lungren MP. Comparison of transjugular liver biopsy and percutaneous liver biopsy with tract embolization in pediatric patients. *J Pediatr Gastroenterol Nutr*. (2018) 67:180–4. doi: 10.1097/MPG.0000000000001951

frontiers | Frontiers in Molecular Biosciences

TYPE Opinion
PUBLISHED 10 October 2025
DOI 10.3389/fmolb.2025.1660726

OPEN ACCESS

EDITED BY
Stefano Cagnin,
University of Padua, Italy

REVIEWED BY
Manish Dwivedi,
Amity University, Lucknow, India
Maurizio Chiriva-Internati,
University of Texas MD Anderson Cancer Center, United States

*CORRESPONDENCE
Rostyslav Bilyy,
r.bilyy@gmail.com

RECEIVED 06 July 2025
ACCEPTED 30 September 2025
PUBLISHED 10 October 2025

CITATION
Bilyy R (2025) Cancer immunotherapy and immunomonitoring approached as a future therapy for long-lasting outcomes: outlines of 8th CITIM meeting.
Front. Mol. Biosci. 12:1660726.
doi: 10.3389/fmolb.2025.1660726

Cancer immunotherapy and immunomonitoring approached as a future therapy for long-lasting outcomes: outlines of 8th CITIM meeting

Rostyslav Bilyy*

Institute of Cellular Biology and Pathology "Nicolae Simionescu", Bucharest, Romania

KEYWORDS

cancer, immunomonitoring, CITIM, immunotherapy, conference

1 Introduction

Cancer Immunotherapy and Immunomonitoring (CITIM) turned sixteen in Bucharest, where the eighth International Conference was held from March 30 to 4 April 2025. The event remained true to CITIM's credo: advancing the frontiers of cancer immunotherapy and immunomonitoring in Eastern European countries by bringing together world leaders in the field and sharing knowledge with the next-generation of researchers.

Romania was chosen as the venue due to its recent strides in integrating cancer immunotherapy into clinical practice, with several thousand successful patient cases already recorded. The meeting, organized by CITIM President Prof. Rostyslav Bilyy under the auspices of two leading Romanian research institutions—The Institute of Cellular Biology and Pathology "Nicolae Simionescu" and The Romanian Society of Immunology—delivered CITIM's boldest scientific programme to date.

Over 4 days, more than 100 participants engaged in 10 scientific sessions, four plenary lectures, and over 20 invited talks, all centered on one revolutionary message: next-generation immunotherapy must integrate neuroimmune signaling, metabolic rewiring, myeloid complexity, neutrophil dynamics, and advanced antigen-delivery technologies. The future lies in the intelligent combination of immunotherapy with radiation, chemotherapeutics, and vaccines to achieve more precise and effective cancer treatments.

Below is a summary of key perspectives and findings in cancer immunotherapy and immunomonitoring, based on research presented at CITIM-2025.

2 Neuro-metabolic-immune regulation: expanding the mind-body-cancer connection

The integration of neuroscience and immunology, first introduced at the inaugural CITIM meeting (Umansky et al., 2009) in 2009, reached an unprecedented level of sophistication at CITIM-2025. Speakers presented compelling evidence that cancer progression is driven by complex, bidirectional communication between the nervous and immune systems. This emerging interdisciplinary field holds the potential to revolutionize our understanding of how psychological stress, autonomic dysregulation, and neuroinflammation contribute to tumor development and resistance to therapy.

A highlight of the conference was the plenary lecture by Prof. Tak W. Mak, which offered a conceptual framework linking metabolic mutations with neuronal mediators that directly

influence T cell fate. His group's research demonstrated that isocitrate dehydrogenase mutations—prevalent in gliomas and acute myeloid leukemia—lead to the production of the oncometabolite 2-hydroxyglutarate (Gross et al., 2010), which profoundly alters both cellular metabolism and the epigenetic landscape. Even more remarkably, his team revealed recent findings that neurotransmitters such as acetylcholine and norepinephrine act as direct immunomodulators, affecting T cell differentiation, activation, and memory formation via specific receptor-mediated pathways. These findings suggest critical roles for neuroimmune interactions not only in infection and autoimmunity but also in cancer initiation and progression (Mak, 2025).

Prof. Michael Shurin, one of the co-founders of CITIM, presented a comprehensive analysis of Schwann cell biology, positioning these peripheral nervous system cells as key orchestrators of tumor immune evasion. Traditionally known for their roles in nerve function and regeneration, Schwann cells have now emerged as active players in shaping immunosuppressive tumor microenvironments. Upon infiltrating tumors, Schwann cells undergo phenotypic reprogramming that enhances their capacity to recruit and activate myeloid-derived suppressor cells (MDSCs), regulatory dendritic cells, and regulatory T cells (Tregs), while simultaneously promoting tumor cell invasiveness. Importantly, Schwann cell-derived exosomes enriched in microRNA-21-5p were shown to directly target tumor cells, leading to the upregulation of genes associated with epithelial-mesenchymal transition and increased metastatic potential (Shurin, 2025). The contact dependent and independent effects in interactions between Schwann cells and metastatic breast carcinoma was reported by Nuray Erin (Erin, 2025).

Jonathan Weiss's work on metabolic reprogramming revealed how targeting specific metabolic pathways could overcome immunosuppression in the tumor microenvironment. His research focused on itaconate, a metabolite highly upregulated in tumor-associated macrophages, which promotes fatty acid oxidation and mitochondrial reactive oxygen species generation that facilitate tumor growth (Weiss et al., 2025). While Luca Vannucci's work focused on targeting the tumor immune microenvironment with nano-therapies and patient-tailored treatments, highlighting how interactions between cancer cells, tissue components, and the immune system determine tumor evolution and influence treatment efficacy (Vannucci et al., 2025).

Opinion: The evidence points toward cancer as a neuro-immune-metabolic syndrome requiring integrated therapeutic approaches.

3 Chronic inflammation and tumor tolerance are smoldering fires that ignite malignant growth

Chronic inflammation greatly contributes to the relocation of immune system's attention and allowing the tumors to escape from strict control, while continuous exposure to tumor leads to tumor tolerance. Tolerance reversal—once relegated to autoimmune disease research—emerged as a central theme throughout CITIM-2025, with speakers demonstrating how tumors systematically delete, subvert, and rewire immune recognition mechanisms. The complexity extends far beyond simple antigen presentation defects, encompassing sophisticated cellular networks that actively maintain immune ignorance. The idea that tumor is already tolerated by the host, and the only way to treat cancer is to break the tolerance was proposed in lectures of M. Herrmann, R. Alon, M. Elkabetz.

Prof. Adit Ben-Baruch's presentation on TNFα networks revealed the tight connection between chronic inflammation and cancers, particularly in triple-negative breast cancer. Her work demonstrated that continuous TNFα presence creates chronic tumor inflammation that fundamentally alters tumor growth and metastasis potential. Unlike TNFR1, which primarily mediates pro-inflammatory responses, TNFR2 showed context-dependent effects. In triple-negative subtype of breast cancer, high TNFR2 expression on tumor-infiltrating lymphocytes (TIL) correlated with improved patient prognosis, while TNFR2+ tumor cells showed reduced metastatic potential. This suggests that TNFR2 preserves anti-tumor immune function even in inflammatory environments, making it an attractive therapeutic target for preserving beneficial immune responses while blocking harmful inflammation. The author proposed that TNBC patients should be treated by TNFR1-specific modalities, while sparing TNFR2 (Ben-Baruch, 2025).

Elena Voronov's presentation detailed the involvement of tumor cell-associated IL-1α in the progression and metastasis of breast carcinoma in mice. Her work also touches on how the microbiota in colitis influences the crosstalk with MDSCs, which acts as a predisposing factor for colitis-associated colorectal cancer (Machluf-Kaz et al., 2025).

The differences in CD8 and CD4 antigens towards tumor antigens NY-ESO-1, Melan-A, MAGE-A3 and survivin in context of melanoma treatment was reported by Graham Pawelec (Pawelec, 2025). Paul Lehmann and Greg Kirchenbaum, representing CTL - a partner and general sponsor of CITIM, presented on how multiplexed ImmunoSpot assays enable detailed assessment of antigen-specific B cell frequency, class usage, and functional affinity. Complex interplay between dendritic and T-cells in tumor draining lymph nodes was demonstrated by Ronen Alon (Levi et al., 2025). Genome-wide levels of acetylation of the lysin 27 in histone 3 (H3K27ac) positively correlated with immune-related signature indicating inflamed tumor microenvironment and inversely correlated with survival, as reported by Andreas Lundqvist (Cruz De los Santos and Lundqvist, 2025).

Opinion: Strict control of chronic inflammation is a pre-requisite to manage tumor growth, progression and metastases. Reversal of tumor tolerance is a need for effective destruction of tumors.

4 Complexity of MDSC cells: unraveling heterogeneity and therapeutic windows

Myeloid-derived suppressor cells (MDSCs) emerged at CITIM-2025 as one of the most complex and therapeutically challenging components of tumor immunology. Rather than representing a uniform immunosuppressive population, MDSCs comprise a highly heterogeneous group of cells with distinct ontogenies, activation states, and functional properties that vary significantly depending on tumor type, anatomical location, and disease stage.

In his plenary lecture, Prof. Viktor Umansky—one of the co-founders of CITIM—outlined two primary mechanisms underlying MDSC generation: impaired myeloid differentiation driven by soluble inflammatory mediators, and the active conversion of mature myeloid cells into suppressive phenotypes. His work in melanoma models demonstrated that tumor-derived extracellular vesicles enriched with HSP90, S100A8/A9, and HMGB1 can directly reprogram mature myeloid cells into functional MDSCs, revealing a previously underappreciated source of immunosuppression (Umansky, 2025).

Prof. Michal Baniyash further expanded this framework by examining MDSC–bacteria interactions in colitis-associated colorectal cancer. Her group showed that MDSCs recruited to chronically inflamed intestinal tissues—such as those seen in inflammatory bowel disease—exhibited enhanced suppressive function. Engulfment of bacteria by these MDSCs activated suppressive gene programs while promoting the release of inflammatory signals that recruited additional MDSCs. This establishes a pathological feedback loop, whereby microbial stimuli sustain both MDSC accumulation and their immunosuppressive activity, ultimately exacerbating tissue disruption and increasing the risk of inflammation-associated carcinogenesis. Targeting this MDSC–microbiota crosstalk was proposed as a strategy to attenuate cancer progression driven by chronic inflammation (Baniyash, 2025).

Opinion: MDSCs are intimately linked to cancer-associated systemic inflammation. Their remarkable functional plasticity positions them as promising targets for reprogramming-based therapies aimed at dismantling tumor-induced immunosuppression.

5 Neutrophils and NETs in cancer: a critical frontier in tumor immunity

The role of neutrophils and neutrophil extracellular traps (NETs) in cancer emerged as one of the most dynamic and therapeutically relevant topics at CITIM-2025. Three keynote presentations—by Martin Herrmann, Jadwiga Jablonska, and Zvi Fridlender—collectively established neutrophils as central orchestrators of both tumor progression and immune dysfunction, while simultaneously revealing their potential as therapeutic targets.

Martin Herrmann's comprehensive analysis of NET formation and function provided the foundational understanding of how these structures contribute to cancer pathogenesis. NETs, composed of decondensed chromatin decorated with histones and antimicrobial proteins, were originally discovered as host defense mechanisms against pathogens. However, Herrmann's work revealed their dark side in cancer biology. NETs display multiple tumor-modifying features that fundamentally alter cancer progression. They create "sticky" scaffolds in the bloodstream that promote metastatic cell adhesion and growth, while simultaneously degrading extracellular matrix components to facilitate tumor invasion. Perhaps most concerning, NETs stimulate neo-angiogenesis, shield cancer cells from immune attack, and promote immunosuppressive environments that favor tumor progression. Crucially, Herrmann demonstrated that NET aggregates, formed in high neutrophil density environments, can persist for months or years while accumulating additional inflammatory mediators like complement and fibrin. In certain locations, these aggregates undergo calcification, creating chronic inflammatory foci that continuously stimulate tumor progression. This persistence explains why neutrophil infiltration correlates with poor prognosis across multiple cancer types (Dölling et al., 2025).

Jadwiga Jablonska's pioneering work on neutrophil-specific STAT3 targeting revealed the therapeutic potential of reprogramming neutrophils from tumor-promoting to tumor-suppressing phenotypes. Her research demonstrated that STAT3 signaling in neutrophils drives their acquisition of immunosuppressive functions, and that selective STAT3 inhibition could reverse this process (Jablonska, 2025).

Zvi Fridlender's investigation of NET-immune cell interactions revealed unexpected complexity in neutrophil-mediated immune regulation. His team discovered that neutrophils from lung cancer patients produce smaller amounts of NETs compared to healthy donors, but these cancer-associated NETs retain potent biological activities that influence both tumor cells and immune responses. NETs enhanced T cell activation through mechanisms that were partially DNA-dependent for CD8 T cells. Involvement of additional metabolic pathways for CD4 and CD8 T cells was reported suggesting that NETs function as complex signaling platforms that integrate multiple activation pathways (Al-Sharif et al., 2025).

Opinion: The evidence supports the relevance of neutrophil-targeted combination therapies that could include selective STAT3 inhibitors, optimized NET modulators, and neutrophil reprogramming agents.

6 Novel approaches to target immunity with radiation and chemicals: engineering immune synergy

The integration of radiation therapy with immunotherapy reached new levels of sophistication at CITIM-2025, with speakers demonstrating that radiation should be viewed not merely as a tumor-killing modality but as a programmable immune stimulus capable of generating antigen, adjuvant, and favorable microenvironmental changes simultaneously.

Udo Gaipl's lecture established the conceptual framework by demonstrating how radiation dose, dose rate, fractionation, and timing can be precisely calibrated to generate optimal immune responses. His work on FLASH radiotherapy—ultra-high dose rate radiation delivery—revealed that temporal aspects of radiation delivery fundamentally alter immune consequences. FLASH protocols generated strong immunogenic cell death signals while minimizing normal tissue immunosuppression, creating therapeutic windows previously thought impossible (Gaipl, 2025).

Yona Keisari's presentation on Diffusing Alpha-emitters Radiation Therapy (DaRT) exemplified next-generation approaches to radio-immunotherapy integration. This novel approach delivers radioactive sources directly into tumors, creating controlled ablation zones that generate massive antigen release combined with danger signal production. Unlike external beam radiation, DaRT creates sustained antigen availability over days to weeks,

providing prolonged immune stimulation that promotes memory T cell formation (Keisari, 2025).

Klaus Spohr's innovative work on immunotherapy-supported Boron Neutron Capture Therapy represented a paradigm shift toward immune cell-delivered radiation. His team developed methods to load immunocompetent cells with boron nanoparticles, effectively creating "cellular radiopharmaceuticals" that selectively deliver radiation to tumor sites. This approach combines the targeting specificity of immune cell trafficking with the precision of nuclear medicine (Spohr et al., 2025).

Rostyslav Bilyy's work on reversible thiol binder demonstrated how chemical agents can be designed to simultaneously kill cancer cells and stimulate immune responses. This compound selectively accumulates in cancer cell lysosomes, increases reactive oxygen species production, and triggers lysosomal disruption leading to immunogenic cell death. The resulting immune activation proved sufficient to generate long-term anti-tumor immunity in animal models (Arkhypov et al., 2025).

Perspective: The field is transitioning from simple combination approaches to engineered immune-radiation/chemical synergy. The goal is creating programmable immune activation were radiation and chemicals function as precision tools for immune system education and activation.

7 Novel vaccine approaches: from precision targeting to multi-modal activation

Cancer vaccination strategies presented at CITIM-2025 revealed a sophisticated evolution beyond traditional peptide-based approaches toward complex, multi-component systems designed to simultaneously engage multiple immune pathways while overcoming established tolerance mechanisms.

Angel Porgador's plenary presentation on current immunotherapy status established the conceptual challenges facing cancer vaccination (Porgador, 2025). Michael Nishimura in his lecture summarized currently used CAR, TCR and TIL therapies, with a special attention paid to CD19 CAR T cells' use in clinical setting (Nishimura, 2025).

Sjoerd van der Burg's groundbreaking work on TEIPP vaccination (T cell epitopes associated with impaired peptide processing) exemplified next-generation antigen selection strategies. TEIPP antigens are generated by defective proteasomal processing in cancer cells, creating neo-epitopes that are absent from normal tissues. This approach salvages immunotherapy responses in checkpoint inhibitor-resistant lung cancer by targeting antigens that remain available even when classical MHC class I presentation is compromised. TEIPP vaccination showed efficacy in patients who had failed conventional immunotherapy, suggesting that antigen selection strategies could overcome resistance mechanisms (Emmers et al., 2025).

Flavio Salazar-Onfray's presentation on TRIMELVax demonstrated how vaccination strategies could harness innate immune system activation to drive adaptive responses. This melanoma vaccine combines heat shock-conditioned cancer cell lysates with mollusk hemocyanin adjuvant, creating a complex antigenic mixture that rapidly induces neutrophil-driven inflammation and subsequent dendritic cell activation (Salazar-Onfray, 2025).

Moshe Elkabets presented research on the development of an AXL/PD-1 Bi-specific-Cell-Engager that targets AXL and PD1 (BiCE AXL/PD1) and increase the interaction between the AXL-expressing tumor cell and $CD8^+$ T cells resulting in enhanced anti-tumor lytic activity of the T cells against AXL-expressing tumor cells (Yegodayev and Elkabets, 2025).

Anahid Jewett's presentation on NK101 supercharged NK cells represented a paradigm shift toward cellular vaccination approaches. Rather than simply providing antigens for T cell recognition, this strategy involves *ex vivo* activation and expansion of natural killer cells that are subsequently reinfused to provide immediate anti-tumor activity while potentially priming adaptive immune responses (Jewett, 2025).

Opinion: The most promising approaches to cancer treatment will likely combine antigen diversity with innate immune activation and tolerance-breaking strategies. Success will require personalized antigen selection guided by individual patient immune profiles and tumor characteristics.

8 Progress in tumor immunology and monitoring from Romanian research centers

One of the defining strengths of the CITIM conference lies in its ability to unite internationally renowned scientists with leading local researchers, fostering an environment of cross-border collaboration and mutual inspiration. This year's meeting exemplified that mission by bringing together representatives from 11 Romanian research institutions, highlighting Romania's growing leadership in the field of cancer immunotherapy. Experts from key academic and clinical centers—including Bucharest, Cluj-Napoca, Măgurele, and Timișoara—played an active role not only as participants but also as speakers, session chairs, and contributors to high-level scientific discussions. Their strong presence ensured that CITIM-2025 was not only a platform for global exchange but also a catalyst for national capacity-building in cancer immunology.

Livia Sima's groundbreaking work on tissue transglutaminase (TG2) in ovarian cancer revealed how stromal proteins can function as immunomodulatory targets. Her research demonstrated that TG2 expression in cancer-associated fibroblasts (CAFs) correlates inversely with $CD8^+$ T cell infiltration in human ovarian cancer samples. Using TG2 knockout mouse models, her team showed that TG2 deletion in the host significantly reduced tumor burden and increased survival, accompanied by enhanced $CD8^+$ T cell infiltration and activation (Sima et al., 2025).

Manuela Banciu's comprehensive investigation of tumor microenvironment rewiring through lipid nanoparticles demonstrated how nanotechnology approaches could simultaneously target multiple cellular components. Her team developed simvastatin-loaded long-circulating liposomes (LCL-SIM) that showed natural tropism for tumor-associated macrophages while delivering therapeutic payloads to reshape the immune landscape (Patras et al., 2025). While Agata Mlynska, representing previous CITIM host country–Lithuania - reported

the deciphering of immune tumor subtypes through profiling of their microenvironment (Mlynska et al., 2025).

Monica Neagu's work provided insights into genetic and epigenetic traits in cutaneous melanoma, aiming to identify new therapy targets by evaluating genetic alterations in the EGFR-RAS-RAF pathway (Neagu et al., 2025). Their group also explored the impact of adipokines and gut microbiome on melanoma outcomes and the anti-tumor effects of TLR7/8 agonists on NK cells in melanoma models.

Opinion: The CITIM platform has proven to be an exceptional forum for the exchange of ideas between international experts and local institutions leading to long-lasting collaborative projects.

9 Perspectives and limitations

Based on the experience gained through the CITIM conferences and numerous discussions with scientists, clinicians, and policymakers from various countries, we have identified key scientific and policy-related barriers that must be addressed to successfully integrate immunomonitoring and cancer immunotherapy into standard clinical practice in developing regions.

Scientific barriers:

a. Lack of local training and expertise. Established research centers in countries with a developed cancer immunotherapy landscape can serve as excellent training hubs. However, they should adopt a structured policy that ensures trained personnel return to their home institutions and continue building local capacity rather than remaining centralized.
b. Limited infrastructure. Insufficient access to advanced equipment and facilities remains a major challenge. This barrier can be partially overcome by consolidating and sharing existing resources among multiple institutions working toward a common goal.
c. Absence of standardized protocols and biobanking. Non-standardized immunomonitoring protocols, lack of harmonized data management, and limited biobanking capacity hinder progress. These challenges can be addressed through structured support and mentoring from countries that have already established these systems. Similar solutions apply to issues related to licensing, access to novel cell lines, and intellectual property (IP) rights.

Policy-related barriers:

a. High costs of immunotherapy. Initially, the cost of treatments such as CAR-T therapy reached approximately USD 1 million per patient. The introduction of point-of-care manufacturing models has significantly reduced costs, with current prices reported at USD 97,000 in Spain and USD 30,000 in Brazil (Hildreth, 2025). While these reductions are encouraging, costs remain a critical barrier for most low- and middle-income countries.
b. Regulations and reimbursement policies. The lack of national treatment guidelines, regulatory frameworks, and state or insurance-based reimbursement mechanisms limits the adoption of immunotherapy. To overcome this barrier, active involvement of decision-making stakeholders from developing countries is essential—a process already initiated within CITIM activities.

Strengthening local research networks is a prerequisite for overcoming both scientific and policy challenges. Such networks should bring together oncologists, immunologists, and healthcare professionals to promote the sustainable development of cancer immunotherapy. A successful example is the coordination initiative in Lithuania, led by CITIM co-organizer Vita Pašukonienė, which demonstrates how collaboration can accelerate progress.

Similar networks are needed in every country. We strongly encourage CITIM participants and all interested parties to build bridges by engaging with local oncology and immunology societies—which are present in most Eastern European countries—and to organize joint events in the coming year. These interactions will reveal numerous shared challenges and opportunities for collaboration. Such initiatives can serve as a starting point for involving policymakers, ultimately addressing the most pressing limitations to implementing immunotherapy in clinical practice.

10 Summary

Recent findings clearly demonstrate that immune regulation is a fundamental component of tumor development. Effective cancer treatment is nearly impossible without a comprehensive understanding of the complex interactions between tumors and the immune system—including direct cell-cell contact, metabolic crosstalk, cytokine signaling, and other factors shaping the tumor microenvironment. In his concluding lecture, Prof. Isaac Witz introduced the concept of the "Cancer Ecosystem", emphasizing the integrated nature of these interactions. He not only summarized key advances in our understanding of cancer–immune system dynamics but also underscored the vast number of unanswered questions that continue to challenge the field. (Witz, 2025).

Recent advances in targeted anti-tumor cell therapies, novel anti-cancer vaccine strategies, and combination treatments with radio- and chemotherapy designed to enhance immunogenicity—along with the development of tumor- and immune-specific delivery systems—have significantly increased our ability to combat cancer more effectively.

Bringing together leading scientists through platforms like CITIM has proven to be a highly effective strategy for advancing knowledge, particularly in countries where cancer immunotherapy and immunomonitoring are only beginning to be integrated into standard clinical practice. As demonstrated by CITIM, such meetings not only raise general awareness of the immune system's critical role in cancer development but also foster productive, long-term collaborations that often lead to novel and impactful scientific discoveries.

Author contributions

RB: Writing – original draft, Writing – review and editing, Resources, Conceptualization, Funding acquisition, Project administration.

Funding

The author(s) declare that financial support was received for the research and/or publication of this article. The work of RB was supported by the European Union – NextGenerationEU and the Romanian Government through the National Recovery and Resilience Plan, Component 9 - Investment 8, HeartCure project, Financing Contract no. 760063/23.05.2023, CF93/15.11.2022.

Acknowledgments

CITIM thanks to their constant sponsor and partners – CTL (Cellular Technology Limited), and specifically Dr. Paul V. Lehmann and Dr. Greg Kirchenbaum.

Conflict of interest

The author declares that the research was conducted in the absence of any commercial or financial relationships that could be construed as a potential conflict of interest.

The author(s) declared that they were an editorial board member of Frontiers, at the time of submission. This had no impact on the peer review process and the final decision.

Generative AI statement

The author(s) declare that Generative AI was used in the creation of this manuscript. During the preparation of this work, the author used ChatGPT-4.1 in order to enhance text readability and length. After using this tool/service, the author reviewed and edited the content as needed and takes full responsibility for the content of the published article.

Any alternative text (alt text) provided alongside figures in this article has been generated by Frontiers with the support of artificial intelligence and reasonable efforts have been made to ensure accuracy, including review by the authors wherever possible. If you identify any issues, please contact us.

Publisher's note

References

Al-Sharif, N., Qaisi, M., Kaisar, N., Padawer, D., Bohana, O., Volman, Y., et al. (2025). Neutrophil extracellular Traps (NETs) in cancer and beyond. *South East Eur. J. Immunol.* 8, 036. doi:10.3889/seejim.2025.6097

Arkhypov, A., Klemt, I., Bila, G., Attia, D., Chernii, S., Bilyy, R., et al. (2025). Targeting lysosomal thiols for immunogenic cancer cell death. *Angew. Chem. Int. Ed.* 64, e202417509. doi:10.1002/anie.202417509

Baniyash, M. (2025). Immune landscape in chronic inflammation: complications and risks. *South East Eur. J. Immunol.* 8, 031. doi:10.3889/seejim.2025.6092

Ben-Baruch, A. (2025). Partners in crime: tnfα-based networks promoting cancer progression. *South East Eur. J. Immunol.* 8, 026. doi:10.3889/seejim.2025.6087

Cruz De los Santos, M., and Lundqvist, A. (2025). Epigenetic modulation drives inflammatory responses in sarcoma. *South East Eur. J. Immunol.* 8, 042. doi:10.3889/seejim.2025.6104

Dölling, M., Schauer, C., and Herrmann, M. (2025). The role of NETs and their aggregates in disease. *South East Eur. J. Immunol.* 8, 038. doi:10.3889/seejim.2025.6099

Emmers, M., Welters, M. J. P., Dietz, M. V., Santegoets, S. J., Boekesteijn, S., Stolk, A., et al. (2025). TEIPP-Vaccination in checkpoint-resistant non-small cell lung cancer: a first-in-human phase I/II dose-escalation study. *Nat. Commun.* 16, 4958. doi:10.1038/s41467-025-60281-8

Erin, N. (2025). Interactions between Schwann cells and metastatic breast carcinoma: contact-dependent and independent effects. *South East Eur. J. Immunol.* 8, 035. doi:10.3889/seejim.2025.6096

Gaipl, U. S. (2025). New concepts and challenges in radio-immunotherapies. *South East Eur. J. Immunol.* 8, 037. doi:10.3889/seejim.2025.6098

Gross, S., Cairns, R. A., Minden, M. D., Driggers, E. M., Bittinger, M. A., Jang, H. G., et al. (2010). Cancer-associated metabolite 2-hydroxyglutarate accumulates in acute myelogenous leukemia with isocitrate dehydrogenase 1 and 2 mutations. *J. Exp. Med.* 207, 339–344. doi:10.1084/jem.20092506

Hildreth, C. (2025). Ways to curb the sky-high costs of CAR-T cell therapy. Available online at: https://bioinformant.com/ways-to-curb-the-sky-high.

Jablonska, J. (2025). Targeting STAT3 in neutrophils alters their immunoregulatory activity in cancer. *South East Eur. J. Immunol.* 8, 039. doi:10.3889/seejim.2025.6101

Jewett, A. (2025). First in human clinical Study demonstrating the safety and efficacy of NK101 (supercharged NK cells) in the treatment of patients with cancer. *South East Eur. J. Immunol.* 8, 040. doi:10.3889/seejim.2025.6102

Keisari, Y. (2025). Tumor destruction *in situ* as a tool to trigger a robust anti-tumor immune response. *South East Eur. J. Immunol.* 8, 041. doi:10.3889/seejim.2025.6103

Levi, N., Kozlovski, S., Kizner, M., Biton, M., and Alon, R. (2025). ICAM-1 on cDC1 promotes the survival of stem-like memory CD8 T cells generated in tumor draining lymph nodes. *South East Eur. J. Immunol.* 8, 028. doi:10.3889/seejim.2025.6089

Machluf-Kaz, N., Stalin, S., Barsky, G., Bersudsky, M., Apte, R. N., Moadi, L., et al. (2025). The role of tumor microenvironment IL-1β in Colorectal Cancer. *South East Eur. J. Immunol.* 8, 053. doi:10.3889/seejim.2025.6117

Mak, T. W. (2025). Metabolic and neural regulation of immunity and cancer. *South East Eur. J. Immunol.* 8, 025. doi:10.3889/seejim.2025.6088

Mlynska, A., Zymantaite, E., Butkute, A., Dobrovolskiene, N., Krasko, J. A., Karaman, O., et al. (2025). Deciphering immune tumor subtypes through microenvironment profiling. *South East Eur. J. Immunol.* 8, 043. doi:10.3889/seejim.2025.6105

Neagu, M., Elena-Georgiana, D., Constantin, C., Surcel, M., Munteanu, A., and Zurac, S. (2025). Insights in genetic and epigenetic traits in cutaneous melanoma - new therapy targets. *South East Eur. J. Immunol.* 8, 044. doi:10.3889/seejim.2025.6106

Nishimura, M. I. (2025). Lessons learned from using TCR and CAR gene modified T cells for treating cancer patients. *South East Eur. J. Immunol.* 8, 045. doi:10.3889/seejim.2025.6107

Patras, L., Sesarman, A., Negrea, G., Dragan, S.-M., Meszaros, M.-S., Licarete, E., et al. (2025). Cancer therapeutic strategies to rewire tumor microenvironment. *South East Eur. J. Immunol.* 8, 030. doi:10.3889/seejim.2025.6091

Pawelec, G. (2025). Antigen-specific peripheral immune cell dynamics predicting clinical responses to checkpoint blockade in melanoma. *South East Eur. J. Immunol.* 8, 047. doi:10.3889/seejim.2025.6109

Porgador, A. (2025). Immunotherapy of cancer: are we already there? *South East Eur. J. Immunol.* 8, 048. doi:10.3889/seejim.2025.6110

Salazar-Onfray, F. (2025). TRIMELVax: a novel innate immune-engaging vaccine for malignant melanoma targeting neutrophil-driven antigen presentation and T-Cell activation. *South East Eur. J. Immunol.* 8, 050. doi:10.3889/seejim.2025.6113

Shurin, M. R. (2025). Schwann cells and the neuro-immune axis in the tumour microenvironment. *South East Eur. J. Immunol.* 8, 023. doi:10.3889/seejim.2025.6086

Sima, L. E., Chen, S., Cardenas, H., Zhao, G., Wang, Y., Ivan, C., et al. (2025). Tissue transglutaminase as a new immunomodulatory target in ovarian cancer tumor microenvironment. *South East Eur. J. Immunol.* 8, 058. doi:10.3889/seejim.2025.6127

Spohr, K. M., Bleotu, G. P., Cristea, M., Doria, D., Ivan, A., Jurca, M., et al. (2025). A new pathway towards immunotherapy-supported radiology for targeted Boron Neutron Capture therapy (BNCT). *South East Eur. J. Immunol.* 8, 057. doi:10.3889/seejim.2025.6128

Umansky, V. (2025). MDSCs as major inducers of immunosuppression in melanoma. *South East Eur. J. Immunol.* 8, 024. doi:10.3889/seejim.2025.6100

Umansky, V., Malyguine, A., and Shurin, M. (2009). New perspectives in cancer immunotherapy and immunomonitoring. *Futur. Oncol.* 5, 941–944. doi:10.2217/fon.09.62

Vannucci, L., Rajsiglova, L., Stakheev, D., Lukac, P., Tenti, P., Sushystskyi, L., et al. (2025). The tumor immune microenvironment as a target for nano-therapies and patient-tailored treatments. *South East Eur. J. Immunol.* 8, 052. doi:10.3889/seejim.2025.6116

Weiss, J. M., Palmieri, E. M., Gonzalez-Cotto, M., Bettencourt, I. A., Kurian, S., O'Keefe, B., et al. (2025). Targeting metabolic programming in the tumor microenvironment. *South East Eur. J. Immunol.* 8, 054. doi:10.3889/seejim.2025.6118

Witz, I. P. (2025). Cancer ecosystem - quo vadis? *South East Eur. J. Immunol.* 8, 056. doi:10.3889/seejim.2025.6120

Yegodayev, K. M., and Elkabets, M. (2025). Development of a AXL/PD-1 BiCE as novel immunotherapy agent. *South East Eur. J. Immunol.* 8, 034. doi:10.3889/seejim.2025.6095

frontiers | Frontiers in Oncology

TYPE Original Research
PUBLISHED 21 October 2025
DOI 10.3389/fonc.2025.1666891

OPEN ACCESS

EDITED BY
Valentyn Oksenych,
University of Bergen, Norway

REVIEWED BY
Payam Behzadi,
Islamic Azad University Shahr-e-Qods Branch, Iran
Xuanhong He,
Sichuan University, China
Anastassia Serguienko,
University of Bergen, Norway
Mengying Xu,
Nanjing University, China

*CORRESPONDENCE
Juan Ren
Ren869491533@qq.com

RECEIVED 19 August 2025
ACCEPTED 06 October 2025
PUBLISHED 21 October 2025

CITATION
Chen M, Wang X, Bai S, Lan N, Wang J, Chen Y, Gao Y, Wang W, Shang X, Jiao M, Zhang X, Li W, Wu F, Liu W, Hu F, Chen L and Ren J (2025) Recognition of the novel items for prediction of bone metastasis in colorectal cancer. *Front. Oncol.* 15:1666891. doi: 10.3389/fonc.2025.1666891

Recognition of the novel items for prediction of bone metastasis in colorectal cancer

Min Chen[1], Xuan Wang[1], Shuheng Bai[1], Ning Lan[1], Junyang Wang[2], YanKe Chen[2], Ying Gao[1], WenJuan Wang[3], Xiao Shang[3], Min Jiao[3], Xiangxiang Zhang[1], Wenyang Li[1], Fang Wu[1], Wanyi Liu[1], Fengyuan Hu[1], Ling Chen[4] and Juan Ren[1]*

[1]Department of Radiotherapy Oncology, the First Affiliated Hospital of Xi'an Jiaotong University, Xi'an, China, [2]School of Basic Medical Sciences of Xi'an Jiaotong University, Xi'an, China, [3]Department of Oncology, the First Affiliated Hospital of Xi'an Jiaotong University, Xi'an, China, [4]Department of Medical Oncology, the First Affiliated Hospital of Xi'an Jiaotong University, Xi'an, China

Objective: To explore whether uric acid (UR), neutrophil/lymphocyte ratio (NLR) and uric acid/albumin ratio (UAR) can predict bone metastasis in colorectal cancer (CRC).

Methods: A single-center retrospective study was conducted studying patients diagnosed with colorectal cancer attending The First Affiliated Hospital of Xian JiaoTong University between January 2016 and December 2021. Patients were categorized into groups with and without bone metastasis. Receiver operating characteristic (ROC) curve analysis assessed the diagnostic accuracy of CRC bone metastases, with subsequent combined ROC curve analysis. Differences among the AUCs were calculated and compared by Delong test. Logistic regression analysis was utilized to assess the impact of these parameters on CRC bone metastasis.

Results: A total of 156 patients (32%) exhibited bone metastases from CRC. In these patients, levels of uric acid (UA), uric acid ratio (UAR), neutrophil-to-lymphocyte ratio (NLR), carcinoembryonic antigen (CEA), carbohydrate antigen 199 (CA199), and carbohydrate antigen 724 (CA724) were significantly elevated. The diagnostic performance of UA, UAR and NLR is surpassed that of traditional colorectal cancer markers. The area under the curve (AUC) for the combination UA, UAR and NLR with colorectal cancer tumor markers was significantly more effective in predicting bone metastasis ($P < 0.001$) compared to the AUC without this combination. Multiple logistic regression analysis identified UA, NLR and CEA as independent risk factors for bone metastasis in colorectal cancer.

Conclusions: UA, UAR and NLR serve as valuable makers for predicting bone metastases in patients with colorectal cancer. The integration of UA, UAR, NLR, CEA, CA199 and CA724 may enhance the prediction of bone metastases in colorectal cancer.

KEYWORDS

colorectal cancer, bone metastasis, uric acid, neutrophil/lymphocyte ratio, uric acid/albumin ratio

Introduction

Colorectal cancer (CRC) ranks as the second deadliest cancer globally, with 1.93 million new cases and 903,859 deaths reported in 2022, according to Global Cancer Data statistics (1). Approximately 3-7% of colorectal cancer patients develop bone metastases (2). Nevertheless, routine follow-up does not include screening for bone metastases in colorectal cancer (3). Diagnosis typically occurs through targeted imaging following the emergence of bone-related events, such as pathological fractures, severe bone pain, or spinal cord compression. Once bone metastasis occurs in colorectal cancer patients, the prognosis is dire, with a 5-year survival rate of less than 5% and a median survival time ranging from 5 to 21 months (4). Furthermore, bone metastases associated with bone-related events significantly impair patients' quality of life and are compounded by a lack of effective interventions and treatments. Consequently, there is an urgent need for timely, effective and non-invasive monitoring of bone metastases occurrence in colorectal cancer patients.

Serum uric acid (UA), the serum uric acid/serum albumin ratio (UAR), and the neutrophil/lymphocyte ratio (NLR) are biochemical markers that are easily measurable, cost-effective, and non-invasive for patients. UA is the final product of purine metabolism, generated through the oxidation of various purines and subsequently excreted in urine. Increasing evidence suggests that elevated UA levels serve as a risk factor for several cancers by inducing inflammatory responses and oxidative stress (5, 6). Albumin, the principal component of serum protein, reflects nutritional status and cancer aggressiveness and is frequently incorporated into prognostic scoring systems in numerous studies (7). Neutrophils, as key components of white blood cells, significantly contribute to cancer progression and have emerged as independent risk factors for various malignant tumors (8, 9), closely associated with tumor metastasis (10). However, the relationships among UA, UAR and NLR, particularly concerning bone metastasis in colorectal cancer have not been systematically investigated. Therefore, this study aimed to utilize retrospective data to examine the diagnostic utility of UA, UAR and NLR in identifying bone metastasis in colorectal cancer patients, facilitating timely and non-invasive detection to enhance patient quality of life and improve survival rates.

Materials and methods

Participant selection

This study was a single-center, retrospective analysis of patients with colorectal cancer bone metastasis, diagnosed through pathology and who had not received any form of treatment, including surgery, radiotherapy, chemotherapy, molecular targeted therapy, or immunotherapy, at the First Affiliated Hospital of Xi'an Jiaotong University in Shaanxi, China. We utilized hospital records form the First Affiliated Hospital of Xi'an Jiaotong University to identify all patients diagnosed between January 2016 and December 2021. The ICD-10 diagnostic codes C18–20 were employed to extract patient data from the electronic records. A researcher reviewed these hospital records to gather information on gender, age, serum uric acid levels, bone metastasis status, neutrophil/lymphocyte ratio, albumin levels, and the uric acid/albumin ratio among other variables.

Patients were eligible for this study if they satisfied the following criteria:

1. A diagnosis of colorectal cancer was confirmed through pathological examination.
2. The patient presented for their first visit without any prior treatment, including surgery, radiation therapy, chemotherapy, molecular targeted therapy, or immunotherapy.
3. The medical records were complete, including blood routine and biochemical test reports obtained within three weeks prior to the pathological examination.

Patients were excluded if they met any of the following criteria:

1. A history of gout or other conditions associated with pathologically elevated uric acid levels.
2. The presence of other malignant tumors or platelet-related disorders.
3. Severe hepatic or renal insufficiency.
4. Recent or long-term use of glucocorticoids.

Our study used retrospective data to screen potential patients based on the inclusion and exclusion criteria confirmed by the initial research design. Then, the patient was divided into bone metastasis group and non-bone metastasis group according to whether there was bone metastasis. Finally, a total of 488 patients were included in this study, of which 156 were in the bone metastasis group and 332 were in the non-bone metastasis group. Therefore, we used the non-bone metastasis group as the negative group and the bone metastasis group as the positive group, and a series of subsequent analyses were also based on this grouping.

Hematology and biochemical index detection

For patients with colorectal cancer bone metastasis who had not received any prior treatment, including anti-tumor therapies such as surgery, radiotherapy, chemotherapy, molecular targeting and immunotherapy, peripheral venous blood was drawn after an 8-hour fasting period. The sample were sent to our hospital's laboratory for analysis, adhering strictly to the instrument and reagent instructions. The serum uric acid test utilized the JDYFY-SH-YQA-25 instrument and its corresponding reagents. The normal range for serum uric acid in males was 208-428umol/L,

Abbreviations: UR, Uric Acid; UAR, Uric acid/Albumin Ratio; NLR, Neutrophil/Lymphocyte Ratio; CRC, Colorectal Cancer; ROC, Receiver operating characteristic curve; AUC, Area under the curve; CI, Confidence Interval; CEA, carcinoembryonic antigen; CA199, carbohydrate antigen 199; CA724, carbohydrate antigen 724.

while in females, it was 155-357umol/L. The normal values for neutrophil count and lymphocyte count were 1.8-6.3*10^9/L and 1.1-3.2*10^9/L, respectively, and the normal range for albumin was 40–55 g/L. Neutrophil count (N) and lymphocyte count (L) were measured using an automated hematology analyzer (BC-6800Plus). The neutrophil/lymphocyte ratio (NLR) was calculated as N/L, and the uric acid/albumin ratio was calculated as UA/Ab.

Diagnostic criteria for bone metastases of colorectal cancer

According to the expert consensus on the Multidisciplinary Comprehensive Treatment of Colorectal Cancer Bone Metastases in China (2020 edition) (11), the diagnosis of colorectal cancer bone metastases must satisfy one of the following two criteria:

1. A clinical or pathological diagnosis of colorectal cancer, with a bone lesion biopsy confirming colorectal cancer metastasis;
2. A clear pathological diagnosis of colorectal cancer accompanied by typical imaging findings indicative bone metastases.

Statistical analysis

The Kolmogorov-Smirnov test was conducted on the continuous data prior to analysis to assess the normality of the variables. Continuous variables were presented as mean ± standard deviation (SD), while categorical variables were expressed as percentages. The independent sample t-test was employed for continuous variables exhibiting a normal distribution, whereas the Mann-Whitney rank sum test was utilized for data that did not follow a non-normal distribution. Count data were analyzed using the Chi-square test. Correlation analysis was performed using the Spearman method. Multiple logistic regression analysis was applied to identify factors potentially associated with bone metastasis in colorectal cancer. A receiver operating characteristic (ROC) curve and area under the curve (AUC) value were employed to evaluate the sensitivity and specificity of each factor in assessing colorectal cancer bone metastasis. Differences among the AUCs were calculated and compared using the Delong test. All statistical analyses were performed using SPSS version 26 (IIBM Corporation, Armonk, NY). A *P*-value of less than 0.05 was considered statistically significant.

Results

A total of 488 patients who met the inclusion and exclusion criteria were enrolled in this study (Figure 1). This cohort comprised 364 males (74.6%) and 124 females (25.4%), with 156 patients (32.0%) exhibiting bone metastasis (metastasis group) and 332 patients (68.0%) without bone metastasis (non-metastasis group). Results from the Kolmogorov-Smirnov test indicated that age, UA, UAR, CEA, CA199, CA724 and NLR exhibited non-normal distributions between the two groups (Table 1). Consequently, these data were reported as medians (P25-P75) and

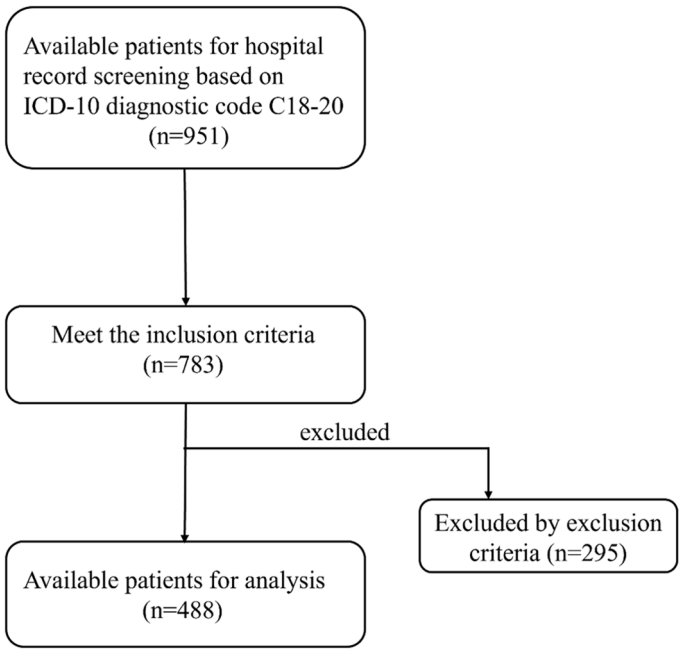

FIGURE 1
Flow chart of patient selection.

TABLE 1 Kolmogorov-Smirnov test of measurement data.

Measurement data	Group	Statistical value	Significance
Age	Non-metastasis	0.059	0.008
	Metastasis	0.089	0.004
Albumin, g/L	Non-metastasis	0.028	0.2
	Metastasis	0.064	0.2
Globulin, g/L	Non-metastasis	0.044	0.2
	Metastasis	0.052	0.2
Uric acid, umol/L	Non-metastasis	0.052	0.032
	Metastasis	0.106	<0.001
UAR	Non-metastasis	0.086	<0.001
	Metastasis	0.103	<0.001
CEA, ng/mL	Non-metastasis	0.435	<0.001
	Metastasis	0.442	<0.001
CA199, U/mL	Non-metastasis	0.303	<0.001
	Metastasis	0.405	<0.001
CA724, U/mL	Non-metastasis	0.379	<0.001
	Metastasis	0.405	<0.001
Lymphocyte, 10^9/L	Non-metastasis	0.067	0.001
	Metastasis	0.178	<0.001
Neutrophil, 10^9/L	Non-metastasis	0.166	<0.001
	Metastasis	0.118	<0.001
NLR	Non-metastasis	0.238	<0.001
	Metastasis	0.298	<0.001
Erythrocyte, 10^{12}/L	Non-metastasis	0.342	<0.001
	Metastasis	0.09	<0.001
Hemoglobin, g/L	Non-metastasis	0.086	<0.001
	Metastasis	0.153	<0.001
Leukocyte, 10^9/L	Non-metastasis	0.121	<0.001
	Metastasis	0.114	<0.001
Platelet, 10^9/L	Non-metastasis	0.069	0.001
	Metastasis	0.079	0.018
Monocyte, 10^9/L	Non-metastasis	0.105	<0.001
	Metastasis	0.385	<0.001

UAR, Uric acid to Albumin Ratio; CEA, carcinoembryonic antigen; CA199, carbohydrate antigen 199; CA724, carbohydrate antigen 724; NLR, Neutrophil to Lymphocyte Ratio.

compared between groups using the rank sum test. No statistically significant differences were observed in age, gender, albumin, leukocyte and monocyte counts between the two groups. However, levels of CEA, CA199 and CA724 in the bone metastatic group were significantly higher than those in the non-metastatic group ($P< 0.001$, $P = 0.006$, $P = 0.005$). The metastasis group also demonstrated significantly increased absolute UA and decreased absolute albumin, resulting in a significantly elevated UAR ($P< 0.001$). Additionally, the neutrophil count in the metastasis group was elevated, while the lymphocyte count also increased ($P = 0.004$, $P < 0.001$) (Table 2).

UA, UAR and NLR can predict more effectively colorectal cancer bone metastases than tumor maker

ROC curve analysis was employed to assess the diagnostic efficacy of various parameters for detecting bone metastasis in CRC. The optimal cut-off values for UA, UAR, NLR, CEA, CA199 and CA724 were determined to be 309.9 (sensitivity 55.1%, specificity 74.1%), 7.69 (sensitivity 62.2%, specificity 66.5%), 4.201 (sensitivity 50.6%, specificity 84.9%), 3.97 (sensitivity 71.2%, specificity 56.2%), 9.975 (sensitivity 76.9%, specificity 39.3%) and 7.79 (sensitivity 56.0%, specificity 60.2%), respectively. The AUC values for UA, UAR, NLR, CEA, CA199 and CA724 in predicting bone metastasis were 0.705 [95% CI: 0.658–0.752, P < 0.001], 0.698 [95% CI: 0.650–0.746, P < 0.001], 0.738 [95% CI: 0.690–0.786, P < 0.001], 0.602 [95% CI: 0.549–0.655, P < 0.001], 0.576 [95% CI: 0.522–0.630, P = 0.007] and 0.578 [95% CI: 0.521–0.635, P = 0.005]. The predictive efficacy of UA, UAR and NLR was found to be comparable to that of established CRC tumor markers (Figure 2). The predicted probabilities for combining CRC markers with UA, UAR and NLR was derived using binary logistic regression. The optimal cut-off values for P1, P2, P3, P4 and P5 were identified as 0.278 (sensitivity 70.5%, specificity 54.3%), 0.248 (sensitivity 80.1%, specificity 51.0%), 0.301 (sensitivity 62.8%, specificity 70.5%), 0.330 (sensitivity 53.8%, specificity 87.1%) and 0.218 (sensitivity 75.0%, specificity 76.0%). The AUC values for P1, P2, P3, P4 and P5 were 0.628 (95% CI: 0.576–0.680, P < 0.001), 0.723 (95% CI: 0.676–0.770, P < 0.001), 0.719 (95% CI: 0.671–0.767, P < 0.001), 0.759 (95% CI: 0.712–0.807, P < 0.001) and 0.825 (95% CI: 0.787–0.863, P < 0.001) (Table 3). As indicated in Table 4, significant differences were observed except for three pairs P2 vs P3, P2 vs P4, P3 vs P4). The similar AUCs of P2 (AUC = 0.723), P3 (AUC = 0.719) and P4 (AUC = 0.759) suggested their equivalent diagnostic accuracy for bone metastasis in CRC. Notably, the combination of UA, UAR, NLR and tumor markers significantly enhanced diagnostic efficacy (Figure 3; Table 4).

The correlation among UA, UAR, NLR and other diagnostic parameters were presented in Table 5. In patients with CRC, UA and UAR exhibited positive correlations with CEA and CA724 (r = 0.091, 0.102, 0.106 and 0.124, respectively, all P < 0.05). However, no significant correlation was observed between UA and CA199 (P = 0.205). Additionally, NLR demonstrated positive correlations with CEA, CA199 and CA724 (r = 0.122, 0.093 and 0.136, respectively, all P < 0.05).

TABLE 2 Demographic and laboratory characteristics of patients.

Characteristics	Non-metastasis (n=332)	Metastasis (n=156)	*P*-value
Sex, no. (%)			0.556
Male	245(73.8)	119(76.3)	
Female	87(26.2)	37(23.7)	
Age, years	61(52-67)	59(51.3-68)	0.943
Albumin, g/L	37.6 ± 4.6	37.5 ± 4.7	0.748
Globulin, g/L	25.2 ± 4.1	26.2 ± 4.0	0.011
Uric acid, umol/L	263.3(215.2-315.1)	312.1(268.2-378.0)	<0.001
UAR	7.01(5.7-8.5)	8.58(6.9-10.1)	<0.001
CEA, ng/mL	1.68(3.4-59.7)	7.12(3.0-109.7)	<0.001
CA199, U/mL	12.88(6.2-207.2)	26.98(10.5-141.6)	0.006
CA724, U/mL	4.33(1.9-28.8)	10.1(2.4-34.9)	0.005
Lymphocyte, 10^9/L	1.47(1.1-2.0)	0.72(0.4-1.6)	<0.001
Neutrophil, 10^9/L	3.19(2.4-4.2)	3.54(2.8-4.7)	0.004
NLR	2.02(1.4-3.3)	4.23(2.2-8.5)	<0.001
Erythrocyte, 10^{12}/L	4.24(3.8-4.7)	3.9(3.4-4.4)	<0.001
Hemoglobin, g/L	127(107.0-141.0)	133(104.3-155.0)	0.017
Leukocyte, 10^9/L	5.44(4.3-6.8)	5.51(4.5-6.8)	0.488
Platelet, 10^9/L	206(162.3-260.0)	195(140.3-251.5)	0.025
Monocyte, 10^9/L	0.42(0.3-0.6)	0.45(0.3-0.6)	0.083

UA and NLR can be independent risk factors for bone metastasis of colorectal cancer

The diagnostic parameters were categorized based on their optimal cut-off values, resulting in two groups: high and low. Univariate logistic regression analysis revealed that elevated UA (OR: 3.46, 95% CI: 2.321-5.157, P < 0.001), elevated UAR (OR: 3.186, 95% CI: 2.146-4.731, P < 0.001), elevated NLR (OR: 5.786, 95% CI: 3.747-8.937, P < 0.001), elevated CEA (OR: 3.142, 95% CI: 2.088-4.728, P < 0.001), elevated CA199 (OR: 2.174, 95% CI: 1.41-3.348, P < 0.001) and elevated CA724 (OR: 2.178, 95% CI: 1.478-3.209, P< 0.001) were identified as risk

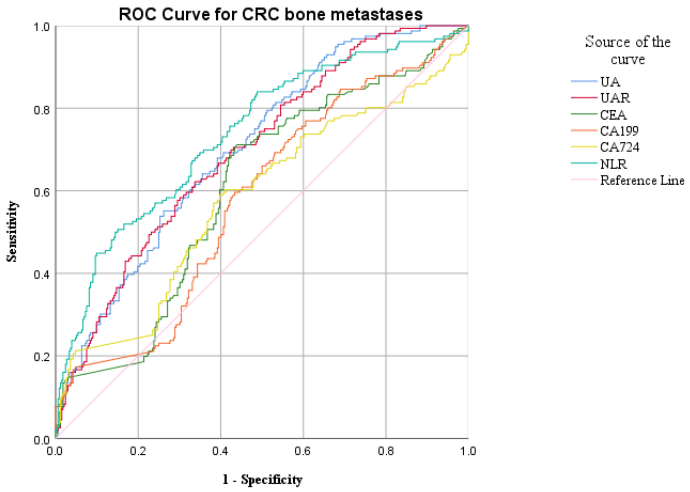

FIGURE 2
ROC analysis for the prediction of CRC bone metastasis. AUC indicates the diagnostic power of UA, UAR, NLR, CEA, CA199 and CA724 for bone metastasis.

TABLE 3 The ROC curve determined the optimal cut-off values for the diagnostic parameters of bone metastases in colorectal cancer.

Parameters	AUC	95% CI	Cut-off	Sen	Spe	Youden index	P value
UA	0.705	0.658-0.752	309.9	0.551	0.741	0.291	<0.001
UAR	0.698	0.650-0.746	7.69	0.622	0.665	0.287	<0.001
CEA	0.602	0.549-0.655	3.97	0.712	0.562	0.273	<0.001
CA199	0.576	0.522-0.630	9.975	0.769	0.393	0.162	0.007
CA724	0.578	0.521-0.635	7.79	0.56	0.602	0.191	0.005
NLR	0.738	0.690-0.786	4.201	0.506	0.849	0.355	<0.001
P1	0.628	0.576-0.680	0.278	0.705	0.543	0.247	<0.001
P2	0.723	0.676-0.770	0.248	0.801	0.51	0.31	<0.001
P3	0.719	0.671-0.767	0.301	0.628	0.705	0.333	<0.001
P4	0.759	0.712-0.807	0.33	0.538	0.871	0.409	<0.001
P5	0.825	0.787-0.863	0.281	0.75	0.76	0.509	<0.001

AUC, Area under receiver operating characteristics; CI, Confidence Interval; UA, Uric acid; Sen, Sensitivity; Spe, Specificity; P1, Prediction probability obtained by binary logistic regression combining CEA, CA199 and CA724; P2, Prediction probability obtained by binary logistic regression combining CEA, CA199, CA724 and UA; P3, Prediction probability obtained by binary logistic regression combining CEA, CA199, CA724 and UAR; P4, Prediction probability obtained by binary logistic regression combining CEA, CA199, CA724 and NLR; P5, Prediction probability obtained by binary logistic regression combining CEA, CA199, CA724, UA, UAR and NLR.

factors for colorectal cancer metastasis (Table 4). Furthermore, multivariate logistic regression analysis indicated that elevated UA (OR: 2.73, 95%CI: 1.399-5.328, P = 0.003), elevated NLR (OR: 6.42, 95%CI: 3.914-10.532, P < 0.001) and elevated CEA (OR: 2.365, 95%CI: 1.423-3.93, P = 0.001) were independent risk factors for colorectal cancer bone metastasis (Table 6).

Discussion

In our study, we investigated serum UA levels, UAR and NLR in patients diagnosed with colorectal cancer. Our finding indicated that serum UA, UAR, NLR and CEA levels were significantly elevated in patients with bone metastatic colorectal cancer compared to those without such metastasis. Furthermore, multiple logistic regression analysis revealed that higher serum UA, NLR and CEA levels were associated with bone metastatic colorectal cancer. However, we did not observe a significant association between UAR and tumor bone metastasis in this patient population.

TABLE 4 Comparison of AUC values between any two of the P1-P5.

	DBA (95% CI)	*P* value
P1 vs P2	-0.095 (-0.153, -0.037)	0.001
P1 vs P3	-0.091 (-0.148, -0.034)	0.002
P1 vs P4	-0.131 (-0.188, -0.075)	<0.001
P1 vs P5	-0.197 (-0.252, -0.142)	<0.001
P2 vs P3	0.004 (-0.017, 0.026)	0.693
P2 vs P4	-0.036 (-0.100, 0.027)	0.264
P2 vs P5	-0.102 (-0.141, -0.063)	0.001
P3 vs P4	-0.041 (-0.105, 0.024)	0.215
P3 vs P5	-0.106 (-0.144, -0.068)	<0.001
P4 vs P5	-0.065 (-0.102, -0.029)	<0.001

DBA Difference between AUCs, AUCs were compared via Delong test.
CI Confidence interval, *AUC* Area under the curve.

Previous prospective studies have demonstrated that elevated serum UA level was associated with poorer prognoses in cancer patients (5). Additionally, serum UA level has been identified as an independent risk factor for esophageal carcinoma, colorectal cancer and oral squamous cell carcinoma (12–14). Currently, there was limited research on the relationship between serum UA levels and tumor bone metastasis in colorectal cancer patients. The findings of this study indicated that serum UA level in the bone metastasis group was significantly higher than that in the group without bone metastasis. Univariate logistic regression analysis revealed that serum UA levels exceeding 309.9 umol/L were linked to an increased likelihood of bone metastasis. Furthermore, multivariate logistic regression analysis suggested that individuals with elevated UA levels were more susceptible to a higher incidence of bone metastasis, with the difference reaching statistical significance. In summary, this study identified elevated UA levels as a risk factor for bone metastasis in colorectal cancer, suggesting that high UA levels may serve as a predictor for such metastasis. Previous research indicated that elevated uric acid concentrations can induce inflammation and oxidative stress, promote tumor cell proliferation and angiogenesis, and facilitate the invasion and metastasis of tumor cells (15, 16). However, there is a paucity of studies examining the relationship between serum uric acid and bone metastasis, and the underlying molecular mechanisms remain unclear. Further, basic research and large-scale cohort studies are necessary to investigate.

Hypoalbuminemia represents another adverse prognostic factor for colorectal cancer. In survival studies involving patients with colorectal cancer who received both surgical and non-surgical treatments, albumin has been utilized either as a component of the study or as part of a prognostic score. Li X et al. demonstrated that a high albumin-to-globulin ratio serves as a reliable indicator of overall survival and disease-free survival (17). Our research indicated that, while low albumin levels alone did not significantly predict bone

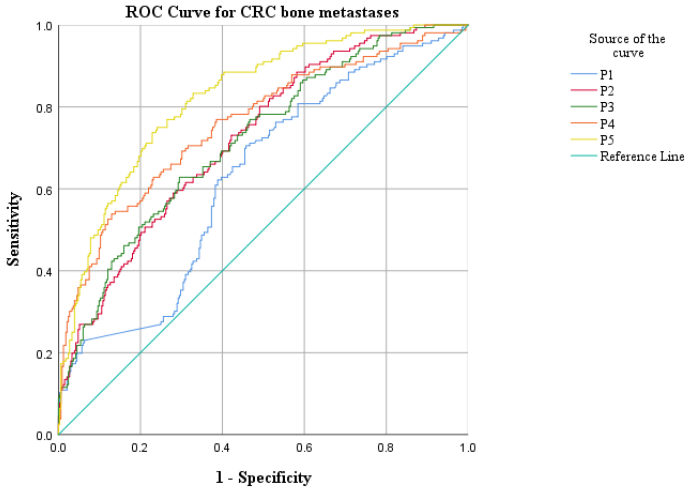

FIGURE 3
ROC analysis for the prediction of CRC bone metastasis. AUC indicates the diagnostic power of prediction probability for bone metastasis. P1: Prediction probability obtained by binary logistic regression combining CEA, CA199 and CA724; P2: Prediction probability obtained by binary logistic regression combining CEA, CA199, CA724 and UA; P3: Prediction probability obtained by binary logistic regression combining CEA, CA199, CA724 and UAR; P4: Prediction probability obtained by binary logistic regression combining CEA, CA199, CA724 and NLR; P5: Prediction probability obtained by binary logistic regression combining CEA, CA199, CA724, UA, UAR and NLR.

metastases in colorectal cancer, the UAR was significantly associated with such metastases, as revealed by further ROC analysis. In our study, the incidence of bone metastases was notably higher in the high UAR group. To date, no studies have reported a correlation between UAR and bone metastases in colorectal cancer. To our knowledge, this investigation was the first to establish that elevated UAR levels predict bone metastases in colorectal cancer.

Studies have demonstrated a close relationship between inflammation and tumors (18). Previous research has indicated that the proportion of neutrophils in peripheral blood increases as malignant tumors progress (19, 20). An elevated NLR signifies either a relative increase in neutrophils numbers or a relative decrease in lymphocytes counts. Evidence suggests that neutrophils can enhance the release of inflammatory mediators and facilitate tumor neovascularization. Conversely, neutrophils may diminish the body's anti-tumor capacity by inhibiting the activity of lymphocytes and natural killer cells, thereby promoting distant tumor metastasis. Lymphocytes not only inhibit tumor cell proliferation and metastasis, but also directly induce tumor cells death (21). A decrease in lymphocyte numbers indicated a weakened anti-tumor immune function, which can lead to tumor invasion and progression. The finding of this study revealed that the NLR in the bone metastasis group was significantly higher than that in the non-bone metastasis group, establishing a close association between NLR and bone metastasis in colorectal cancer. Consequently, a high NLR is more likely to be associated with bone metastasis, suggesting that NLR may serve as a novel marker for assessing tumor bone metastasis in patients with colorectal cancer.

TABLE 5 Correlation between UA, UAR, NLR and diagnostic parameters of bone metastases in colorectal cancer.

	Spearman correlation		
	UA	UAR	NLR
UA		0.908**	0.066
UAR	0.908**		0.086
NLR	0.066	0.086	
CEA	0.091*	0.106*	0.122**
CA199	0.05	0.025	0.093*
CA724	0.102*	0.124**	0.136**

*/**Statistically significant. **P-value<0.01; *P-value<0.05.

The predictive and prognostic effects of UA and NLR in cancer have been extensively investigated. Most studies have concentrated on elevated UA and NLR as indicators of long-term survival in cancer patients or have examined the role of NLR in assessing lymph node metastasis (10, 22–24). However, the predictive capacity of UA and NLR in evaluating bone metastasis has received comparatively less attention. While the involvement of UA and NLR in distant metastases among tumor patients has been documented, researchers have not yet compared the diagnostic efficacy of UA and NLR with traditional tumor markers. In our study, we demonstrated that UA and NLR outperformed conventional tumor markers in assessing bone metastasis. The optimal cut-off values for UA and NLR were determined to be 309.9 umol/L and 4.201, respectively, with sensitivities of 55.1% and 50.6%, and specificities of 74.1% and 84.9%. Among these indices, the combination of UA, the UAR, NLR and tumor markers exhibited the highest predictive accuracy for bone metastasis in CRC, whereas CA199 and CA724 demonstrated the lowest performance as indicated by logistic regression and ROC analysis. Further research is requires to ascertain whether the detection and targeted therapy of UA and neutrophils can enhance the prognosis of colorectal cancer and facilitate clinical treatment.

However, our study has several limitations. First, it is a single-center retrospective analysis, which may introduce bias and errors.

TABLE 6 Univariate and multivariate binary logistic regression analyses of variables for colorectal cancer bone metastases.

	Univariate analysis			Multivariate analysis		
	Odds ratio	95% CI	*P* value	Odds ratio	95% CI	*P* value
Age, years						
≥67.5 vs. <67.5	1.377	0.903-2.101	0.137	1.133	0.687-1.869	0.624
UA						
High vs. low	3.46	2.321-5.157	<0.001	2.73	1.399-5.328	0.003
UAR						
High vs. low	3.186	2.146-4.731	<0.001	1.836	0.944-6.57	0.074
NLR						
High vs. low	5.786	3.747-8.937	<0.001	6.42	3.914-10.532	<0.001
CEA						
High vs. low	3.142	2.088-4.728	<0.001	2.365	1.423-3.93	0.001
CA199						
High vs. low	2.172	1.41-3.348	<0.001	1.504	0.887-2.55	0.13
CA724						
High vs. low	2.178	1.478-3.209	<0.001	1.008	0.619-1.64	0.976

The reference of age, NLR, CEA, CA19–9 and CA72–4 was age < 67.5, UA < 309.9, UAR < 7.69, NLR < 4.201, CEA < 3.97, CA199 < 9.975 and CA724 < 7.79.

The conclusions further validation through additional basic studies, as well as multi-center and large-sample cohort studies. Second, certain confounders related to UA, such as diet, exercise, and alcohol consumption, were not included in the analysis. Furthermore, additional clinical parameters reflecting disease severity are necessary to elucidate the relationships among UA, UAR NLR and bone metastatic status in the multivariate regression analysis. Finally, we analyzed the relationships among UA, UAR, NLR and clinical prognosis in CRC patients. Despite these limitations, our findings indicate that UA, UAR and NLR may serve as novel markers for assessing tumor bone metastasis in patients with CRC.

Conclusion

In summary, our findings indicate that the combination of UA, UAR, NLR and tumor markers exhibits the highest diagnostic performance for bone metastasis in CRC. Both UA and NLR serve as valuable indicators for predicting bone metastases in CRC patients. Consequently, clinicians should closely monitor patients with UA levels exceeding 309.9 umol/L and NLR values greater than 2.91. Furthermore, they should undertake additional examinations to identify bone metastases at the earliest opportunity.

Data availability statement

The original contributions presented in the study are included in the article/supplementary material. Further inquiries can be directed to the corresponding author.

Ethics statement

The studies involving humans were approved by the Institutional Review Board of The First Affiliated Hospital of Xian JiaoTong University, Xian, China. The studies were conducted in accordance with the local legislation and institutional requirements. Written informed consent for participation was not required from the participants or the participants' legal guardians/next of kin in accordance with the national legislation and institutional requirements due to the retrospective nature of the study.

Author contributions

MC: Writing – original draft, Conceptualization, Writing – review & editing, Investigation, Data curation, Methodology. XW: Writing – review & editing, Investigation, Data curation. SB: Writing – review & editing, Conceptualization, Methodology. NL: Writing – review & editing. JW: Writing – review & editing. YC: Writing – review & editing. YG: Writing – review & editing. WW: Writing – review & editing. XS: Writing – review & editing. MJ: Writing – review & editing. XZ: Writing – review & editing. WeL: Writing – review & editing. FW: Writing – review & editing. WaL: Writing – review & editing. FH: Writing – review & editing. LC: Writing – review & editing. JR: Writing – review & editing, Funding acquisition, Supervision.

Funding

The author(s) declare financial support was received for the research and/or publication of this article. This manuscript is

supported by National Natural Science Foundation of China (Juan Ren, 82473252, 81772793); the Scientific and Technological Research Foundation of Shan'xi Province, Key Research and Development Project, General project (Juan Ren, 2023-YBSF-666); supported by the Shaanxi Provincial Key Research and Development Plan Project (Key support projects Category A) (Juan Ren, 2021A011); supported by the Basic and Clinical Integration Innovation Project of Xi' an Jiao tong University (Juan Ren,YXJLRH2022006; Ying Gao, YXJLRH 2022004). Nanjing Tianqing Scientific Research Fund of First Affiliated Hospital of Xi'an Jiaotong University (Juan Ren, TQ202205).

Acknowledgments

We would like to thank the patients who participated in this study and the Precision Medicine Center of the First Affiliated Hospital of Xi'an Jiaotong University, Xi'an, Shaanxi Province, 710061, P.R. China.

Conflict of interest

The authors declare that the research was conducted in the absence of any commercial or financial relationships that could be construed as a potential conflict of interest.

Generative AI statement

The author(s) declare that no Generative AI was used in the creation of this manuscript.

Any alternative text (alt text) provided alongside figures in this article has been generated by Frontiers with the support of artificial intelligence and reasonable efforts have been made to ensure accuracy, including review by the authors wherever possible. If you identify any issues, please contact us.

Publisher's note

References

1. Bray F, Laversanne M, Sung H, Ferlay J, Siegel RL, Soerjomataram I, et al. Global cancer statistics 2022: GLOBOCAN estimates of incidence and mortality worldwide for 36 cancers in 185 countries. *CA Cancer J Clin.* (2024) 74:229–63. doi: 10.3322/caac.21834

2. Christensen TD, Jensen SG, Larsen FO, Nielsen DL. Systematic review: Incidence, risk factors, survival and treatment of bone metastases from colorectal cancer. *J Bone Oncol.* (2018), 13:97–105. doi: 10.1016/j.jbo.2018.09.009

3. Hong EK, Chalabi M, Landolfi F, Castagnoli F, Park SJ, Sikorska K, et al. Colon cancer CT staging according to mismatch repair status: Comparison and suggestion of imaging features for high-risk colon cancer. *Eur J Cancer.* (2022), 165–75. doi: 10.1016/j.ejca.2022.06.060

4. Cervantes A, Adam R, Roselló S, Arnold D, Normanno N, Taïeb J, et al. Metastatic colorectal cancer: ESMO Clinical Practice Guideline for diagnosis, treatment and follow-up. *Ann Oncol.* (2023) 34:10–32. doi: 10.1016/j.annonc.2022.10.003

5. Strasak AM, Rapp K, Hilbe W, Oberaigner W, Ruttmann E, Concin H, et al. The role of serum uric acid as an antioxidant protecting against cancer: prospective study in more than 28–000 older Austrian women. *Ann Oncol.* (2007) 18:1893–7. doi: 10.1093/annonc/mdm338

6. Mi S, Gong L, Sui Z. An unrecognized role of uric acid in cancer development and the potential anticancer effects of uric acid-lowering drugs. *J Cancer.* (2020) 11:5236–44. doi: 10.7150/jca.46200

7. Takamori S, Takada K, Shimokawa M, Matsubara T, Fujishita T, Ito K, et al. Clinical utility of pretreatment Glasgow prognostic score in non-small-cell lung cancer patients treated with immune checkpoint inhibitors. *Lung Cancer.* (2021) 152:27–33. doi: 10.1016/j.lungcan.2020.11.026

8. Tang H, Li B, Zhang A, Lu W, Xiang C, Dong J. Prognostic significance of neutrophil-to-lymphocyte ratio in colorectal liver metastasis: A systematic review and meta-analysis. *PloS One.* (2016) 11:e0159447. doi: 10.1371/journal.pone.0159447

9. Magdy M, Hussein T, Ezzat A, Gaballah A. Pre-treatment peripheral neutrophil-lymphocyte ratio as a prognostic marker in gastric cancer. *J Gastrointest Cancer.* (2019) 50:763–8. doi: 10.1007/s12029-018-0144-x

10. Aoyama T, Takano M, Miyamoto M, Yoshikawa T, Kato K, Sakamoto T, et al. Pretreatment neutrophil-to-lymphocyte ratio was a predictor of lymph node metastasis in endometrial cancer patients. *Oncology.* (2019) 96:259–67. doi: 10.1159/000497184

11. Liu Z, Xu SF, Liu ER, Wang LQ, Huang HY. Colorectal oncology committee of chinese medical doctor association. *[Chinese Expert consensus Multidiscip Treat Bone metastasis colorectal Cancer (2020 version)].* (2020) 42:433–7. doi: 10.3760/cma.j.cn112152-20200402-00295

12. Chen YF, Li Q, Chen DT, Pan JH, Chen YH, Wen ZS, et al. Prognostic value of pre-operative serum uric acid levels in esophageal squamous cell carcinoma patients who undergo R0 esophagectomy. *Cancer biomark.* (2016) 17:89–96. doi: 10.3233/CBM-160621

13. Liao W, Wang Y, Zhang W. Serum uric acid and the risk of colorectal cancer: a meta-analysis. *Eur J Cancer Prev.* (2024) 33:19–28. doi: 10.1097/CEJ.0000000000000834

14. Ara SA, Ashraf S, Patil BM. Evaluation of serum uric acid levels in patients with oral squamous cell carcinoma. *Indian J Dent Res.* (2016) 27:178–83. doi: 10.4103/0970-9290.183128

15. Liu J, Xu C, Ying L, Zang S, Zhuang Z, Lv H, et al. Relationship of serum uric acid level with non-alcoholic fatty liver disease and its inflammation progression in non-obese adults. *Hepatol Res.* (2017) 47:E104–12. doi: 10.1111/hepr.12734

16. Hulsegge G, Herber-Gast GC, Spijkerman AM, Susan H, Picavet J, van der Schouw YT, et al. Obesity and age-related changes in markers of oxidative stress and inflammation across four generations. *Obes (Silver Spring).* (2016) 24:1389–96. doi: 10.1002/oby.21515

17. Li X, Qin S, Sun X, Liu D, Zhang B, Xiao G, et al. Prognostic significance of albumin-globulin score in patients with operable non-small-cell lung cancer. *Ann Surg Oncol.* (2018) 25:3647–59. doi: 10.1245/s10434-018-6715-z

18. Nishida A, Andoh A. The role of inflammation in cancer: mechanisms of tumor initiation, progression, and metastasis. *Cells.* (2025) 14:488. doi: 10.3390/cells14070488

19. Diakos CI, Charles KA, McMillan DC, Clarke SJ. Cancer-related inflammation and treatment effectiveness. *Lancet Oncol.* (2014) 15:e493–503. doi: 10.1016/S1470-2045(14)70263-3

20. Pastore CA, Orlandi SP, Gonzalez MC. The Inflammatory-Nutritional Index; assessing nutritional status and prognosis in gastrointestinal and lung cancer patients. *Nutr Hosp.* (2014) 29:629–34. doi: 10.3305/nh.2014.29.3.7195

21. Bastid J, Bonnefoy N, Eliaou JF, Bensussan A. Lymphocyte-derived interleukin-17A adds another brick in the wall of inflammation-induced breast carcinogenesis. *Oncoimmunology.* (2014) 3:e28273. doi: 10.4161/onci.28273

22. Howard R, Kanetsky PA, Egan KM. Exploring the prognostic value of the neutrophil-to-lymphocyte ratio in cancer. *Sci Rep.* (2019) 9:19673. doi: 10.1038/s41598-019-56218-z

23. Moon G, Noh H, Cho IJ, Lee JI, Han A. Prediction of late recurrence in patients with breast cancer: elevated neutrophil to lymphocyte ratio (NLR) at 5 years after diagnosis and late recurrence. *Breast Cancer.* (2020) 27:54–61. doi: 10.1007/s12282-019-00994-z

24. Wang Y, Zhai J, Zhang T, Han S, Zhang Y, Yao X, et al. Tumor-associated neutrophils can predict lymph node metastasis in early gastric cancer. *Front Oncol.* (2020), 10:570113. doi: 10.3389/fonc.2020.570113

frontiers | Frontiers in Oncology

TYPE Case Report
PUBLISHED 24 October 2025
DOI 10.3389/fonc.2025.1613500

OPEN ACCESS

EDITED BY
Oleksandr Kamyshnyi,
Ternopil State Medical University, Ukraine

REVIEWED BY
Yifeng Sun,
Canhelp Genomics, China
Çiğdem Özdemir,
Afyonkarahisar Saglik Bilimleri Universitesi Hastanesi, Türkiye

*CORRESPONDENCE
Xiaodong Zhang
zhangxd0829@163.com

RECEIVED 17 April 2025
ACCEPTED 30 September 2025
PUBLISHED 24 October 2025

CITATION
Yang Y, Sun W, Jia J, Yu J, Sun Z, Du F, Shi Y, Sun J, Gao S, Xiao Y and Zhang X (2025) Metastatic squamous cell carcinoma of unknown primary: a case report and brief literature review. *Front. Oncol.* 15:1613500. doi: 10.3389/fonc.2025.1613500

Metastatic squamous cell carcinoma of unknown primary: a case report and brief literature review

Ying Yang[1], Wei Sun[2], Jun Jia[1], Jing Yu[1], Zhiwei Sun[1], Feng Du[1], Youwu Shi[1], Jing Sun[1], Songlin Gao[1], Yanjie Xiao[1] and Xiaodong Zhang[1]*

[1]Key Laboratory of Carcinogenesis and Translational Research (Ministry of Education, China), The VIP-II Gastrointestinal Cancer Division of Medical Department, Peking University Cancer Hospital and Institute, Beijing, China, [2]Key Laboratory of Carcinogenesis and Translational Research (Ministry of Education), Department of Pathology, Peking University Cancer Hospital and Institute, Beijing, China

Carcinoma of unknown primary (CUP) is a rare malignancy characterized by metastatic disease without an identifiable primary tumor, even after extensive diagnostic evaluation. This case report described a 70-year-old female patient with squamous cell CUP (SCCUP) who initially presented with elevated carbohydrate antigen 19–9 and a diaphragmatic mass. Despite comprehensive workup, including ^{18}F-fluorodeoxyglucose positron emission tomography–computed tomography and a 90-gene expression assay, the primary site remained unclear. The patient underwent surgical resection followed by two cycles of systematic therapy and achieved a disease-free survival of 14 months. This case underscores the limitations of the current diagnostic tools and the potential role of multimodal therapy in the management of CUP. The discordance between molecular testing and the clinical findings further emphasizes the perplexing nature of CUP. This report also reviews the literature on diagnosis and therapeutic options. Due to the absence of standardized regimens, future international collaboration and comprehensive genomic profiling are warranted to advance the understanding of this heterogeneous disease.

KEYWORDS

carcinoma of unknown primary, squamous cell carcinoma, multimodal therapy, comprehensive workup, molecular testing

Introduction

Carcinoma of unknown primary (CUP) presents only metastatic cancers without an identifiable primary tumor site, even after thorough clinical evaluations and various tests. Primary lesions have been identified only in less than 30% of patients despite comprehensive examinations (1, 2). Currently, the detection rate is still as low as 50%

even diagnosed by positron emission tomography–computed tomography (PET-CT) and biopsy (3–5). It is assumed that the primary tumor of CUP is below the minimum detectable lesion by current techniques, which may be due to the natural disease regression. The reported incidence of CUP ranges from 2.3% to 5% (6–8), with a median age at diagnosis of 65 years and a slight male predominance (8, 9). The median overall survival (OS) is 6–10 months (7, 10), while the 5-year survival is 5%–15% (11). Adenocarcinoma accounts for 40%–60% of CUP cases, and squamous cell carcinoma represents 15%–20% (10, 11). Here, we present a case of CUP diagnosed and treated by our cancer division.

The patient provided written informed consent for the publication of this case report, including all associated clinical details and images. All identifying information has been anonymized to protect the patient's privacy.

Case description

General information

The patient was a 70-year-old Chinese Han woman with an Eastern Cooperative Oncology Group Performance Status (ECOG PS) of 1. She was 155 cm in height and 63 kg in weight and with a body surface area of 1.62 m^2. Her blood group is Rh-negative type B. The patient did not report any obvious discomfort, and physical examinations revealed no remarkable findings. She had a medical history of hypertension that was well controlled by oral valsartan/hydrochlorothiazide combination therapy. She denied any history of tobacco or alcohol use, as well as any family history of malignancy.

Diagnostic workup

Carbohydrate antigen 19-9 (CA19-9) was incidentally found to be elevated, i.e., 56 U/ml (normal range = 0–37 U/ml), in October 2020, but no abnormal imaging findings were detected in November. Her CA19–9 had been progressively increasing since then. In May 2022, a colonoscopy showed no abnormalities. In March 2023, non-contrast abdominal CT revealed a space-occupying lesion near the spleen in the subphrenic region, but was not given attention for further investigation. The CT imaging changes are shown in Figure 1. In April 2023, gastroscopy identified a 2 cm × 1.5 cm pedunculated polyp near the cardia of the gastric greater curvature. This was pathologically confirmed as a hyperplastic polyp.

On November 13, 2023, her carcinoembryonic antigen (CEA) level was 43.52 ng/ml (normal range = 0–5 ng/ml), CA19–9 was 387 U/ml, and neuron-specific enolase (NSE) was 17.3 ng/ml (normal range = 0–15.2 ng/ml). Enhanced abdominal and pelvic CT revealed post-polypectomy changes in the stomach, with no obvious wall thickening or abnormal enhancement of the gastric wall. A spindle-shaped lesion with soft tissue density was observed below the left diaphragm, measuring approximately 5 cm × 1.5 cm. The lesion exhibited heterogeneous enhancement, smeared-out boundaries, and indistinct separation from the diaphragm. The spleen was shoved. The lesion was highly suspicious for a mesenchymal tumor, although malignant metastasis could not be ruled out. The left pleura appeared slightly thickened, and a patchy consolidation was noted adjacent to the pleura in the lower lobe of the left lung. On December 11, 2023, ^{18}F-fluorodeoxyglucose (FDG) PET-CT revealed an irregular soft tissue mass in the left diaphragmatic area with a maximum standardized uptake value (SUV_{max}) of 11.4, which measured approximately 3.9 cm × 3.4 cm × 2.4 cm. The lesion was growing toward the diaphragm; and its boundaries with the diaphragm and the spleen were unclear. PET-CT also demonstrated local thickening of the adjacent left pleura with a mildly increased radiotracer uptake (SUV_{max} = 2.3), as well as local discoid atelectasis of the lung. No enlarged or hypermetabolic lymph nodes were observed in the retroperitoneum or abdominal cavity. The lesion was considered suspicious for a mesenchymal tumor. The CT and PET-CT images are shown in Figure 2. However, the patient did not undergo a biopsy due to her Rh-negative blood type.

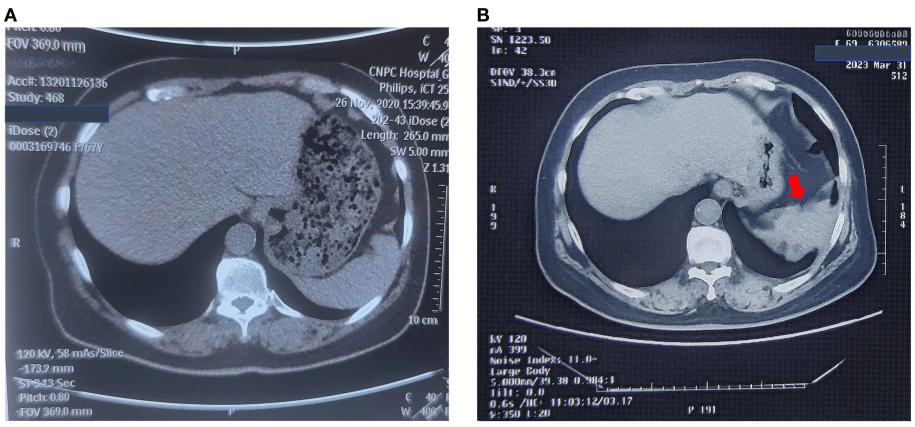

FIGURE 1
No-contrast abdomen CT changes before November, 2023. **(A)** No-contrast abdomen CT on November 26th, 2020. **(B)** No-contrast abdomen CT on March 31st, 2023.

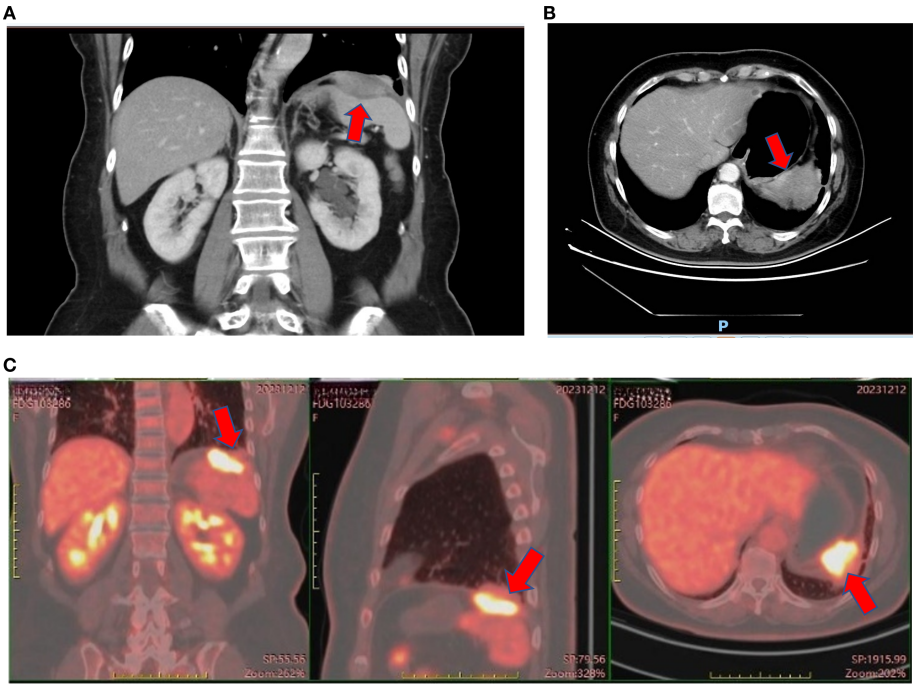

FIGURE 2
Enhanced CT and PET-CT of the left subdiaphragmatic mass. **(A)** Coronal view of enhanced CT of the left subdiaphragmatic mass on November 14th, 2023. **(B)** Axial view of enhanced CT of the left subdiaphragmatic mass on November 14th, 2023. **(C)** PET-CT of the left subdiaphragmatic mass on December 12th, 2023.

Treatment

On January 5, 2024, the patient underwent resection of the diaphragmatic mass and the spleen. The pathology findings were as follows:

1. The spleen measured 8.5 cm × 6 cm × 4 cm and the diaphragm 9.5 cm × 8 cm × 2 cm. A mass was observed within the diaphragm, measuring 6 cm × 5 cm × 2 cm. The cut section was grayish white and grayish yellow, solid, firm, and poorly demarcated from the surroundings. The focal lesion was in close proximity to the spleen.
2. The squamous cell carcinoma was moderately differentiated.
3. The tumor did not involve the spleen parenchyma, and no tumor was observed at the diaphragmatic resection margin.
4. The immunohistochemical results showed P16 (mixed +), P40 (+), CK5/6 (cytokeratin 5/6) (+), calretinin (−), D2-40 (focal +), WT1 (Wilms tumor protein 1) (−), EBER (Epstein–Barr virus-encoded small ribonucleic acid, RNA) (−), and PD-L1(22C3) [programmed death-ligand 1 (22C3 clone)] combined positive score (CPS) of 40.

The pathology images are shown in Figure 3. The pathologist recommended a thorough examination to rule out metastasis. A postoperative follow-up on March 1, 2024, showed a CEA of 1.38 ng/ml, CA19-9 of 10.1 U/ml, and NSE of 18.0 ng/ml.

From March 14 to April 7, 2024, two cycles of postoperative systematic therapy were administered. The regimen included albumin-bound paclitaxel (300 mg on day 1), carboplatin (500 mg on day 1), and pembrolizumab (200 mg on day 1), administered every 21 days. The main side effect was a grade 2 rash. After two cycles, the patient refused to continue.

CUP workup

On March 26, 2024, a 90-gene expression assay (Canhelp®-Origin; Canhelp® Genomics, Hangzhou, China) for CUP was conducted to identify the suspected origin. The results showed that the possible origin was the cervix uteri. The molecular analysis for origin is shown in Figure 3.

Pelvic enhanced magnetic resonance imaging showed a thickened mucous membrane of the cervical canal, which was a patchy long T1 and long T2 signal lesion and measured approximately 12 mm × 8 mm × 18 mm. The lesion exhibited a high signal on diffusion-weighted imaging (DWI) and a strong enhancement, with a continuous low signal at the local cervical junctional zone. The images are presented in Figure 4. However, on April 3, 2024, a gynecologic examination and colposcopy did not find any abnormalities. The cervical pathology displayed in Supplementary Figure S1 suggested atrophic signs, and the high-risk human papillomavirus (HPV) subtypes were all negative.

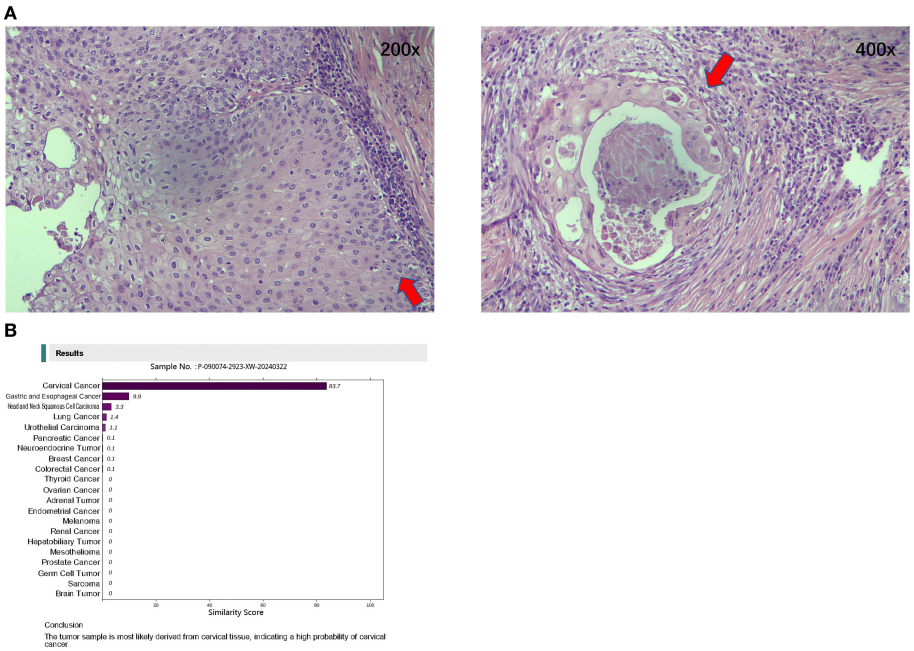

FIGURE 3
Hematoxylin and Eosin-stained pathological diagnosis and the Canhelp®-Origin 90-gene expression assay of resected lesions. **(A)** Hematoxylin and Eosin stained pathological diagnosis of resected lesions (Left: 200x; Right: 400x). **(B)** Canhelp®-Origin 90-gene expression assay of resected lesions.

Follow-up

On November 28, 2024, carbohydrate antigen 724 (CA724) was found to be elevated at 1,502 U/ml (normal range = 0–6.7 U/ml) during routine follow-up, but there were no abnormal signs on the CT scan. Compared with the PET-CT on December 11, 2023, the most recent imaging did not find any recurrent or metastatic features. The size of the bilateral hilar lymph nodes remained unchanged from previous imaging, with newly noted mild uptake increase (SUV_{max} = 4.0), which was suggestive of an inflammatory change, as seen in Supplementary Figure S2. On December 5, 2024, the CA724 level decreased to 203 U/ml. The changes in the tumor markers during the entire clinical course are shown in Supplementary Figure S3.

Up to April 17, 2025, when this manuscript was submitted, the disease-free survival (DFS) had been 15 months.

The timeline with relevant data and events is shown in Supplementary Table S1.

Discussion

We presented a case of squamous cell CUP (SCCUP). The 70-year-old female patient underwent surgery and remained without evidence of disease for more than 15 months. The 90-gene expression assay (Canhelp®-Origin) suggested a primary origin in the cervix uteri. However, colposcopy and its corresponding pathology findings and the HPV test were negative.

A systematic review on 24 reported SCCUP cases in the pelvic, abdominal, and retroperitoneal regions demonstrated a median age at diagnosis of 56.5 years (range = 27–78 years), with a female-to-male ratio of 3:1, and HPV infection was confirmed in 2 out of 10 patients tested (12). The optimal treatment strategy for this designated SCCUP remains debatable. Cisplatin-based chemoradiation has been the most widely employed, and surgical resection may be considered for bulky disease (12). Another study indicated that localized abdominal SCCUP may predict more favorable outcomes compared with other CUP subgroups (13). The case presented here shares similar features to those of previous reports.

Two cycles of systematic therapy combining albumin-bound paclitaxel, carboplatin, and pembrolizumab were administered after surgery, but was discontinued due to patient refusal, consistent with the limited evidence for postoperative chemotherapy in CUP. The majority of previous studies have explored chemotherapy as a palliative treatment, and no definitive regimen has been established. Briasoulis et al. (14) reported a response rate of carboplatin plus paclitaxel of 38.7% [95% confidence interval (CI) = 27.5–49.9] and a median OS of 13.0 months. A small-sample study conducted by Nishimori et al. (15) reported that cisplatin plus docetaxel showed a response rate of 62.5%, with a median OS of 22.7 months. A meta-analysis conducted by Lee et al. (16) reported a median OS for CUP of 9.0 months (95%CI = 8.1–9.8) and demonstrated an improved survival trend with platinum- or taxane-based regimens compared with other chemotherapy regimens. However, this association did not reach statistical significance with prolonged follow-up and after multivariate adjustment. A multidisciplinary treatment that integrated palliative surgery, radiotherapy, and chemotherapy suggests a possible survival benefit (17). Our case exhibited better outcomes than those reported in the meta-analysis. This good prognosis may

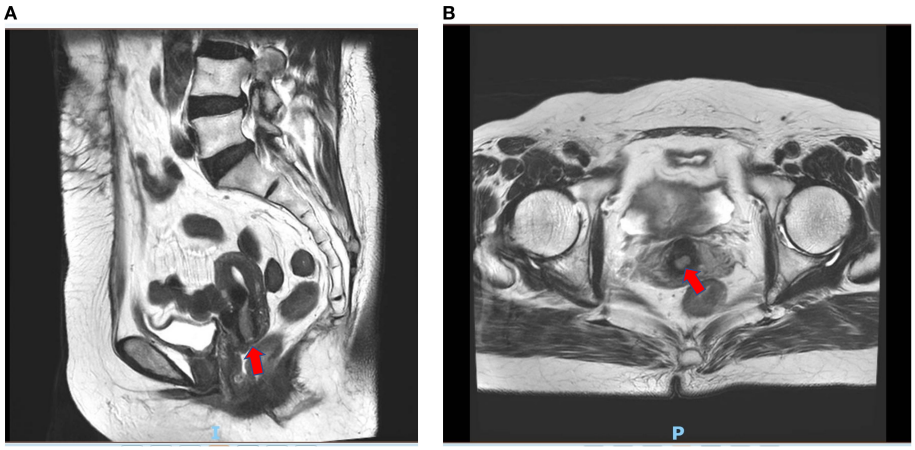

FIGURE 4
Enhanced magnetic resonance imaging of suspected cervical lesion on April 20th 2024. **(A)** Sagittal view of enhanced magnetic resonance imaging of suspected cervical lesion on April 20th 2024. **(B)** Axial view of enhanced magnetic resonance imaging of suspected cervical lesion on April 20th 2024.

further verify the suspected primary of cervical cancer that showed a less aggressive biological behavior. It could also reflect the effectiveness of the comprehensive treatment strategy comprising surgery, chemotherapy, and immunotherapy. In addition, in patients administered carboplatin plus paclitaxel therapy, the researchers observed that those with a PS of 0–1 and no bone metastasis had significantly better survival compared with patients with a PS of ≥2 or with bone metastasis (1-year OS = 67.1% *vs.* 36.8%, $p = 0.0003$) (18). Our patient had a PS of 1, with no evidence of bone or visceral metastasis, and underwent radical surgery. These factors may have also contributed to the better survival outcome.

Canhelp®-Origin is a 90-gene expression profiling assay created for differential diagnosis among 21 prevalent malignancies. These tumor specimens include breast, lung, colorectal, prostate, ovarian, and pancreatic carcinomas, as well as adrenal, renal, thyroid, hepatic, endometrial, cervical, gastroesophageal, and neuroendocrine lesions. In addition, the assay detects melanomas, mesotheliomas, sarcomas, germ cell tumors, and malignancies of the head and neck region and the urinary tract. This methodology employs reverse transcription polymerase chain reaction analysis, utilizing total RNA obtained from formalin-fixed, paraffin-embedded tumor tissues (19). The performance of the 90-gene assay has been verified, demonstrating a sensitivity of 95.7% and a specificity of 99.0% for cervical cancer. The accuracy for squamous cell carcinoma is 91.0%, which is slightly lower than that for adenocarcinoma (95.2%) (20). Despite the high sensitivity, specificity, and accuracy of the test, no malignant lesions were identified in the patient's cervix. This provides further proof of the challenge of identifying the origin of CUP and may suggest that the primary lesion has regressed during the disease course. Several mechanisms have been proposed for the regression. For example, early metastasis occurs before the primary tumor is clinically detectable, followed by immune-mediated elimination of the primary lesion, while metastatic clones continue to grow. Furthermore, the metastatic cells may acquire a pro-metastatic phenotype with genetic or epigenetic changes and thrive independently of the primary tumor. Moreover, modern techniques may fail to detect a tiny primary tumor (21).

Another advantage of the 90-gene expression assay is that it guides site-specific therapy. In the Fudan CUP-001 study, 91 of the 182 patients received site-specific therapy based on the results of the 90-gene expression assay, among whom 45% were administered targeted agents or immunotherapy, such as bevacizumab, PD-1 inhibitors, and epidermal growth factor receptor tyrosine kinase inhibitors (EGFR-TKIs). The other 91 patients received empirical chemotherapy, and only 26% were administered targeted agents or immunotherapy. The median progression-free survival (PFS) was 9.6 months, while the median OS was 28.2 months for patients who received site-specific therapy *versus* the corresponding 6.6 and 19.0 months for those who received empirical chemotherapy [PFS: unadjusted hazard ratio (HR) = 0.68, 95%CI = 0.49–0.93, p=0.017; OS: unadjusted HR = 0.74, 95%CI = 0.52–1.06, p=0.098]. Notably, among the 40 patients with SCCUP, site-specific therapy significantly improved the PFS compared with empirical chemotherapy (median PFS = 17.2 *versus* 4.7 months, HR = 0.41, p=0.017) (22). In our case, the patient received two cycles of chemotherapy combined with immunotherapy following surgery. However, given the postoperative setting and the limited number of treatment cycles, any definitive conclusions should be drawn with caution.

The major limitations of CUP, in particular SCCUP, include the lack of large-scale clinical studies and biological experiments elucidating the underlying molecular mechanisms. A recent large-scale comprehensive genomic profiling (CGP) study of 443 cases of SCCUP has revealed unique molecular characteristics distinct from those of non-squamous CUP, including actionable biomarkers (23). The integration of CGP into diagnostic workflows could improve the management of this challenging malignancy, which is a potential future direction. Given the rarity of this disease, multicenter collaboration, potentially on an international scale, is essential to accumulate sufficient cases in order to explore the nature of CUP.

Data availability statement

The original contributions presented in the study are included in the article/Supplementary Material. Further inquiries can be directed to the corresponding author.

Ethics statement

The studies involving humans were approved by Peking University Cancer Hospital and Institute, Beijing, China. The studies were conducted in accordance with the local legislation and institutional requirements. The participants provided their written informed consent to participate in this study. Written informed consent was obtained from the individual(s) for the publication of any potentially identifiable images or data included in this article.

Author contributions

YY: Writing – original draft. WS: Writing – review & editing. JJ: Writing – review & editing. JY: Writing – review & editing. ZS: Writing – review & editing. FD: Writing – review & editing. YS: Writing – review & editing. JS: Writing – review & editing. SG: Writing – review & editing. YX: Writing – review & editing. XZ: Writing – review & editing.

Funding

The author(s) declare that no financial support was received for the research, and/or publication of this article.

Conflict of interest

The authors declare that the research was conducted in the absence of any commercial or financial relationships that could be construed as a potential conflict of interest.

Generative AI statement

The author(s) declare that no Generative AI was used in the creation of this manuscript.

Any alternative text (alt text) provided alongside figures in this article has been generated by Frontiers with the support of artificial intelligence and reasonable efforts have been made to ensure accuracy, including review by the authors wherever possible. If you identify any issues, please contact us.

Publisher's note

Supplementary material

The Supplementary Material for this article can be found online at: https://www.frontiersin.org/articles/10.3389/fonc.2025.1613500/full#supplementary-material

SUPPLEMENTARY FIGURE 1
Cervical pathology (40x).

SUPPLEMENTARY FIGURE 2
Follow-up PET-CT on November 29th, 2024.

SUPPLEMENTARY FIGURE 3
Tumor marker change trends during the disease course. **(A)** CA19-9 change trends during the disease course. **(B)** CEA change trends during the disease course. **(C)** CA724 change trends during the disease course. **(D)** NSE change trends during the disease course.

References

1. Oien KA, Dennis JL. Diagnostic work-up of carcinoma of unknown primary: from immunohistochemistry to molecular profiling. *Ann Oncol.* (2012) 23 Suppl 10: x271–7. doi: 10.1093/annonc/mds357

2. Losa F, Iglesias L, Pané M, Sanz J, Nieto B, Fusté V, et al. 2018 consensus statement by the Spanish Society of Pathology and the Spanish Society of Medical Oncology on the diagnosis and treatment of cancer of unknown primary. *Clin Trans Oncol.* (2018) 20:1361–72. doi: 10.1007/s12094-018-1899-z

3. Blaszyk H, Hartmann A, Bjornsson J. Cancer of unknown primary: clinicopathologic correlations. *Apmis.* (2003) 111:1089–94. doi: 10.1111/j.1600-0463.2003.apm1111203.x

4. Lee MY, Fowler N, Adelstein D, Koyfman S, Prendes B, Burkey BB, et al. Detection and oncologic outcomes of head and neck squamous cell carcinoma of unknown primary origin. *Anticancer Res.* (2020) 40:4207–14. doi: 10.21873/anticanres.14421

5. Soni N, Ora M, Aher PY, Mishra P, Maheshwarappa RP, Priya S, et al. Role of FDG PET/CT for detection of primary tumor in patients with extracervical metastases from carcinoma of unknown primary. *Clin Imaging.* (2021) 78:262–70. doi: 10.1016/j.clinimag.2021.06.022

6. Fizazi K, Greco FA, Pavlidis N, Pentheroudakis G. Cancers of unknown primary site: ESMO Clinical Practice Guidelines for diagnosis, treatment and follow-up. *Ann Oncol.* (2011) 22 Suppl 6:vi64–8. doi: 10.1093/annonc/mdr389

7. van de Wouw AJ, Janssen-Heijnen ML, Coebergh JW, Hillen HF. Epidemiology of unknown primary tumours; incidence and population-based survival of 1285 patients in Southeast Netherlands, 1984-1992. *Eur J Cancer.* (2002) 38:409–13. doi: 10.1016/S0959-8049(01)00378-1

8. Pavlidis N, Fizazi K. Carcinoma of unknown primary (CUP). *Crit Rev Oncol Hematol.* (2009) 69:271–8. doi: 10.1016/j.critrevonc.2008.09.005

9. Siegel RL, Kratzer TB, Giaquinto AN, Sung H, Jemal A. Cancer statistics, 2025. *CA Cancer J Clin.* (2025) 75:10–45. doi: 10.3322/caac.21871

10. Matsubara N, Mukai H, Nagai S, Itoh K. Review of primary unknown cancer: cases referred to the National Cancer Center Hospital East. *Int J Clin Oncol.* (2010) 15:578–82. doi: 10.1007/s10147-010-0112-3

11. Yentz S, Bhave M, Cobain E, Baker L. "Cancer of unknown primary". In: DeVita VTJ, Lawrence TS, Rosenberg SA, editors. *DeVita, Hellman, and Rosenberg's Cancer Principles & Practice of Oncology*. Philadelphia, Baltimore, New York: Walters Kluwer Health (2023). p. 1856–62.

12. El Rassy E, Kattan J, Pavlidis N. A new entity of abdominal squamous cell carcinoma of unknown primary. *Eur J Clin Invest*. (2019) 49:e13111. doi: 10.1111/eci.13111

13. Randén M, Helde-Frankling M, Runesdotter S, Gunvén P. Unfavorable cancers of unknown primaries: presentation and prognostic factors. A population-based 8-year experience. *Med Oncol*. (2013) 30:706. doi: 10.1007/s12032-013-0706-5

14. Briasoulis E, Kalofonos H, Bafaloukos D, Samantas E, Fountzilas G, Xiros N, et al. Carboplatin plus paclitaxel in unknown primary carcinoma: a phase II Hellenic Cooperative Oncology Group Study. *J Clin Oncol*. (2000) 18:3101–7. doi: 10.1200/JCO.2000.18.17.3101

15. Nishimori H, Takahashi S, Kiura K, Ennishi D, Kobayashi T, Sano K, et al. Cancer of unknown primary site: a review of 28 cases and the efficacy of cisplatin/docetaxel therapy at a single institute in Japan. *Acta Med Okayama*. (2010) 64:285–91.

16. Lee J, Hahn S, Kim DW, Kim J, Kang SN, Rha SY, et al. Evaluation of survival benefits by platinums and taxanes for an unfavourable subset of carcinoma of unknown primary: a systematic review and meta-analysis. *Br J Cancer*. (2013) 108:39–48. doi: 10.1038/bjc.2012.516

17. Pentheroudakis G, Lazaridis G, Pavlidis N. Axillary nodal metastases from carcinoma of unknown primary (CUPAx): a systematic review of published evidence. *Breast Cancer Res Treat*. (2010) 119:1–11. doi: 10.1007/s10549-009-0554-3

18. Kodaira M, Takahashi S, Yamada S, Ueda K, Mishima Y, Takeuchi K, et al. Bone metastasis and poor performance status are prognostic factors for survival of carcinoma of unknown primary site in patients treated with systematic chemotherapy. *Ann Oncol*. (2010) 21:1163–7. doi: 10.1093/annonc/mdp583

19. Ye Q, Wang Q, Qi P, Chen J, Sun Y, Jin S, et al. Development and clinical validation of a 90-gene expression assay for identifying tumor tissue origin. *J Mol Diagnostics*. (2020) 22:1139–50. doi: 10.1016/j.jmoldx.2020.06.005

20. Sun W, Wu W, Wang Q, Yao Q, Feng Q, Wang Y, et al. Clinical validation of a 90-gene expression test for tumor tissue of origin diagnosis: a large-scale multicenter study of 1417 patients. *J Transl Med*. (2022) 20:114. doi: 10.1186/s12967-022-03318-6

21. Raghav K. Cancer of unknown primary site. *New Engl J Med*. (2025) 392:2035–47. doi: 10.1056/NEJMcp2402691

22. Liu X, Zhang X, Jiang S, Mo M, Wang Q, Wang Y, et al. Site-specific therapy guided by a 90-gene expression assay versus empirical chemotherapy in patients with cancer of unknown primary (Fudan CUP-001): a randomised controlled trial. *Lancet Oncol*. (2024) 25:1092–102. doi: 10.1016/S1470-2045(24)00313-9

23. Robinson HR, Lakritz S, Pavlick DC, Davis SL, Lieu CH, Eule CJ, et al. Squamous cell carcinoma of unknown primary (SCCUP): a genomic landscape study. *ESMO Open*. (2025) 10:105312. doi: 10.1016/j.esmoop.2025.105312

frontiers | Frontiers in Oncology

TYPE Case Report
PUBLISHED 06 November 2025
DOI 10.3389/fonc.2025.1635424

OPEN ACCESS

EDITED BY
Valentyn Oksenych,
University of Bergen, Norway

REVIEWED BY
Huzafa Ali,
CMH Multan Institute of Medical Sciences, Pakistan
José Antonio García Muñiz,
Dr José Eleuterio Gonzalez University Hospital, Mexico

*CORRESPONDENCE
Francois G. Kamar
francois@kamarclinic.com
Jawad K. Zrein
jawad.zrein@gmail.com

†These authors have contributed equally to this work

RECEIVED 25 June 2025
ACCEPTED 21 October 2025
PUBLISHED 06 November 2025

CITATION
El Waary NS, Chami AA, Zrein JK, Houcheimy DA, Akl RT, Fleifel SD and Kamar FG (2025) Case Report: Pitfalls in anatomic pathology and clinical oncology: a case of misdiagnosed pulmonary Ewing sarcoma as SCLC. *Front. Oncol.* 15:1635424. doi: 10.3389/fonc.2025.1635424

Case Report: Pitfalls in anatomic pathology and clinical oncology: a case of misdiagnosed pulmonary Ewing sarcoma as SCLC

Nagham S. El Waary[1,2†], Angelo A. Chami[3†], Jawad K. Zrein[1,2*], Doha A. Houcheimy[3], Ryan T. Akl[3], Siham D. Fleifel[4] and Francois G. Kamar[1,2*]

[1]Department of Hematology and Oncology, Faculty of Medicine, University of Balamand, Beirut, Lebanon, [2]Division of Hematology and Oncology, Mount Lebanon Hospital University Medical Center, Beirut, Lebanon, [3]Faculty of Medicine and Medical Sciences, University of Balamand, Beirut, Lebanon, [4]Department of Pathology, Lebanese American University Medical Center Rizk Hospital, Beirut, Lebanon

In oncology, an accurate pathological diagnosis can often mean the difference between cure and failure, potentially determining a patient's survival. We present the case of a 28-year-old, never-smoking man whose initial diagnosis of small cell lung cancer (SCLC) was confirmed by the anatomic pathology laboratory upon reevaluation, despite initial doubt. This misclassification ultimately led to therapeutic failure following an initial complete remission and likely contributed to the poor outcome after the diagnosis was later corrected to pulmonary Ewing sarcoma. Primary pulmonary Ewing sarcoma is a rare malignancy that is often overlooked in adults. This case underscores not only the striking clinical and histopathological overlap between SCLC and pulmonary Ewing sarcoma but also the potentially fatal consequences of missing key diagnostic red flags, including the patient's young age, non-smoking status, and atypical clinical course. Through this patient's journey, we emphasize the importance of multidisciplinary collaboration, the limitations of relying solely on immunohistochemistry, and the critical role of early molecular testing. This case serves as a stark reminder that behind every pathology report is a human life—one that depends on the vigilance, humility, and thoroughness of the medical team entrusted with their care.

KEYWORDS

lung malignancy, pulmonary Ewing sarcoma, immunohistochemistry, molecular testing, multidisciplinary team, misdiagnosis

1 Introduction

In the ever-evolving and dynamic world of oncology and the classification of thoracic malignancies, one must always keep an open and critical mind when diagnosing cases, no matter how straightforward or routine they might appear. An accurate diagnosis can be especially challenging when making a correct classification of thoracic malignancies such as primary mediastinal malignancies or lung cancers, due to the high overlap in histopathological and immunohistochemical features.

Primary mediastinal or pulmonary Ewing sarcoma (PES), an extremely rare malignancy with around 50 cases reported worldwide (1), can be easily misdiagnosed as a case of small cell lung carcinoma (SCLC) because of their similar morphological features—namely, small round blue cell histology (2, 3), a high nuclear-to-cytoplasmic ratio (2), hyperchromatic nuclei (4), abundant mitotic activity (5), or even necrotic and hemorrhagic features (4).

The following article discusses the discrepancies, overlap, and weak points that led to the misdiagnosis of a young gentleman initially thought to have a typical case of SCLC but later found to have an atypical presentation of PES. The delay in accurate diagnosis led to a suboptimal case outcome and the deferment of the correct chemotherapy regimen as well as any radiotherapy or surgical intervention. This case emphasizes the pitfalls in histopathology, the limitations of IHC alone, and the necessity for molecular testing, as well as highlights the importance of a multidisciplinary team approach in oncology discussions.

2 Case presentation

Our patient was a 28-year-old, never-smoking man with no significant past medical or surgical history. He initially presented to his local dispensary with gastrointestinal (GI) symptoms, including nausea and vomiting, associated with low anterior chest pain and a "pins and needles" sensation. He was prescribed intramuscular (IM) antibiotics and advised to undergo imaging studies. At that time, his initial computed tomography (CT) scan revealed a 9-cm mass in the left lung.

He presented to our clinic 4 months later with dyspnea and an intractable cough. A chest X-ray showed a widened mediastinum, prompting a repeat CT scan. This time, imaging revealed an 11-cm left hilar mass involving the upper and lower main bronchi. Bronchoscopy with biopsy established a diagnosis of small cell lung carcinoma (SCLC), which was confirmed by immunohistochemistry (IHC). The IHC findings were as follows: + CD56, +cytokeratin, -CD45, -CD20, - TTF1 and p63.

The anatomic pathology department had been consulted several times regarding this diagnosis, since the presentation was not classical given the patient's young age and never-smoker status.

Staging workup included a normal brain MRI and an FDG PET-CT scan showing an 11x11x10 cm left hilar mass with an SUV of 13 and no evidence of locoregional or distant metastasis. Given the patient's confined disease, a cisplatin, etoposide, and atezolizumab (Tecentriq) chemotherapy protocol was initiated with concurrent radiotherapy after documenting a major response by FDG PET-CT criteria following the second cycle. This allowed for a significant reduction in the radiation field.

Upon completing the third cycle, another FDG PET scan showed complete remission; therefore, treatment was continued until completion of six cycles. Unfortunately, a post-treatment FDG PET-CT scan showed local recurrence of the disease in the left upper lobe and hilum, with direct invasion into the mediastinum.

The suspiciously short relapse period prompted further investigation, initially requiring a salvage chemotherapy protocol with irinotecan and carboplatin (Campto-Carbo), as well as scheduling an EBUS biopsy at another site, along with re-examination of the same previously embedded paraffin block. The latter was delayed, but upon completion, immunohistochemical and histopathological analyses, which were sent to a reference pathology department in Lebanon, revealed pulmonary Ewing sarcoma, with CD99 (+), vimentin (+), CD56 (+), CD45 (–), synaptophysin (–), desmin (–), TTF-1 (–), and TLE1 (–). Although NKX2.2 immunohistochemistry and EWSR1 rearrangement studies were not available in our setting to definitively exclude BCOR- or CIC-rearranged sarcomas, the characteristic morphology and diffuse membranous CD99 positivity strongly supported the diagnosis of Ewing sarcoma (Figures 1, 2).

Once these findings were revealed, a repeat PET scan showed significant disease progression Figure 3, with a large mass extending from the lower cervical region into the anterior mediastinum and distant metastases to the retroperitoneum and porta hepatis. His condition progressively worsened despite initiation of vincristine, dactinomycin, and cyclophosphamide therapy, ultimately requiring ICU admission. He succumbed to the disease shortly thereafter Figure 4.

3 Discussion

3.1 Why was Ewing sarcoma misdiagnosed as SCLC?

3.1.1 Histopathologic overlap

SCLC and Ewing sarcoma (ES) can both present histologically as small, basophilic cells with granular nuclear chromatin and high mitotic activity on H&E stain. Necrotic and hemorrhagic features are common in both (1, 6). Moreover, although CD56 is the most sensitive marker for SCLC, it is not highly specific, and cases of ES found positive for CD56 have been reported in the literature (7, 8), with the latter being associated with a more aggressive tumor, especially when found in the extraosseous form of ES (8). To add more to the overlap, cytokeratin can be positive in SCLC (6) and, in very rare cases, in ES as well (1).

In the case presented, our misdiagnosis was confirmed at the repeat biopsy by the CD99 and vimentin IHC stains that are sensitive to ES. However, as we will explain further, these stains should not be our sole source of confirmation, as both can show positivity in other types of lung carcinomas, especially in combined forms (9). It is also important to point out that other IHC stains,

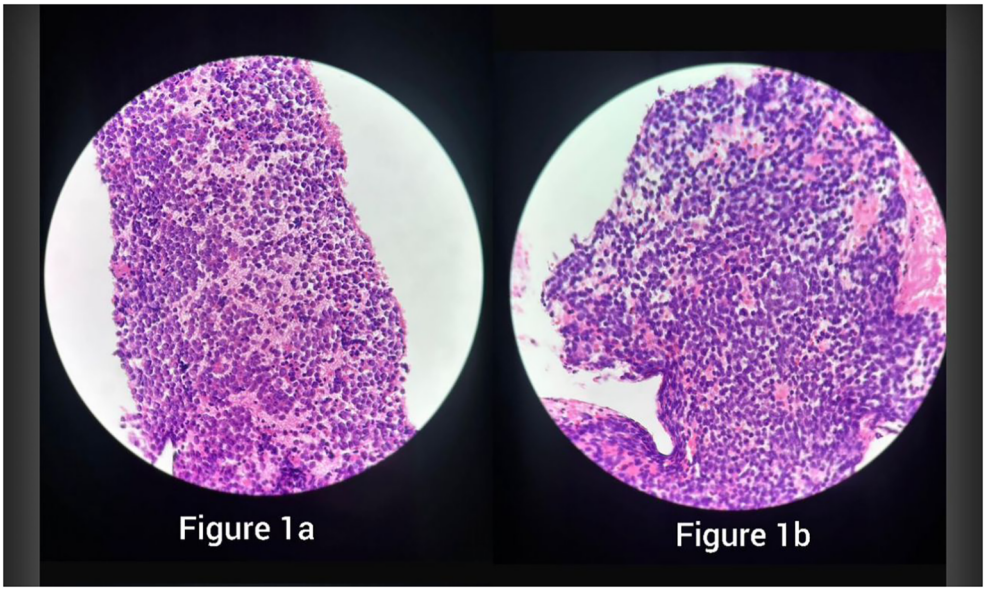

FIGURE 1
H&E sections showing sheets of small round blue cells with scant cytoplasm and fine chromatin, consistent with Ewing sarcoma, in specimen 1 **(a)** and specimen 2 **(b)**.

such as chromogranin A and synaptophysin, are not exclusive to SCLC and that a few cases of extraosseous ES have been reported to display such immunohistological features (1) Table 1.

3.1.2 Role of molecular testing

Since 1994, Delattre et al. have established that, at the molecular level, fusion of the EWSR1 gene on chromosome 22 with a member of the erythroblast transformation-specific (ETS) family of transcription factors—most commonly *FLI1* on chromosome 11 (q24) or ERG on chromosome 21(q22), results in the development of an oncogenic transcription factor that gives rise to Ewing sarcoma in its various forms (10, 11). This translocation remains the most accurate diagnostic standard for Ewing sarcoma and should be considered the gold standard when evaluating these tumors.

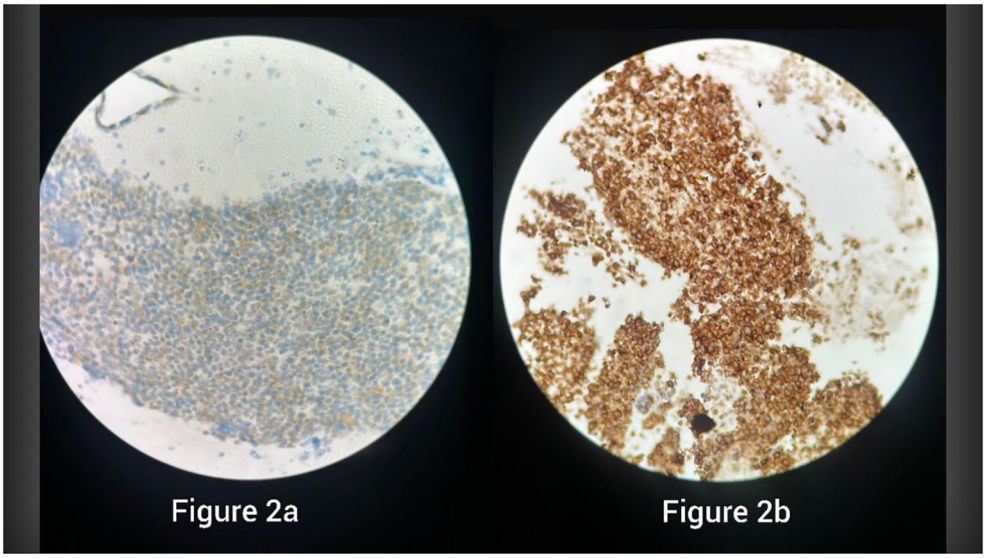

FIGURE 2
Immunohistochemistry showing strong membranous CD99 positivity in specimen 1 **(a)** and specimen 2 **(b)**, supporting the diagnosis of Ewing sarcoma.

More recently, other biomarkers have been identified that can assist in diagnosing ES, although they yet on their own don't hold the same sensitivity and specificity as the latter.

However, the combination of these biomarkers holds promise in achieving the desired sensitivity and specificity. For example, the NKX2.2 and ZBTB16 genes have been found to be a more sensitive combination when compared to CD99 alone or NKX2.2 and CD99 together. This is because ZBTB16 is upregulated by EWS-FLI1 (12). Moreover, cell-free tumor DNA (ctDNA) containing EWS-FLI1 or EWS-ERG fusions shows not only qualitative value but also quantitative importance in assessing and monitoring tumor burden upon diagnosis and throughout the course of therapy (13).

The lack of molecular testing, either by FISH or NGS, at the initial diagnosis may have led to the unfortunate misdiagnosis of the patient reported in this case. This occurrence has also been reported by Abdelghany et al., who described a case initially misdiagnosed with SCLC and later underwent molecular testing by next-generation sequencing after disease metastasis, only to be found to have primary ES of the lung. Thus, missing out on early molecular confirmation can lead to inappropriate chemotherapy choices, as SCLC and primary ES do not share similar management protocols.

3.1.3 Biopsy site and imaging bias

It is without doubt that the site from which the biopsy is extracted plays a role in the diagnostic approach to the type of tumor, especially given that primary ES of the lung has been reported in the literature. Fedeli et al., in a systematic review of primary ES of the lung, reported 50 cases as of 2023 found in the literature. Moreover, SCLC most frequently presents as a hilar mass with ipsilateral mediastinal lymphadenopathy or direct mediastinal extension, with involvement of the upper and lower lobes being a common presentation and infrequent ipsilateral pleural effusions (14). This added to the bias toward the incorrect diagnosis.

3.2 Clinical consequence of misdiagnosis

3.2.1 Inappropriate treatment

The patient's disease stage prompted initiation of etoposide and a platinum base, a standard of care that has been in use for decades. Our patient was started on cisplatin due to its decreased side effects of myelosuppression and better overall survival in younger patients (6). The patient was also placed on atezolizumab, which has shown modest improvement in overall and progression-free survival (6). The patient additionally received radiation therapy in a VMAT and IGRT fashion between his third and fourth chemotherapy sessions. The aim of management was hopeful, as the patient was young, and complete remission was the goal.

However, SCLC is known to be aggressive, especially in advanced stages, with a 5-year overall survival rate of 40% in early stage, 29% in extensive stage, and 18% in broadly metastatic extensive stage (15). Ewing sarcoma management is considered more intensive and aims for complete remission, as survival rates are high if initiated early. The US-based standard of care, later validated by the Euro Ewing 2012 Phase 3 trial, is the most effective and least toxic, with a shortened duration. The regimen is composed of vincristine, cyclophosphamide, and doxorubicin alternated with ifosfamide and etoposide (16, 17). The chemotherapy regimen can then be followed by radiation therapy or surgical resection, either of which is case dependent.

.

3.2.2 Delayed correct treatment and prognostic implications

Both treatments differ significantly, sharing only etoposide as a common agent, which could explain the false hope created by the partial response to treatment. Thus, the delay in uncovering the true diagnosis led to critical time being lost and disease progression beyond the reach of the standard Ewing regimen, eventually resulting in metastasis and the unfortunate demise of our patient.

Primary pulmonary Ewing sarcoma is an aggressive disease, particularly in the absence of surgical intervention, and carries a very poor prognosis. In the review by Fedeli et al., among 36 reported cases, 14 patients had died by the time of publication, with a median survival of 11.5 months (95% CI, 1.8–25.2). Thirteen patients were alive at a median follow-up of 18 months (95% CI, 14.1–41.1 months), six were alive at 36 months from diagnosis, and three remained disease-free for 48 months (1).

Stork et al., in a retrospective study analyzing nine patients with primary Ewing sarcoma of the mediastinum, reported an overall 5-year survival rate of 64%. Interestingly, patients who underwent local R0 resection for primary, non-metastatic disease achieved a 100% survival rate (18). These findings suggest that high-dose chemotherapy, followed by surgical resection when feasible, could have provided a better prognosis for our patient.

3.3 Lessons learned

3.3.1 When to suspect primary Ewing sarcoma instead of SCLC

Recognizing the demographic discrepancy of having a never-smoker young patient with SCLC should have been a warning sign to look deeper into the true etiology of the malignancy. In addition, the poor response and early relapse of the disease were other red flags that should have prompted us to question the primary diagnosis. With Ewing sarcoma being less aggressive and more responsive to dose-intensive regimens of chemoradiotherapy (CRT), precious time was lost in attaining the correct diagnosis, which could have given our patient a better chance of survival.

SCLC's median age of presentation in both genders was around 68–69 years in 2019 (15, 19), which presents a significant gap when compared with the median age of the rare cases of primary Ewing sarcoma of the lung reported, which was around 30.5 years in both sexes (1). It is also important to examine the risk factors for each malignancy. SCLC occurs in approximately 95% of cases in smokers, with an increased risk in groups that have smoked at low intensity over a long period compared with those who have

TABLE 1 Immunohistochemical and molecular differences between pulmonary Ewing sarcoma and small cell lung carcinoma.

Marker/feature	Ewing sarcoma	Small cell lung carcinoma
CD99	Diffuse Strong Membranous Positivity	Negative or weak and focal
Vimentin	Positive	Negative
Cytokeratin	Rare (weak)	Diffuse Positivity
NKX2.2	Nuclear Positivity	Negative
FL1-1	Nuclear Positivity	Negative
TTF-1	Negative	Positive in majority of cases
Neuroendocrine Markers (Synatophysin, Chromogranin, CD56)	Negative or rare weak focal positivity	Diffuse positivity for at least one marker
Ki-67 Proliferation Index	High, but variable	Very High (usually ~ 70-90%)
Molecular Confirmation	Most commonly EWSR1-FL1 fusion	Frequent TP53 or RB1 inactivation

smoked at higher intensity over a shorter period, even when overall pack-years are the same. The overall risk ranges between 17.1 and 38.6 for 30 years of smoking (20). Only 2%–3% of cases are reported in non-smokers, with the remainder attributed to environmental exposure to carcinogenic materials, mainly radon (20).

As for Ewing sarcoma, no external risk factors are known, and molecular susceptibility to mutations remains the primary cause. Imaging plays a major role in establishing the differential diagnoses of lung tumors, especially given the overlapping features between the two types. Some key radiologic signs of Ewing sarcoma to look out for include a well-circumscribed mass with a heterogeneous appearance (21, 22). Invasion of adjacent structures is rare (21), while ipsilateral pleural effusions and calcifications have been reported (21, 22). On FDG-PET, the malignancy demonstrates increased uptake, which aids in border and invasion detection as well as in identifying bone marrow metastases.

3.3.2 Role of a multidisciplinary team

Accurate diagnosis of complex or unclear pathologies relies significantly on multidisciplinary teams (MDTs), including oncologists, pathologists, and radiologists, particularly in lesions of the lung, where clinical, radiologic, and histopathologic features often overlap in pulmonary masses. In our case, the importance of the MDT is highlighted by the initial pathology report misdiagnosing our patient with SCLC mainly because key IHC markers were not included. When diagnosing Ewing sarcoma of the lung, the central role lies in distinguishing the histological findings of ES from its mimics, as well as identifying essential IHC markers such as CD99, FLI1, and NKX2.2. When morphological features alone are inconclusive or overlapping, these markers are of great importance.

As in our case, the omission of these stains in the initial pathology report delayed the correct diagnosis and, consequently, the correct treatment. This underscores the need for standardized

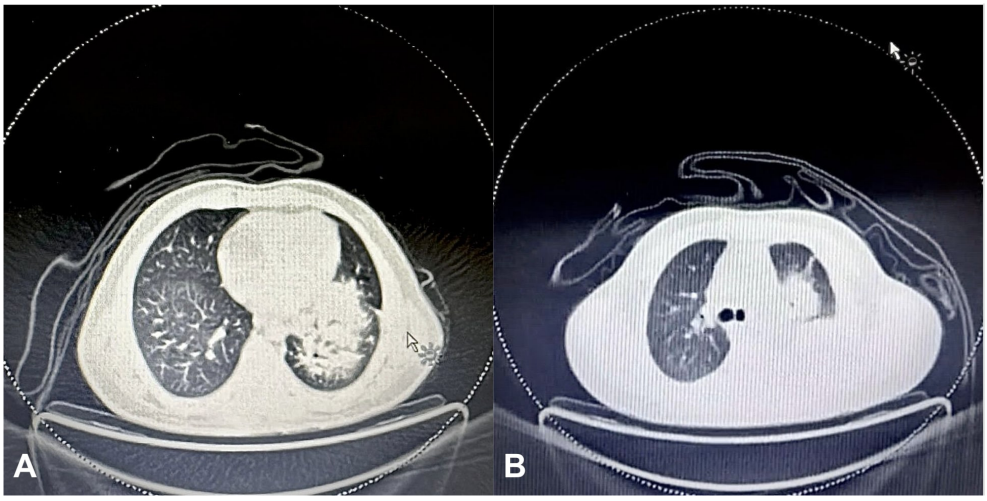

FIGURE 3
(A) Initial FDG PET scan of the chest showing an 11x11x10 cm soft tissue mass in the left lung perihilar region, encasing the left lobar bronchus and extending from the medial pleural surface to the lung periphery. **(B)** Final FDG PET scan showing a marked interval increase in the size of the soft tissue mass in the left lung perihilar region (12x12x8 cm), extending into the upper and lower lobes and reaching the pleural and pericardial surfaces.

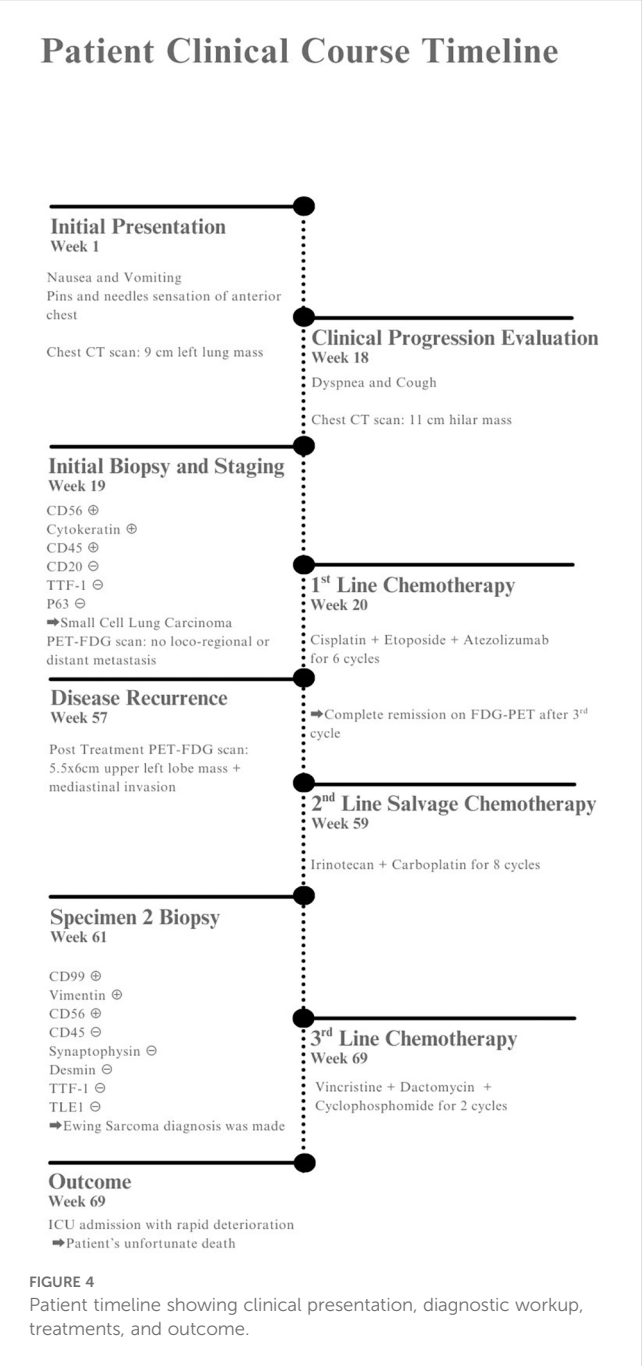

FIGURE 4
Patient timeline showing clinical presentation, diagnostic workup, treatments, and outcome.

diagnostic protocols to ensure timely identification of the disease. Similarly, the radiologist's role lies in recognizing the characteristic radiographic features of ES. When imaging modalities reveal aggressive features of malignancy—such as a well-circumscribed mass invading adjacent structures, with signs of pleural effusion and calcifications (21, 22)—especially in young patients, these findings should be emphasized when setting the differential.

In a study conducted by Pang et al. concerning the role of multidisciplinary teams in guiding the diagnosis and treatment of bone and soft tissue tumors, the teams were able to correctly diagnose the type of tumor in 95.42% of cases, compared with a rate of 90.84% when multidisciplinary discussions were not held. Additionally, the team achieved a 100% success rate in identifying relapses (23). Our case aims to highlight the critical role of communication between specialties in achieving an accurate and timely diagnosis.

If an MDT discussion had taken place during our patient's workup, the pathologist might have considered ES in the differential diagnosis, taking into account the patient's demographic and clinical presentation, and thus included the necessary IHC markers in the report—leading to an accurate diagnosis from the outset. Consequently, standardizing a diagnostic workflow that mandates a full panel of IHC stains in relevant, highly suspicious cases will improve diagnostic accuracy and prevent delays in initiating the correct treatment.

We also emphasize the inclusion of molecular testing, especially in patient demographics that may present with signs and symptoms of SCLC but do not fit the typical profile, particularly with respect to age and risk factor exposure. Although molecular testing is a more expensive and less accessible option—especially in less developed institutions with limited funding—we cannot rely solely on IHC, as the discrepancies described could lead to similar events in the future. Thus, molecular testing remains a safeguard for accurate diagnosis and should be incorporated early in the diagnostic workflow.

4 Conclusion

This case highlights the key points that led to the initial misdiagnosis of Ewing sarcoma (ES) as a typical case of small cell lung cancer (SCLC). Moreover, it reveals areas in the standard diagnosis of thoracic neoplasms that could divert diagnosticians from accurately identifying the pathology at hand, especially when it mimics a more prevalent malignancy both in histopathology and immunohistochemical profile. This prompts a deeper look into molecular diagnostics as a crucial pillar in future pathology confirmations across all oncology scopes and not only in thoracic neoplasms. The early reliance on FISH or next-generation sequencing (NGS) to identify the EWSR1 translocation would have greatly altered the treatment and would optimally have led to a better prognosis.

An essential role must be recognized for multidisciplinary approaches as well as early and accurate molecular studies to

improve the outcomes of future cases, establishing the above-mentioned techniques as essentials rather than luxuries.

Data availability statement

The original contributions presented in the study are included in the article/supplementary material. Further inquiries can be directed to the corresponding authors.

Ethics statement

Written informed consent was obtained from the individual(s) for the publication of any potentially identifiable images or data included in this article. Consent was received from patient's family and treating physician. Written informed consent was obtained from the participant/patient(s) for the publication of this case report.

Author contributions

NE: Writing – original draft, Writing – review & editing. AC: Writing – original draft, Writing – review & editing. DH: Writing – original draft. JZ: Writing – review & editing. RA: Writing – original draft. SF: Writing – review & editing, Investigation. FK: Supervision, Writing – original draft, Conceptualization, Funding acquisition, Project administration, Writing – review & editing.

Funding

The author(s) declare that no financial support was received for the research, and/or publication of this article.

Acknowledgments

We would like to express our gratitude to Dr Francois G Kamar for their guidance in the preparation of this case report. We also extend our gratitude to the pathology department at LAU Rizk Hospital for reinterpreting the pathology results.

Conflict of interest

The authors declare that the research was conducted in the absence of any commercial or financial relationships that could be construed as a potential conflict of interest.

Generative AI statement

The author(s) declare that no Generative AI was used in the creation of this manuscript.

Any alternative text (alt text) provided alongside figures in this article has been generated by Frontiers with the support of artificial intelligence and reasonable efforts have been made to ensure accuracy, including review by the authors wherever possible. If you identify any issues, please contact us.

Publisher's note

References

1. Fedeli MA, Marras V, Fara AM, Deiana A, Lobrano R, Cossu A, et al. Primary Ewing sarcoma of the lung: A systematic review of the recent literature. *Ann Diagn Pathol*. (2023) 65:152152. Available online at: https://linkinghub.elsevier.com/retrieve/pii/S1092913423000503 (Accessed March 25, 2025).

2. Desai SS, Jambhekar NA. Pathology of Ewing's sarcoma/PNET: Current opinion and emerging concepts. *Indian J Orthop*. (2010) 44:363–8. doi: 10.4103/0019-5413.69304

3. Raso MG, Bota-Rabassedas N, Wistuba II. Pathology and classification of SCLC. *Cancers*. (2021) 13:820. Available online at: https://www.mdpi.com/2072-6694/13/4/820 (Accessed March 25, 2025).

4. Basumallik N, Agarwal M. *Small cell lung cancer* (2019). Nih.gov. StatPearls Publishing. Available online at: https://www.ncbi.nlm.nih.gov/books/NBK482458/.

5. Hamilton G. Comparative characteristics of small cell lung cancer and Ewing's sarcoma: a narrative review. *Transl Lung Cancer Res*. (2022) 11:185–98. Available online at: https://tlcr.amegroups.com/article/view/65249/html (Accessed March 25, 2025).

6. Dingemans AMC, Früh M, Ardizzoni A, Besse B, Faivre-Finn C, Hendriks LE, et al. Small-cell lung cancer: ESMO Clinical Practice Guidelines for diagnosis, treatment and follow-up. *Ann Oncol*. (2021) 32:839–53. Available online at: https://linkinghub.elsevier.com/retrieve/pii/S0923753421011133 (Accessed March 25, 2025).

7. MaChado I, Navarro S, López-Guerrero JA, Verdini L, Picci P, Giner F, et al. Neuroendocrine differentiation in a large series of genetically-confirmed Ewing's sarcoma family tumor: Does it provide any diagnostic or prognostic information? *Pathol - Res Pract*. (2021) 219:153362. Available online at: https://linkinghub.elsevier.com/retrieve/pii/S0344033821000236 (Accessed March 25, 2025).

8. Ash S, Luria D, Cohen IJ, Goshen Y, Toledano H, Issakov J, et al. Excellent prognosis in a subset of patients with ewing sarcoma identified at diagnosis by CD56 using flow cytometry. *Clin Cancer Res*. (2011) 17:2900–7. Available online at: https://aacrjournals.org/clincancerres/article/17/9/2900/12906/Excellent-Prognosis-in-a-Subset-of-Patients-with (Accessed March 25, 2025).

9. Thunnissen E, Borczuk AC, Flieder DB, Witte B, Beasley MB, Chung JH, et al. The use of immunohistochemistry improves the diagnosis of small cell lung cancer and its differential diagnosis. An international reproducibility study in a demanding set of cases. *J Thorac Oncol*. (2017) 12:334–46. Available online at: https://linkinghub.elsevier.com/retrieve/pii/S1556086416335729 (Accessed March 25, 2025).

10. Delattre O, Zucman J, Melot T, XS G, JM Z, GM L, et al. The Ewing family of tumors–a subgroup of small-round-cell tumors defined by specific chimeric transcripts. *New Engl J Med*. (1994) 331:294–9. Available online at. doi: 10.1056/NEJM199408043310503

11. Gamberi G, Cocchi S, Benini S, Magagnoli G, Morandi L, Kreshak J, et al. Molecular diagnosis in ewing family tumors. *J Mol Diagn*. (2011) 13:313–24. Available

online at: https://linkinghub.elsevier.com/retrieve/pii/S1525157811000225 (Accessed March 25, 2025).

12. Daher M, Zalaquett Z, Chalhoub R, Abi Farraj S, Abdo M, Sebaaly A, et al. Molecular and biologic biomarkers of Ewing sarcoma: A systematic review. J. *Bone Oncol.* (2023) 40:100482. Available online at: https://linkinghub.elsevier.com/retrieve/pii/S2212137423000155 (Accessed March 25, 2025).

13. Krumbholz M, Hellberg J, Steif B, Bäuerle T, Gillmann C, Fritscher T, et al. Genomic EWSR1 fusion sequence as highly sensitive and dynamic plasma tumor marker in ewing sarcoma. *Clin Cancer Res*. (2016) 22:4356–65. Available online at: https://aacrjournals.org/clincancerres/article/22/17/4356/119821/Genomic-EWSR1-Fusion-Sequence-as-Highly-Sensitive (Accessed March 25, 2025).

14. Lee D, Rho JY, Kang S, Yoo KJ, Choi HJ. CT findings of small cell lung carcinoma: Can recognizable features be found? *Med (Baltimore)*. (2016) 95:e5426. Available online at: https://journals.lww.com/00005792-201611220-00034 (Accessed March 25, 2025).

15. Dumoulin DW, Aarts MJ, De Ruysscher D, Aerts JGJV, Dingemans AMC. Trends in the epidemiology of small-cell lung cancer: a Dutch nationwide population-based study over 1989–2020. *Eur J Cancer*. (2023) 191:112985. Available online at: https://linkinghub.elsevier.com/retrieve/pii/S0959804923003374 (Accessed March 25, 2025).

16. Pretz JL, Barysauskas CM, George S, Hornick JL, ChandrajitP R, Chen YLE, et al. Localized adult ewing sarcoma: favorable outcomes with alternating vincristine, doxorubicin, cyclophosphamide, and ifosfamide, etoposide (VDC/IE)-based multimodality therapy. *Oncologist*. (2017) 22:1265–70. Available online at: https://academic.oup.com/oncolo/article/22/10/1265/6444585 (Accessed March 25, 2025).

17. Brennan B, Kirton L, Marec-Bérard P, Gaspar N, Laurence V, Martín-Broto J, et al. Comparison of two chemotherapy regimens in patients with newly diagnosed Ewing sarcoma (EE2012): an open-label, randomised, phase 3 trial. *Lancet*. (2022) 400:1513–21. Available online at: https://www.thelancet.com/journals/lancet/article/PIIS0140-6736(22)01790-1/fulltext (Accessed March 25, 2025).

18. Stork T, Ranft A, Aigner C, Jurgens H, Ladenstein RL, Timmermann B, et al. Primary mediastinal ewing's sarcoma: post hoc analysis from two international multicenter prospective randomized trials. *Cancers*. (2025) 17:118. Available online at: https://www.mdpi.com/2072-6694/17/1/118 (Accessed March 25, 2025).

19. Cittolin-Santos GF, Knapp B, Ganesh B, Gao F, Waqar S, Stinchcombe TE, et al. The changing landscape of small cell lung cancer. *Cancer*. 130:2453–61. doi: 10.1002/cncr.35281

20. Wang Q, Gümüş ZH, Colarossi C, Memeo L, Wang X, Kong CY, et al. SCLC: epidemiology, risk factors, genetic susceptibility, molecular pathology, screening, and early detection. *J Thorac Oncol*. (2023) 18:31–46. Available online at: https://linkinghub.elsevier.com/retrieve/pii/S1556086422018512 (Accessed March 25, 2025).

21. Shet N, Stanescu L, Deutsch G. Primary extraosseous Ewing sarcoma of the lung: Case report and literature review. *Radiol Case Rep*. (2013) 8:832. Available online at: https://linkinghub.elsevier.com/retrieve/pii/S1930043315303915 (Accessed March 25, 2025).

22. Tsetsou I, Moschouris H, Spanomanolis N, Soumpourou E. Ewing sarcoma of the lung: imaging of a rare tumor. *Cureus*. (2022). Available online at: https://www.cureus.com/articles/126712-ewing-sarcoma-of-the-lung-imaging-of-a-rare-tumor (Accessed March 25, 2025).

23. Pang K, Guo X, Liu T, Wang L, Chen R, Zhang Z, et al. The role of a multidisciplinary team in the diagnosis and treatment of bone and soft tissue sarcomas: A single-center experience. *J Pers Med*. (2022) 12:2079. Available online at: https://www.mdpi.com/2075-4426/12/12/2079 (Accessed March 25, 2025).

Frontiers in
Molecular Biosciences

Explores biological processes in living organisms on a molecular scale

Focuses on the molecular mechanisms underpinning and regulating biological processes in organisms across all branches of life.

Discover the latest Research Topics

See more →

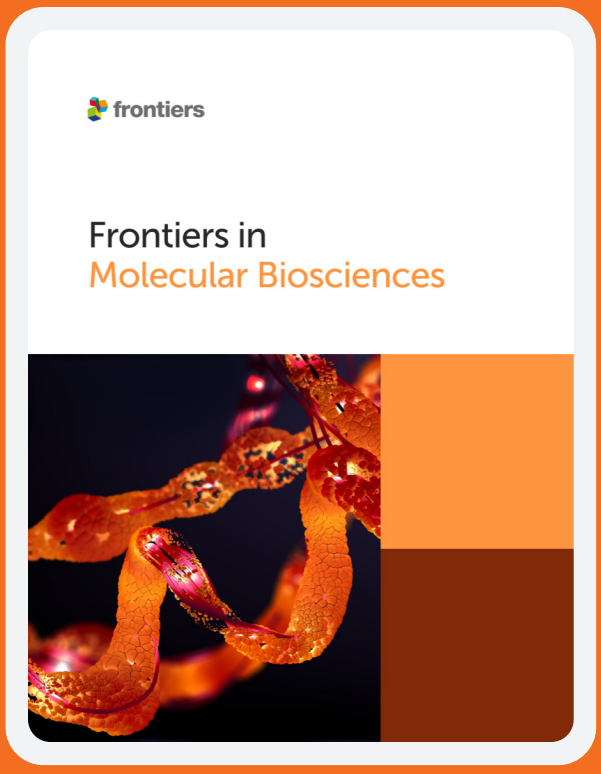

Frontiers

Avenue du Tribunal-Fédéral 34
1005 Lausanne, Switzerland
frontiersin.org

Contact us

+41 (0)21 510 17 00
frontiersin.org/about/contact